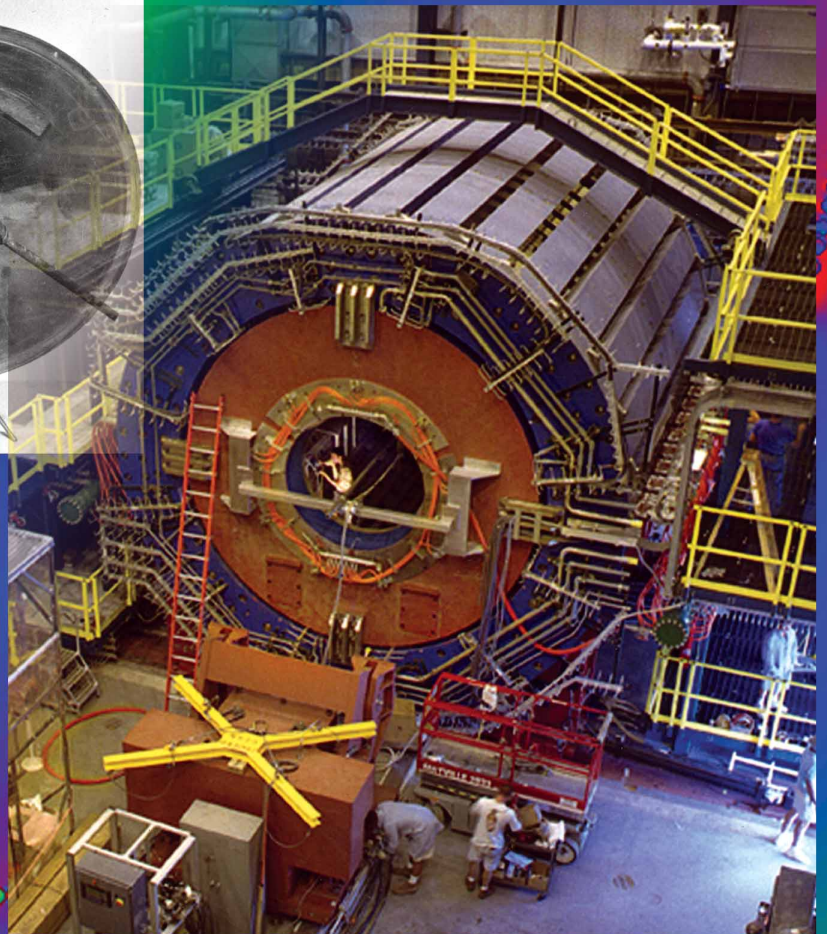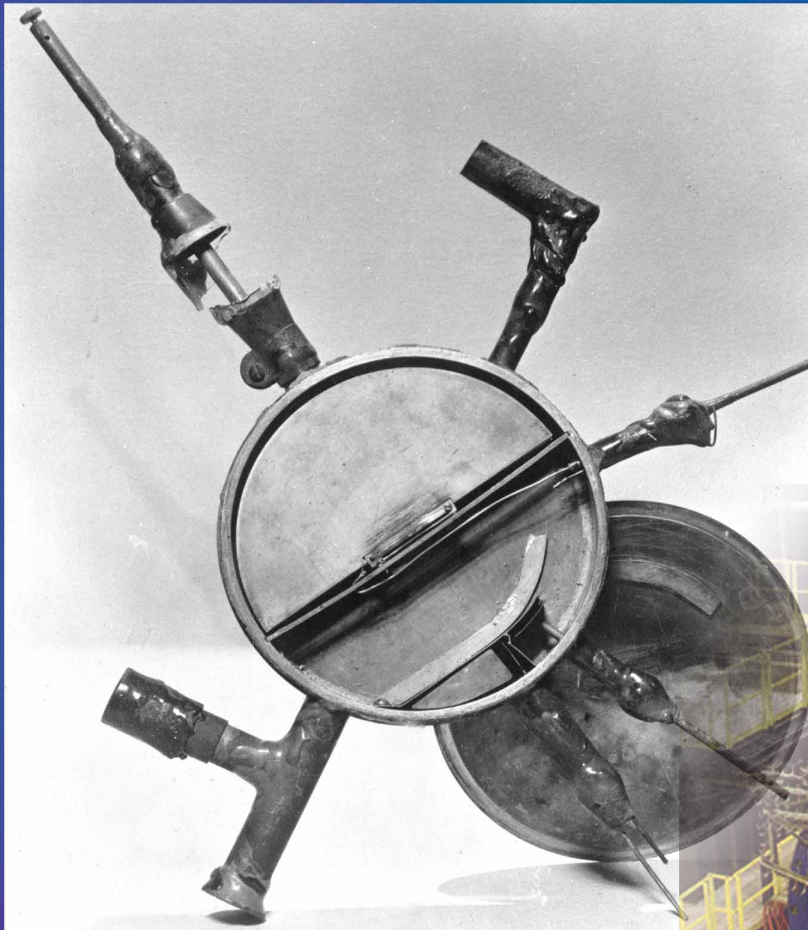# Journal of Undergraduate Research

OFFICE OF
SCIENCE
U.S. DEPARTMENT of ENERGY

A NOTE FROM THE EDITOR: THE NEW SCIENCE

*T*here are more scientists alive today than have ever lived before, and this formidable, intellectual force is reaching wherever human imagination directs it. Any scientist can easily feel overwhelmed by the rapid progress in his/her own specialty, let alone in the broader field to which s/he belongs. There are currently thousands of scientific journals published monthly, and a simple Internet search of a term as specific as "microarray" can generate as many as 116,000 "hits."

Along with this avalanche of information, publications that bring to bear various scientific disciplines in an attempt to reveal a comprehensive, multidimensional understanding of nature are increasingly common. Investigations that cut across disciplines are revealed in the titles and language of recent publications. If language, as poets tell us, reveals the nature of a culture, what should we make of terms like biogeochemistry, DNA semiconductors, and unifying theory? It suggests that our scientific disciplines are converging and that the reductionalist and fragmentary approaches, which typify a science in its childhood, are giving way to an era of synthesis. This is apparent in the physical sciences where the "Standard Model" provides a substantially integrated picture of the subatomic world. Scientists of this world of inner space are often contributing to the work of cosmologists in the understanding of the Earth, its evolution and the destiny of the greater universe. Certainly, the central questions regarding dark energy and the CP violation indicate our science is still adolescent, but the advancements we have made in the last century are amazing. We can look to the collaboration of scientists of inner and outer space for another century of expanding scientific frontiers, leading to a heightened, collective understanding.

> **"...the reductionalist and fragmentary approaches, which typify a science in its childhood, are giving way to an era of synthesis.**

New research into DNA-based semiconductors, organic high-temperature superconductors and molecular organic machinery is an indication of the scientific culture of merging disciplines and technologies which, like nanotechnology, defy categorization. Underpinning all these sciences is the modern computer. Before 1950, a dictionary was unlikely to include the definition of a computer. The ability of computers to input, store and intelligently mine massive amounts of data is central to modern science and has spurred a radical change in how science is done. Scientific advances like the Human Genome Project would have been impracticable without them. All organisms on Earth are DNA based, and there is considerable similarity among the genomes of all life forms. High-throughput gene machines are rapidly deciphering the genomes of numerous organisms, and with massive computer data-banks comparative genomics should soon be able to make an accurate model of all the genes on the planet...a sort of planetary genome.

Microorganisms are well recognized to have changed the atmospheric composition of this planet through photosynthetic oxygenation, nitrogen fixation and carbon sequestration. It is only recently that geologists, chemists, meteorologists, and biologists have come together to begin creating an integrated picture of our living planet's mantle to tens of kilometers in depth where microorganisms have been found to be a substantial geological force. It should be clear to our nation's academic institutions, National Laboratories, and populace that the future of our economy and the science that drives our economy is in an environment where the term "interdisciplinary science" is a redundancy.
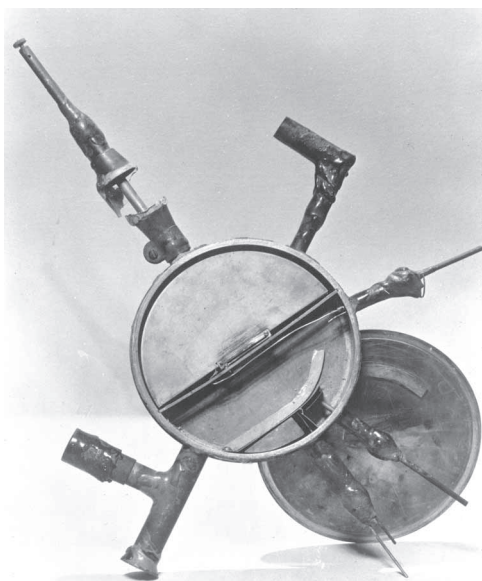
Peter Faletra, Ph.D.
Editor-In-Chief
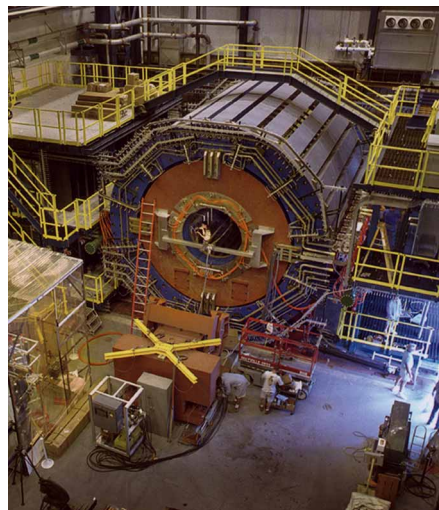
ABOUT THE COVER

Courtesy of Lawrence Berkeley National Laboratory

The first successful cyclotron (left) built by E.O. Lawrence and his graduate student M. Stanley Livingston, accelerated a few hydrogen molecule ions to an energy of 80,000 electron volts. Since each ion received an accelerating kick twice in a circuit as it entered and left the single flat semicircular electrode or "dee," those that managed to reach full energy and fall into the collecting cup 4.50 cm from the center of the instrument had made no fewer than forty turns. The result, reported at the January 1931 American Physical Society meeting, earned Livingston his Ph.D. and Lawrence $500 from the National Research Council towards the construction of a machine that might be useful for nuclear physics. Who would have predicted that this machine that "might be useful" would grow eventually to the size of a small city, cost many millions of dollars, and allow scienti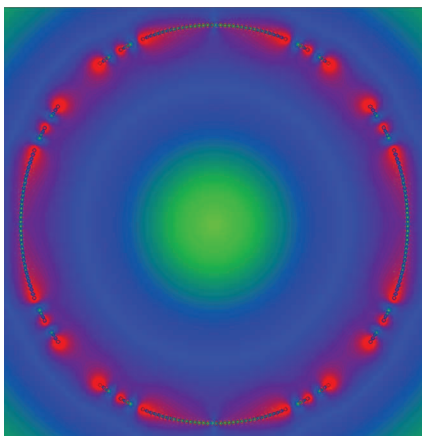sts of all disciplines to study matter in forms ranging from the most basic of particles to complex life-systems. Arguably, Lawrence's cyclotron was the birth of the Department of Energy and the beginning of today's big science.

Many of today's most advanced scientific tools, including particle accelerators and advanced light sources, have evolved from the cyclotron. The STAR (Solenoidal Tracker at RHIC) Detector (right), one of four detectors at the Relativistic Heavy Ion Collider (RHIC) at Brookhaven National Laboratory, tracks and analyzes the thousands of particles that may be produced by each gold ion collision inside the detector. As big as a house, STAR will search for signatures of the form of matter that RHIC aims to create: the quark-gluon plasma. It will also investigate the behavior of matter at high energy densities by making measurements over a large area. Particle accelerators work in large part because of the advances in human ability to control electromagnetic forces. The image of the strength of a magnetic field (left), produced by a superconducting quadrupole magnet built by the Brookhaven National Laboratory (BNL) Superconducting Magnet Division for the Hadron-Electron Ring Accelerator (HERA) at the DESY Laboratory in Hamburg, Germany, was built using technology developed at BNL for manufacturing some of the specialized magnets for the RHIC facility.

Courtesy of Brookhaven National Laboratory

Courtesy of Brookhaven National Laboratory

TABLE OF CONTENTS

Electron and positron collisions and their decay products interact with the layered subsystems of the BaBar Detector to provide information that could help physicists learn about the earliest moments in our universe and the fundamental interactions of matter. The BaBar Detector, the work of 500 physicists from over 780 organizations worldwide, is part of Stanford Linear Accelerator Center's B Factory Systems. It will be used to study B and anti-B mesons—particle-antiparticle pairs that scientists believe will help in our understanding of nature and matter.

WHY RESEARCH EXPERIENCE?

"...on fait la science avec des faits comme une maison avec des pierres; mais une accumulation de faits n'est pas plus une science qu'un tas de pierres n'est une maison."
"...one builds science with facts, as (one builds) a house with stones. But a collection of facts is no more a science than a heap of stones is a house."
— Jules Henri Poincaré (Science and Hypothesis, 1908)

Any science student learns a lot of facts. But the enterprise of science, as Poincaré stresses earlier in the essay that I quote above, is fundamentally one of doing experiments and making observations, and, equally critical, developing a theory that comprehends the past observations and makes predictions for the outcome of future experiments. That is the enterprise of research. Research is the essence of science. The facts, (by which Poincaré means the things learned by past observations and experiment), and the theories that comprehend these facts are a product of research. Without some knowledge of the process by which these facts and theories were obtained a student cannot know what science is all about, nor distinguish scientific information from myth or speculation.

None of us has the time, nor the resources, to reproduce all the experiments and redevelop all of the theories. In learning science one mostly learns just the results, the facts and theories, without learning very much about how these results were obtained. Even laboratory classes only scratch the surface of the problem. All too often the experiments have been reduced to rote following of procedure. The iterative process of interaction between experiment and theory, the uncertainty, the missteps and wrong guesses, are rarely met.

> **The iterative process of interaction between experiment and theory, the uncertainty, the missteps and wrong guesses, are rarely met.**

A research experience allows a student to see the process of science firsthand, to struggle, as researchers must, with the confusion of not knowing what is going on, with the uncertainty and the excitement of a new idea. The student can experience the detective-like hunt for a clue, for a way to make an experiment work, or for an interpretation of an unexpected outcome. This experience brings the student face to face with issues that do not appear when learning means finding out about what others already know.

Research is so different from learning science in the classroom that anyone considering a career in science should seek out every opportunity to experience it. In studying science, a student may experience the fascination of the big ideas and be excited when reading of a new theory in the paper. While that excitement indicates the student may like being a scientist, it is only the first step. The real test comes with some actual experience of having a problem to solve that is not just an exercise. It must be a problem to which no one quite knows the answer yet. Beyond that, the student needs to experience what it means to be part of a research team, with others who rely on your results to push forward the joint endeavor, as you rely on them for their insights and advice on your part of the problem, as well as for their results.

Some students may perhaps feel that, despite strong interest, they are not quite cut out for a career in science because others in their classes read and understand faster, or do better on the exams. However, once in the research lab, some of these students find that other skills that they possess are more important than those that make it easy to get good grades. Skills in making equipment function, skills in envisaging a change in the setup that will overcome a problem you are experiencing with it, skills in working as part of a team and combining your ideas with those of others; all these are critical in research but seldom tapped in the classroom. The research experience lets a student learn about these skills and demonstrate them too — and a letter of recommendation from a research mentor can be the key to admission to a first rate graduate school.

On the other hand, a student may find that living with uncertainty and confusion appeals not at all. If so, this too is invaluable knowledge. A career in research is probably not the best choice for such a person. Their interest and skills in learning about science can lead to other options: teaching, science writing, working as a hospital radiation physicist, to name but a few. The sooner the student knows this the better educational choices can be tuned towards the careers that will be most rewarding.
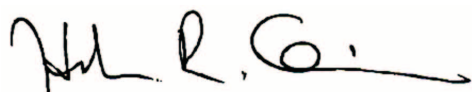
Whether the research experience steers the student away from or toward research as a career direction, it will be invaluable. The experience teaches the student things about herself, or himself, and about science, that no classroom can teach. Experience of the process by which scientific results are obtained is valuable for anyone. At some level it needs to be part of basic science education.

> **"The experience teaches the student things about herself, or himself, and about science, that no classroom can teach.**

The opportunity to experience research in the real world of advanced scientific laboratories, such as those supported by the Department of Energy, is particularly precious. The students who have had this experience, whose research abstracts and papers are published in this journal, will never again take a scientific result for granted. Some will go on to be the leaders of their fields of science in future careers. All will be well-informed citizens when considering issues of science in society and in their lives. We wish them well, and hope many more like them will apply to the program next year.

Helen Quinn, Ph.D.
Stanford Linear Accelerator Center

DISCLAIMER

The views and opinions of authors expressed in this journal do not necessarily state or reflect those of the United States Government or any agency thereof and shall not be used for advertising or product endorsement purposes. Reference herein to any specific commercial product, process, or service by its trade name, trademark, manufacturer, or otherwise, does not necessarily constitute or imply its endorsement, recommendation, or favoring by the United States Government or any agency thereof. This document was prepared as an account of work sponsored by the United States Government and, while it is believed to contain correct information, neither the United States Government nor any of its agencies or employees makes any warranty, expressed or implied, or assumes any legal liability or responsibility for the accuracy, completeness, or usefulness of any information, apparatus, product, or process disclosed, or represents that its use would not infringe privately owned rights.

ARGONNE NATIONAL LABORATORY
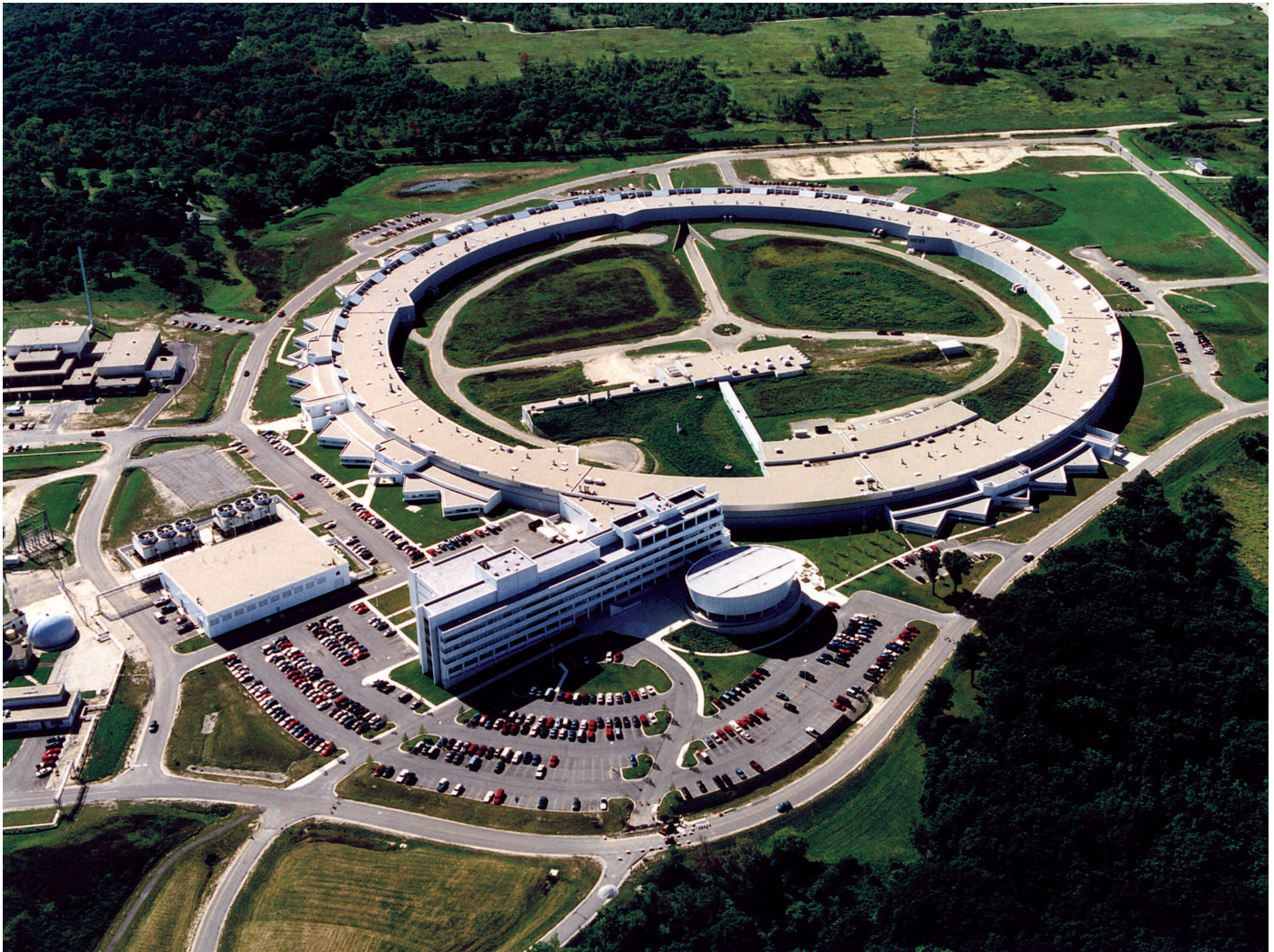
Argonne National Laboratory (ANL) is a Department of Energy, Office of Science facility on 1,700 acres located 28 miles southwest of Chicago. ANL was the country's first National Laboratory and focuses on research areas including nuclear reactor development, energy and environmental technology, biomedical and environmental research, and basic sciences research. Some of ANL's significant accomplishments include: (1) the development of many of the nuclear power reactor types in use today; (2) development and construction of large superconducting magnets; (3) pioneering work in cancer diagnosis and therapy; and (4) development of lithium-metal sulfide batteries for vehicle propulsion and peak-load leveling for utilities. ANL is home to the Advanced Photon Source, a 1,104 meter circumference synchrotron-radiation light source producing high-brilliance x-ray beams used to carry out basic and applied research in the fields of biology, physics, chemistry, environmental, geophysical, and planetary sciences along with innovative x-ray instrumentation.

ANL's other site (ANL-W) is about 35 miles west of Idaho Falls, Idaho. Research at ANL-W is typically focused on areas of national concern including those relating to energy, nuclear safety, dealing with spent nuclear fuel, nonproliferation, decommissioning and decontamination technologies, and similar work.

BROOKHAVEN NATIONAL LABORATORY

Brookhaven National Laboratory (BNL) is an Department of Energy, Office of Science site that conducts research in the physical, biomedical, and environmental sciences, as well as in energy technologies. Located on a 5,300-acre site on Long Island, New York, BNL also builds and operates major facilities available to university, industrial, and government scientists. Chief among these is the Relativistic Heavy Ion Collider (RHIC), which drives two intersecting beams of gold ions head-on in a subatomic collision to study what the universe may have looked like a few moments after its creation.

FERMI NATIONAL ACCELERATOR LABORATORY
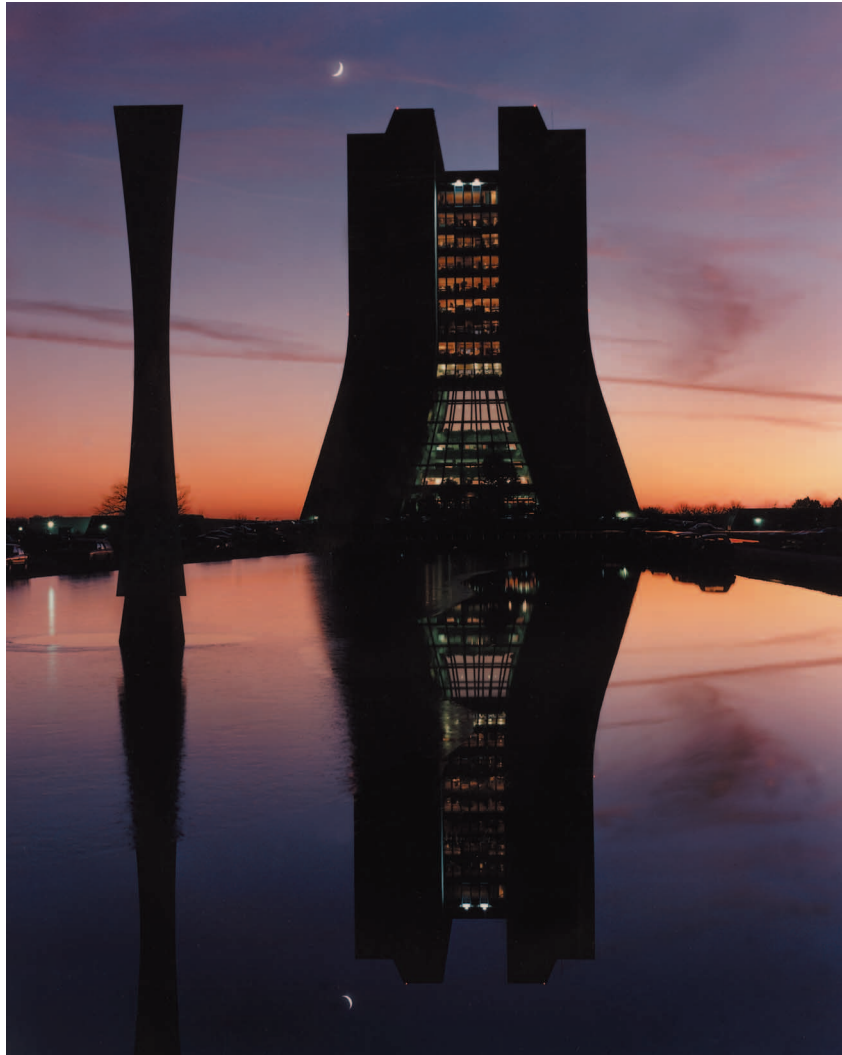
Fermi National Accelerator Laboratory (Fermilab) is one of the world's foremost laboratories dedicated to high energy physics research. The laboratory is operated for the Department of Energy, Office of Science by a consortium of 89 leading research-oriented universities primarily in the United States, with members also in Canada, Italy and Japan. Fermilab is located on a 6,800 acre site about 45 miles west of Chicago. Fermilab is home to the Tevatron, which at four miles in circumference is the world's highest energy particle accelerator. Its 1,000 superconducting magnets are cooled by liquid helium to -268ºC. Two major components of the Standard Model were discovered at Fermilab: the bottom quark and the top quark.

IDAHO NATIONAL ENGINEERING AND ENVIRONMENTAL LABORATORY

The Idaho National Engineering & Environmental Laboratory (INEEL) is a multi-purpose national laboratory delivering specialized science and engineering solutions for the DOE. The INEEL offers research opportunities in environmental stewardship, subsurface science, Generation IV Nuclear Energy Systems, advanced computing and collaboration, advanced waste management solutions, biotechnology, and engineering.

The INEEL is the lead DOE laboratory in environmental management and environmental stewardship. In partnership with Argonne National Laboratory, the INEEL is the DOE lead nuclear energy laboratory.   It is home to one of the largest concentrations of technical professionals in the northern Rocky Mountain region.

Located in southeastern Idaho, the INEEL covers 889 square miles of the Snake River Plain between Idaho Falls and Arco, Idaho. Offices and laboratories are also in the city of Idaho Falls, Idaho, (population 50,000), located about two hours from Grand Teton National and Yellowstone National Parks.

LAWRENCE BERKELEY NATIONAL LABORATORY

Lawrence Berkeley National Laboratory's research and development includes new energy technologies and environmental solutions with a focus on energy efficiency, electric reliability, carbon management and global climate change, and fusion. Frontier research experiences exist in nanoscience, genomics and cancer research, advanced computing, and observing matter and energy at the most fundamental level in the universe. Ernest Orlando Lawrence founded the Berkeley Lab in 1931. Lawrence is most commonly known for his invention of the cyclotron, which led to a Golden Age of particle physics—the foundation of modern nuclear science—and revolutionary discoveries about the nature of the universe. Berkeley Lab's Advanced Light Source is its premier national user facility centrally located on the lab site overlooking the San Francisco Bay.

NATIONAL RENEWABLE ENERGY LABORATORY

As the nation's leading center for renewable energy research, the National Renewable Energy Lab (NREL) is developing new energy technologies to benefit both the environment and the economy. NREL's mission is to develop renewable energy and energy efficiency technologies and practices, advance related science and engineering, and transfer knowledge and innovations to address the nation's energy and environmental goals. NREL's 300-acre campus is located at the foot of South Table Mountain in Golden, Colorado.

OAK RIDGE NATIONAL LABORATORY

Originally known as Clinton Laboratories, Oak Ridge National Laboratory (ORNL) was established in 1943 to carry out a single, well-defined mission: the pilot-scale production and separation of plutonium for the World War II Manhattan Project. From this foundation, the laboratory has evolved into a unique resource for addressing important national and global energy and environmental issues. Today, ORNL pioneers the development of new energy sources, technologies, and materials and the advancement of knowledge in the biological, chemical, computational, engineering, environmental, physical, and social sciences. In addition, ORNL is responsible for the civil construction, project management, design integration, and ultimately the operation of the Spallation Neutron Source (SNS). Designed and constructed by a partnership of six Department of Energy National Laboratories (Argonne, Berkeley, Brookhaven, Jefferson, Los Alamos, and Oak Ridge), the SNS is a new, accelerator-based science facility that will provide neutron beams greater than ten times more intense than any other such source in the world. SNS will provide the opportunity for up to 2,000 researchers each year from universities, National Labs, and industry for basic and applied research and technology development in the fields of materials science, magnetic materials, polymers and complex fluids, chemistry, and biology.

PACIFIC NORTHWEST NATIONAL LABORATORY

Pacific Northwest National Laboratory (PNNL) in Richland, Washington, has research facilities within the 560-square-mile government reservation known as Hanford. This Department of Energy, Office of Science laboratory delivers breakthrough science and technology to meet key national needs in security, biomolecular sciences, energy, health, and the environment. PNNL is home to the Environmental Molecular Sciences Laboratory, a national user facility where fundamental research is conducted in molecular and computational sciences to achieve a better understanding of biological and environmental effects associated with energy technologies.

PRINCETON PLASMA PHYSICS LABORATORY
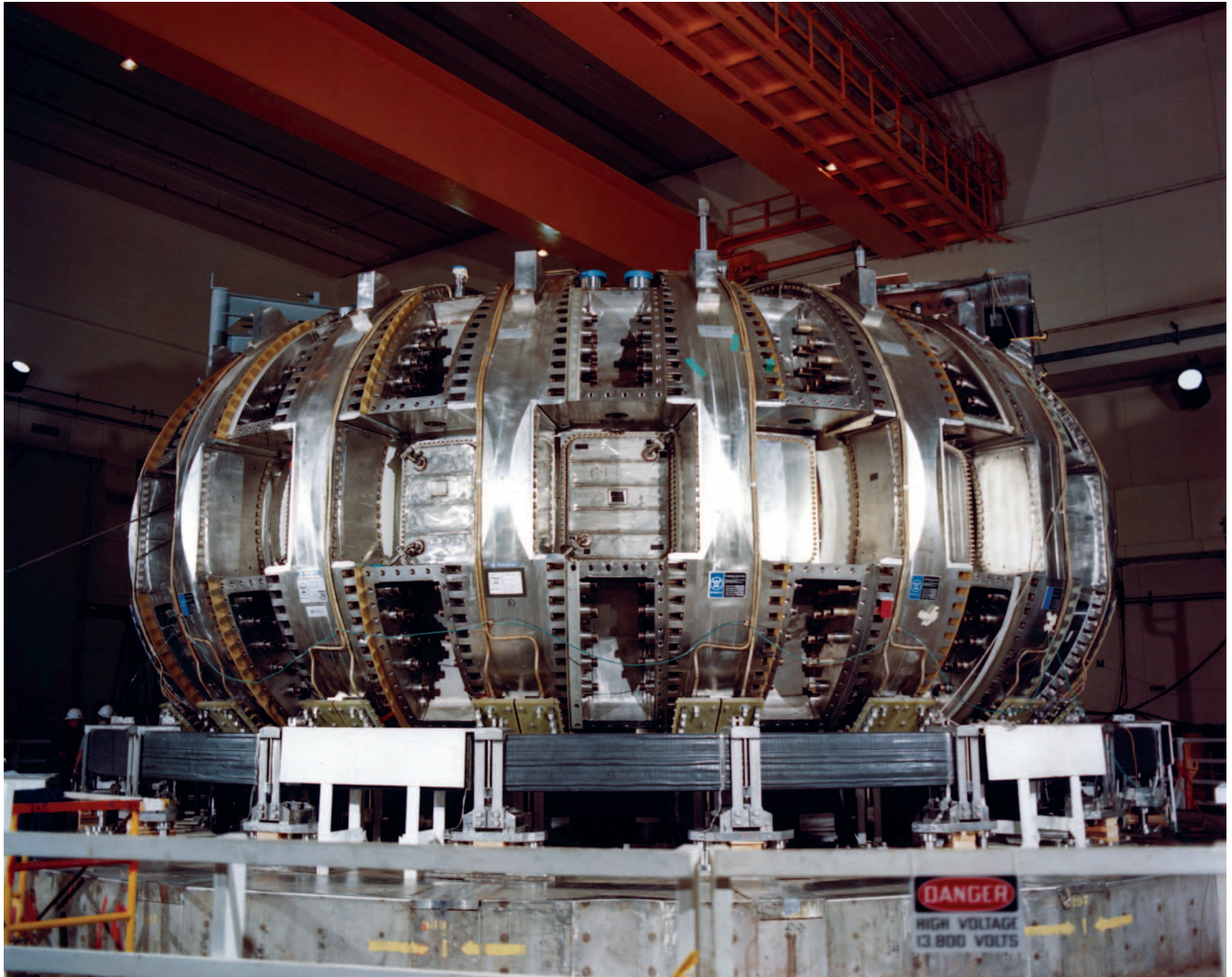
Princeton Plasma Physics Laboratory (PPPL), established in 1951, is a single-purpose research lab of the Department of Energy, Office of Science, managed by the trustees of Princeton University. Its primary mission is to conduct basic and applied research and development to improve the understanding of controlled nuclear fusion. Above is pictured the Tokamak Fusion Test Reactor (TFTR). The goal of the TFTR is to achieve fusion break-even, that is, to produce fusion power output equal to the plasma-heating input. A fusion reaction requires a density of 1/100,000 that of air at sea level and a temperature of 100 million degrees Celsius, with a confinement time of one second.

STANFORD LINEAR ACCELERATOR CENTER

The Stanford Linear Accelerator Center (SLAC) is operated by Stanford University for the Department of Energy, Office of Science. The center's main instrument for support of research is a two-mile-long linear electron accelerator that can produce intense beams of electrons and positrons with energies up to 50 billion electron volts (GeV). SLAC facilities include the accelerator for producing the high-energy particle beams, two electron-positron colliding beam storage rings, and a complement of large experimental detection devices used in particle physics experiments, including a bubble chamber and several magnetic spectrometers. SLAC is located on a 426 acre site approximately 50 miles south of San Francisco, California.

THOMAS JEFFERSON NATIONAL LABORATORY

Thomas Jefferson National Accelerator Facility (J-Lab) is a Department of Energy, Office of Science laboratory that uses advanced superconducting technology to accelerate a high energy, high current continuous electron beam. The electron beam begins orbiting in an underground racetrack containing a superconducting linear accelerator that drives electrons to higher energies. Magnets steer the beam from one section of the tunnel to another. After a few orbits, the electron beam is split for use in three simultaneous experiments. J-Lab is located in Newport News, Virginia.

DNA MICROARRAY TECHNOLOGIES: A NOVEL APPROACH TO GENOMIC RESEARCH

Rochelle Hinman[A], Brian Thrall, Ph.D.[B], and Kwong-Kwok Wong, Ph.D.[B]

ABSTRACT

A cDNA microarray allows biologists to examine the expression of thousands of genes simultaneously. Researchers may analyze the complete transcriptional program of an organism in response to specific physiological or developmental conditions. By design, a cDNA microarray is an experiment with many variables and few controls. One question that inevitably arises when working with a cDNA microarray is data reproducibility. How easy is it to confirm mRNA expression patterns? In this paper, a case study involving the treatment of a murine macrophage RAW 264.7 cell line with tumor necrosis factor alpha (TNF-α) was used to obtain a rough estimate of data reproducibility. Two trials were examined and a list of genes displaying either a > 2-fold or > 4-fold increase in gene expression was compiled. Variations in signal mean ratios between the two slides were observed. We can assume that erring in reproducibility may be compensated by greater inductive levels of similar genes. Steps taken to obtain results included serum starvation of cells before treatment, tests of mRNA for quality/consistency, and data normalization.

INTRODUCTION

"Reconstructing the genome is just the beginning. Figuring out how the 30000 genes played like piano keys give rise to the rhythms and melodies of life is going to take even more calculating power."
　　　　　　　 - George Johnson (Johnson, 2001)

The media frenzy started with a simple press conference. United States President Bill Clinton announced in June of 2000 that scientists working under Francis S. Collins and J. Craig Venter had succeeded in completing the first map of the human genome (Cawley, 2001). The news spread rapidly. The Human Genome Project soon became the front headline in every facet of the media.

Reporters were correct in labeling the map of the human genome as well as those of other organisms as a major discovery. Yet, the work of biologists is far from complete. As George Johnson of the New York Times so aptly put it, reconstruction is just the beginning. The task of figuring out how sections of the code interact with one another and outside stimuli is still at hand. It is here where cDNA microarray technology is an important tool.

A cDNA microarray allows biologists to examine the expression of thousands of genes simultaneously. Researchers may analyze the complete transcriptional program of an organism in response to specific physiological or developmental conditions (Lodish et al., 2000). The construction of a cDNA microarray experiment is a lengthy process involving multiple steps. These steps are broadly divided into three main sections: array fabrication; probe preparation and hybridization; and data collection, data mining, and analysis (Hegde et al., 2000).

During array fabrication, cDNA clones representing the genes of interest, either in the form of known or expressed sequence tags (ESTs), are amplified by PCR techniques. Clones are then mechanically spotted/adhered to a glass microscope slide or other surfaces. Probe preparation begins with mRNA extraction from selected tissues or cell lines and their corresponding controls. The mRNA is reverse transcribed and undergoes fluorescent tagging. Hybridization against the clones on the slide takes place, and the slide is then scanned with two lasers. Each laser detects a different fluorescent label: one for the tissue/cell line probe; the other for the control probe. Images are overlapped and analysis software is used to compare the resulting signals at each spot and identify which genes have undergone a change in expression. These genes may then be examined in detail.

There are many possible uses for cDNA microarray technology. It may be used to compare the genomes of different subspecies (Lashkari et al., 1997). An important application is towards an understanding of the effects of chemicals (Schena et al., 1996) and/or diseases (Nelson, 1999). The reconstruction of complex gene control networks is a future goal (Herzel et al., 2001). Yet, in all cases the use of technology can present problems.

One question that inevitably arises when working with cDNA microarrays is data reproducibility. How easy is it to confirm mRNA expression patterns? A cDNA microarray is by design an experiment with many variables. Sample to sample fluctuations in mRNA preparation as well as varying success rates with reverse transcription and labeling can occur. It is also possible for target-spot sizes to fluctuate and unspecific hybridization to take place. Many factors must be taken into consideration when analyzing data.

Yet, certain steps can be taken in order to obtain reliable re-

A: Whitworth College, Spokane, WA; B: Pacific Northwest National Laboratory, Richland, WA

sults. In this paper, a case study involving the treatment of a murine macrophage RAW 264.7 cell line with tumor necrosis factor alpha (TNF-α) will be used in order to outline several of these steps. Steps include serum starvation of cells before treatment, tests of mRNA for quality/consistency, data normalization, and trail repetition.

MATERIALS AND METHODS

ARRAY FABRICATION

The cDNA microarray slides used in this experiment were printed on site. The slides were printed using Cartesian Technologies PixSys 5000 workstation. They were printed with twenty-four ArrayIt™ ChipMaker Micro Spotting Pins on amino-silane coated slides. Clones were suspended in 50% DMSO and loaded into 384-well plates before printing. Approximately 6185 mouse cDNA clones, as well as a series of controls, were printed on each slide. Spots were then adhered to the slides by baking at 80 °C for two hours.

EXTRACTION OF mRNA

Four sets of cells from a murine macrophage RAW 264.7 cell line were prepared. Sets were 80% confluent and contained approximately five million cells. All cell sets were serum-starved overnight to minimize invariant cell-cycle differences that may hinder the impending results. Two cell sets were then treated with 25 ng/mL TNF-α. Two other cell sets were treated with an equal volume of DMSO as control. All cell sets were allowed to incubate for one hour before mRNA extraction. A Qiagen RNeasy® Midi Kit was used for mRNA extraction.

Extracted mRNA was resuspended in 200 μL RNAse free water. Optical densities on all samples were taken to determine concentration. A 1% agarose gel was run using 3 μg of each RNA sample in order to test for RNA purity. Samples were stored at -80 °C when not in use.

PROBE PREPARATION AND HYBRIDIZATION

A MICROMAX™TSA™ Labeling and Detection kit was used to prepare probes and hybridize them to the printed slides. Probes of cDNA were prepared separately from each of the four mRNA samples using 3 μg of mRNA in each case. Probes originating from mRNA of TNF-α treated cells were labeled with fluorescein. Probes originating from mRNA of control cells were labeled with biotin.

Two pools of probes were prepared, each containing a TNF-α and control set. These pools were suspended in 20 μL of hybridization buffer. Each pool was hybridized against a separate slide (#1 and #2 respectively) overnight at 65 °C. At the end of hybridization, slides were washed. In the washing process, a Cy5 dye was bound to the biotin labeled control cDNA. A Cy3 dye was bound to the fluorescein labeled TNF-α cDNA. Slides were then spun dry in preparation for scanning.

DATA COLLECTION, DATA MINING, AND ANALYSIS

Slides were scanned on ScanArray® 3000. This machine uses two lasers. One laser detects Cy3 and the other detects Cy5. Scanning was done sequentially, with Cy3 and Cy5 scans completed separately. Both slides were scanned two times with each laser.
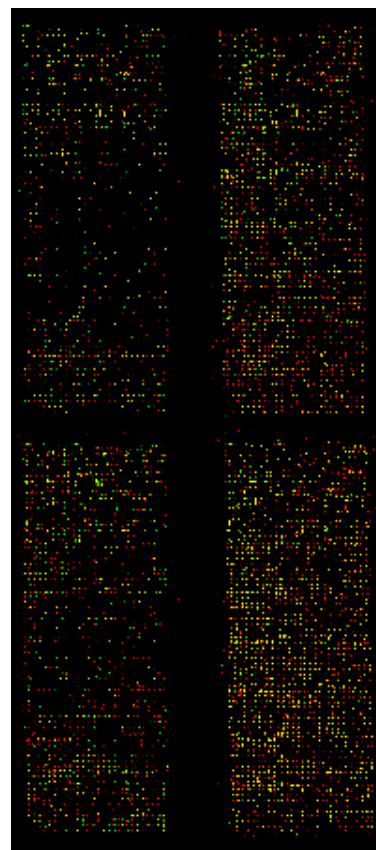
Figure 1.
Top Left Panel: Normal Scan of Slide #1
Top Right Panel: High Scan of Slide #1
Bottom Left Panel: Normal Scan of Slide #2
Bottom Right Panel: High Scan of Slide #2

One scanning was done at a high power; the other was done at a low power. The resulting images were loaded into ImaGene™ version 4.2 for analysis.

In ImaGene™ 4.2 corresponding Cy3 and Cy5 images for each scan type were overlaid. Cy3/TNF-α images were shown in red; Cy5/Control images were shown in green. For the resulting compilation, a red spot indicated a gene induced by TNF-α, a green spot indicated a gene repressed by TNF-α, and a yellow spot indicated a gene unchanged by the treatment. Some spots did not light up at all.

ImaGene™ 4.2 was used to calculate the Cy3 and Cy5 signals at each spot. Calculations were completed both with and without provided normalization methods. Provided normalization methods subtracted local background hybridization and took spot quality into account. Scatterplots and data tables were then produced. The resulting signal mean ratios (SMR) between Cy3/ TNF-α and Cy5/Control were compiled for further analysis. A signal mean ratio greater than one indicated that the gene was induced by TNF-α. A signal mean ratio less than one indicated a suppression of expression. In normalized data, all negative signal mean ratios were assigned a value of one. Thus, for purposes of this analysis, only genes induced 2-fold or greater were considered.

Table 1. Comparison of differences between Signal Mean Ratios (SMR) in Slide #1 and Slide #2.

	High Scan Non-normalized	High Scan Normalized	Normal Scan Non-normalized	Normal Scan Normalized
Difference Between SMR > 0.25	5293	4212	5669	4287
Difference Between SMR > 0.5	4169	2601	4899	2673
Difference Between SMR > 0.75	3225	1667	4210	1693
Difference Between SMR > 1.0	2498	1150	3578	1129
Difference Between SMR > 2.0	959	480	1858	452
Difference Between SMR > 3.0	402	301	1006	275

Table 2. Comparison of gene induction levels in Slide #1 and Slide #2.

	#1 High Scan Normalized	#2 High Scan Normalized
Genes Induced > 2 Fold	683	734
Genes Induced > 4 Fold	157	192

RESULTS

Compiled images of both slides (Figure 1) were visually compared. While some differences within the slides were evident, the slides displayed many of the same general trends in expression patterns. This was especially evident in those images produced via high scanning.

Comparisons of signal mean ratios between the two slides were made (Table 1). The differences between signal mean ratios in non-normalized data were higher than those in normalized data. High scanning produced signal mean ratios in closer correlation than normal scanning.

For high scanning, the number of genes induced by factors greater than two, three, four, six, eight, and ten-fold were determined (Table 2). For each slide, the number of these genes was slightly different. For example, slide #1 was shown to have 683 genes induced by a factor greater than two-fold. Slide #2 had 734 genes induced by the same factor. Although both treated slides shared just 147 common genes (20% reproducibility), differences in induction levels between the two were low (Table 3). Interestingly, when we examined the common genes that were induced by greater than four-fold, 20 genes (11% reproducibility) were markedly induced in both data sets (Table 4).

Several genes of interest were identified based on the compiled gene expression profiles. These genes included, but were not limited to, tumor necrosis factor, zinc finger protein 36, immunoresponsive gene 1, and leptin receptor.

DISCUSSION AND CONCLUSIONS

In a sense, a cDNA microarray can be thought of as a high throughput Northern Blot. Thousands of genes undergo a generalized procedure to obtain expression data (Chin, 2000). It is important to remember that conditions may not be optimal for all the genes involved. Certain genes may never register on the slide although mRNA for these genes is present in the cells.

In working with many expression profiles generated simultaneously, an exact duplication of results is extremely difficult. However, certain steps may help to ensure that results from multiple trials do have some correlation. In this study, all cells were serum-starved overnight. This process put all cells at the same stage of their life cycle before the experiment started. Differences in mRNA expression based on cell cycle stage were therefore minimized.

All mRNA extracted from the cells underwent a gel electrophoresis test for purity. The mRNA was shown to be pure and without degradation. This is important. Degraded mRNA can still undergo reverse transcription to create cDNA probes. However, these probes will anneal to the microarray slide in random fashion. They will anneal wherever their shorter cDNA sequences can be found, not necessarily on the spot corresponding to their genetic origin. Consequently, collected expression profiles will be difficult, if not impossible, to duplicate. For this reason, it is always a good idea to test mRNA quality before probe preparation, especially if some time has passed since the mRNA was extracted.

Data normalization in a cDNA microarray experiment can aid in obtaining reproducible results. Normalization processes can be used to correct for variations in background fluorescence on the slide. The degree of background on a slide can vary greatly from experiment to experiment. Normalization also compensates when one dye naturally fluoresces more than another dye. Spot size is taken into consideration as well as signals from surrounding spots. As indicated in this experiment, normalization can result in greater correlation between signal mean ratios on different slides.

In this experiment, two trials were run. Each trial used different sources of mRNA. These two trials were enough to obtain a rough estimate of data-reproducibility and identify probable genes of interest. However, further trials are necessary. Switching dyes would verify that the data obtained was not the result of dye location. Testing the two controls against one another would locate genes where differences in expression were a result of baseline mRNA variations and not TNF-α exposure. It would also be helpful to hybridize each of the TNF-α probes against the opposite control.

Once enough genes of interest have been identified, a smaller cDNA microarray may be printed for further experimentation. In a smaller microarray, additional steps may be taken in order to verify results. Clones may be spotted multiple times on the slide. These spots may be centered in one location on the slide or spread out evenly across the surface. In either case, the result is multiple signal mean ratios that can be compared and averaged for each experiment.

The technology available through a cDNA microarray has many applications. The vast majority of these applications center

Table 3. Genes induced by a factor greater than two-fold on Slide #1 and Slide #2 (High Scan Normalized Data).

Gene ID	SM R #1	SM R #2
tumor necrosis factor	25.936	24.575
"AI385562""CytochromeP450,2b9,phenobarbitolinducible,typea"""	3.9947	4.8613
"AI894223""Musmusculusp38deltaMAPkinasemRNA,completecds"""	3.4195	2.3631
acetylcholine receptor epsilon	2.0807	3.6037
serum-inducible kinase	4.2471	2.4695
protein kinase C and casein kinase substrate in neurons 1	12.359	3.79
AI323310Fos-likeantigen2	2.2174	2.3988
AI323330SRY-boxcontaininggene17	4.2432	2.094
426318ESTs	2.24	81.142
AI426345ESTs	4.4362	3.3971
AI429085ESTs	2.0703	2.6932
AI449073ESTs	8.6087	2.8756
AI528691B-cellleukemia/lymphoma3	2.1262	2.0028
AI528708MYELOIDDIFFERENTIATIONPRIMARYRESPONSEPROTEINMYD116	2.8851	3.8973
AI430953ESTs	4.6128	7.5741
AI447215EST	6.1161	4.0212
AI447814ESTs	2.8165	2.2979
AI464404ESTs	3.1168	2.2491
procollagen, type III, alpha 1	2.9925	2.1645
AI528691B-cellleukemia/lymphoma3	2.1262	2.0028
AI893411Zincfingerprotein36	10.958	14.238
AI428386ESTs	3.4921	2.1343
AI448307ESTs	3.7874	2.8138
AI452258ESTs	3.2407	9.0342
AI447233ESTs	2.7646	2.1711
"AI447335""EST,HighlysimilartosimilartoAL031532[H.sapiens]"""	2.6391	2.8585
AI451116EST	5.8156	5.3604
small inducible cytokine subfamily D, 1 Scyd1	16.972	5.4329
"AI323555""Solutecarrierfamily2(facilitatedglucosetransporter),member2"""	2.0114	2.3185
AI323680IMMEDIATEEARLYPROTEINGLY96	6.2085	4.0352
"AI414038""ESTs,WeaklysimilartoapolipoproteinA-IVprecursor[M.musculus]"""	2.8466	2.1769
AI447522ESTs	2.0874	2.1013
"AI451916""Ubiquitouslytranscribedtetratricopeptiderepeatgene,XChromosome"""	2.7528	3.8049
5'-CCACCACTTCAGTGTGGTTTGGAAAAGGGACAGATGAGCCCCTGAAGACGAGGTGAAAGTCAATTTTAC-3'	4.3773	6.58
Homo sapiens TNF-alpha stimulated ABC protein (ABC50) mRNA,	10.905	3.2333
"AI660999""ESTs,WeaklysimilartoNG28[M.musculus]"""	2.338	2.524
AI414026ESTs	5.1666	6.2979
AI414480ESTs	3.9582	2.477
AI425989ESTs	2.3381	2.6646
"AI426007""ESTs,HighlysimilartoNEURONALPROTEINNP25[Rattusnorvegicus]"""	2.05	7.5056
AI450130ESTs	4.9952	28.109
Mus musculus WNT-2 gene, partial cds; putative ankyrin-related protein	3.1488	4.2211
AI385610SemaphorinF	4.4217	2.1641
AI323667Immunoresponsivegene1	9.5027	5.6812
AI413231ESTs	2.9306	2.9918
AI413235ESTs	6.246	2.891
AI447645ESTs	2.1168	2.8712
"AI449667""ESTs,ModeratelysimilartoCTM[M.musculus]"""	26.67	2.4479
5'-TCCAGTTCCTGTCCCAGCAGACTGGATGAACCGTGTGGAGATGAACGAGACCCAGTACAGTGAAATGTTT-3'	3.9799	14.039
Mus musculus ferritin light chain 1 (Ftl1), mRNA	12.583	2.5916
Mus musculus serine protease inhibitor 6 (Spi6), mRNA	11.247	2.8004

Table 3. (Continued)

Gene ID	SM R #1	SM R #2
adrenergic receptor, beta 3	3.1604	4.5372
AI415019ESTs	3.3453	2.2811
AI430799ESTs	4.1444	3.6952
AI449378ESTs	3.053	3.8083
small inducible cytokine subfamily B, member 15	3.0449	2.7636
"AI426665""ESTs,WeaklysimilartoCALCIUM-BINDINGPROTEINP22[R.norvegicus]"""	2.6975	2.5254
AI452320ESTs	2.6611	2.5237
cytokine inducible SH2-containing protein 2 Cish	2.8703	2.7936
ESTs, Highly similar to ATRIAL NATRIURETIC PEPTIDE CLEARANCE RECEPTOR PRECURSOR [Rattus norvegicus]	3.0732	3.2623
AI666741ESTs	2.8351	6.5842
AI528709Mousegeneformuchainassociationprotein(8hs20)	7.1497	6.4497
AI430805EST	3.9898	5.8722
"AI431039""ESTs,WeaklysimilartoKIAA0584protein[H.sapiens]"""	2.6259	6.8584
AI426162ESTs	2.6697	2.0884
"AI426674""EST,WeaklysimilartosimilartoTRNA[H.sapiens]"""	3.4883	2.0884
AI428422ESTs	2.4028	2.3146
AI464549ESTs	3.1995	3.0491
"AI323701""MusmusculusSKD3mRNA,completecds"""	9.2152	4.1922
AI414514EST	16.772	2.7323
AI414525EST	9.7347	2.0268
ESTs, Highly similar to PROBABLE G PROTEIN-COUPLED RECEPTOR GPR18 [H.sapiens]	2.7856	32.813
Mm.29844 ESTs	2.7781	3.0611
AXL receptor tyrosine kinase	2.033	2.1216
AI385752Distal-lesshomeobox5	3.1178	2.3148
"AI326823""ESTs,HighlysimilartoLENSFIBERMEMBRANEINTRINSICPROTEIN[M.musculus]"""	2.4196	6.5354
"AI414810""ESTs,ModeratelysimilartoS-ACYLFATTYACIDSYNTHASETHIOESTERASE,MEDIUMCHAIN[R.norvegicus]"""	2.1662	3.55
AI414821ESTs	2.6085	2.5915
AI429810ESTs	3.347	3.3936
"AI426455""MusmusculusSin3-associatedprotein(sap30)mRNA,completecds"""	2.5355	2.0139
AI451295ESTs	2.8999	3.5372
small inducible cytokine A2	2.5952	6.392
AI449520ESTs	2.3186	2.3155
AI447908ESTs	2.5892	2.0078
gap junction membrane channel protein beta 5 Gjb5	2.2108	4.4055
nuclear receptor subfamily 0, group B, member 2	2.2327	2.2174
AI449420ESTs	2.2606	2.1599
AI447436ESTs	3.2093	2.9957
homeodomain interacting protein kinase 2	2.8656	2.2825
AI528743Myxovirus(influenzavirus)resistance2	3.7441	3.3611
AI326155MusmusculusmRNAforvery-long-chainacyl-CoAsynthetase(VLACS)	3.4356	2.0425
AI428447EST	2.3858	2.1103
interleukin 15 receptor, alpha chain	4.8704	2.0444
cytochrome P450, 4a10	23.493	2.3457
AI451958ESTs	2.2101	3.4445
"AI448672""MusmusculuscloneL5uniformgroupof2-cell-stagegenefamilymRNA,completecds"""	3.5762	2.5035
AI447753EST	2.6478	2.9979
AI447183ESTs	3.0624	2.8211
AI447862ESTs	2.7553	3.0587
AI449628EST	2.925	2.1751
AI450841ESTs	2.4811	2.9297
AI451315EST	2.2694	2.2659
AI465471ESTs	4.035	4.7052
small inducible cytokine B subfamily (Cys-X-Cys), member 10	2.691	2.8823
procollagen, type VII, alpha 1	5.735	2.2219
endothelial-specific receptor tyrosine kinase	2.6609	2.3717
AI323614Myelocytomatosisoncogene	2.6817	2.2608
AI528697Zincfingerprotein62	2.2608	3.5774
AI426040ESTs	4.2577	8.0409

Table 3. (Continued)

Gene ID	SM R #1	SM R #2
AI430784ESTs	2.2549	7.1683
AI447507EST	3.2541	3.2948
AI449234CD48antigen	2.2482	2.1122
Mus musculus SWI/SNF related, matrix associated, actin dependent	2.4076	2.3079
growth accentuating protein 43	2.0039	4.1651
trefoil factor 1	2.2367	2.123
T-cell receptor gamma, variable 4	2.9209	2.4972
CD3 antigen, zeta polypeptide	2.2674	2.3616
"AI528680""MusmusculustranscriptionfactorGIFmRNA,completecds"""	4.3126	2.0259
lung carcinoma myc related oncogene 1	2.1714	4.6654
"AI323965""ATPase,Na+/K+transporting,beta1polypeptide"""	2.1048	2.3011
AI448121ESTs	4.018	3.7943
AI428470ESTs	2.7799	2.0604
AI449547ESTs	5.394	3.2503
AI447293EST	2.3183	2.0301
AI447603ESTs	6.2375	2.5641
AI448810ESTs	3.2941	2.8877
AI662536ESTs	2.3631	2.2141
"AI464440""ESTs,WeaklysimilartoHYPOTHETICAL139.1KDPROTEINC08B11.3INCHROMOSOMEII[Caenorhabditiselegans]"""	2.2688	2.0232
AI464450ESTs	3.5499	2.4294
Cytochrome P450, 2a4	2.8682	2.9134
phospholipase A2, group IB, pancreas, receptor	5.9435	2.0658
"AI661491""Guaninenucleotidebindingprotein,alphao"""	2.5411	2.0717
"AI323836""Colonystimulatingfactor,macrophage"""	2.2982	2.4251
AI449557EST	2.2322	4.8917
AI449453EST	2.0107	2.0181
AI449461ESTs	3.825	6.1049
AI447443ESTs	2.3871	2.047
AI464308ESTs	5.5826	2.2535
AI465162ESTs	6.699	2.6199
toll-like receptor 2	3.7917	3.2385
cAMP response element binding protein-related protein	3.0204	6.0496
uracil-DNA glycosylase	2.3573	2.4672
AI327008M.musculusmRNAforcytochromeP450IIIA25	17.853	3.1653
AI415104ESTs	3.3717	2.7119
AI447289ESTs	3.7061	2.1763
AI447940ESTs	2.5051	2.1495
Mus musculus cytochrome P450 CYP2D22 mRNA, complete cds	27.356	2.2019

Table 4. Genes Induced by a Factor Greater than 4-fold on Slide #1 and Slide #2 (High Scan Normalized Data)

Gene ID	SM R #1	SM R #2
"AI385598""MurineGlvr-1mRNA,completecds"""	5.16	4.78
AI414709ESTs	5.17	4.05
tumor necrosis factor	25.94	24.58
AI661215ESTs	6.67	7.14
AI325160MARCKS-RELATEDPROTEIN	5.26	4.16
AI430953ESTs	4.61	7.57
AI447215EST	6.12	4.02
AI893411Zincfingerprotein36	10.95	14.24
AI451116EST	5.82	5.36
small inducible cytokine subfamily D, 1 Scyd1	16.97	5.43
AI323680IMMEDIATEEARLYPROTEINGLY96	6.21	4.04
5'-CCACCACTTCAGTGTGGTTTGGAAAAGGGACAGATGAGCCCCTGAAGACGAGGTGAAAAGTCAATTTTAC-3'	4.38	6.58
AI414026ESTs	5.17	6.3
AI450130ESTs	5	28.11
AI323667Immunoresponsivegene1	9.5	4.68
AI528709Mousegeneformuchainassociationprotein(8hs20)	7.15	6.45
"AI385688""MousemRNAforZfp-57,completecds"""	5.19	13.71
"AI323701""MusmusculusSKD3mRNA,completecds"""	9.22	4.19
AI323343Leptinreceptor	6.82	10.09
AI465471ESTs	4.03	4.71

on deciphering the genetic code of life. Although many factors must be considered, the technology still generates a list of genes of interest faster than would be possible if working with traditional methods on a gene-by-gene basis. Based on the differences in generation of signal mean ratios between the two similarly treated slides, we can assume that greater inductive levels of similar genes may alleviate variations in reproducibility.

REFERENCES

Cawley, Janet (2001, January). Biography of the year. Biography. 50-59.

Chin, B.Y. "Bioformatics." John Hopkins University, Baltimore. 12 Febuary 2000.

Hegde, P., Qi, R., Abernathy, K., Gay, C., Dharap, S., Gaspard, R., Hughs, J.E., Snesrud, E., Lee, N., & Quackenbush, J. (2000, September). A concise guide to cDNA Microarray Analysis. BioTechniques, 29, 548-562.

Herzel, H., Beule, D., Kielbasa, S., Korbel, J., Sers, C., Malik, A., Eickhoff, H., Lehrach, H., & Schuchhardt, J. (2001, March). Extracting information from cDNA arrays. CHAOS, 11 (1), 98-106.

Johnson, George (2001, March 25). All science is computer science. The New York Times, pp. 4.1.

Lashkari, D.A., DeRisi, J.L., McCusker, J.H., Namath, A.F., Gentile, C., Hwang, S.Y., Brown, P.O., & Davis, R.W. (1996, October). Yeast microarrays for genome wide parallel genetic and gene expression analysis. Proc. Natl. Acad. Sci. USA, 94, 13057-13062.

Lodish, H., Berk, A., Zipursky, S.L., Matsudaira, P., Baltimore, D., & Darrell, J. (2000). Molecular Cell Biology (4th ed.) New York: W.H. Freeman and Company.

Nelson, N.J. (1999, December). Genetic profiling for cancer surfaces slowly in the clinic. J. Natl. Cancer Inst., 91, 1990-1992.

Schena, M., Shalon, D., Heller, R., Chai, A., Brown, P.O., & Davis, R.W. (1996, October). Parallel human genome analysis: Microarray-based expression monitoring of 1000 genes. Proc. Natl. Acad. Sci. USA, 93, 10614-10619.

DNA DILEMMA: A PERSPECTIVE ON CURRENT U.S. PATENT AND TRADEMARK OFFICE PHILOSOPHY CONCERNING LIFE PATENTS

KALE FRANZ[A] AND PETER FALETRA, PH.D.[B]

ABSTRACT

The lack of a solid set of criteria for determining patentability of subject matter—particularly subject matter dealing with life—has recently been of increasing public concern in the United States. Alarm for patent practices related to life systems ranges from patents being granted on biochemical processes and the knowledge of these processes to the patenting of entire organisms. One of the most volatile concerns is the patenting of human genes or parts of genes since this genetic material is the basic informational molecule for all life. Current patent law, legislated in 1952, has been interpreted by the U.S. Supreme Court to allow broad patents of DNA, biochemical processes, and what are generally considered "inventions" of life systems. Several issues are addressed in this paper regarding the unsound reasoning underlying both the interpretation and execution of patent law. Lapses in logic provide a gateway for businesses and individuals to take patenting to an illogical and unworkable extreme. Patent Office disorder of this magnitude is unnecessary and has great potential for harming the mission that the patent office was designed to serve. Recently disclosed patent-granting guidelines suggest the United States Patent and Trademark Office is not upholding its Constitutional responsibility of promoting the progress of science.

"Living organisms are able to reproduce themselves even if they are patented, and in view of this special quality of living organisms, the scope of a patent is difficult to define, which makes it nearly impossible to find a balance between private and public interests."[1]

INTRODUCTION

Patents on life, ranging from DNA fragments to entire organisms, have reached mainstream concern in the past few decades. It is now obvious that several fundamental problems exist with United States patent law and the system that has been established to execute that law. Through the United States Patent and Trademark Office's interpretation of Supreme Court decisions[2], patents on DNA have been deemed grantable. As this paper illustrates, it is now theoretically possible to acquire a patent on any life-related subject matter, whether the subject matter is in essence a duplication of nature or otherwise. Through the current practice of granting life patents, fundamental problems arise because of the distinct differences that exist between life and inanimate objects. At this time, the patent system needs to undergo a significant reevaluation to ensure that it is promoting the best interest of science in a sound and logical manner.

The magnitude of the current challenges facing the patent office is easily seen in the number of pending genetically related patents. Through the end of December 2000, approximately 25,000 DNA-based patents were granted.[2] Several forms of life-related subject matter have been successfully patented: Expressed Sequence Tags (EST), which serve as gene markers along a DNA strand; Single Nucleotide Polymorphisms (SNP), which are single-base variations within DNA that could potentially cause disease; and regulatory sequences—all only gene fragments—have been patented. Entire genes, such as a gene called CCR5 that helps in the process of allowing HIV entrance into immune cells, have also been patented. An entire chromosome of a vertebrate is yet to be patented.[4]

LEGAL JUSTIFICATION FOR DNA PATENTING

To obtain a patent on DNA of any type or scope, the DNA fragment must be isolated and purified from its (thus far) observed natural state, or the fragment must be produced in purified form in a laboratory. More specifically, the following eligibility conditions as stated in the United States Patent and Trademark Office (USPTO) Utility Examination Guidelines, must be met:

> (1) an excised gene is eligible for a patent as a composition of matter or as an article of manufacture because that DNA molecule does not occur in that isolated form in nature, or (2) synthetic DNA preparations are eligible for patents because their purified state is different from the naturally occurring compound.[5]

A: Colorado School of Mines, Golden, CO; B: U.S. Department of Energy, Headquarters, Washington, D.C.

Thus, it is not acceptable to patent the exact genes as they exist in an individual.[6] However, several other logical conflicts and practical dilemmas arise from this patent philosophy.

As Condition (1) infers, one method by which DNA patents can be acquired is through patenting DNA that has been extracted from its natural environment. Since DNA is patentable, and by its very nature is part of all living organisms, any organism should be patentable by a similar mechanism to that established for the patenting of DNA. This brings about startling possibilities, the consequences of which the USPTO may have never anticipated or desired.

Entire organisms like plants, bacteria, even mice, have indeed been patented. All such patents, however, have been of an entirely different nature than DNA patents. These organisms have been fundamentally changed in some way by human ingenuity to improve upon their previous functions, abilities, and characteristics. Bacteria were genetically altered for oil-spill bioremediation purposes[7]; numerous plants have been transgenically altered for production purposes and other specific qualities[8]; mice are commonly genetically engineered as in the case of the "knockout" mice[9]: patents have been granted in all of these situations. The purification and isolation of DNA does not resemble such accomplishments. Patented DNA has simply been stripped of some of the critical parts it needs to function in a natural setting, but the base code still remains intact and unchanged by human influence.

CONDITION (1): PATENTING A TREE

Let us now consider patenting a tree by the same process that one would undertake to patent a DNA fragment under the first USPTO-defined condition. Though patenting a tree at first seems completely absurd, it is quite conceivable given current patent law and USPTO guidelines. While attempting to satisfy the requirements for patent approval legislated by Congress and interpreted by the USPTO in its execution of that legislation, the *Metasequoia glyptostroboides*—long thought extinct—will serve as our hypothetical example, though someone has yet to apply for a patent on this tree or any tree by such means. Several criteria need to be met in order to obtain a patent on *Metasequoia*. Formally, these criteria consist of non-obviousness, novelty, utility, and enablement. The first criterion however, and perhaps most logically troublesome, is that the tree must be an invention of human design. At first thought most individuals would believe it impossible for humans to invent the *Metasequoia*; it has already been created by nature. But the USPTO has a different view and exercises its duties accordingly. Patent law states that:

> Whoever invents or discovers any new and useful process, machine, manufacture, or composition of matter, or any new and useful improvement thereof, may obtain a patent therefor, subject to the conditions and requirements of this title.[10]

Just as DNA must be removed (purified and isolated) from the environment in which it has been observed, so too must the tree. To "invent" the *Metasequoia* we simply need to take it from central China and plant it in our own backyard. As an extra measure, we will thoroughly clean the tree so that none of the native dirt is attached to its roots, no naturally growing fungi or bacteria indigenous to the region are residing on the tree, and all other foreign material such as birds and their nests are free from the tree's limbs. *Metasequoia* has now been isolated and purified and thus is our own "invention."

The tree must be non-obvious, which is defined by the USPTO to mean that the claimed subject matter must not be obvious to a person of ordinary skill in light of what was previously known.[11] Since *Metasequoia* was thought to be extinct, its existence on Earth today was not common knowledge to those of ordinary skill in the field of botany. Given this, *Metasequoia* would also conform to the novelty requirement as well, which states that a patent cannot be granted for an entity that has already been invented by someone else.[12] While no human invented the tree as it existed in nature, and because we invented the tree as it exists outside of nature, the novelty requirement is satisfied.

Metasequoia must have utility.[13] In other words, it must be useful in at least one way. "The patentee is required to disclose only one utility, that is, teach others how to use the invention in at least one way."[14] *Metasequoia*, as in the nature of all trees, is useful in any of a number of applications. Thus, our tree fits perfectly with the utility requirement. To meet the final requirement, our *Metasequoia* patent must show enablement.

> The specification shall contain a written description of the invention, and of the manner and process of making and using it…to enable any person skilled in the art to which it pertains…to make and use the same.[15]

To satisfy this requirement, we must simply describe in what fashion the tree was transplanted from its native land to our backyard as well as how to use it to benefit from the previously described utility.

CONDITION (2): PATENTING A PROTON

As formerly alluded to, the second condition—Condition (2)—that makes DNA eligible for patenting is satisfied after the DNA has been "synthesized in a laboratory from chemical starting materials."[16] Hence, biologists must simply prove that they can recreate in a laboratory setting that which has already been created by nature. If patenting practices of this form are adopted by other science disciplines, perplexing and possibly undesirable consequences could result. For example, ever since Einstein proposed his famous equation $E = mc^2$, a result of the Special Theory of Relativity, it has been understood that all matter is simply a form of energy.[17] Today, scientists have the ability to manipulate energy in the vast number of particle accelerators that exist all over the world to create the various elementary particles of nature[18]—particles as common as the proton and as exotic as the Z boson. If DNA can be patented simply by synthetically creating it from more basic materials and meeting the four other conditions and requirements outlined by patent law, a proton or Z boson should theoretically be patentable because it can likewise be created. The ramifications of such patents being granted are incomprehensible.

THE DENIAL OF EXAMPLE PATENT APPLICATION IDEAS

Would the patent office ever grant a patent on *Metasequoia* or a proton in the manner that has been suggested, even though the application would comply with all of the outlined requirements in the same way DNA patent applications do? Since the patent office has yet to encounter a patent on a tree or a proton, one can only speculate upon the outcome. It inherently seems absurd to any rational person for a patent to be granted on a tree. In all probability, the patent office would reject a patent application on a tree not because of the apparent absurdity, but because of the size scale on which the patent is being proposed. The USPTO would likely not see the isolation and purification process used with *Metasequoia* as comparable to the isolation and purification that is undergone with DNA. The isolation and purification of the tree as described above is a fully tangible and visually understandable process, unlike the isolation and purification of DNA, which by its technical nature is more abstract. This dichotomy would almost certainly be enough to sway the patent office's view on the purification of the tree and thus reject the patent for not meeting the standard criteria. With the application of simple logic one can see that purification processes differing in physical size and technological scale can otherwise be quite similar. Given this, the USPTO seems to unwittingly hold a standard for patentability based on size and technological level.

Such a patent system based ultimately on size is inherently ambiguous. Size, like most any continuous system, presents natural difficulties when trying to establish arbitrary boundaries within the system. At what size does an object move from the non-patentable realm into the patentable? If DNA is patentable, then is an entire cell patentable? If an entire cell is patentable, then certainly a free-living, single-celled organism would be patentable material. If a single celled organism is patentable, then why not a multi-celled organism? Though, as mentioned earlier, patents have been granted on multi-celled organisms, all patented organisms have, to this day, been in some way genetically altered by humans and not simply the product of nature.

Similarly, it would probably be considered equally absurd to grant a patent on the proton. Protons are basic building blocks of all matter. But it follows that DNA is a basic structure of all life. For DNA to be patentable, all entities on Earth, whether devised by the creativity of humans or otherwise, must be in essence patentable. This certainly defies Congress's original intention when writing current patent law in 1952 that "anything under the sun that is *made by man*"[19] (emphasis added) be patentable subject matter.

PLAGIARIZING NATURE'S WORK

Another fundamental problem exists with the patenting of DNA. Historically, patents have been granted for inventions of an original mechanical nature or process. Plows, automobiles, and oil refinement processes have all been patented. More recently, computer chip designs and biological processes such as the polymerase chain reaction have been patented. Those pat-

ents are intrinsically different from patents on DNA fragments since they are processes or creations of humanity and not extant physical entities in nature.

Traditional patents encourage further innovation and ingenuity because it is physically possible to *invent around* the patented subject matter with a new and novel idea. However, DNA was not a human innovation, but a manifestation of nature that has undergone millions of years of evolution. By purifying and isolating DNA to patent it, humans are simply plagiarizing nature's work. Because of the innate characteristics of DNA, it is inherently impossible to re-invent it or even invent around it. Thus a patent on DNA has power above and beyond that of a typical patent.

In this regard the USPTO seems confused. The USPTO likens DNA patenting to patents on television sets and the picture tubes therein, as explained by the USPTO Director of Biotechnology Examination.

> "The USPTO views this situation as analogous to having a patent on a picture tube. The picture tube patent does not preclude someone else from obtaining a patent on a television set. However, the holder of the picture tube patent could sue the television set makers for patent infringement if they use the patented picture tube without obtaining a license."[20]

A dissection of this analogy is revealing. A Single Nucleotide Polymorphism (SNP) would be analogous to the picture tube, and a cure for a disease is analogous to the television set. Consequently an SNP patent does not preclude someone else from obtaining a patent on a cure for a disease, which is attributable to that SNP. However, the holder of the SNP patent could sue the "disease-cure" manufacturer for patent infringement if that manufacturer uses the patented SNP without obtaining a license.

The USPTO analogy is confusing, though a simple conclusion results. It is entirely possible for the television set maker to choose any of a number of picture tubes that have already been patented to use in a television set. More importantly, the television set maker can opt to design its own picture tube because it is physically possible to invent around patented picture tube innovations. Conversely, a competitor of the "inventor" of the SNP cannot pick and choose among other SNPs for a cure for the same disease since the originally patented SNP was the natural cause for that disease. Furthermore, DNA is wholly unique to this planet not because of human invention and action, but because of the forces that allowed it to evolve. Inventing around DNA therefore is entirely impossible without redesigning billions of years of evolution and "remaking" life systems altogether.

THE ROLE OF THE UNITED STATES PATENT AND TRADEMARK OFFICE

In addition to current patent guidelines seeming illogical, strong potential exists for the hindrance of the advancement of science and engineering innovation. The United States Constitution provides:

The Congress shall have Power…To promote the Progress of Science and useful Arts, by securing for limited Times to Authors, and Inventors the exclusive Right to their respective Writings and Discoveries.[21]

The USPTO was established to execute this Constitutional mandate. Keen observers may deduce that it is the current position of the USPTO to interpret this statement with emphasis on "securing for limited Times…exclusive Right to…Discoveries." However, the purpose of the patent office is not to simply impart patents without regard for the objectives it was created to serve. The USPTO should take special care to fulfill its first and foremost duty, which is "To promote the Progress of Science and useful Arts." Strong economic and scientific advancement arguments exist on both sides of the DNA patenting issue; individuals in the scientific, academic, research, economic, and law communities are heavily divided. Through all of the controversy, it appears that the patent office is not seeking the avenue that will truly yield the most success for accomplishing its purpose, but is simply upholding previously established patent precedent. The USPTO should be more forthright about fighting to uphold its constitutional obligation of promoting the state of science. Even though "it is a long tradition in the United States that discoveries from nature which are transformed into new and useful products are eligible for patents,"[22] precedent should not supersede purpose.

That the patent woes of other nations might be just as daunting as those of the United States was recently illustrated by John Keogh who successfully applied for and received a patent in Australia for…the wheel. He does not expect to make money from the patent but did receive worldwide attention and the 2001 Ig Nobel Award in Technology.[23]

ACKNOWLEDGEMENTS

REFERENCES

1. Committee on Agriculture and Rural Development, Parliamentary Assembly - Council of Europe, Biotechnology and Intellectual Property Doc. 8459, July 1999.

2. *Diamond v. Chakrabarty*, 447 U.S. 303 (1980)

3. Cook-Deegan, R. M., & McCormack, S. J. "Patents, Secrecy, and DNA." Science, 293, (2001, July 13) 217.

4. Root, M. J., & Kay, M. S., & Kim, P. S. "Protein Design of an HIV-1 Entry Inhibitor." Science, 291, (2001, February 1) 884-888.

5. Utility Examination Guidelines, 66 Fed. Reg. 1,093 (2001)

6. Utility Examination Guidelines, 66 Fed. Reg. 1,093-1,094 (2001)

7. *Diamond v. Chakrabarty*, 447 U.S. 303 (1980)

8. "Sixty-Five Years of the U.S. Plant Patent Act." ETC Group. http://www.etcgroup.org/article.asp?newsid=204

9. National Research Council. "Sharing Laboratory Resouirces: Genetically Altered Mice." National Academy of Sciences, (1993, March 23-34) 19. http://www.nap.edu/html/mice/

10. 35 U.S.C. § 101

11. 35 U.S.C. § 103

12. 35 U.S.C. § 102

13. 35 U.S.C. § 101

14. Utility Examination Guidelines, 66 Fed. Reg. 1,094 (2001)

15. 35 U.S.C. § 112

16. Thorton, S.T., Rex, A., *Modern Physics for Scientists and Engineers.* Forth Worth: Saunders College Publishing (2000) 63.

17. "The Science of Matter, Space, and Time: How to Find the Smallest Particles." Fermi National Accelerator Laboratory, (2001, Oct. 24) http://www.fnal.gov/pub/inquiring/matter/smallest/

18. Utility Examination Guidelines, 66 Fed. Reg. 1,093 (2001)

19. S. Rep. No. 1979, 82d Cong., 2d Sess., 5 (1952); H.R. Rep. No. 1923, 82d Cong., 2d Sess., 6 (1952)

20. Doll, J. J. "The patenting of DNA." Science, 280, (1998, May 1) 689-690.

21. United States Constitution, Article 1, Section 8, Clause 8

22. Utility Examination Guidelines, 66 Fed. Reg. 1,093 (2001)

23. "Scientific Prizes." Science, 294 (2001, Oct. 12) 285.

EVALUATION OF THE *IN VIVO* AND *EX VIVO* BINDING OF NOVEL CB1 CANNABINOID RECEPTOR RADIOTRACERS

ASHLEY MILLER[A], JOHN GATLEY, PH.D.[B], AND ANDREW GIFFORD, PH.D.[B]

ABSTRACT

The primary active ingredient of marijuana, Δ9-tetrahydrocannabinol, exerts its psychoactive effects by binding to cannabinoid CB1 receptors. These receptors are found throughout the brain with high concentrations in the hippocampus and cerebellum. The current study was conducted to evaluate the binding of a newly developed putative cannabinoid antagonist, AM630, and a classical cannabinoid Δ8-tetrahydrocannabinol as potential PET and/or SPECT imaging agents for brain CB1 receptors. For both of these ligands *in vivo* and *ex vivo* studies in mice were conducted. AM630 showed good overall brain uptake (as measure by %IA/g) and a moderately rapid clearance from the brain with a half-clearance time of approximately 30 minutes. However, AM630 did not show selective binding to CB1 cannabinoid receptors. *Ex vivo* autoradiography supported the lack of selective binding seen in the *in vivo* study. Similar to AM630, Δ8-tetrahydrocanibol also failed to show selective binding to CB1 receptor rich brain areas. The Δ8-tetrahydrocanibol showed moderate overall brain uptake and relatively slow brain clearance as compared to AM630.

Further studies were done with AM2233, a cannabinoid ligand with a similar structure as AM630. These studies were done to develop an *ex vivo* binding assay to quantify the displacement of [131I]AM2233 binding by other ligands in Swiss-Webster and CB1 receptor knockout mice. By developing this assay we hoped to determine the identity of an unknown binding site for AM2233 present in the hippocampus of CB1 knockout mice. Using an approach based on incubation of brain slices prepared from mice given intravenous [131I]AM2233 in either the presence or absence of AM2233 (unlabelled) it was possible to demonstrate a significant AM2233-displacable binding in the Swiss-Webster mice. Future studies will determine if this assay is appropriate for identifying the unknown binding site for AM2233 in the CB1 knockout mice.

INTRODUCTION

The hemp plant, *Canabis sativa*, has been used for medicinal and recreational purposes for many centuries. Its popularity is derived primarily from its ability to alter mood and behavior. Known also as marijuana, the extracts of the hemp plant have a wide variety of therapeutic effects including the ability to act as an antiemetic, anti-inflammatory, antiglaucoma, analgesic, and appetite-enhancing agent (Felder, 1998). These physiological effects are mediated by the active compound in marijuana, Δ9-tetrahydrocannabinol (Δ9-THC), for which specific receptors were identified in the brain (Devane, 1988). High levels of these receptors were reported in substantia nigra, globus pallidus, hippocampus, and cerebellum. Other regions, including the brain stem and the thalamus, contain low or negligible concentrations of this receptor. These concentrations have been proven through *in vitro* autoradiographic studies with radiolabeled high-affinity ligands (Herkenham, 1990). Based on the areas of high concentration of CB1 receptors in the brain and the well-known behavioral effects of cannabinoid agonists (Mechoulam, 1986), it is likely that this receptor regulates short-term memory, coordination of movement and emotions.

The relatively high densities of the CB1 receptors in the brain have turned interests towards developing radiotracers capable of imaging CB1 receptors *in vivo* using PET or SPECT imaging. The imaging of these receptors *in vivo* would be of potential value in addressing several research questions. Such questions include determining the degree of occupancy of cannabinoid receptors necessary to produce therapeutic actions of cannabinoids, determining if new therapeutic agents posses significant binding to cannabinoid receptors *in vivo*, determining if cannabinoid receptors are up or down regulated as a result of chronic drug use or psychiatric conditions, and monitoring the loss of neuronal cell types possessing cannabinoid receptors.

The primary classes of chemical compounds that have been found to be active at CB1 cannabinoid receptors are the classical and non-classical cannabinoids, anandamides, aminoalkylindoles, and pyrazoles (Gifford, manuscript in preparation). To date, pyrazoles have been mostly targeted as lead compounds for the development of CB1 cannabinoid PET and SPECT radiotracers. These compounds are antagonists and/or inverse agonists at the CB1 receptor and are typified by SR141516A (Gifford, manuscript in preparation). Pyrazole derivatives developed so far for *in vivo*

A: University of Connecticut, Storrs, CT; B: Brookhaven National Laboratory, Upton, NY
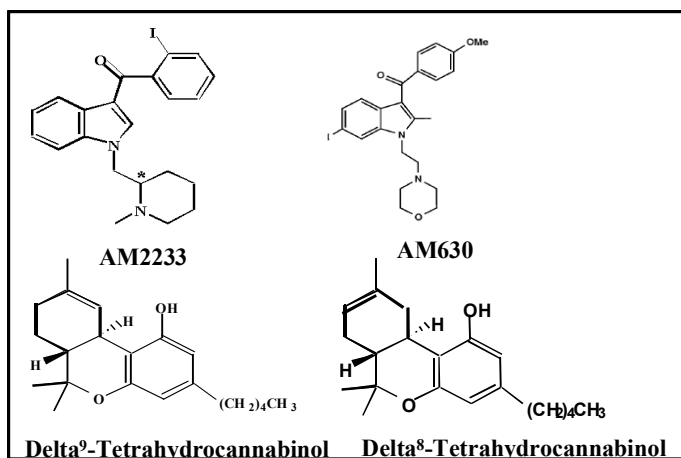
Figure 1: Structures of cannabinoid ligands evaluated in this study.

imaging have included [123I]AM281 for SPECT (Gatley, 1998) and [18F]SR144385 and [18F]SR147963 for PET (Mathews, 2000). These radiotracers have shown reasonable specificity in binding to CB1 receptors *in vivo*, but they have mediocre brain uptake which suggests they have limited potential as SPECT or PET radiotracers.

In addition to the pyrazole derivatives, the aminoalkylindoles have also shown promise for developing *in vivo* imaging agents for CB1 receptors. Similar to the pyrazole derivatives, the aminoalkylindoles have a relatively low lipophilicity compared to that of the classical and non-classical cannabinoids. However, where the pyrazole derivatives are antagonists/inverse agonists, the aminoalkylindoles are generally agonists (Compton, 1992). Because of this, the information obtained from these radiotracers will be different since agonist radiotracers will mostly bind to receptors in the high agonist affinity state where as the antagonists will bind to both high and low agonist affinity states. Inverse agonists bind preferentially to the low agonist affinity states.

One of the most potent aminoalkylindoles, developed to date, at the CB1 receptor is WIN 5512-2 (D'Ambra, 1992). This compound is useful in pharmacological and behavioral studies, but it lacks an iodine or fluorine group to make it useful for *in vivo* imaging of the CB1 receptor. The present study was conducted to evaluate a newly developed putative cannabinoid antagonist, AM630, based on an aminoalkylindole structure with an iodine group, and a classical cannabinoid, Δ8-THC, as imaging agents. Also, further study was done on AM2233, an aminoalkylindole with a higher affinity than WIN 5512-2, and an iodine group, making it potentially useful as an *in vivo* radiotracer.

MATERIALS AND METHODS

Male mice (Swiss-Webster strain) were purchased from Taconic Farms. CB1 receptor knockout mice were bred at Brookhaven National Laboratory. Federal guidelines for the care and use of animals were strictly followed. Studies were approved by the institutional review committee.

Δ8-THC was obtained from NIDA. AM630 and AM2233 were generously provided by Alexandros Makriyannis of the University of Connecticut.

[131I]AM630 and [131I]AM2233 were prepared by radioiododestannylation of their respective tributyltin precursors and purified by HPLC. AM2233 and its precursors were prepared as described by Deng (manuscript in preparation).

AM630 AND Δ8-THC *IN VITRO* BRAIN UPTAKE

Mice were injected via a tail vein with [131I]AM630 and [3H]Δ8-THC dissolved in .2 mL 40% 2-hydroxypropyl-β-cyclodextrin and 3-5% bovine serum albumin. Animals were killed by decapitation at 5, 15, 30 minutes, 1 and 2 hours, and the cerebellum, brain stem, and hippocampi were dissected out. These were weighed, solubulizer was added, after dissolving, scintillate was added and levels of [131I] were determined with a γ-counter. After the appropriate number of half-lives, the vials were again counted via liquid scintillation counting for [3H] levels.

EX VIVO AUTORADIOGRAPHY

Mice were injected via a tail vein with either [131I]AM630 or [131I]AM2233 dissolved in .2 mL 40% 2-hydroxypropyl-β-cyclodextrin. Animals were killed by decapitation after 40 minutes. The hippocampal region of the brain was dissected out, immersed in ice-cold saline, glued to a plastic block, and slices were cut 300 µm thick using a vibratome from the fresh brain tissue. After the sections were cut, they were placed on glass coverslips and allowed to air-dry on a slide warmer. Following drying, the sections were exposed to a phosphoimager plate (Molecular Dynamics) and the plates scanned after an exposure time of 12–20 hours.

AM223 *EX VIVO* ASSAY

Mice were injected via a tail vein with [131I]AM2233 dissolved in .2 mL 40% 2-hydroxypropyl-β-cyclodextrin. Animals were killed by decapitation after 30 minutes. The hippocampus was dissected out and was sliced in 300 µm slices using a tissue chopper. Then one hippocampi was add to a vial containing cold AM2233 and 5 mL of 50 mM Tris-HCL (pH 7.4), from now on referred to as buffer, and the other to a vial containing only 5 mL of the buffer. The vials were then counted in a γ-counter. After incubation in a 30°C water bath for 30 minutes, the vials were removed and either underwent filtration or centrifugation.

FILTRATION

After being removed from the water bath, each vial was added to a larger vial containing 10 mL of the ice-cold buffer. The smaller vial was rinsed with approximately 1 mL of ice-cold buffer, then the solution was homogenized using a tissue tearer for 20 seconds. The contents of the vial were then sucked up into a 20 cc syringe and filtered through a glass fiber filter. The filter was then washed with 20 mL of ice-cold buffer, removed and placed in another vial. Scintillate was then added to the vial and after sitting for four hours, the vials were counted in a liquid scintillation γ-counter.

CENTRIFUGATION

After being removed from the water bath, each vial was added to a large centrifugation tube containing 10 mL of ice-cold buffer.

The smaller vials were rinsed with approximately 1 mL of ice-cold buffer, and then the solution was homogenized using a tissue tearer for 20 seconds. The tubes were then placed in the centrifuge and spun at 8000 rpms for 3 minutes. After they had been spun the supernatant was poured off and the pellet resuspended in 1 mL of ddH$_2$O. Then the solution was pipetted into a large vial, scintillate was added, and the vials were counted in a liquid scintillation counter.

RESULTS

TIME-COURSE OF BRAIN UPTAKE

Mice were given [131I]AM630 intravenously and the time course of brain uptake of the radiotracer followed Figure 2a. Maximal brain uptake of [131I]AM630 was already reached by the first sacrifice time point at 1 minute post-injection. Thereafter, radioactivity declined moderately rapidly, reaching about half of its peak value after 30 minutes. Uptake was not significantly higher in the hippocampus or cerebellum, areas with high densities of cannabinoid receptors, relative to the brain stem, an area with a low density of receptors.

Mice were given [3H]Δ8-THC intravenously and the time course of brain uptake of the radiotracer was followed in Figure 2b. Maximal brain uptake of [3H]Δ8-THC was reached by the first sacrifice time point 5-minute post-injection in the hippocampus and the brain stem, however the cerebellum did not reach maximal brain uptake until 30-minute post-injection. Uptake of [3H]Δ8-THC was moderate compared to [131I]AM630, and its clearance from the brain was relatively slow compared to [131I]AM630. Again the hippocampal and cerebellum values were similar to the values for the brain stem.

EX VIVO AUTORADIOGRAPHY

Mice were injected intravenously with [131I]AM630 and sacrificed at 30-minute time points after radiotracer administration (Figure 3a). *Ex vivo* autoradiography showed generally a uniform brain distribution, with only a very weak indication of localization to CB1 receptor brain areas, as suggested by *in vitro* binding assays.

Mice were injected intravenously with [131I]AM2233 and sacrificed at 20- and 40-minute time points after radiotracer administration (Figure 3b). *Ex vivo* autoradiography indicated a strong regional localization in the brain radioactivity that closely paralleled that of the brain CB1 receptor, as shown in Gifford (manuscript in preparation).

AM2233 *EX VIVO* ASSAY

Mice were injected intravenously with [131I]AM2233 and sacrificed at 30 minutes after radiotracer administration. The hippocampi were then incubated with and without cold AM2233. The tissue was then either centrifuged or filtered to maintain the receptors. Centrifugation did not give a large signal to noise ratio (Figure 4a), as seen by the close values of total and nonspecific binding. Filtration, however, gave a two-fold difference between total and non-specific binding in Swiss-Webster mice.
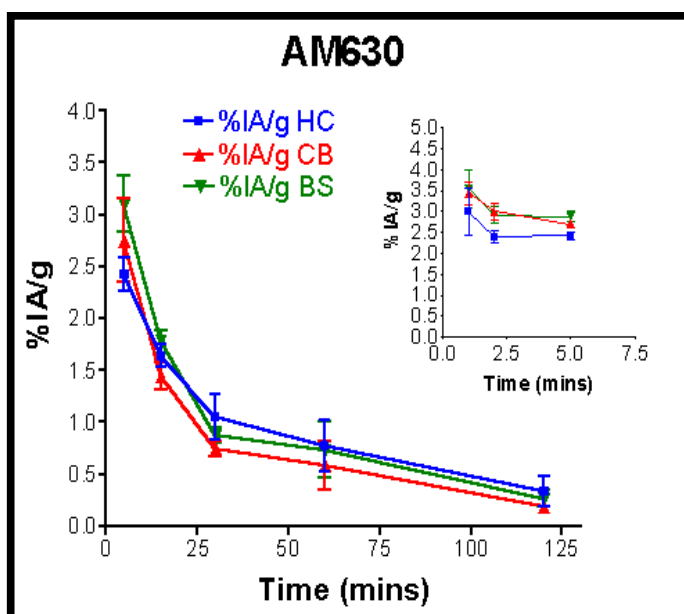
Figure 2a. Time activity curves.
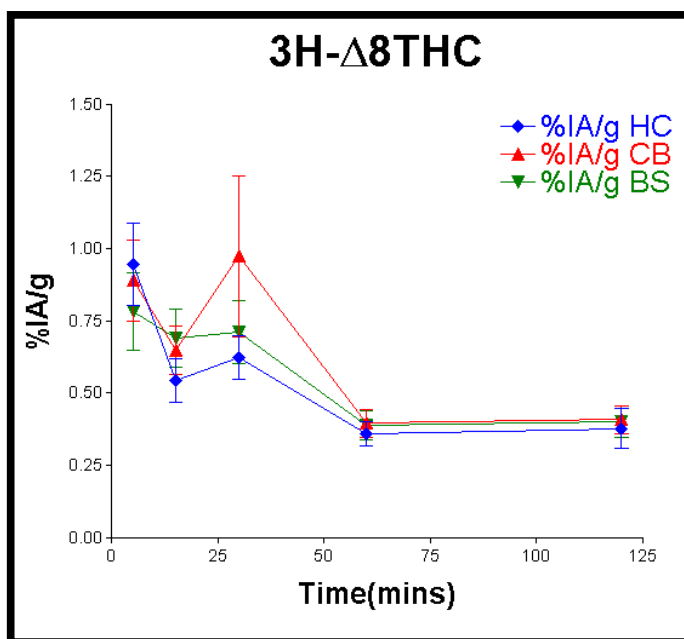
Figure 2b. Time activity curves.

DISCUSSION AND CONCLUSION

The present study was an attempt to show labeling of CB1 receptors using an aminoalkylindole cannabinoid antagonist, and a classical cannabinoid agonist. Earlier attempts by our group at labeling brain CB1 receptor with a cannabinoid agonist employed fluorine-18 labeled Δ8-THC. In both mice and baboon experiments, this radiotracer did not show selective localization in CB1 receptor-rich brain regions, presumably because of too low an affinity combined with a high non-specific binding. This proved to be true with tritium labeled Δ8-THC, as well.

The aminoalkylindoles have more suitability for labeling CB1 cannabinoid receptors *in vivo* than classical cannabinoids and

other classes of cannabinoid agonists because of their good receptor affinity combined with a significant lower lipophilicity. In earlier studies, AM2233 proved to be a good candidate for *in vivo* imaging because of its high CB1 receptor affinity combined with the fact that it possesses a SPECT-labelable iodine group (Gifford, manuscript in preparation). AM630 is an aminoalkylindole like AM2233 and also possesses a SPECT-labelable iodine group, however it did not show CB1 receptor affinity *in vivo* or in *ex vivo* autoradiography.

In the *ex vivo* biodistribution studies, [131I]AM2233 binding showed a distribution typical of that for binding to brain CB1 receptors, suggesting that binding was mostly or wholly to this receptor. In CB1 knockout mice, specific binding was largely absent although some weak binding did appear to be present in the hippocampus. However, no regionally selective binding of AM2233 was observed in *in vitro* autoradiography on cryostat cut sections from CB1 knockout mice and thus the cause of the weak hippocampal binding in *ex vivo* studies in these mice is unclear.

The development of an *ex vivo* binding assay was performed to help quantify the displacement of [131I]AM2233 binding by other ligands in Swiss-Webster and CB1 receptor knockout mice. By quantifying this displacement we will be able to begin studies to determine the identity of the unknown binding site for [131I]AM2233 present in the hippocampus of CB1 knockout mice.

In conclusion, though AM630 possesses the structure to be a SPECT-labelable radioligand, *in vitro* binding studies and *ex vivo* autoradiography showed that it lacks the affinity for CB1 receptors necessary to make it an ideal SPECT radiotracer. Δ8-THC also lacked the affinity necessary, and showed low brain uptake consistent with lipophilic classical cannabinoid agonists, which prevents it from being an ideal SPECT radiotracer. The *ex vivo* binding assay developed to quantify the displacement of [131I]AM2233 by unlabelled AM2233, however, showed promise with a two-fold difference in total and non-specific binding utilizing filtration in Swiss-Webster mice. Further studies in CB1 receptor knockout mice will be necessary to identify the unknown binding site for [131I]AM2233 in the hippocampus of CB1 knockout mice.

ACKNOWLEDGMENTS

AM630 Non-Specific Binding

Hippocampal Region

Cerebellum
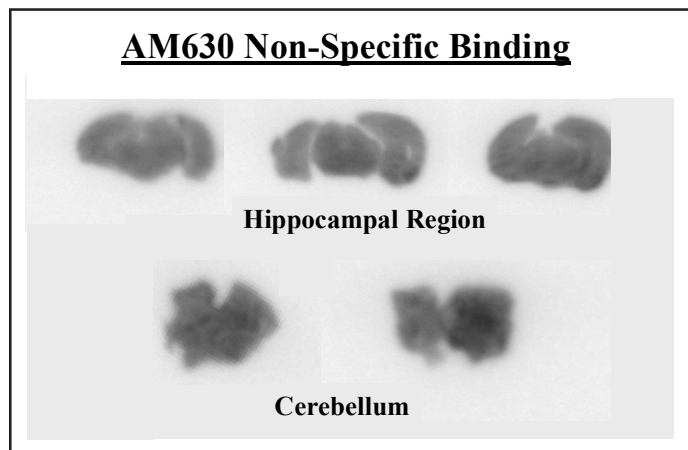
Figure 3a. Phosphoimager studies with AM630.

AM2233 Cannabinoid Specific Binding

Frontal Cortex   Striatum   Globus Pallidus   Entopeduncular Nucleus

Thalamic Region   Hippocampus   Substantia Nigra   Cerebellum
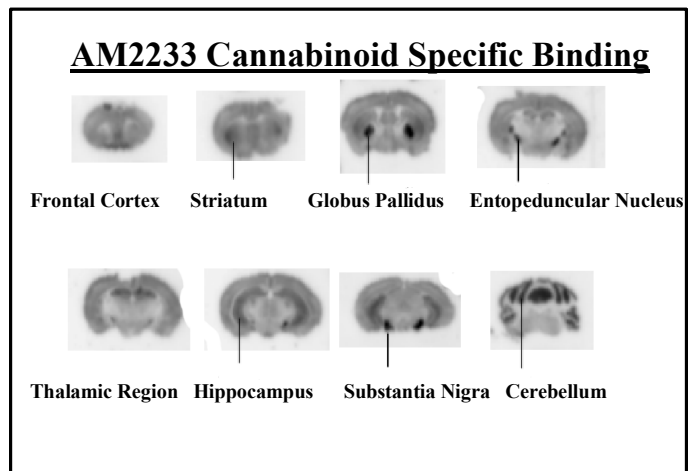
Figure 3b. Phosphoimager studies with AM2233.
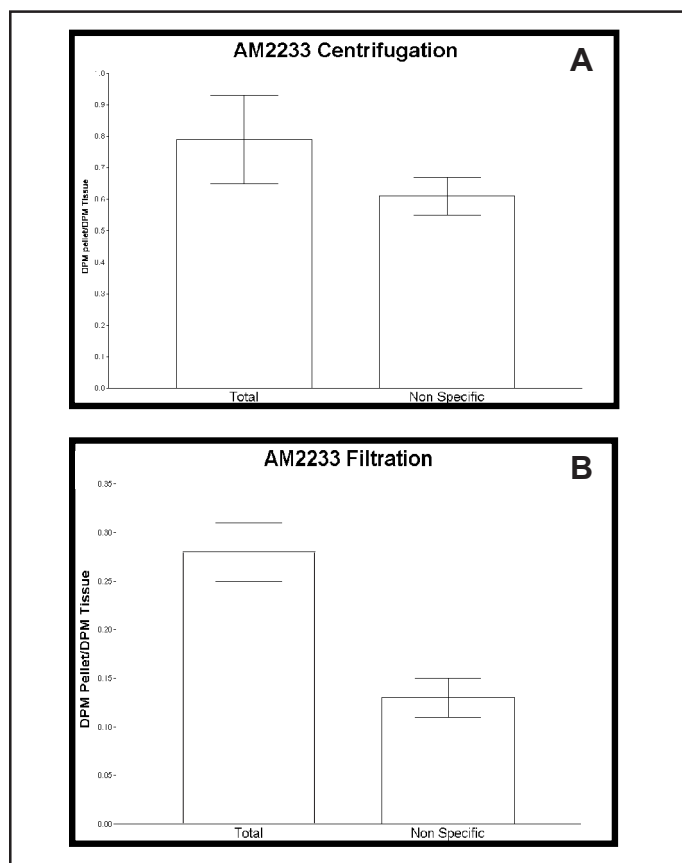
Figure 4. Development of an *ex vivo* binding assay for CB1 receptors.

sponsored by the United States Department of Energy's Office of Health and Environmental Research and located in Upton, New York.

REFERENCES

Compton Dr, Gold LH, Ward SJ, Balster Rl and Martin BR (1992) Aminoalkylindole analogs: Cannabimimetic activity of a class of compounds structurally distinct from delta 9-tetrahydroconnabinol. J.Pharmacol Exp Ther 263:1118-1126.

D'Ambra TE, Estep KG, Bell MR, Eissenstat MA, Josef KA, Ward SJ, Haycock DA, Baizman ER, Casiano FM, Beglin NC, et al. (1992) Conformationally restrained analogues of pravadoline: nanomolar potent, enantioselective, aminoalkylindole agonists of the cannabinoid receptor. J Med Chem 35(1):124-35.

Devane WA, Dysarz FA, Johnson MR, Melvin LS and Howlett AC (1988) Detmination and characterization of a cannabinoid receptor in the rat brain. Mol Pharmaco 34:605-613. Felder CC, Glass M. (1998) Cannabinoid receptors and their endogenous agonists.Annu Rev Pharmacol Toxicol 38:179-200.

Herkenham M, Hynn AB, Little MD, Johnson MR, Melvin LS, DeCosta BR, Rice KC (1990) Cannabinoid receptor localization in brain. Proc Natl Acad Sci 87:1932-1936.

Mathews WB, Scheffel U, Fineley P, Ravert HT, Frank RA, Rinaldi-Caroma M, Barth F, Dannals RF (2000) Biodistribution of [18F] Sr 144385 and [18F] SR147963 selective radioligands for positron emission tomographic studies of brain cannabinoid receptors. Nuc Med and Bio 27:757-762.

Mechoulan R (1986) Cannabinoids as Therapeutic Agents. CRC Press, Boca Raton, Fl.

ISOLATION OF TWO UNKNOWN GENES POTENTIALLY INVOLVED IN DIFFERENTIATION OF THE HEMATOPOIETIC PATHWAY, AND STUDIES OF SPERMIDINE/SPERMINE ACETYLTRANSFERASE REGULATION

CATHRYN KUBERA[A], IGOR GAVIN, PH.D.[B], AND ELIEZER HUBERMAN, PH.D.[B]

ABSTRACT

Differential display identified a number of candidate genes involved with growth and differentiation in the human leukemia cell lines HL-60 and HL-525. Two of these genes were previously unknown, and one is the gene for the enzyme spermidine/spermine acetyltransferase (SSAT). One of our objectives is to isolate and sequence the unknown genes, 631A1 and 510C1, in order to characterize them and determine their functions. The other is to determine how SSAT is regulated, and look at how the polyamines that SSAT regulates effect macrophage differentiation. By screening the CEM T-cell DNA library and the fetal brain library, we were able to identify clones that had inserts with homology to the 631A1 cDNA probe sequence. The insert was amplified using the polymerase chain reaction (PCR) and is currently being sent to the University of Chicago for automated sequencing. The library screens for 510C1 are currently underway, but hybridization of the 510C1 cDNA probe with nylon membranes containing CEM library λ-phage DNA produced strong signal, indicating the gene is there. SSAT experiments identified that the rate-limiting enzyme that marks the polyamines spermidine and spermine for degradation is regulated by PKC-β and a transcription factor called Nrf2. The knowledge of regulation and function of these genes involved in macrophage differentiation will provide new insight into this cellular process, potentially making it possible to discover the roots of the problems that cause cancerous diseases.

INTRODUCTION

Hematopoiesis is the process by which stem cells differentiate into the components of blood in humans. The branch stemming from the myeloid stem cells ends in the formation of monocytes and granulocytes (Figure 1). Final differentiation of a monocyte yields a macrophage. It is possible to study the process of macrophage differentiation in hematopoiesis *in vitro* using a human myeloid leukemia cell line called HL-60, and an HL-60 variant called HL-525, which is differentiation resistant. HL-60 is thought to exist in the phase between CFU-GM and the next step, enabling it to differentiate into neutrophils, or monocytes and macrophages. The fact that HL-525 cells cannot differentiate is the primary difference between the two cell lines. In other words, assuming that the ability to differentiate is at the genomic level, the difference between HL-60 and HL-525 can be attributed to the presence or absence of genes in HL-525, or to altered gene regulation in HL-525.

Another difference between the two cell lines is the presence or absence of the protein kinase C-β (PKC-β) pathway. It has been shown by Tonnetti, Henning-Chubb, Yamanishi, & Huberman (1994) that the PKC pathway is required for macrophage differentiation in HL-60 cells by re-enabling HL-525 to differentiate by transfecting PKC-β deficient HL-525 cells with expression vectors containing cDNA for PKC-β. So if PKC-β is required for macrophage differentiation, then any genes that are dependent on PKC-β for expression might also be involved in differentiation. These genes can be found using a technique called differential display.

First reported by Liang and Pardee (1992), differential display is a powerful technique that highlights the differences in RNA expression in different cell lines. We have used this method to screen for the genes showing the difference in expression between HL-60 and HL-525, as well as between induced and noninduced HL-60. The technique utilizes methods capitalizing on the polymerase chain reaction (PCR). A poly-T plus one base primer that anneals to the 3' poly-A tail of RNA is used along with an arbitrary 5' primer in reverse transcription reaction followed by PCR, making a number of cDNAs for the expressed RNAs in the cell. Sequencing gels are then run to compare the cDNAs of the two cells. Changes in the pattern of the expression are a red flag for genes possibly involved in differentiation. Differences in expression are then confirmed by using the cDNA as a probe on a Northern blot. By using this technique, eight genes were identified for HL-60 or HL-525, both known and unknown. We chose to focus on three of these genes: two unknown genes, temporarily called 631A1 and 510C1, and spermidine/spermine N1-acetyltransferase (SSAT).

A: Cornell University, Ithica, NY; B: Argonne National Laboratory, Argonne, IL

Not that much is known about 631A1 or 510C1. 631A1 is expressed in HL-60 cells, but not in HL-525. It is induced with PMA after 32 hours of incubation, suggesting it somehow plays a role in differentiation (Gavin, 2001). 510C1, on the other hand, is found in HL-525 and not in HL-60. 510C1 has a homeo-domain in the known fragment sequence hinting that it may be a transcription factor of some kind (Gavin, 2001).

Spermidine/spermine N1-acetyltransferase is a rate-limiting enzyme that acetylates spermidine and spermine in polyamine metabolism, tagging them for degradation by polyamine oxidase. Polyamines have long been known to play a role in growth and differentiation, but how these vital cations are regulated is still unclear. It is important to understand the metabolic pathway for polyamines if we are to learn more about polyamine regulation (Figure 2). Ornithine decarboxylase (ODC) is the rate-limiting biosynthetic enzyme, and it was originally thought that polyamines

Figure 1. The process of hematopoiesis. HL-60 cells exist in the phase around CFU-GM and can differentiate into granulocytes or neutrophils, and monocytes. Monocytes differentiate further into macrophages. *Figure adapted from Socolovsky, Lodish, & Daley (1998).*

Figure 2. Polyamine biosynthetic pathway. Spermine and spermidine are acetylated by SSAT, marking them for degradation. *Figure adapted from Casero & Pegg (1993).*

were regulated by the synthetic pathway. However, findings that spermine decreases while spermidine and putrescine increase during phorbol 12-myristate 13-acetate (PMA) induced macrophage differentiation suggests that regulation of polyamines occurs by degradation (Huberman, Weeks, Callaham, & Slaga, 1981). Since SSAT is responsible for the initial steps of polyamine catabolism, how it is regulated is a logical question to ask. We have done a number of experiments with SSAT and polyamines to observe the effects on macrophage differentiation and determine how SSAT is regulated.
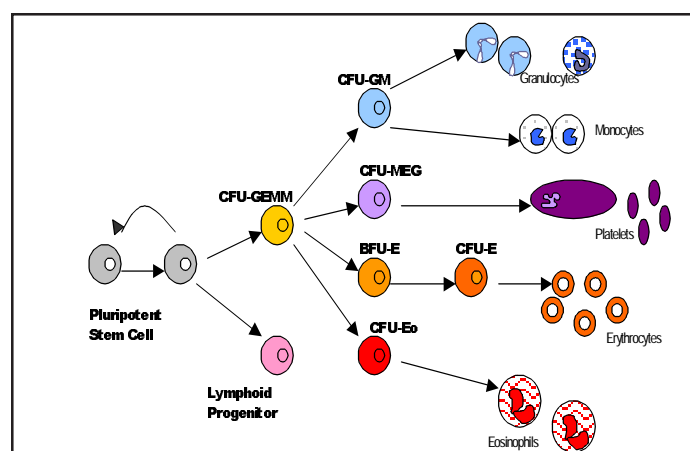
MATERIALS & METHODS

631A1

Testing three DNA libraries, a Northern blot determined expression of 631A1 was highest in the human CEM T-cell DNA library from Clontech Laboratories. Polymerase Chain Reaction (PCR) was used to amplify 631A1 cDNA probes. Y1090 strain of Escherichia coli was infected with the CEM library in lambda Zap phage, and plated on 150mm LB-agar $MgSO_4$ plates. We also used human fetal brain plasmid library in pcDNA1, also by Clontech, plated on 150mm LB-agar plus half ampicillin, full tetracycline plates. After overnight incubation at 37 °C, the colonies and plaques were lifted with Magna lift nylon transfer membranes by Osmonics Inc. The CEM membranes were crosslinked with a Stratagene UV Stratalinker-2400 at 1200 µJ. The fetal brain membranes were baked at 80 °C in an oven for one hour. The membranes were then hybridized with P^{32} labeled 631A1 cDNA probe, and exposed to film. The plates were lined up with the developed film. Ten picks were made from the CEM library; five picks were made from the fetal brain library.

The CEM picks were cleaned with 250 µL of phage dilution buffer (35 mM Tris pH 7.5, 10 mM $MgSO_4$, 0.01% gelatin, 0.1 M NaCl, H_2O) and 25 µL chloroform, used to infect Y1090, and plated on 80 mm LB-agar $MgSO_4$ plates. The fetal brain picks were used to streak new 80 mm LB-agar half ampicillin, full tetracycline plates. A second round of lifting and hybridizing was done. This time, six CEM picks were freeze-thawed in water three times. Five fetal brain picks were boiled 10 minutes in colony lysis buffer. The CEM picks were PCR amplified with T7 and T3 primers; the fetal brain picks were PCR amplified with pcF/R primers. Five additional fetal brain picks were made and put in 100 µL LB to be grown up overnight. DNA was prepared with the Qiagen QIAprep Miniprep Kit (250), and then double digested with BamHI and XbaI restriction endonucleases.

The digests and PCR products were electrophoresed on a 1% agarose gel. Two bands from the digest were excised, and two PCR products were subject to a second round of PCR. PCR products were then purified with the Qiagen Qiaquick PCR Purification Kit (50). A fraction of DNA was then digested with EcoRI, and run out on a 1% agarose gel. The vector Bluescript Sk(+) was prepared for subcloning by digesting with EcoRI, EcoRV and BamHI/XbaI. DNA was obtained from gels using the Quigen QIAEX II Gel Extraction Kit.

Ligation reactions were set up for EcoRV digested Sk(+) and blunt ended PCR products, EcoRI digested Sk(+) and EcoRI cut PCR product, and BamHI/XbaI digested Sk(+) and BamHI/XbaI
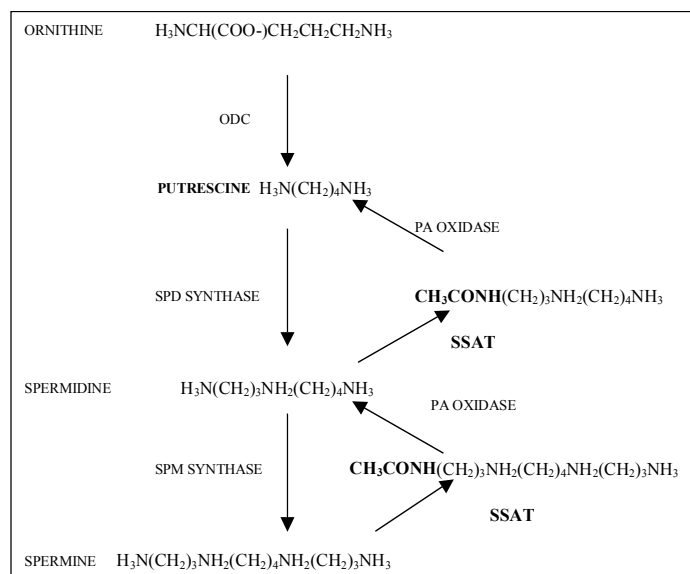
cut fetal brain plasmid. The ligations were purified by phenol chloroform extraction, and transformed into electrocompetent bacteria by electroporation with a BioRad Gene Pulser (1.8 kV, 20 Ω, 25 µFD). The bacteria were then plated on full ampicillin/tetracycline plates with 100 mM IPTG and X-gal DMFA for blue-white screening. A total of 28 picks were made and cultured. Minipreps were done to prepare DNA. The DNA was then digested with EcoRI, EcoRV, and BamHI/XbaI, as before, and electrophoresed on a 1% agarose gel.

A culture of the positive clone was grown up overnight and miniprepped. A glycerol stock for 631A1 in the fetal brain library was made. We then sequenced the BamHI/XbaI cut fetal brain plasmid and one of the CEM PCR products. Since only a small segment of DNA can be sequenced at once, we digested with SstI and NotI to prepare the DNA binding site, and did an ExoIII timed deletion reaction to obtain varying fragment lengths. After the ExoIII reaction, vectors were re-ligated and transformed into bacteria by electroporation. Colony PCR was done to check them, and cultures were miniprepped. DNA was digested with PvuII and run on a 1% agarose gel. The plasmid was then sent for automated sequencing.

510C1

The same cDNA libraries—CEM and fetal brain—were initially screened for 510C1 by hybridizing P[32] labeled cDNA probe with the original library membranes. However, after secondary screening, this proved ineffective, so new libraries were plated. Only the CEM library was plated. Plaque lifts were performed, and then the membranes were hybridized with the 510C1 radiolabeled probe. 15 picks for the secondary screening were made and plated.

SSAT RELATED EXPERIMENTS

Induction of HL-60 with spermine: $4x10^4$ HL-60 cells were added to each of 8 wells with 100 µL of serum free media on a chamber slide. Spermine and SSAT antisense were added to the wells as shown in Table 1. The cells were incubated at 37 °C four hours, when fetal bovine serum was added to 10%. The cells were placed at 37 °C for an additional hour, then PMA was added to 3nM as indicated in Table 1. The cells were again placed at 37 °C for about 19 hours more.

Cells were resuspended and transferred to microwells. They were fixed in 4% formaldehyde for 10 minutes at room temperature,

Table 1. Variables for Induction of HL-60 with Spermine

Plate	PMA	Spermine	SSAT antisense
1	-	-	-
2	3 nM	-	-
3	-	2 µM	-
4	-	4 µM	-
5	3 nM	2 µM	-
6	3 nM	4 µM	-
7	3 nM	2 µM	200 µM
8	3 nM	4 µM	200 µM

and then stained with anti-MacI antibodies (1:20) for one hour at 4 °C. Anti-mouse FITC conjugated secondary antibodies (1:100) were incubated with cells 30 minutes at room temperature. Cells were then cytospun onto glass slides for 5 minutes at 770 rpm.

Activity of SSAT antisense with PMA and no spermine in HL-60: $4x10^4$ HL-60 cells were added to 100 µL serum free media in 3 wells of a chamber slide. Though SSAT antisense should have been added to 200 µM in one well, there was only enough antisense to make it about 100 µM. The cells were incubated 4 hours at 37 °C when serum was added to 10%. After another hour of incubation, PMA was added to 3 nM in the antisense well and one other. The well with nothing but cells acted as the control.

After 8 hours incubation with PMA, cells were cytospun onto slides and fixed with 100% methanol 5 minutes. They were blocked with PBS/BSA 10 minutes and then stained with 1:100 anti-SSAT antibodies 30 minutes at room temperature. Goat anti-rabbit FIT C conjugated antibodies (1:100) were then added and incubated for 30 minutes at room temperature.

Determination of spermidine and putrescine toxicity in HL-60: HL-60 cells in culture were resuspended and counted with a hemacytometer. About $24x10^4$ cells were transferred to 1.5 mL serum free media. One plate was left as control, adding nothing. To four plates, 100 µM, 200 µM, 500 µM and 1 mM putrescine was added. To four other plates, 100 µM, 200 µM, 500 µM and 1 mM spermidine was added. These were incubated at 37 °C 4 hours, then serum was added to 10%. Cells were then taken at 19 hours and 48 hours of incubation for DAPI staining.

After 19 hours cells were spun down in a microcentrifuge, and fixed with 100% methanol for 5 minutes. They were stained with 1:30 DAPI and 1:500 hydroethidine in PBS for 7 minutes, and cytospun onto slides. After 48 hours, cells were cytospun onto slides first, and then fixed with 100% methanol for 5 minutes. Then they were stained with DAPI and hydroethidine as above.

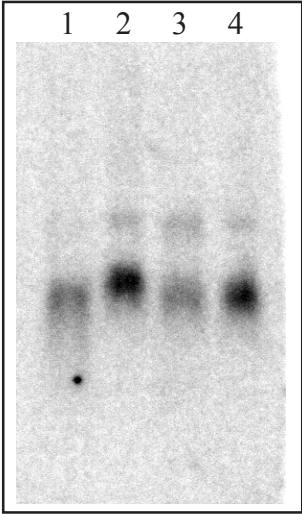**Figure 3.** Northern blot hybridized with 631A1 probe to test expression in different DNA libraries. Lane 1 is 631A1 expression in the prostate PG-3 library. Lane 2 is expression in the CEM library. Lane 3 is expression in the Breast AC 565 library. And lane 4 is 631A1 expression in HL-60. Since expression was comparatively higher in the CEM library, that is the library we chose to screen for 631A1.

The spermidine toxicity experiment was repeated with about 44×10^4 cells per plate at concentrations of 3 µM, 10 µM, 30 µM and 100 µM. They were stained by spinning in a microcentrifuge first, fixing with 4% formaldehyde, adding DAPI and hydroethidine as before, and then cytospinning.
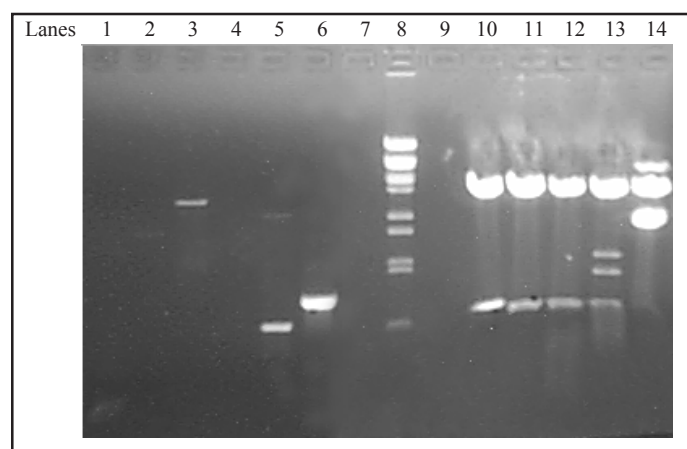
ODC probe synthesis: Ornithine decarboxylase cDNA probe was made from ODC mRNA using a reverse transcriptase reaction. In a PCR cycler, the mRNA plus 1x RT buffer, 20 µM dNTPs, 0.2 µM ODC reverse primer and RNAse-free treated water was held at 68 °C for 10 minutes. The block cooled to 37 °C where the cycle was paused and 0.5 µL MMLV reverse transcriptase was added to the reaction. It was then held at 37 °C for 1 hour, heated to 75 °C for 5 minutes, and then stored at 4 °C infinitely. The RT reaction was then amplified using Taq polymerase by normal PCR. The probe was used to look at ODC expression during PMA induction of HL-60.

RNA gel of 3-2 cells: RNA was prepared for 3-2 and HL-525 cells that were treated with PMA. A 1% agarose gel with MOPS and formaldehyde was run, and the gel was transferred onto a membrane by capillary action.

RESULTS

631A1

Three DNA libraries were tested for expression of 631A1 with a northern blot. The expression in HL-60 behaves as a positive control. The CEM library demonstrates the highest expression (Figure 3). When the CEM and fetal brain libraries were plated out, lifted, and membranes were hybridized with 631A1 probe, the fetal brain library yielded fewer, yet stronger hits. The CEM library had more hits that had weaker signal. Background was very low. In secondary screening, the signal, when present, was very strong.

The secondary CEM picks that were PCRed showed three promising bands when they were electrophoresed. The fetal brain plasmid picks digested with BamHI and XbaI yielded fragments around 1kb, which was the expected cDNA length for 631A1. Based on this, we isolated DNA from picks 6 and 9, two of the CEM PCR products, and picks 1 and 5, two of the digested fetal brain plasmids (Figure 4). The PCR products were digested with EcoRI to make sticky end ligation possible. Pick number 6 had an internal EcoRI restriction site, suggesting that perhaps there were two library inserts in that clone, since the smaller fragment was then very close in size to that expected (Figure 5).

The blue-white screening yielded only one clone positive for the expected 631A1 insert size of 1kb out of forty picks. We also tried ligating again into new vector, and plating on S-gal plates (brown-white screening media from Sigma), but this did not yield any positive results either. Even so, we continued by sequencing the positive BamHI/XbaI digested clone and the CEM PCR product number 9 that was the expected size.

Initial sequencing yielded no results for the plasmid, and only sequence from one primer in the CEM fragment. Trouble-shooting indicated that there was little to no DNA in the fetal brain plasmid prep. The T7 primer was found to be ineffective for the CEM fragment sequencing. A second miniprep and new T7 primer then yielded about 300bp of 631A1 sequence. The 3' end of the cDNA sequence matched the sequence of the 631A1 probe.

The ExoIII deletion reaction worked as expected, deleting about 200bp per 30 seconds. This can be seen on the step-like gel of the eight time points. The first time point has the largest fragment; the last time point has the smallest fragment (Figure 6).

PCR of the time points from the ExoIII reaction yielded strange results. The PCR only work for the 2 minute time point, and all four picks resulted in fragments of differing sizes. Digestion of miniprepped

Figure 4. Agarose gel of CEM library PCR products and BamHI/XbaI digested fetal brain library plasmid. Lanes 1-6 contain the PCR products from the CEM library. Lane 3 and lane 6 contain picks 6 and 9, which were arbitrarily chosen to be subcloned. Lane 8 is the high molecular weight marker λ–BstE II. Lanes 10-14 are fetal brain plasmids digested with BamHI and XbaI. Lanes 10 and 14, or picks 1 and 5 were also chosen to be subcloned. All of these clones were isolated from 631A1 secondary screening.

Figure 5. Results of EcoRI digestion of CEM picks 6 and 9. Lane 1 is the high molecular weight marker λ–BstE II. Lane 2 is pick #6 PCR product. Lane 3 is #6 digested with EcoRI. Notice that it is split into two bands, and that the smaller is nearly identical to #9 in size, which is around 1kb. Lane 4 is pick #9 PCR product, and lane 5 is #9 digested with EcoRI.
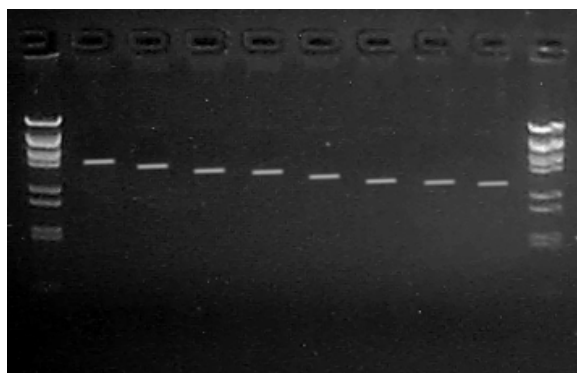
Figure 6. Agarose gel of Bluescript plus the 631A1 insert at 8 time points of the ExoIII deletion reaction. The length of insert becomes progressively smaller as the enzyme deletes about 400bp per minute. The loose end of vector DNA was protected by a 3' overhang. The samples were run with the λ–BstE II marker.

DNA with PvuII yielded bands of the same size for all time points and all were too large. Only the control looked correct in size.

510C1

Hybridization of the 510C1 probe to the original library membranes resulted in much higher background than the 631A1 screening. The strongest hits failed to produce colonies or plaques on the secondary plates. Signal after the secondary membranes were hybridized were also very weak. The picks that were made from the secondary plates were all determined to be negative for 510C1 insert when there was no DNA amplified by PCR. We then plated and hybridized new CEM libraries. The newly plated library yielded very strong signal with extremely low background.

SSAT EXPERIMENTS

Induction of HL-60 with spermine: When spermine was added to the media in concentrations similar to that naturally in the cell, PMA induction of differentiation in HL-60 was blocked. Table 2 indicates the level of cell attachment and MacI expression. PMA induced cells had both positive attachment and MacI expression. Concentrations of spermine resulted in no attachment of MacI expression. PMA plus spermine resulted in some attachment with $2 \mu M$ spermine. Minimal attachment was seen at $2 \mu M$ spermine with PMA and SSAT antisense.

Activity of SSAT antisense with PMA: This experiment tests whether the SSAT antisense functions as it is expected to. Here we saw induction of SSAT, and not very much blocking of SSAT expression. The experiment was repeated with new antisense and only 4 hours of PMA induction, and SSAT expression was blocked.

Spermidine and putrescine toxicity: Cells appeared healthy at all concentrations of putrescine, therefore putrescine is not toxic to HL-60 cells. Spermidine caused a significant number of cells to be apoptotic at $100 \mu M$, so the experiment was repeated. At $3 \mu M$, $10 \mu M$ and $30 \mu M$, cells appeared healthy, although it was apparent that there were more apoptotic cells at $30 \mu M$ than the lower concentrations. Cells once again were apoptotic at $100 \mu M$ spermidine.

ODC probe: Hybridization of the ODC probe to a RNA membrane for PMA induced HL-60 cells showed normal levels of ODC expression at 3 hours, but decreasing levels of expression after 8 hours of induction.

3-2 cell blot: Hybridization of the blot for 3-2 and 3-30 cells with SSAT probe showed expression of SSAT at 8 hours of PMA induction. There was no induction of SSAT in the HL-525 control.

DISCUSSION & CONCLUSIONS

The rationale behind spending time screening for desired genes and sequencing is as follows: Although the human genome is supposedly sequenced, there is still a significant percentage of unknown genes, and there is little knowledge about the function of many genes. By screening a library with a cDNA probe, we are able to isolate the gene. Then sequencing enables us to learn a great deal about the gene. Similarities to other known sequences may infer the gene's function. The presence of known domains in the sequence might hint at how the gene is regulated. Finding the open reading frames would make it possible to determine the amino acid sequence of the gene. Finally, having the gene sequence enables one to determine the 3' antisense. Obtaining the antisense is important for functional studies of the gene because it blocks expression of the gene, essentially creating a knockout model cell.

In our experiments described here, we initially attempted subcloning the 631A1 insert into Bluescript Sk(+) instead of immediately sequencing the positive clone so that we could do the ExoIII deletion reaction. This would allow us to do several sequencing reactions in parallel and obtain the entire gene sequence manually instead of having to make a new primer for the next 300 bp region in the gene each round. While the ExoIII reaction worked, some kind of plasmid contamination made transformants impossible to find easily. This encouraged us to discontinue manual sequencing efforts and send the positive clone to the University of Chicago for automated sequencing. We had already confirmed that we had the gene we were looking for because the 3' end that was manually sequenced matched that of the probe. The 5' sequenced end had identity with some sequences in the database, which is strong evidence that the cDNA sequence is full.

Learning from our experience with 631A1, after a positive clone is found and isolated for 510C1, we will most likely forego subcloning and manual sequencing, and send it for automated sequencing directly, using subcloning and manual sequencing only for confirmation.

Thus far, experiments with SSAT have shown that the antisense is capable of blocking SSAT expression, and so is capable of blocking differentiation in HL-60 by itself. Spermine alone, however is unable to block differentiation. The combination of antisense and spermine together is also capable of blocking macrophage differentiation. This, along with the knowledge of toxicity levels of polyamines in the cell will facilitate planning future functional studies of SSAT and the polyamines.

Expression studies have also yielded some interesting findings. SSAT expression in 3-2 and 3-30 cells, but not in HL-525 indicate that PKC-β may play a role in SSAT regulation. 3-2 and

Table 2. Spermine Induction Results

	c	p	2uM s	4uM s	2uM sp	4uM sp	2uM spa	4uM spa
cell attachment	-/+	+	-	-	+/-	-	-/+	-
MacI expression	-	+	-	-	-	-	-	-

c = control   p = 3nM PMA   s = spermine   a = SSAT antisense

3-30 are cell lines derived from HL-525, and are stably transfected with a plasmid coding for PKC-β. There is also a transcription factor called Nrf2 that is expressed after 3 hours of PMA induction in HL-60 (Gavin, 2001). This might also play a role in regulating SSAT, because SSAT is not expressed until 8 hours.

The isolation and sequencing of 631A1 and 510C1 will be completed soon. Obtaining the antisense sequence will enable us to learn much more about the function of these currently unknown genes. It will be interesting to discover where in the scheme of macrophage differentiation these new genes fit in. We can only hope that it will make what we now know about differentiation even more clear. In addition, knowing how SSAT is regulated is the beginning of a new understanding of polyamine regulation in the cell. This could lead to identification of new targets for cell growth and differentiation control, giving us yet another tool for finding treatments for cancer.

The research presented here was done at Argonne National Laboratory, a scientific research facility owned by the U.S. Department of Energy, and managed by the University of Chicago in Argonne, Illinois. The experimental data was collected in the summer of 2001.

REFERENCES

Casero, R.A., & Pegg, A.E. (1993). Spermidine/spermine N1-acetyltransferase- the turning point in polyamine metabolism. The FASEB Journal, 7(May), 653-661.

Gavin, I. (2001). (Personal communication, July, 2001). Huberman, E., Weeks, C., Herrmann, A., Callaham, M., & Slaga, T. (1981). Alterations in polyamine levels induced by phorbol diesters and other agents that promote differentiation in human promyelocytic leukemia cells. Cell Biology, 78(2), 1062-1066.

Liang, P., & Pardee, A.B. (1992). Differential display of eukaryotic messenger RNA by means of the polymerase chain reaction. Science, 257(Aug. 14), 967-971.

Socolovsky, M., Lodish, H.F., & Daley, G.Q. (1998). Control of hematopoietic differentiation: lack of specificity in signaling by cytokine receptors. Proceedings of the National Academy of Sciences of the United States of America, 95(12), 6573-6575.

Tonnetti, D.A., Henning-Chubb, C., Yamanishi, D.T., & Huberman, E. (1994). Protein kinase C-b is required for macrophage differentiation of human HL-60 leukemia cells. The Journal of Biological Chemistry, 269(37), 23230-23235.

REDUCING BORON TOXICITY BY MICROBIAL SEQUESTRATION

Tracy Hazen[A] and Tommy J. Phelps, Ph.D.[B]

ABSTRACT

While electricity is a clean source of energy, methods of electricity-production, such as the use of coal-fired power plants, often result in significant environmental damage. Coal-fired electrical power plants produce air pollution, while contaminating ground water and soils by build-up of boron, which enters surrounding areas through leachate. Increasingly high levels of boron in soils eventually overcome boron tolerance levels in plants and trees, resulting in toxicity. Formation of insoluble boron precipitates, mediated by mineral-precipitating bacteria, may sequester boron into more stable forms that are less available and toxic to vegetation. Results have provided evidence of microbially-facilitated sequestration of boron into insoluble mineral precipitates. Analyses of water samples taken from ponds with high boron concentrations showed that algae present contained 3-5 times more boron than contained in the water in the samples. Boron sequestration may also be facilitated by the incorporation of boron within algal cells. Experiments examining boron sequestration by algae are in progress. In bacterial experiments with added ferric citrate, the reduction of iron by the bacteria resulted in an iron-carbonate precipitate containing boron. An apparent color change showing the reduction of amorphous iron, as well as the precipitation of boron with iron, was more favorable at higher pH. Analysis of precipitates by X-ray diffraction, scanning electron microscopy, and inductively coupled plasma mass spectroscopy revealed mineralogical composition and biologically-mediated accumulation of boron precipitates in test-tube experiments.

INTRODUCTION

Coal-fired power plants have continuously played an important role in the production of electricity for government, economic, and personal use. Although electrical power plants positively influence humanity, their methods of waste disposal often threaten the health of vegetation and wildlife living on adjacent land. The production of energy often indirectly results in environmental degradation of areas such as wetlands, with visible effects that appear only after a significant length of time. For example, the effects of boron toxicity on wetlands surrounding coal-fired electrical power plants may often be seen as a lack of plant growth or inability of the boron-rich soils and groundwater to sustain a variety of plant and animal species.

The use of natural or artificially-constructed wetlands as a method of waste-water reclamation has increased substantially over the past 30 years (Cole, 1998) due to relative effectiveness, low cost of construction, and the passive maintenance approach commonly applied in leachate pond treatments. Coal-fired power plants often employ the use of wetlands as settling basins, which serve to contain coal fly-ash that is discharged from electrical power plants.

The presence of toxic metals in natural or artificial wetlands is often amplified through methods of pollution control, including the discharge of coal fly-ash from coal-fired electrical power plants. Coal that is burned to obtain electricity at power plants often contains naturally-occurring metals, including boron, which remains in the resulting fly-ash and is subsequently discharged into wetland areas surrounding the power plants. At normal levels, boron poses no threat to environmental health, instead serving as an essential nutrient for plant growth. The presence of boron in soils at continuous levels is required for processes of plant growth and seed production (Brown & Shelp, 1997); however, the accumulation of excess boron in soil and groundwater has negative impacts on plant health, due to the increase in adsorption of boron by roots. Boron often occurs in the form of boric acid, which is soluble in water, making the boron more readily available to plants (Nable, Bañuelos, & Paul, 1997). Continuous accumulation of boron within the environment eventually exceeds the tolerance levels of many plants.

The potential use of microorganisms to facilitate in precipitation of boron from the fly-ash ponds associated with coal-fired electrical power plants would provide an environmentally-friendly remediation alternative in returning healthful conditions to a disrupted ecosystem such as a treatment wetland. Naturally-occurring bacteria and algae in a wetland may prove beneficial in reducing the effects of boron toxicity by bacterially-mediated precipitation or incorporation of the mineral within algal cells or precipitates. Sequestration of the excess boron into an unreactive precipitate would potentially decrease boron toxicity by reducing the amount of boron available for plant adsorption.

A: University of California, Davis, Davis CA; B: Oak Ridge National Laboratory, Oak Ridge, TN

METHODS AND MATERIALS

A medium with 52 mg/L boron concentration was created by the addition of boric acid. The medium was then transferred to test tubes in the presence of N_2 gas and autoclaved. Separate solutions of amorphous iron, ferric citrate, calcium chloride, potassium phosphate, and a pH 9.6 buffer, containing HEPES (4-(2-hydroxyethyl)-1-piperazineethanesulfonic acid) and Mops, were prepared and autoclaved for approximately one hour. The pH of each tube was adjusted to approximately 7, 8, and 9, in order to show variable chemically- and biologically-mediated precipitation at different alkalinities. Following the adjustment of pH in each tube, different combinations of calcium, phosphate, and either amorphous iron or ferric citrate were added, maintaining tubes with all three of the alkalinities for every specific mineral combination. Sets of tubes containing the various mineral combinations at each alkalinity were inoculated with bacteria from different sample sites, allowing the establishment of nine different culture sets. A set of abiotic controls at the different alkalinities was also established. After 2 weeks of incubation, 5 mL of the supernatant were removed from the test tubes. The precipitate was then filtered from the remaining supernatant onto 0.4-micron Gelman filter discs and rinsed three times with molecular water of pH 11 in order to remove any residue left by the supernatant.

The incorporation of boron from solution into algal cells was tested by the construction of an algae medium to which boric acid was added, resulting in a boron concentration of 73 mg/L. A 9 mL portion of the algae medium was then transferred into test tubes and the alkalinity increased to approximately pH 7, 8, or 9 using a pH 9 buffer solution. The test tubes were then inoculated by addition of one drop, 0.1 mL, 0.3 mL, or 0.5 mL of the algae site sample as well as serial dilutions within each pH for the 2 different algae site samples. The algal cultures were placed in a light incubator and allowed to grow for 2 to 3 weeks. The entire contents of the test tubes were filtered onto 0.4 micron Gelman filter discs, and the filter and contents were then dried and used in later precipitate analyses, with 5 mL of the supernatant remaining after filtration, for each tube, were saved for later analyses.

Table 1. Visual observations of tube contents color change and precipitate formation for bacterial culture sets and abiotic controls.

Composition	pH 7	pH 8	pH 9
Control			
Ferric Citrate, Ca, P	no precipitate	no precipitate	no precipitate
Amorphous Iron	precipitate	precipitate	precipitate
Amorphous Iron, Ca	precipitate	precipitate	precipitate*
Amorphous Iron, Ca, P	precipitate	precipitate*	precipitate
Set 1			
Ferric Citrate, Ca, P	gray precipitate	precipitate	precipitate
Amorphous Iron	no precipitate	darker	brown precipitate
Amorphous Iron, Ca	precipitate	slightly darker	brown precipitate
Amorphous Iron, Ca, P	slightly darker	slightly darker	slightly darker
Set 2			
Ferric Citrate, Ca, P	darker **	precipitate	precipitate
Amorphous Iron	no precipitate	slightly darker	darker **
Amorphous Iron, Ca	no precipitate	slightly darker	darker
Amorphous Iron, Ca, P	slightly darker	slightly darker	slightly darker
Set 3			
Ferric Citrate, Ca, P	darker	precipitate	precipitate
Amorphous Iron	precipitate	darker	brown precipitate
Amorphous Iron, Ca	slightly darker	darker **	brown precipitate*
Amorphous Iron, Ca, P	slightly darker	slightly darker	darker
Set 4			
Ferric Citrate, Ca, P	precipitate	precipitate*	gray precipitate*
Amorphous Iron	precipitate	slightly darker	dark precipitate
Amorphous Iron, Ca	precipitate	gray precipitate	gray precipitate
Amorphous Iron, Ca, P	precipitate*	slightly darker*	darker*

*Samples on which ICP analyses were performed. **Samples analyzed by ICP as well as SEM-EDX.

In order to show existence of boron in the bacterial culture precipitates, as well as contained in the algal cultures, inductively coupled plasma spectroscopic (ICP) analyses of the precipitates were performed. Analyses were conducted using 1 mL of a solution obtained by dissolving the precipitate on a measured one-third section of the filter disc in 5 mL of 10 M hydrochloric acid, which was then diluted with molecular water. The supernatants for the microbial trials were also diluted using molecular water and analyzed by ICP.

The mineralogical structure of the precipitates obtained from the bacterial cultures was determined by analyzing sections of the filtered precipitate from select samples using a Hitachi spectral display S-4700 scanning electron microscope with energy dispersive X-ray (SEM-EDX). The selection of samples that were analyzed was based on the amount of precipitate per one-third section of filter disc, as well as color of precipitate.

Precipitate and supernatant samples obtained from both bacterial and algal cultures were also analyzed using a Hach 2010 direct reading spectrophotometer, as well as a Hewlett Packard 8453 spectrophotometer, following reaction with a Hach test kit specifically for boron detection. Results provided the preliminary data used to determine which samples were most beneficial to analyze by the ICP and SEM-EDX. Selection of samples to be analyzed by the spectrophotometer, as well as the ICP and SEM-EDX, was based primarily on precipitate formation at specific mineral combinations, though coloration and quantity of precipitate were also considered. Analyses of the filtered algae cultures and supernatants were performed on tubes which had a noticeable amount of growth based on change in intensity of color.

RESULTS

The ability of microorganisms to mediate boron sequestration through precipitation of boron into insoluble solids, or isolation of boron within algal cultures, was made evident through data obtained by several different methods of analysis. Visual observation of the amount of precipitation and color of precipitates, light spectroscopy, inductively coupled plasma spectroscopy (ICP), and scanning electron microscopy with energy dispersive X-ray (SEM-EDX), all generated data showing the occurrence of boron sequestration through microbial mediation.

The visible traits of precipitates formed in the bacterial cultures served as one factor in selecting samples that were potentially more beneficial for ICP and SEM-EDX analyses. In all tubes of bacterial medium to which amorphous iron was an added mineral, formation of a precipitate occurred before addition of bacteria. Following inoculation with bacteria, and 2 weeks of incubation, there was a noticeable color change among the precipitates within tubes containing amorphous iron, as well as additional precipitation (see Table 1). In tubes containing the mineral combination of calcium and phosphate with ferric citrate, the controls showed no precipitation, however; there was a substantial amount of precipitation in the biotic tubes containing the same minerals. Precipitates formed in the Set 4 bacterial cultures at pH 8 and 9, with a mineral combination of ferric citrate and calcium, plus phosphate, were a gray color that appeared darker, and in greater quantity than the precipitate in Set 4 at pH 7 with the same mineral combination. The amount of precipitation in tubes at the various alkalinities that contained amorphous iron or ferric citrate, plus calcium and phosphate, was much greater than in tubes containing only amorphous iron. At pH 9 for either amorphous iron or ferric citrate combinations, there was more precipitate formation than in tubes with the same added metal composition cultured at pH 7 or 8.

Visual observations of the algal cultures showed the growth of green as well as red algae. Tubes to which the algae site sample was added in a serial dilution had a lighter initial color than tubes that were inoculated through direct addition of the algae sample.

Data from spectrophotometric analyses showed variations between the amount of boron present in precipitates and supernatants of the bacterial cultures compared to the boron concentration reported in analyses of the abiotic controls, although

Table 2. ICP analyses reporting concentration of boron present in precipitates for select bacterial culture sets and abiotic controls.

Culture Analyzed	Composition	pH	Concentration B (μg)	% B precipitated
Control	Amorphous Iron, Ca	9	10.25	2
Control	Amorphous Iron, Ca, P	8	6.46	1.2
Set 2	Ferric Citrate, Ca, P	7	20.49	3.9
Set 3	Amorphous Iron, Ca	8	18.91	3.6
Set 3	Amorphous Iron, Ca	9	12.53	2.4
Set 4	Ferric Citrate, Ca, P	8	26.57	5.1
Set 4	Ferric Citrate, Ca, P	9	23.73	4.6
Set 4	Amorphous Iron, Ca, P	7	15.59	3
Set 4	Amorphous Iron, Ca, P	8	22.14	4.3
Set 4	Amorphous Iron, Ca, P	9	22.44	4.3

*Composition shows mineral combination specific to each culture. Minerals; present in concentrations 10 mM ferric citrate, 10 mM amorphous iron, 10 mM calcium (Ca), and 20 mM phosphate (P).

Calculated mass of boron in media is 520 μg.

these boron levels varied greatly from the original media. Precipitates from the bacterial cultures contained a greater amount of boron than the precipitates from the controls with the corresponding alkalinities and mineral combinations. Analyses of precipitates and supernatants from cultures containing ferric citrate also proved differing concentrations of boron present at the varying alkalinities and mineral combinations, compared to the amount of boron in the original media, as well as the lack of precipitation in the ferric citrate controls. Results obtained from spectrophotometric analyses served as a guide in selection of samples to further examine by ICP analysis.

Spectrophotometric analyses of the supernatants from the algal cultures showed differing levels of boron present between the cultures containing variable concentrations of the algae site sample. Although spectrophotometric analyses showed considerable contrast between the products from the abiotic and biotic controls, the data was highly variable, therefore no conclusions could be made.

ICP analyses of the precipitates from select bacterial cultures at various alkalinities and mineral combinations detected the presence of boron. The percentage of boron found in the precipitates was calculated from the actual amount of boron reported by ICP analyses (see Table 2), and amount of boron that was added to the original media. There was a noticeable difference in precipitation for the bacterial cultures compared to the controls with the corresponding alkalinities and mineral combinations. The precipitate analyzed from the Set 4 bacterial culture at pH 8 with ferric citrate and calcium, plus phosphate, contained approximately 27 µg of boron from the original 520 µg of boron per tube, (approximately 5%), compared to the ferric citrate control which had no precipitate formation. Inclusion of boron within the precipitates was also evident in the comparison of the Set 4 bacterial culture at pH 8 composed of amorphous iron, calcium, and phosphate, to the control with the same alkalinity and mineral combination. Results showed the rate of boron precipitation was approximately 4% for the bacterial culture, and 1% for the control, suggesting 3% of the boron within the test tube may have been biologically precipitated. Precipitate analyses of the Set 4 bacterial cultures with the mineral combination of amorphous iron and calcium, plus
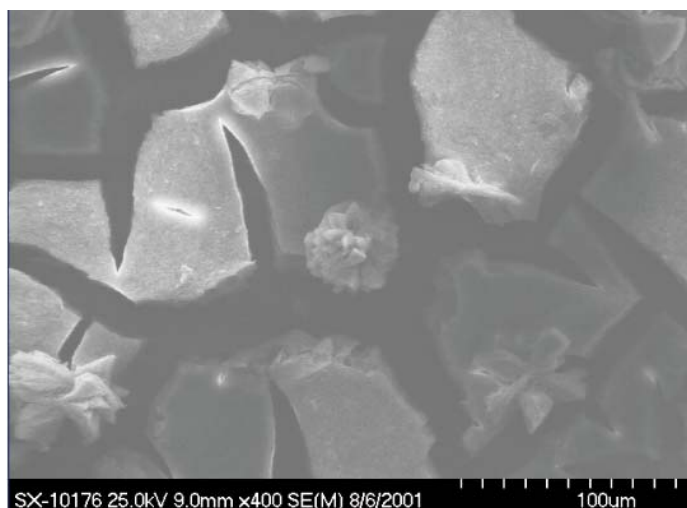
Figure 1A. SEM image showing Bacterial Culture precipitate from tube for Set 2 at pH 7 containing Ferric Citrate, Calcium, and Phosphate.
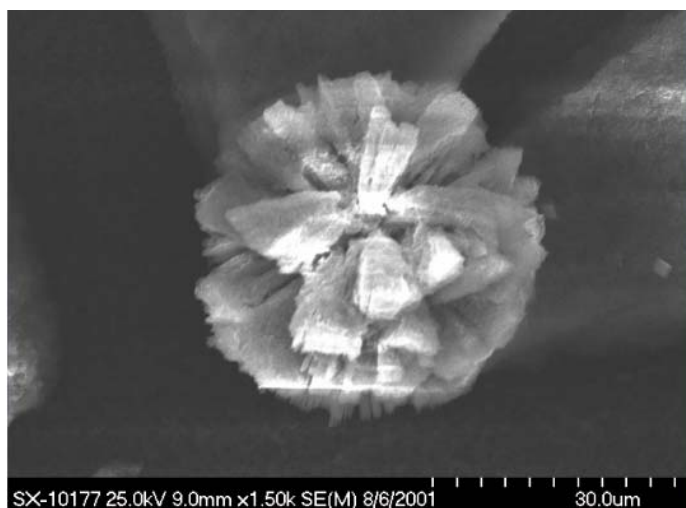
Figure 1B. SEM image showing close-up of select Bacterial Culture precipitate from tube for Set 2 at pH 7 containing Ferric Citrate, Calcium, and Phosphate.
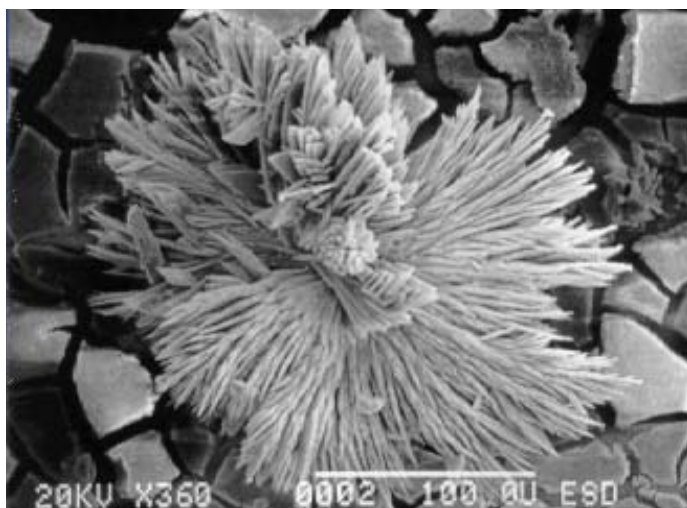
Figure 1C. SEM image showing Bacterial Culture precipitate from tube for Set 2 at pH 7 containing Ferric Citrate, Calcium, and Phosphate.
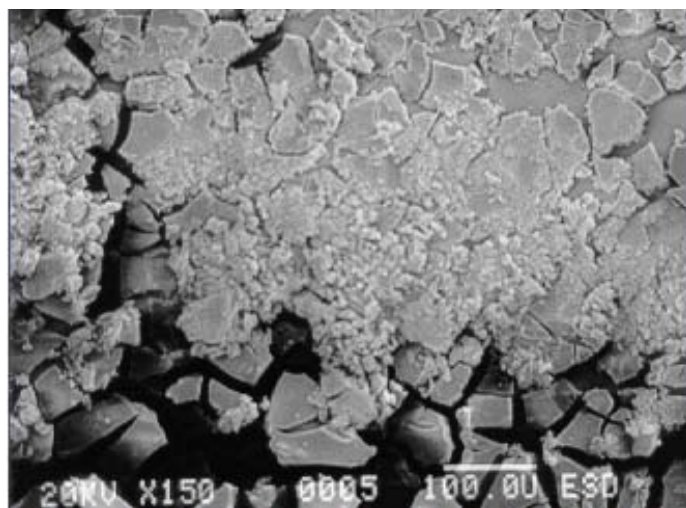
Figure 1D. SEM image showing Bacterial Culture precipitate from tube for Set 2 at pH 7 containing Ferric Citrate, Calcium, and Phosphate.

phosphate, for pH 9 when compared to the pH 7 analysis showed a precipitation rate of approximately 4% to 3%; respectively.

Spectral analyses with the Hitachi S-4700 SEM-EDX, performed on the contents of the tubes for several of the bacterial cultures, showed further evidence of boron precipitation. The precipitates formed at pH 7 in the presence of ferric citrate, calcium, and phosphate, for the Set 2 bacterial culture (see Figures 1A and 1B), were in the shape of spherical rosettes. Formation of various types of precipitates within culture Set 2 was also shown by SEM images (see Figures 1C and 1D), revealing the presence of conical and crystalline precipitates as well. Energy dispersive X-ray analysis (see Figure 1E) of the selected SEM image shown in Figures 1A and 1B, revealed that the precipitate contained large amounts of iron and phosphate, as well as boron. The presence of boron in the precipitate was indicated as a peak located next to carbon on the graph, though due to its close relation with carbon, was subsequently left unlabeled by the graphics program. The SEM images taken of the precipitate formed in the tube for the Set 2 bacterial culture at pH 9 containing amorphous iron, revealed two distinct types of precipitation. The smooth surfaces of the precipitates shown in Figure 2A suggested microbially-mediated precipitation, while the shape of the precipitate in Figure 2B was characteristic of the chemically-mediated precipitate formation of vivianite. Energy dispersive X-ray analysis of the precipitate formed in the tube for the Set 2 bacterial culture (see Figure 2C) showed high levels of carbonate formation in comparison to the presence of iron in the precipitate. The SEM image of the Set 3 bacterial culture at pH 8 containing amorphous iron and calcium (see Figure 3A), also revealed the presence of crystalline precipitates. Formation of additional precipitates over an existing crystalline precipitate (see Figure 3B) was shown in the SEM image of a different section for the same bacterial culture viewed in Figure 3A. The EDX analysis (see Figure 3C) exam-
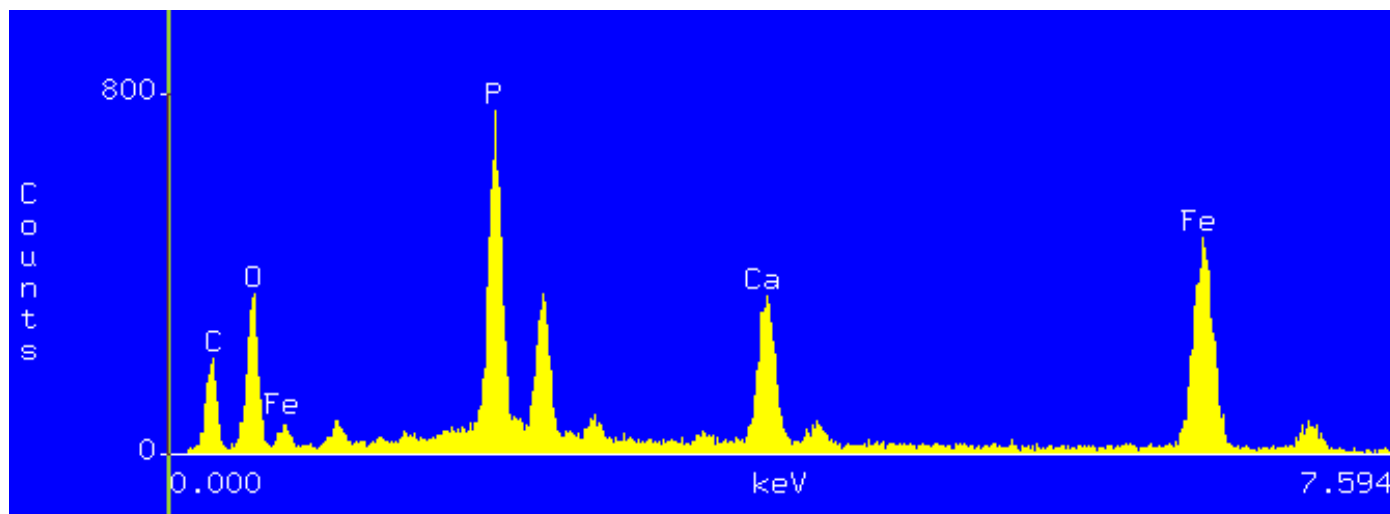
Figure 1E. EDX analysis of bacterial culture precipitate from tubes for Set 2 at pH 7 containing ferric citrate, calcium, and phosphate. Accelerating Voltage: 25 KeV; Take Off Angle: 30°; Live Time: 100 seconds; Dead Time: 15.4

Figure 2A. SEM image showing Bacterial Culture precipitate from tube for Set 2 at pH 9 containing Amorphous Iron.
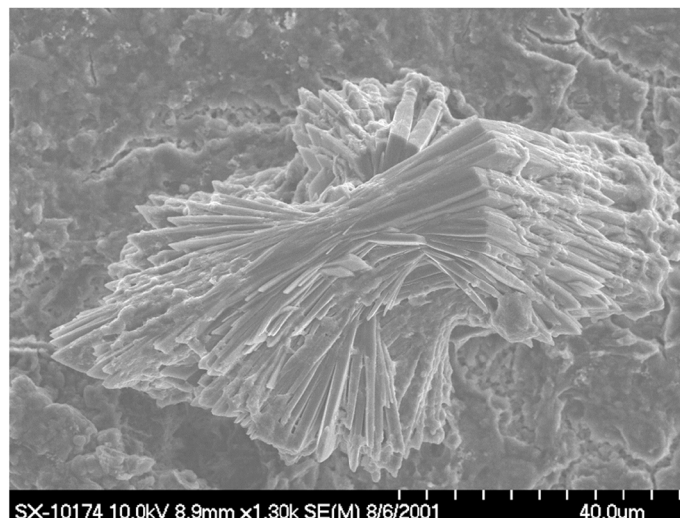
Figure 2B. SEM image showing Bacterial Culture precipitate from tube for Set 2 at pH 9 containing Amorphous Iron.

ining the selected portion of the precipitate shown in the SEM image in Figure 3A for the Set 3 bacterial culture confirmed the existence of boron.

Preliminary analyses performed on the two different algae site samples by Activation Laboratories Limited reported boron concentration of the algae as 52,000 mg/L and 27,400 mg/L, compared to the boron concentration of the water in each sample, which was 2,010 mg/L and 2,680 mg/L, respectively (data not shown). The high levels of boron within the algae compared to the water, suggested the ability of algae to incorporate boron into cells. Inclusion of boron within algal cultures was partially verified by ICP analyses, revealing the presence of boron in the contents of the cultures that remained on the filter disc after filtration, although it was not determined whether the boron was present within the cells or in algae precipitates.

DISCUSSION AND CONCLUSIONS

The microbially-mediated sequestration of boron was demonstrated by the precipitation of insoluble solids in the presence of bacteria, and the incorporation of boron from solution within algal cultures. The method by which bacteria facilitated the precipitation of boron was unclear, although data gathered by SEM-EDX analyses showing high levels of iron in the precipitates, suggested it might have been related to the reduction of iron.

Visual observations of the bacterial cultures provided evidence of biologically-mediated precipitation, shown by the formation of precipitates in tubes containing mineral combinations with ferric citrate, when compared to abiotic controls with identical compositions, which had no visible precipitation. A noticeable change of color from brown to dark gray, which occurred to the precipitates in a majority of the tubes contain-

Figure 2C. EDX analysis of bacterial culture precipitate from tube for Set 2 at pH 9 containing amorphous iron. Accelerating Voltage: 25 KeV; Take Off Angle: 30°; Live Time: 100 seconds; Dead Time: 7.5
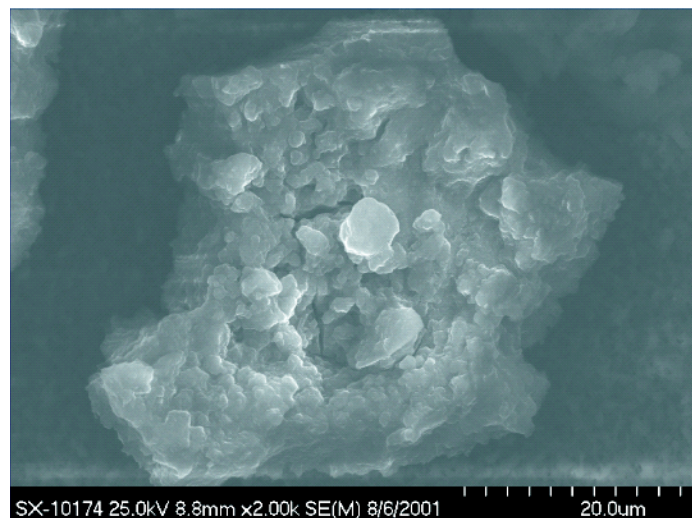
Figure 3A. SEM image showing Bacterial Culture precipitate from tube for Set 3 at pH 8 containing Amorphous Iron and Calcium.

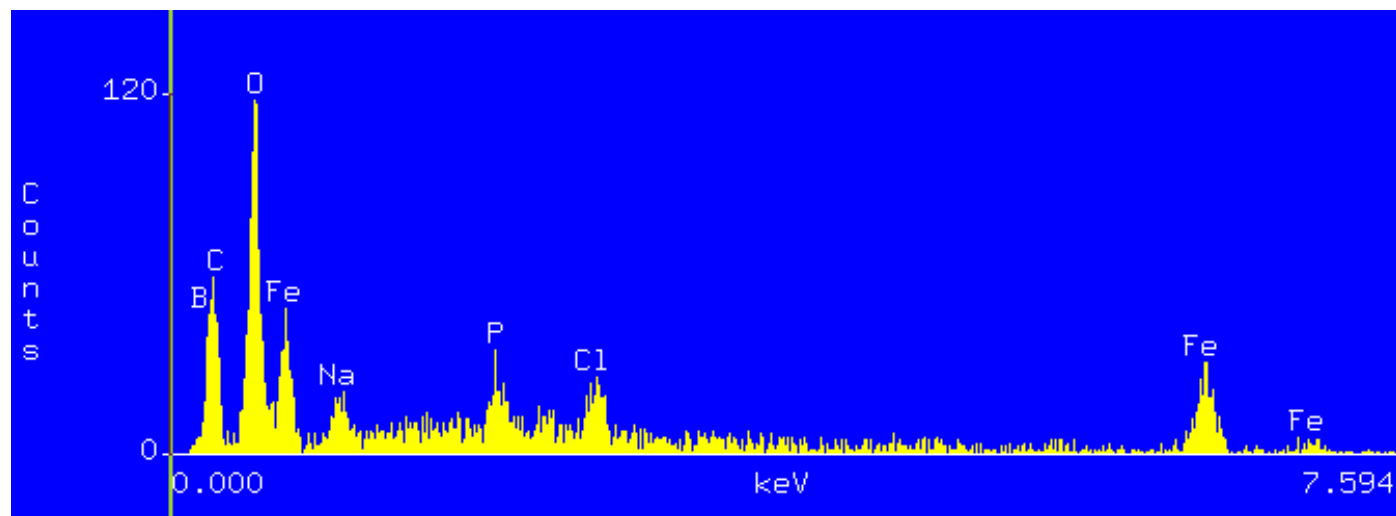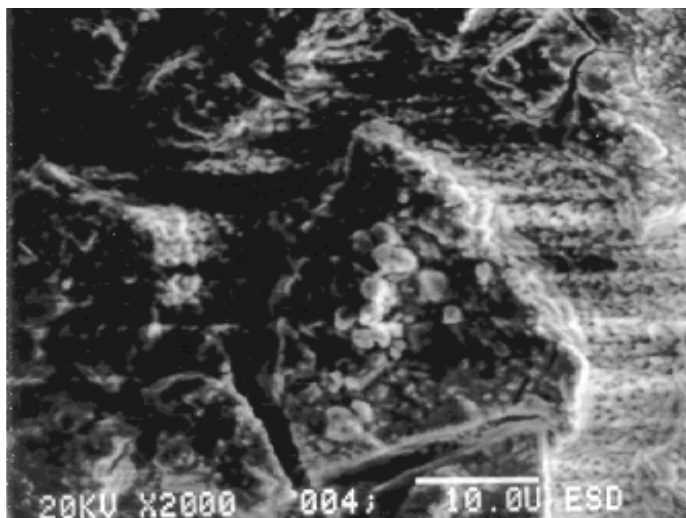**Figure 3B.** SEM image showing Bacterial Culture precipitate from tube for Set 3 at pH 8 containing Amorphous Iron.
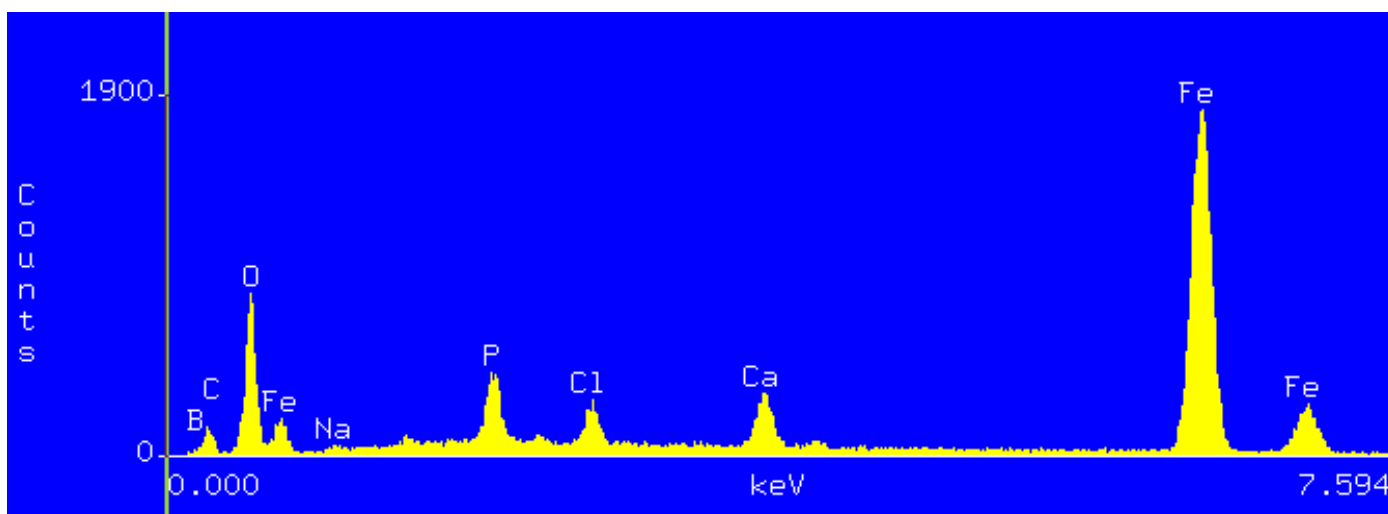
Figure 3C. EDX analysis of bacterial culture precipitate from tube for Set 3 at pH 8 containing amorphous iron and calcium. Accelerating Voltage: 35 KeV; Take Off Angle: 30°; Live Time: 100 seconds; Dead Time: 21.3

ing amorphous iron, after addition of bacteria, suggested that the added bacteria facilitated the reduction of iron. The change in reactivity of amorphous iron following its reduction may have resulted in the formation of additional precipitates containing iron and several of the other added minerals. High levels of iron in select portions of the precipitates were reported by SEM-EDX analyses. Precipitation occurred in a greater number of bacterial cultures containing ferric citrate under pH 9 conditions when compared to tubes at pH 7, suggesting that conditions with higher alkalinity were preferential. In several of the bacterial culture sets, formation of precipitates in tubes containing ferric citrate occurred only at pH 7, suggesting the existence of several different types of bacteria mediating precipitate formation. A greater amount of precipitation in tubes that contained either ferric citrate or amorphous iron, with calcium and phosphate, compared to tubes containing only iron, suggested that calcium and phosphate, as well as iron, were incorporated into the precipitates, as shown by SEM-EDX analyses.

Further evidence of boron precipitation through mediation by bacteria was provided by ICP analyses. Comparison of analyses for bacterial culture precipitates to controls of identical alkalinity and mineral composition show that bacteria served a significant role in increasing the amount of boron precipitation. Data from ICP analyses of the precipitates also revealed that a greater amount of boron precipitation occurred at higher alkalinity, as well as with additional mineral constituents, coinciding with the visual observation that more precipitates had formed.

Mineralogical analyses performed on select sections of several precipitates with SEM-EDX verified the presence of boron, shown in relation to levels of additional minerals present in specific combinations within the various tubes. Energy dispersive X-ray analyses on sections of the bacterial culture precipitates revealed the presence of high levels of iron and phosphate for cultures containing amorphous iron as well as ones with ferric citrate. Although precipitates were formed in the controls containing amorphous iron, the lack of precipitation that occurred in the ferric citrate controls suggested the inclusion of iron and phosphate within the precipitates was facilitated by bacteria. Formation of carbonates through incorporation of CO_2 within the precipitates was shown in the EDX analysis of the precipitate for the Set 2 bacterial culture at pH 9 containing amorphous iron.

The potential application of technologies incorporating principles of environmentally friendly pollution control methods, such as microbially-mediated sequestration of boron into a form that is less reactive and toxic to plants and animals, may provide a way to remediate the effects of environmental degradation while encouraging biological growth and preserving wetland health.

REFERENCES

Brown, Patrick H., & Shelp, Barry J. (1997). Boron mobility in plants. Plant and Soil, 193, 85-101.

Cole, Stephen (1998). The emergence of treatment wetlands. Environmental Science and Technology, 32, 218A-223A.

Hu, Hening, & Brown, Patrick H. (1997). Absorption of Boron by plant roots. Plant and Soil, 193, 49-58.

Nable, Ross O., Bañuelos, Gary S., & Paul, Jeffrey G. (1997). Boron toxicity. Plant and Soil, 198, 181-198.

HYBRID CALORIMETER ALGORITHM DEVELOPMENT FOR PRIMEX EXPERIMENT

Eugene Motoyama[A], Ashot Gasparian, Ph.D.[B], and Aron Bernstein, Ph. D.[A]

ABSTRACT

The PrimEx Collaboration seeks to measure the lifetime of the π^0 meson (neutral pion) at high precision. The decay rate of the pion is considered to be the most fundamental prediction of low-energy quantum chromodynamics (QCD). Pions will be produced by the Primakoff Effect: a few GeV photon interacts with the coulomb field of a nucleus to produce a pion. The pion then decays almost immediately (~10^{-16} seconds) into two photons. The decay photons will be detected by an electromagnetic hybrid calorimeter (HYCAL), an array of lead tungstate and lead glass crystals. An algorithm is needed to calculate the angular separation of the two decay photons (and thus the invariant mass of the pion) from the energies deposited in HYCAL. A GEANT Monte Carlo simulation of the experiment is used to test and develop the algorithm to achieve the best angular resolution. The development of the algorithm is essential to the PrimEx project.

INTRODUCTION

Agreement between theoretical predictions and experimental results is the essence of a good theory. The modern theories of quantum physics have survived decades of experiments. Textbooks boast that predictions of quantum theory and their corresponding experimental measurements show an amazing amount of agreement. Yet some of these predictions have not yet been tested with high precision. One of these, the lifetime of the π^0 meson (neutral pion), is a fundamental prediction of low-energy quantum chromodynamics (QCD). All previous experiments have measured this value with levels of precision around 10%. With the modern technology, it has become possible to conduct a higher-precision experiment. The goal of the PrimEx Collaboration is to measure the π^0 lifetime to within approximately 1.4%. The PrimEx experiment thus pins down this important piece of particle data.

QCD is the theory of the nuclear strong force and deals with the interaction of quarks. The familiar proton and neutron (examples of baryons) consist of three quarks, whereas mesons, such as the π^0, consist of two. The π^0 is the lightest of all mesons and usually decays into two high-energy photons (gamma rays). It has an extremely short lifetime of about 10^{-16} seconds, and it is therefore difficult and unfeasible to set up a high-precision experiment to directly measure the time of decay. The PrimEx Collaboration will instead make use of the Primakoff Effect (Primakoff, 1951). The Primakoff Effect is a form of photopion production; a high-energy photon interacts with the coulomb field of a nucleus to produce a π^0 meson (Figure 1). This is essentially the reverse action of the $\pi^0 \rightarrow \gamma\gamma$ decay, and the cross-section of the outgoing π^0 angle (θ_π) can be used to extract the lifetime of the π^0 meson.

The PrimEx experiment will take place in Experimental Hall B at the Thomas Jefferson National Accelerator Facility (Jefferson Lab),

and will utilize the Hall B photon tagging system. The photon beam hits a Primakoff target (a thin, meticulously prepared sheet of carbon-12, tin-116, or lead-208) to produce the pions, which almost immediately decay into pairs of photons. These pairs of photons hit the PrimEx Hybrid Calorimeter (HYCAL), a matrix of 663 lead glass Cherenkov counters and 480 lead tungstate ($PbWO_4$) scintillating crystals (Figure 2). HYCAL essentially detects the amount of energy that is deposited in each crystal. The incidence positions of the photons are calculated from this data from HYCAL. The cross section of θ_π is then extracted, and the rest mass of the pion is deduced. The pion lifetime can then be calculated from the spectral width (the energy spread) of the pion rest mass. (The
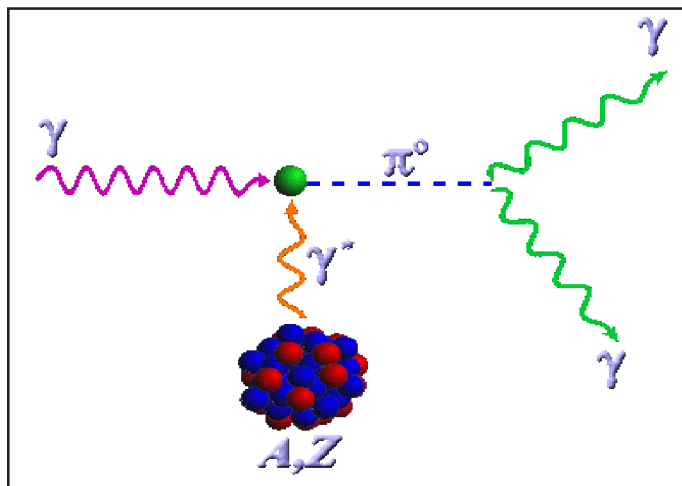
Figure 1. An illustration of the Primakoff Effect
A high-energy photon (γ) interacts with the coulomb field (γ*) of a nucleus (A,Z) to produce a π^0 meson, which then decays into two photons.

A: Massachusetts Institute of Technology, Cambridge, MA; B: Thomas Jefferson National Accelerator Facility, Newport News, VA

lifetime τ of a decay and the spectral width Γ of the rest mass of the decaying particle are intimately related through the Energy-Time Uncertainty Principle: $\tau \cdot \Gamma = \hbar / 2$.) An algorithm must be developed for the task of reconstructing the incidence positions of the photons on HYCAL from the energy data. Since the goal of the experiment is high precision, it is essential that this algorithm be as accurate as possible.

METHODS

Using GEANT, a physics simulator developed by CERN, a Monte Carlo simulation of the PrimEx experiment was used to test the algorithm for reconstructing the incidence positions of the photons (Figure 3). In the simulation, photons ranging from 0.5 GeV to 6 GeV are directed perpendicularly towards HYCAL. (The x and y directions run along the face of HYCAL while z is the direction of the beam.) In each run, the photon generation point (and thus the photon incidence position) is varied in the x direction from the center of one module to the center of the next module. This is done both for the lead glass counters and for the lead tungstate scintillators. Each run consists of roughly 2000 photon-generation events, and in each event the resulting shower of particles in the detector is tracked down to 0.1 MeV.

When a photon hits the calorimeter, most of the energy is deposited in the modules nearest the position of incidence (Figure 4). Reconstructing the incidence position first requires a cluster-finding algorithm, which identifies the modules whose energies are associated with a particular incident photon. Other members of the PrimEx Collaboration are developing a good cluster-finding algorithm, but a very simple algorithm suffices for this one-photon simulation. The module with the most energy deposited is found, and the cluster consists of that module and the eight directly surrounding it. Thus, in the methods that follow, only a three-by-three matrix of modules is used for the calculations. For simplicity, only the reconstruction of the x-coordinate is shown. Since HYCAL is symmetric along the x and y directions, the y-coordinate is reconstructed in a similar manner.

Two methods of reconstructing the incidence positions of the photons were used in developing the algorithm. The first is the linear method, in which the incidence position is estimated to be the center of gravity of the shower

$$x_{\text{calc}} = \frac{\sum_i w_i x_i}{\sum_i w_i} \quad (1)$$

where x_i is the x-coordinate of the center of the i-th module and w_i is taken to be E_i, the energy deposited in the i-th module (Awes et al. 1992). The second method uses a logarithmic weighting scheme. The equation is the same as above, but instead of using $w_i = E_i$, the weights to be used are given by the following expression:

$$w_i = \max\left\{0, \left[w_0 + \ln\left(\frac{E_i}{E_{\text{total}}}\right)\right]\right\} \quad (2)$$

In this equation, E_i is the energy deposited in module i, E_{total} is the total energy in the cluster ($\sum_i E_i$), and w_0 is a free parameter (Awes et al. 1992).

The algorithm developed varies slightly from the equations above. In the calculation of the x-coordinate, for example, the first step is to add the energies of the modules with the same x-value.
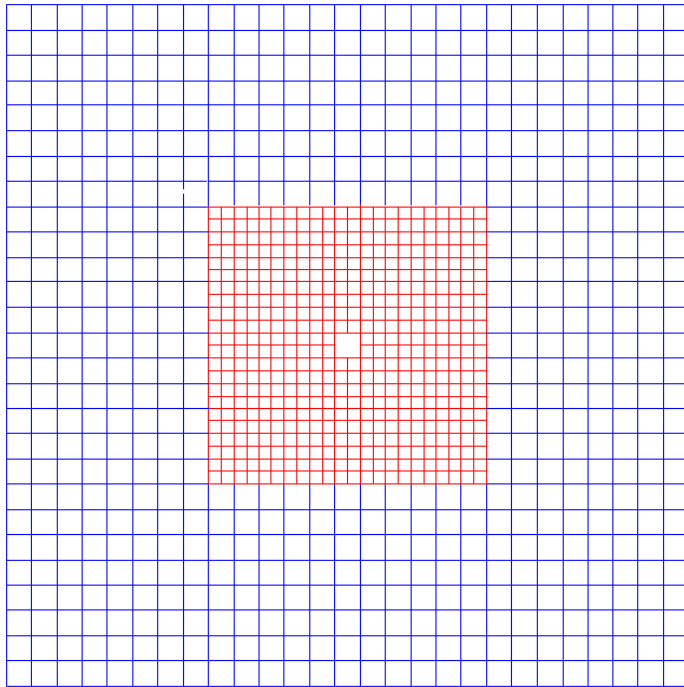
Figure 2. An illustration of the Hybrid Calorimeter (HYCAL) The front face of HYCAL. The outer modules are lead glass; the inner modules are lead tungstate. The square in the center is the beam hole.
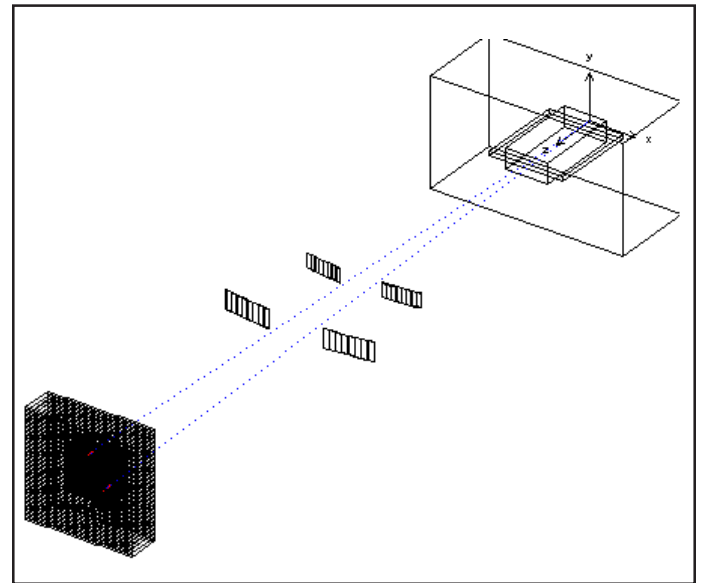
Figure 3. The GEANT setup of the PrimEx experiment. The target sits at the origin of the axes shown. HYCAL is shown at the bottom left. A typical trajectory of a pair of photons is also shown. The large box near the target is a dipole magnet, which deflects the electron-positron pairs that are produced. Between the dipole and HYCAL are the pair spectrometers which detect the electron-positron pairs and thus monitor the photon beam flux.

Since the cluster (in this study) is a three-by-three matrix, the result is three values of energy: E_{left}, E_{center}, and E_{right}. Equation 1 is then applied to these values. In the linear version, the end result is exactly the same (the two approaches are mathematically the same). The logarithmic version yields an answer that is slightly different, but the algorithm is more efficient: in this case three logarithmic computations instead of nine. It was found that this slightly altered logarithmic method had a negligible effect on the results.

RESULTS

When the calculated position is plotted against the true incidence position, the result for the linear method is a well-known S-curve (Figure 5). The S-shape arises because, in reality, the energy of the particle shower formed in the modules drops off exponentially with distances. The result is that there is not enough weight given to the energies of the outer modules, and the reconstructed value does not change much as the incident position is varied. When the incident position approaches the edge between two crystals, the reconstructed value suddenly approaches the true value (since now there are two crystals with approximately equal energies). In the figure, the units for the axes are half-module lengths away from the center of the module (i.e. –1 is the left edge, 0 is the center, and 1 is the right edge). The logarithmic method yields an S-curve situated nearer the ideal 45-degree line (for which the reconstructed value equals the true value) (Figure 6).

In both the linear and logarithmic cases, a polynomial curve fit was used to straighten out the S-shape, to complete algorithms with the best possible agreement between reconstructed position and true incident positions of the photons. Since we must eventually consider energies other than 4.0 GeV, the final version of the algorithm will most likely have an energy-dependent empirical formula for the curve fit. The polynomial fit is as follows:

$$x_{\text{fit}} = a + b(x_{\text{calc}} - 0.5) + (2 - 4a)(x_{\text{calc}} - 0.5)^2 + (4 - 4b)(x_{\text{calc}} - 0.5)^3$$
(3)

In this equation, x_{fit} is the calculated x-coordinate after the curve fit, x_{calc} is the direct result of the linear or logarithmic methods, and a and b are the two parameters of the fit. These values are for the positive values of x (in the units mentioned above), and it is assumed that the negative values are symmetrical. Simply put, the equation is a third-order polynomial fixed at (0,0) and (1,1) with a as the value of x_{fit} at 0.5 (halfway between the center and the edge) and b as the slope of the curve at this same point. Figure 7 shows the curve fit being applied, and Figure 8 shows the results of straightening out the S-curve.

The linear method and the logarithmic method (using a few different values for w_0) were tested for the resolution of incidence position. In each case, the curve fit was applied and a histogram of $x_{\text{calc}} - x_{\text{true}}$ was taken (Figure 9). When tested on the lead tungstate crystals, the standard deviation for $w_0 = 3.25$ was $s = 0.114$ (in the relative units) while $\sigma = 0.128$ for the linear method. Since the lead tungstate crystals are 2.125 cm wide, the resolution is approximately 0.12 cm on the face of the calorimeter. HYCAL is 700 cm away from the target, so this position resolution translates to an angular resolution of 0.00017 radians or 0.01 degrees.
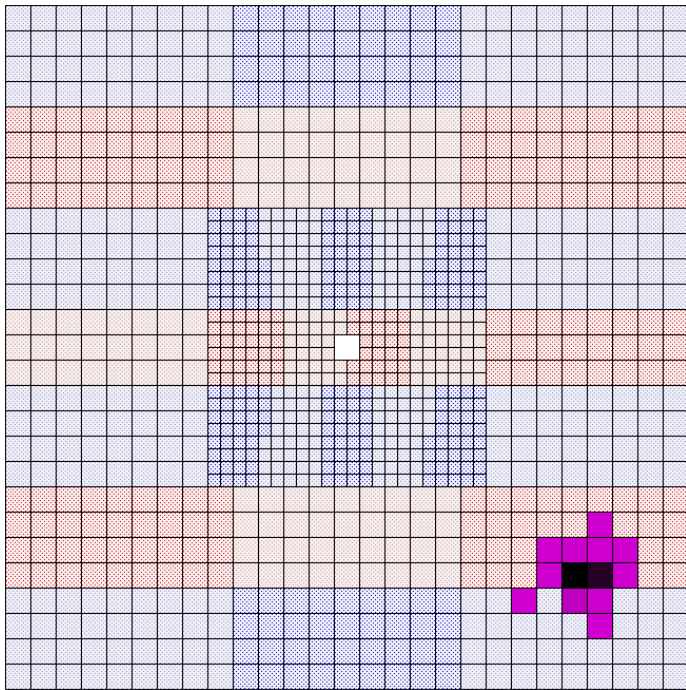
Figure 4. An example of a cluster of deposited energies from a Monte Carlo simulation.
A 4.0 GeV photon was directed at lead glass module (5,5). The modules are numbered starting at the bottom right of each part of the calorimeter.
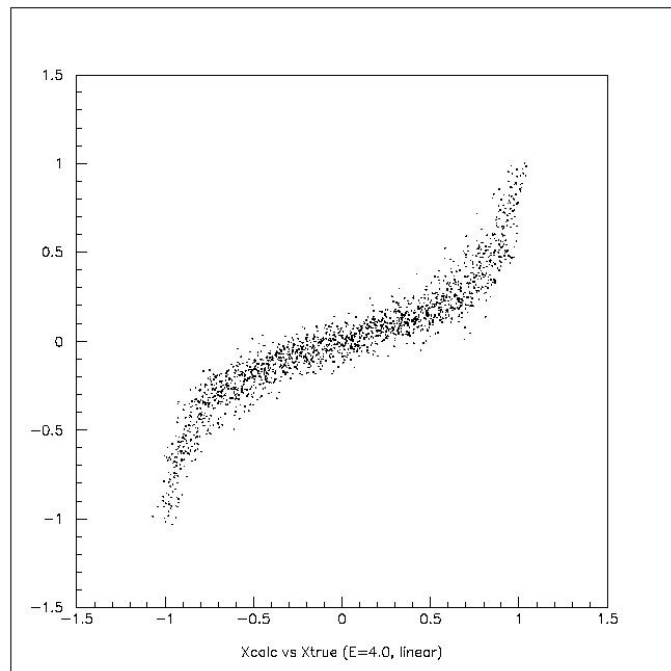
Figure 5. The linear method of incidence position reconstruction. 4.0 GeV photons on lead tungstanate. The units are half-module lengths away from the center of the module (i.e., –1 is the left edge, 0 is the center, and 1 is the right edge).
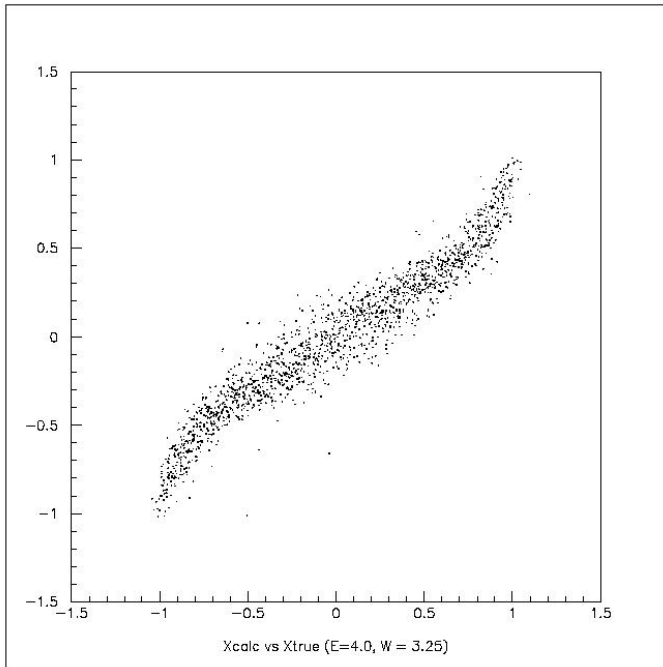
Figure 6. The logarithmic method of incidence position reconstruction. 4.0 GeV photons on lead tungstate. Logarithmic method with w_0= 3.25.
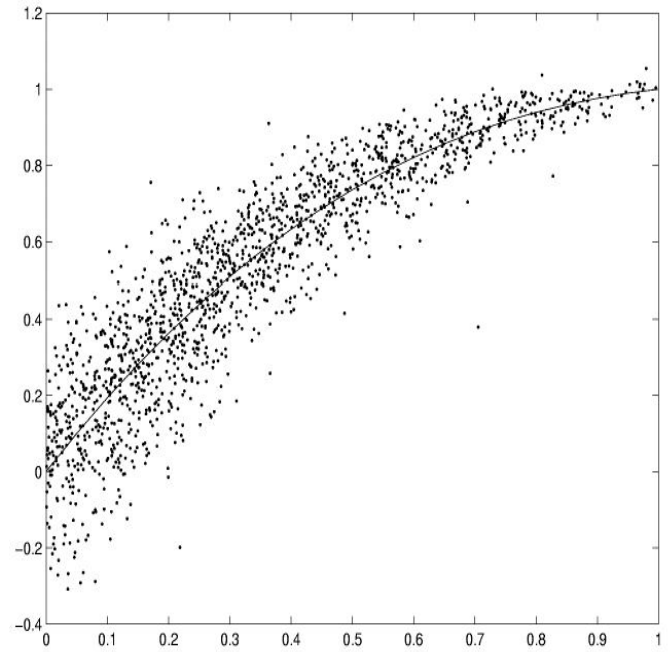
Figure 7: The curve fit applied to the results of the logarithmic method. 6.0 GeV photons on lead glass. Logarithmic method with w_0= 3.25.
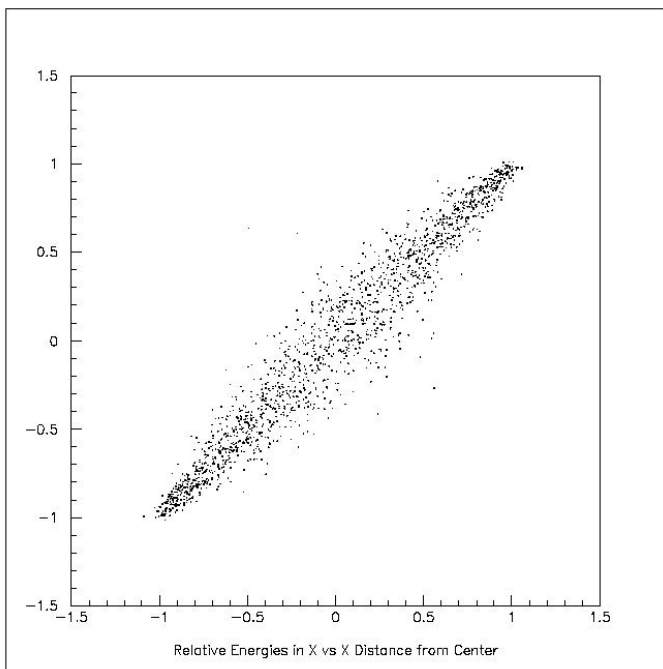
Figure 8. The results of applying the curve fit to the logarithmic method 4.0 GeV photons on lead tungstate. Logarithmic method with w_0= 3.25.
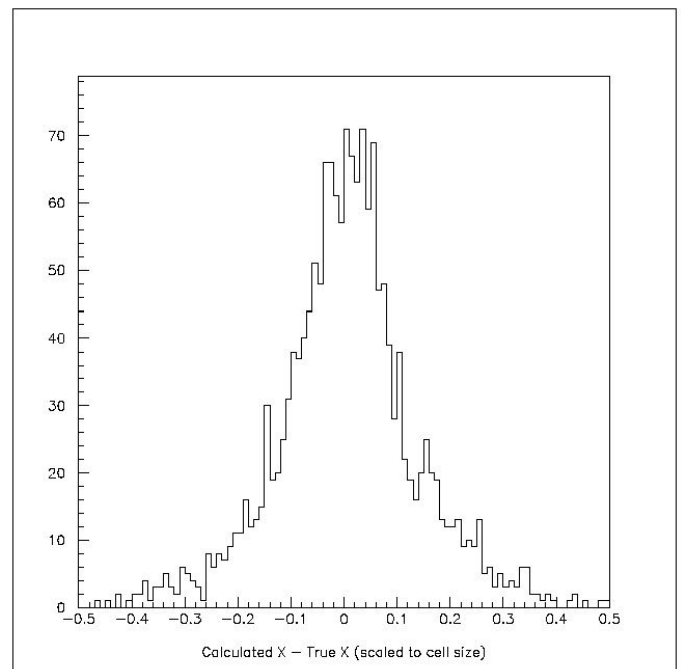
Figure 9. The histogram for $x_{calc} - x_{true}$ after applying the curve fit. 4.0 GeV photons on lead tungstate. Logarithmic method with w_0= 3.25.

DISCUSSION AND CONCLUSION

Based on the results, the final algorithm should have the following steps: A good cluster-finding algorithm should be followed by adding the "columns" or "rows" of energies for the calculations of the x-coordinate and y-coordinate respectively; the logarithmic method of reconstructing the incidence position should be implemented with an appropriate value of w_0; and an empirical equation based on the results of curve-fit testing should be applied to give the final reconstructed incidence positions. From these positions, the rest mass of the π^0 will be determined, which will be used to extract the θ_π cross-section.

The algorithm is by no means in its finished state. Many more tests will need to be done to further develop the algorithm in order to yield the best resolution for position reconstruction. First, the best values for w_0 must be found for both lead tungstate and lead glass modules. The value of 3.25 seems to be relatively good for the lead tungstate, but more testing needs to be done. Second, the empirical formula to "straighten out" the results from the logarithmic method must be realized. The formula must be energy-dependent and will differ for the lead tungstate and lead glass cases. The empirical formula will be based on the two parameters (a and b) mentioned above, and so far there seems to be a smooth dependence of these parameters on the energy (Figure 10). After these tests are done, an actual Monte Carlo simulation of the Primakoff Effect will be performed to determine the resolution of HYCAL.

There are yet other factors that must be taken into consideration. In the current simulation, light attenuation within the crystals is not yet taken into account. Cherenkov light produced at the plane of the detector, for example, will actually yield a smaller signal than the same amount of light produced near the end of the module (nearer the photomultiplier tubes). The effect of light attenuation on the resolution should be determined. It is also uncertain, as yet, whether the plane of the lead tungstate insertion array will be flush with the lead glass array. It should be determined whether having the lead tungstate array recessed by a few centimeters will affect or even improve the resolution.

Finally, since the GEANT simulation cannot match reality perfectly, the detector must actually be tested in the line of the photon beam to see what adjustments must be made to the position-reconstruction algorithm.
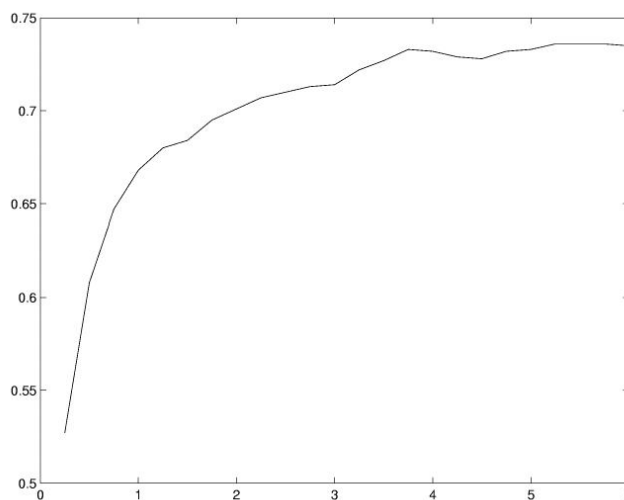
Figure 10. Energy dependence for parameter a in the empirical formula. Value of parameter a versus photon energy (in GeV). Results are for lead glass.

REFERENCES

Awes, T. C., Obenshain, F. E., Plasil, F., Saini, S,. Sorensen, S. P., Young, G. R. (1992). "A Simple Method of Shower Localization and Identification in Laterally Segmented Calorimeters." Nuclear Instruments and Methods in Physics Research. Vol. A311, pp. 130-138.

Primakoff, H. Physical Review Letters. 81, 899 (1951).

The PrimEx Collaboration. (2000). "A Precision Measurement of the Neutral Pion Lifetime via the Primakoff Effect: Conceptual Design Report. Jefferson Lab Experiment E99-014." http://www.jlab.org/primex/documents/PrimEx_CDR.ps

OBJECT-ORIENTED ANALYSIS CODE FOR HALL A VERTICAL DRIFT CHAMBERS

JONATHAN ROBBINS[A] AND JENS-OLE HANSEN, PH.D.[B]

ABSTRACT

The high-resolution spectrometers in Jefferson Lab's Hall A use vertical drift chambers to determine charged particle tracks. The current analysis code for the vertical drift chambers is difficult to maintain and modify, which has prompted the development of an object-oriented version, which will be easier to maintain and more able to adapt to changes in the detector configuration. However, the object-oriented approach involves using a slightly different algorithm than ESPACE, which could lead to different results. In this project, a preliminary version of an object-oriented analysis program for the vertical drift chambers is created and its results are compared to the existing software to determine the impacts of the differences in the reconstruction algorithms. In addition, the algorithms themselves are compared, and minor differences in track reconstruction techniques are reported.

INTRODUCTION

Jefferson Lab is one of the few nuclear physics research facilities in the world to feature a continuous electron beam, which allows unique opportunities to study subatomic structure. The largest of Jefferson Lab's three experimental halls, Hall A, contains two High Resolution Spectrometers (HRSs), which can be used to make precision measurements of the momentum and origin of scattered charged particles. Each of the HRSs has a set of Vertical Drift Chambers (VDCs), which are used to detect charged particle tracks in the focal plane of the spectrometer. The software used to analyze the data collected by the VDCs and extract momentum and position information of particles is discussed in this paper.

Until now, Hall A has been using a software package called ESPACE (Offermann, 1997) for track reconstruction. ESPACE is written in FORTRAN and, for various technical reasons, is difficult to maintain and to modify when changes in the detector configuration are necessary. As a result, an effort has been started to duplicate the capabilities of ESPACE using object-oriented programming. This project is called the C++ Analyzer Project. By using object-oriented techniques, the analysis code is expected to become more maintainable and flexible. The C++ analyzer is based on ROOT (Brun & Rademakers, 2001), an object-oriented data analysis framework that has been developed at CERN since 1995 and that is specialized for physics applications.

The goal of this project is to determine the effect of small differences between the C++ analyzer algorithm and the ESPACE algorithm. The C++ analyzer's object-oriented design encourages encapsulation of data and processing at the object level, while ESPACE uses global processing and does not strongly distinguish separate components of the program. Also, the C++ analyzer was designed to break the analysis into separate coarse and fine tracking stages, rather than having a single stage, like ESPACE.

MATERIALS AND METHODS

The code for the object-oriented analyzer was written in C++ and compiled using the GNU C++ compiler (gcc/g++ 2.91) on a Pentium III 650 MHz computer running RedHat Linux 6.2. ROOT was used to view the results of the object-oriented code. ESPACE was used to analyze the data as a reference, and Paw++ (CERN, 2001) was used to view the results from ESPACE. The input data were obtained as part of the optics study for Hall A experiment E97-111 in September 2000. The data analyzed here were taken with the left arm HRS, using a 9-foil graphite target. The target foils are positioned perpendicular to the beam, and the distance between the foils is 3.988 cm. A sieve slit with 7x7 holes was used to block portions of the beam at the spectrometer entrance, which produces peaks in the angular spectra of the data.

As mentioned earlier, the C++ analyzer uses an object-oriented approach to implement data analysis functions. One of the first steps in the design process of the VDC detector code, therefore, was to define a set of suitable C++ classes, their features, public interfaces, and their interactions with each other. The classes, which are described in detail below, were chosen so as to closely correspond to the physical components of the VDCs and objects relevant to the analysis.

Once the class design was in place, the next step was writing a prototype so that the program could successfully go through each step in the analysis process. Once this was completed, the more challenging task of refining the analysis code began. Initially, it was sufficient to find results that were clearly wrong based on physical reasons and to track down the causes of these errors. Next, ESPACE was used to analyze the same data as the C++ analyzer to look for major differences in the results, which would indicate serious errors in the C++ algorithm. Finally, once there was sufficient agreement between the ESPACE and C++ analyzer results, subtle differences were investigated.

A: University of Richmond, Richmond, VA; B: Thomas Jefferson National Accelerator Facility, Newport News, VA

The VDCs are the most sophisticated detectors in the spectrometers, since they are designed to provide sub-millimeter track position resolution. The Hall A VDC packages consist of 4 gas-filled wire chambers with 368 active wires each (Leathers, 1996; Fissum, 2001). The gas is a mixture of 50% argon and 50% ethane by volume (62% and 38% by mass). The wire chambers are arranged into an upper VDC and a lower VDC, each of which consists of two wire planes whose wires are oriented at 90° to each other. The wire planes are tilted at 45° to the nominal beam direction such that an average of 5 wires receive a signal for each event. The convention used in this paper is that the direction perpendicular to the wires in the first and third wire planes (the "U" wire planes) is the u direction and the direction perpendicular to the wires in the second and fourth wire planes (the "V" wire planes) is the v direction.

When a particle passes through a wire chamber, it creates positively charged ions and free electrons. The wires are kept at ground potential and negatively charged high voltage plates are located above and below the wires, so that the electrons are attracted to the wires (Liyanage, 1999; Wechsler, 1996). As the electrons move, they accelerate and collide with other gas molecules which ionizes them. When this process occurs near the large electric field gradients created by the wires, the result is an avalanche of electrons that strikes the wire, inducing a signal (or "hit") on that wire. The signal is then preamplified and discriminated before reaching a time-to-digital converter (TDC). The TDCs measure the time elapsed between the signal's arrival and the arrival of a common stop signal, triggered by the particle passing through a scintillator panel. As a result, the time resolution of the TDCs, 0.5 ns, determines the time resolution of the VDCs. The time measured by the TDCs can be converted into the so-called drift time, i.e. the time taken for the electrons freed by the charged particles to drift to a wire. The drift time information can be used to determine the position and direction of the particle crossing each wire plane. This information, in turn, allows reconstruction of the particle's track.

TRACK RECONSTRUCTION ALGORITHM

General Track Reconstruction

Track reconstruction for both ESPACE and the C++ analyzer involves the following basic steps. First, hits on adjacent wires, presumably caused by the same particle, are grouped into a "cluster." Next, clusters found in each of the 4 wire planes are matched, and the position at which the track crossed each wire plane is determined. To find this position, it is first necessary to apply an algorithm to convert the drift times measured by the TDCs into the drift distance of the electrons, where the drift distance is defined to be the distance perpendicular to the wire plane from a wire to the particle track. To do this conversion accurately, corrections for the angle of the track and the nonuniformity of the electric field near the wires must be included (Wechsler, 1996). Once drift distances have been calculated, a linear fit is used to determine where the track crossed each wire plane, and the position and direction of the particle when it crossed the focal plane are calculated.

The software uses the u-v and detector coordinate systems

(Offerman, 1997) before producing a final result for the position and direction of the tracks in the TRANSPORT (Brown et al., 1983) coordinate system. In this system, z_T is the nominal direction of the beam, x_T is the direction the beam moves when its momentum is increased an infinitesimal amount, and y_T is the direction appropriate to make a right-handed coordinate system (Figure 1). The angle θ_T is measured from the z-axis to the projection of the track in the xz-plane, and the angle ϕ_T is measured from the z-axis to the projection of the track in the yz-plane. Straightforward trigonometry gives the following equations, used to convert from the u-v coordinate system (u, v, θ_u, θ_v) to TRANSPORT coordinates ($x_T, y_T, \theta_T, \phi_T$):

$$x_T = \frac{u \sin\phi_v - v \sin\phi_u}{\sin(\phi_v - \phi_u)} \cos\rho + z_D \sin\rho$$

$$y_T = \frac{v \cos\phi_u - u \cos\phi_v}{\sin(\phi_v - \phi_u)}$$

$$\tan(\rho + \theta_T) = \frac{\tan\theta_u \sin\phi_v - \tan\theta_v \sin\phi_u}{\sin(\phi_v - \phi_u)}$$

$$\tan\phi_T = \frac{\tan\theta_v \cos\phi_u - \tan\theta_u \cos\phi_v}{\sin(\phi_v - \phi_u)\cos\rho + (\tan\theta_u \sin\phi_v - \tan\theta_v \sin\phi_u)\sin\rho}$$

(1)
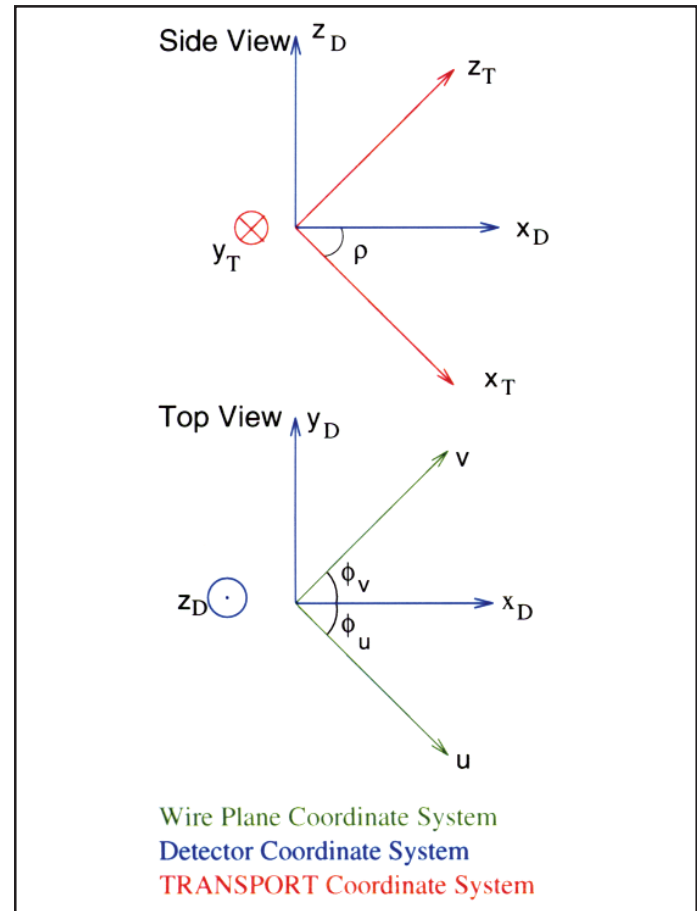
Figure 1. The TRANSPORT coordinate system used to reconstruct tracks in the C++ analysis code.

In the previous equations, ϕ_u and ϕ_v are the angles that the u and v axes make with the projection of the x direction into the uv-plane, ρ is the angle between the detector plane and the z_T axis, z_D is the distance from the focal plane of the spectrometer to the U wire plane in which the track is being reconstructed, and θ_u and θ_v are the angles that the track makes with the u and v axes. In addition, the TRANSPORT coordinates are then projected into the TRANSPORT plane ($z_T = 0$) using

$$x'_T = x_T(1 + \tan\rho\tan\theta_T)$$
$$y'_T = y_T + \tan\rho\tan\phi_T x_T$$

(2)

where x'_T and y'_T are the projected coordinates of the track.

Object-oriented Track Reconstruction

This section describes in detail the C++ analyzer code to convert the raw drift times into actual track information. The first stage is decoding the raw data for each event into hits in a specific wire plane with their associated drift times and wire numbers. The second stage is the "coarse tracking" stage, in which a rough estimate of the particle's track is determined. This stage is particularly useful for situations when a quick estimate of results may be desirable. The third stage is the "fine tracking" stage. During fine tracking, the position and direction of the particle track found in the coarse tracking stage is refined.

During the coarse tracking, the hits are grouped into clusters by identifying hits with no more than one wire separating them. Once clusters have been found, clusters in the U wire plane are paired with clusters in the V wire plane by finding clusters whose hits with largest TDC values had drift times closest to each other. Equation 1 is then used to obtain an estimate of where the track found in the lower VDC would intersect with the upper VDC, and vice versa, and these estimates are used to match the clusters in the upper and lower VDCs. Once clusters from the upper and lower VDCs are matched, the global angles based on the cluster positions in each plane are calculated.

During the fine tracking stage, a drift-time-to-drift-distance (t-x) conversion algorithm is applied to the hits. Changing the t-x conversion algorithm can be accomplished very simply by using class inheritance. In principle, each wire could be associated with a different algorithm. The algorithm used in this analysis employs a polynomial in the angle of the track to provide a correction to the drift distance, where the angle of the track is obtained during the final step of the coarse tracking. Once the drift distance for each hit is known, a linear fit is carried out to calculate the point where the track crossed the wire plane (Figure 2). Equations 1 and 2 are applied again to match clusters from the lower and upper VDCs, and a final calculation of the track is made.

CLASS DESCRIPTION

The classes in the C++ analyzer closely correspond to the physical layout of the detector and to the logical structures that arise from the analysis algorithm. Figure 3 shows the class ownership hierarchy.

• *THaVDC*: The VDC class is the top class in the hierarchy, representing the entire VDC package of a single spectrometer. It contains data applicable to the entire VDC and two UV plane objects. It also contains functions responsible for the final calculation of track position and direction.

• *THaVDCUVPlane*: The UV plane class represents the upper and lower VDCs in the VDC package. Since each VDC has a U and V plane, the UV plane class has two plane objects in addition to other data specific to the VDCs. The UV plane class also generates UV track objects.

• *THaVDCPlane*: The plane class represents an individual wire plane in the VDC package. It contains an array of 368 wire objects, an array of hits, and an array of clusters. The size of the hit and cluster arrays vary with the actual number of hits and clusters. The plane class is responsible for decoding raw data into hits and finding clusters.

• *THaVDCUVTrack*: The UV track describes a track through one of the UV planes. UV tracks are able to search for a partner track in the other UV plane and are considered successfully matched when a track is its partner's partner.

• *THaVDCCluster*: The cluster class describes a cluster of hits. It has an array of pointers to the hits that belong to it. Also,
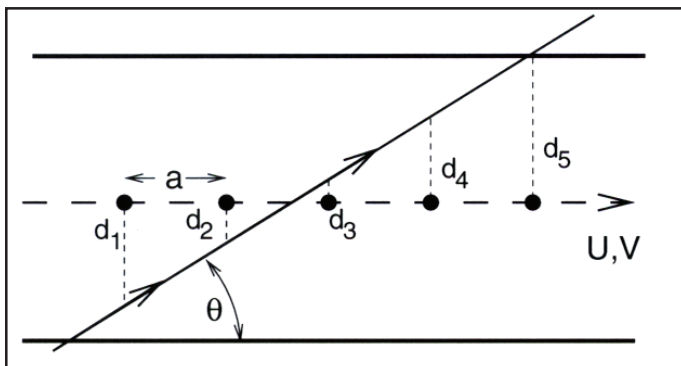
Figure 2. A particle track through a wire plane for a typical 5-wire event. The value d_i is the drift distances for ith wire in the cluster to be hit, a is the wire separation, and θ is the angle of the track with the wire plane.
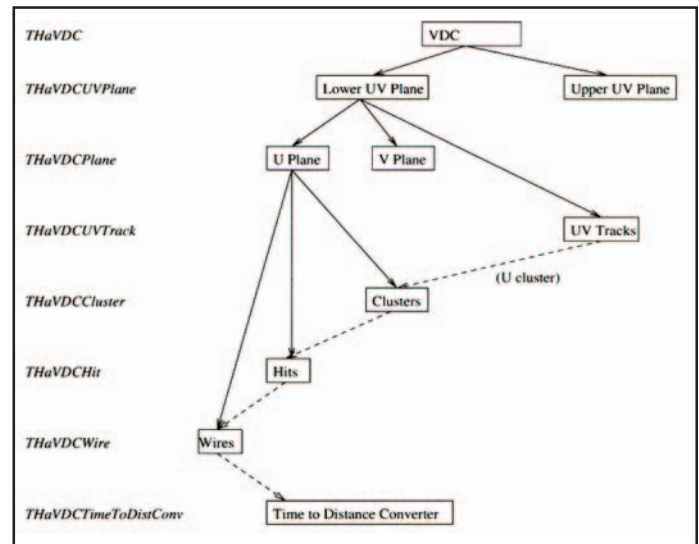
Figure 3. This diagram shows the class ownership hierarchy. The solid arrows indicate classes that are members of other classes. The dashed arrows indicate references to objects of other classes. For example, the VDC class has a lower UV plane object, and hits contain a reference to the wire on which they occurred.

it can perform a linear fit on the hits in order to estimate the point in the cluster where a track intercepts the wire plane and the angle of that track.

• *THaVDCHit*: The hit class represents a single hit on one of the wire planes. It contains the TDC value associated with the hit, the drift time of the electrons that caused the hit, and a pointer to the wire on which the hit occurred.

• *THaVDCWire*: A wire class object represents each wire in the VDC package. Each wire object contains the wire number and position of the wire in the detector. Also, each wire has a pointer to a time-to-distance conversion object for use by hits that occurred on the wire.

• *THaVDCTimeToDistConv*: The time-to-distance conversion class is a base class from which to derive actual *t-x* conversion algorithms. The main feature of the class is a function called `ConvertTimeToDist()`, which takes a drift time and track angle as arguments and returns a drift distance.

RESULTS

Three quantities that are of inherent interest for any VDC are the drift time distribution, the wire efficiency, and the intrinsic timing resolution. The shape of the drift time spectrum for a wire in a VDC is very distinctive. There is a large peak for short drift times due to the increased electric field intensity followed by a long plateau (Wechsler, 1996). Figure 4 shows a sample drift time spectrum for a wire from the VDC package. Other wires show very similar results. The efficiency of a wire can be determined by checking whether or not it fires when the two wires adjacent to it fire. Thus, the wire efficiency is defined by $\varepsilon = \kappa/(\kappa+\lambda)$, where κ is the number of times a wire fires when its neighbors fire and λ is the number of times it does not fire when its neighbors fire (Leathers, 1996). Figure 5 shows the wire efficiency for data with an even distribution of wire hits. The time resolution measures how precisely the firing times of events may be determined. The formula for timing resolution for an event with n hits is $\Delta T = |(t_1-t_2)-(t_n-t_{n-1})|$, where t_i is the time of the ith hit (Fissum et al., 2000). The time resolution as determined by the C++ analyzer is shown in Figure 6.

As mentioned, the data used to compare the ESPACE and C++ analyzer results were part of an optics study with a 9-foil carbon target. Results for both ESPACE and the C++ analyzer are shown in Figures 7-10. For this configuration, one expects a single narrow peak in the x_T direction because x_T depends mostly on the momentum of the scattered electrons, which is nearly constant here (elastic scattering from carbon). The clean peaks in the θ_T spectrum arise because the sieve slit collimator selects well-defined out-of-plane scattering angles at the target. Both y_T and ϕ_T depend in a complex way on the scattering position along the beam and the in-plane scattering angle at the target, and so one expects spectra with some structure due to the sieve slit pattern and target foils. The visible peaks are smeared because the results are projected into the TRANSPORT plane, rather than being in the focal plane of the spectrometer, and because the contributions from the target foils and the sieve slit are convoluted in these one-dimensional spectra. The mean x_T' value of the C++ analyzer results and ESPACE results differ by 2 mm, which is significantly greater than the detector resolution of 0.1 mm. Also, the shape of the x_T' spectra, as seen in Figure 7, is somewhat different,
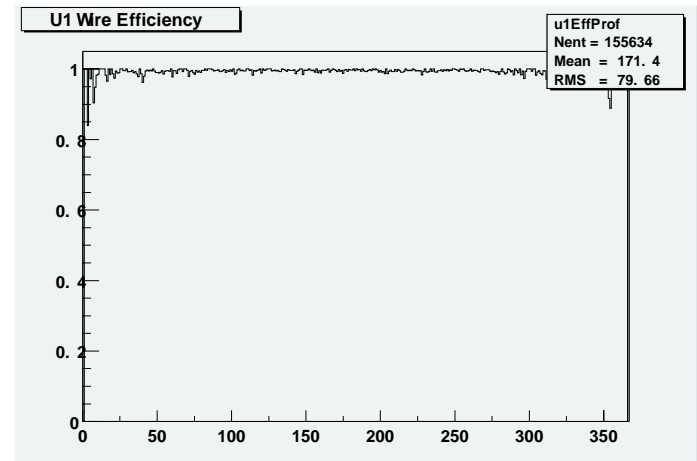
Figure 5. Wire efficiency in the U_1 wire plane, calculated by the C++ analyzer.

Figure 4. Drift time spectrum for wire 233 in the U_1 wire plane, calculated by the C++ analyzer. Note that that there is a peak for short drift times followed by a long plateau, as is expected. The x-axis is in seconds.
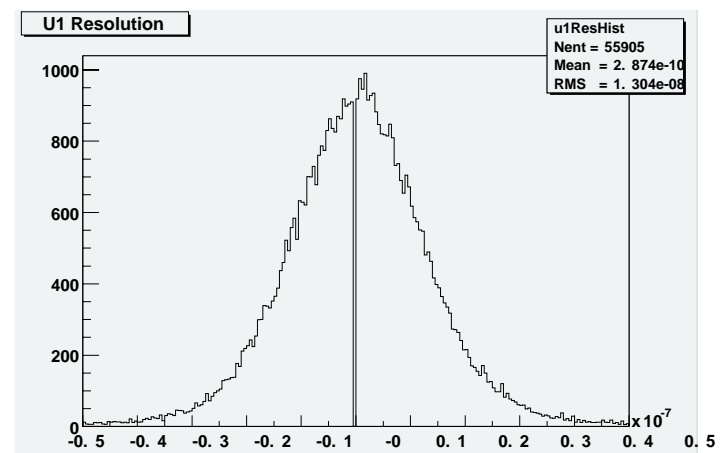
Figure 6. Time resolution for the U_1 wire plane, calculated by the C++ analyzer. The x-axis is in seconds.

especially on the right edge. Since both algorithms are operating on the exact same data, this difference is purely due to differences in the algorithms. The ESPACE results are likely to be more accurate, since ESPACE has been in use for many years, but the best way to determine the accuracy of the two systems would be to test them on theoretical data, where the correct answer is known. In the y_T' direction, 7 peaks are visible in the focal plane, but the projection of these values into the TRANSPORT plane (Figure 8) makes the peaks overlap significantly. The shape of the C++ analyzer and ESPACE results are very similar, though there is a small shift in the results, which may be due to the fact that x_T' and y_T' are coupled (Equation 2). The C++ analyzer results for θ_T and ϕ_T agree very well with the ESPACE results (Figures 9 & 10).

CONCLUSION

The results show that there are indeed differences in the results from the C++ analyzer and ESPACE. The differences are not very large, but they are significant, since the resolution of the detectors is on the order of 0.1 mm. The reason for the differences is purely due to differences in the algorithms, since both act on the same set of data. Hence, it is vital to track down the causes of the differences and determine which algorithm is, in fact, more accurate. Since the ESPACE code has been in use for many years, it is strongly expected to be more accurate at present. The most effective way to verify this would be to run both algorithms on simulated data, where the correct answer is known, rather than on experimental data.

One difference between the C++ analyzer algorithm and the ESPACE algorithm is that the angles used for the t-x conversion are computed differently. ESPACE finds a cluster and then uses characteristics of that cluster in order to compute the angle. The C++ analyzer uses the angle between pairs of clusters in the lower and upper planes, which is obtained during the coarse tracking phase. This means that the C++ results should be more reliable.

A second difference is that clusters are matched in a different order. When handling multiple track events, ESPACE first pairs
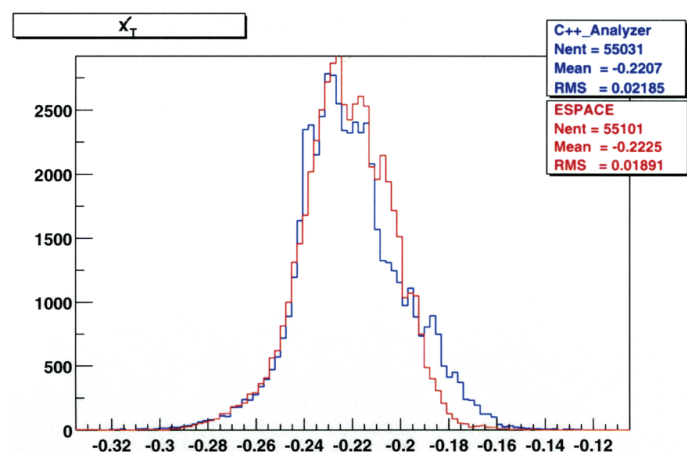
Figure 7. X'_T spectrum from a 9-foil carbon target. The blue results are from the C++ analyzer and the red results are from ESPACE. The x-axis is in meters.
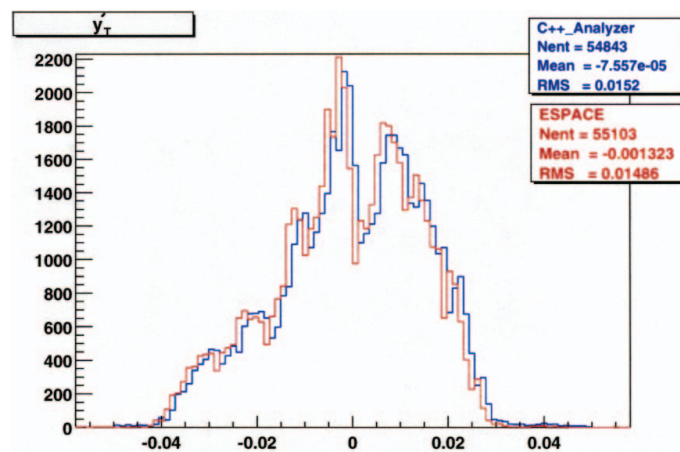
Figure 8: Y'_T spectrum from a 9-foil carbon target. The blue results are from the C++ analyzer and the red results are from ESPACE. The x-axis is in meters.
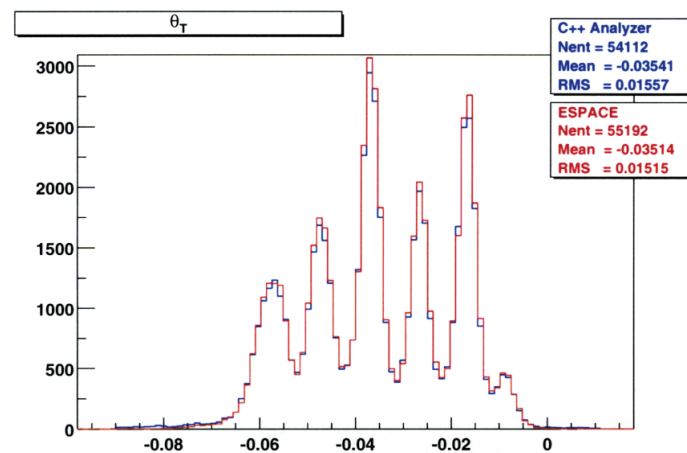
Figure 9. θ_T spectrum from a 9-foil carbon target. The blue results are from the C++ analyzer and the red results are from ESPACE. The x-axis is $\tan(\theta_T)$.
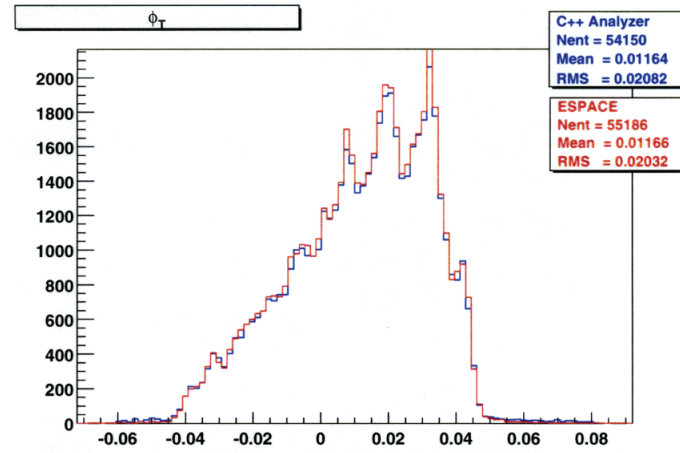
Figure 10. ϕ_T spectrum from a 9-foil carbon target. The blue results are from the C++ analyzer and the red results are from ESPACE. The x-axis is $\tan(\phi_T)$.

clusters from the U_1 and U_2 planes, then pairs clusters from the V_1 and V_2 planes, before finally matching sets of 4 clusters into tracks. The C++ analyzer, however, matches U_1 and V_1 planes, and then matches U_2 and V_2 planes, creating lower and upper UV tracks. The lower and upper UV tracks are then paired in order to form complete tracks. The main difference is that ESPACE is able to form a more precise fit of drift distances to wire positions, since it has access to more points. Although this difference is negligible for low-data-rate experiments where less than 1% of events involve multiple tracks, it could have an impact on high-data-rate experiments.

Unfortunately, neither ESPACE nor the C++ analyzer is currently able to reliably process events with multiple particle tracks. ESPACE's current methods for handling multiple particle tracks are known to be inefficient, but work is under way to improve them. The technique used by the C++ analyzer has not yet been thoroughly tested, so it is impossible to say how efficient it is. The main advantage of the C++ analyzer is that it is being designed in a highly modular fashion, unlike ESPACE, which has many complicated interdependencies between program units. As a result, interchanging algorithms and making changes to the code when the detector configuration changes can be done more rapidly with the new C++ analyzer.

At present, there is still a great deal of work that must be done to compare the performance of the two algorithms. It is important to determine which one is actually more accurate, and to track down the differences in the algorithms leading to the current differences. The speed of the algorithms has not been rigorously tested, though they are roughly equal. A thorough test of speed should occur after the differences in the results have been accounted for and the C++ analyzer has been optimized. Since the ultimate goal of the C++ analyzer is to replace ESPACE, more testing is currently underway.

REFERENCES

Brown, K. L. et al. (1977). TRANSPORT: A Computer Program for Designing Charged Particle Beam Transport Systems. SLAC-91, UC-28.

Brun, R. & Rademakers, F. (2001). The ROOT System Home Page [WWW Page]. URL http://root.cern.ch

CERN. (2001). CERN Program Library [WWW Page]. URL http://cernlib.web.cern.ch/cernlib

Fissum, K.G., et al. (2001). Vertical Drift Chambers for the Hall A High Resolution Spectrometers at Jefferson Lab. Nucl. Instr. Meth. A474, 108.

Leathers, C. (1996). Efficiency Measurements on the CEBAF Hall A VDCs. Undergraduate Thesis, Massachusetts Institute of Technology. Available http://www.jlab.org/~fissum/vdcs/documentation/docs.html

Liyanage, N. K. B. (1999). A Study of the ^{16}O(e,e'p) Reaction at Deep Missing Energies. Doctoral Thesis, Massachusetts Institute of Technology. (unpublished)

Offerman, E. (1997). ESPACE User's Guide. Available http://hallaweb.jlab.org/espace/docs.html

Wechsler, R.H. (1996). Drift-Time Properties of CEBAF Hall A Vertical Drift Chambers. Undergraduate Thesis, Massachusetts Institute of Technology. Available http://www.jlab.org/~fissum/vdcs/documentation/docs.html

INVESTIGATING NEUTRALINO ANNIHILATIONS USING DarkSUSY

Sameh Kamel[A] and Eduardo do Couto e Silva, Ph.D.[B]

ABSTRACT

Physicists do not fully understand the nature of dark matter although we infer its existence from experimental observation. This project is part of the dark matter detection searches with the Gamma-Ray Large Area Space Telescope (GLAST). We are investigating one of the Weakly Interacting Massive Particles (WIMP) candidates called the neutralino, a particle predicted by the Minimal Supersymmetric Standard Model. In particular, we ran a computer simulation called DarkSUSY that predicts the signature that we expect to see in the data from GLAST that pertains to the detection of the neutralino in the galactic halo.

PROJECT DESCRIPTION

The primary objective of this project is to predict the flux of photons from the galactic halo due to neutralino annihilations using the DarkSUSY simulation code[1] so that one can calculate the sensitivity of the GLAST detector for dark matter searches. The secondary objectives of this project are to:

1. Understand and document the DarkSUSY simulation code;
2. Generate output from DarkSUSY in a format useful for analysis in the GLAST framework; and
3. Develop a framework under which one can generate a large number of DarkSUSY events (approximately one million) on the computer infrastructure at SLAC.

INTRODUCTION

The Mass Density Parameter Ω

The mass density of the universe has an important consequence because, according to standard cosmological theory, the value of this density determines whether the universe will expand or collapse. To quantify the state of the universe we define a mass density parameter $\Omega = \rho/\rho_{crit}$ where ρ is the mass density of the universe (homogenous on large scales) and $\rho_{crit} = 3H^2/8\pi G \sim 10^{-38}h^2$ kg/m³.[2] If Ω is less than one then the universe will continue to expand and is said to be open; if Ω is greater than one then the universe will eventually collapse and is said to be closed; if Ω is equal to one then the universe is delicately balanced between the previous two states and is said to be flat. So far Ω is observed to be very close to one (a flat universe).

Now that one understands Ω, one should analyze what contributes to Ω's value. Ω is determined by two contributions: one due to the mass in the universe, Ω_M, and another due to what is labeled the cosmological constant, Ω_Λ. Ω_Λ is a result of solving Einstein's equation and can be thought of as a sort of "dark energy" that we cannot account for but whose existence we infer from observation. Ω_M is experimentally determined to be close to 0.3 while Ω_Λ is close to 0.7. The Ω_M term is subdivided into two terms: the first due to baryonic matter Ω_B and the second due to non-baryonic matter Ω_{NB}. It turns out that only around ten percent of matter in the universe is luminous and the remaining ninety percent consists of matter that we cannot see called dark matter. That is, $\Omega_{NB} \approx 90\%$ of $\Omega_M \sim 0.25$.

Dark Matter

In the galaxy NGC 3198, experimental observation of gravitational effects indicates that more matter exists than what is visible.[2] The rotational velocity of stellar objects (see Figure 1) contradicts Newton's Laws which predict that $v^2 = GM/r$. There are observations from many other galaxies like NGC 3198 that exhibit similar behavior. One way to explain this phenomenon is to postulate there is invisible matter permeating the galaxy and the stellar objects therefore lie in a sphere of mass. In this way, one can assume that the M in Newton's Law is proportional to the radius r and therefore we find that $v^2 \propto GM$, which is a constant of r.

In recent years there has been increasing confidence that dark matter is not made up of ordinary matter and is instead non-baryonic. Among the non-baryonic candidates investigated today are axions and Weakly Interacting Massive Particles (WIMPs). One class of WIMP is the supersymmetric particles predicted by the Minimal Super-symmetric Standard Model (MSSM).[4] The focus of this paper is on models in which the lightest and most stable of the supersymmetric particles called the neutralino exists.

Minimal Super-symmetric Standard Model (MSSM)

The MSSM was actually created by particle physicists to explain problems with the Standard Model:

A: Santa Clara University, Santa Clara, CA; B: Stanford Linear Accelerator Center, Stanford, CA

- **Mass scale problem:** The problem of explaining why particles have the masses that they do. In masses at the scales of the Standard Model (~100 GeV), one can explain the mass hierarchy by introducing the Higgs boson. Grand unified theories, however, introduce masses ~10^{15} GeV for which the Higgs boson is an insufficient explanation. The MSSM accounts for masses at the ~10^{15} GeV scale by introducing four new Higgs bosons.[5]
- **Naturalness problem:** Correction to the Higgs mass can diverge.[5]

The MSSM is the "minimum amount" of new physics that one must add to the Standard Model to account for these problems. The MSSM adds superpartners to some of the particles in the Standard Model: bosons get fermionic superpartners whose names are formed by attaching "-ino" to the end of the bosons' name (e.g., photon goes to photino), whereas fermions get bosonic superpartners whose names are formed by adding an "s" to the beginning of the fermions' name (e.g., quark goes to squark). In particular, the MSSM consists of the following[3]:

1. 4 neutralino mass eigenstates (χ_j^0), which all arise from the mixing between like-sign Higgsino and Gaugino fields;
2. 2 chargino mass eigenstates ($\chi_i^\pm$);
3. spin 1/2 gluino ($\tilde{g}$) and spin 0 squarks ($\tilde{q}$), sleptons ($\tilde{l}$), and sneutrinos ($\tilde{v}$); and
4. 5 physical Higgs bosons.

The particles which the MSSM introduces are often called SUSY particles (SUper-SYmmetric), hence the simulation's name: DarkSUSY.

The Neutralino (χ_1^0)

In some MSSM models, the χ_1^0 neutralino is the Lightest SuperParticle (LSP) and is therefore stable in that it does not decay into other superparticles. Although there are three other neutralino states (see above), in this paper when I refer to the neutralino I am referring to its lightest state, χ_1^0. The χ_1^0 neutralino is a linear combination of Higgsino and Gaugino particles:

$$\chi_1^0 = a_{11}\tilde{B} + a_{12}\tilde{W}^3 + a_{13}\tilde{H}_1^0 + a_{14}\tilde{H}_2^0 \quad (1)$$

The a_{1j} coefficients give weight to the different quantum states that make up the neutralino. There is a quantity called the gaugino fraction which is defined as the following:

$$Z_g = |a_{11}|^2 + |a_{12}|^2 \quad (2)$$

The gaugino fraction is close to one if the neutralino is mainly in the gaugino states ($\tilde{B}$ and $\tilde{W}^3$) and close to zero if the neutralino is mostly in the Higgsino states ($\tilde{H}_1^0$ and $\tilde{H}_2^0$). Although the χ_1^0 neutralino does not decay because it is stable, it does have the following three annihilation channels:

- Line processes

$$-\chi\chi \rightarrow \gamma\gamma$$
$$-\chi\chi \rightarrow Z\gamma$$

- Continuum process

$$-\chi\chi \rightarrow q\bar{q} \rightarrow \cdots \rightarrow \gamma\gamma$$

The line processes are so-called because the gamma particles that result from the annihilation process have a well-defined energy, resulting in a spike in the gamma ray spectrum at a particular energy (see Figure 2). The continuum process, on the other hand, can produce gamma rays with a wide range of energies because of the many channels in which $q\bar{q}$ can annihilate and therefore continuum processes produce gamma ray spectrums which are spread out.

The neutralino is considered one of the favorite WIMP candidates for dark matter because the cross section neutralino annihilations (in times following the Big Bang but before freeze-out) is such that the neutralino could account for the non-baryonic con-
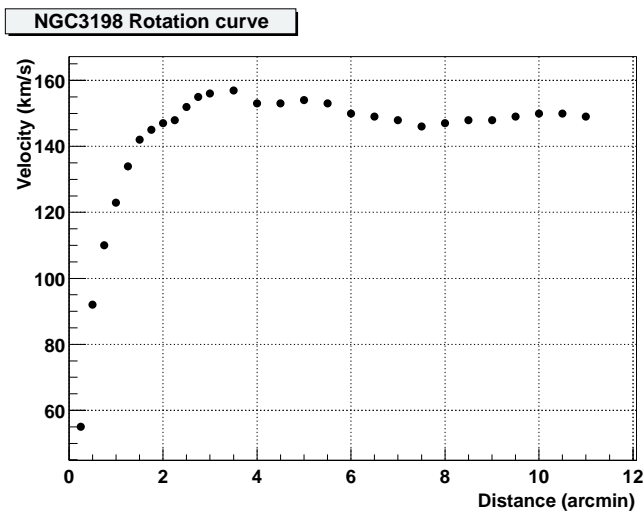
Figure 1. The velocity of stellar objects as a function of distance from the galactic center in the galaxy NGC 3198. Although Newton's laws predict $v^2 = GM/r$ we see clearly that here this is not the case. Galactic rotation curves such as this one imply the existence of dark matter.[3] Data points were extracted from Begeman.
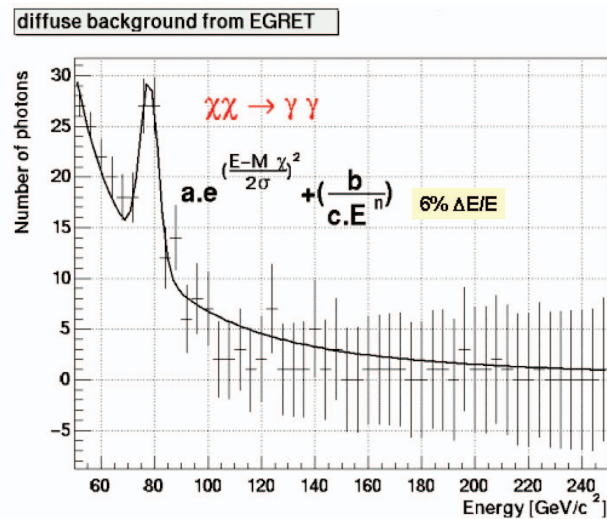
Figure 2. The flux versus the photon energy for a neutralino line process with background simulated from 50 to 250 GeV. The neutralino was generated with energy of 78 GeV, hence the spike at that energy.

tribution to dark matter. The neutralino contribution to Ω_M is given by the following equation[4]:

$$\Omega_\chi \sim \frac{10^{-10} GeV^{-2}}{\langle \sigma_A v \rangle} \quad (3)$$

Notice that as σ_A—the cross section of neutralino annihilations—increases, the Ω_χ contribution decreases because the more neutralinos annihilate the less neutralinos there are to contribute to Ω_M. The quantity v is the relative velocity between neutralinos. For supersymmetric dark matter, $\langle \sigma_A v \rangle \sim \alpha^2/m_W^2 \, 0.1 \sim 10^{-9\pm1}$ (see reference 6) which implies that $\Omega_\chi \sim 10^{-1\pm1}$. This range allows for Ω_χ to account for $\Omega_{NB} \sim 0.25$.

GLAST (GAMMA-RAY LARGE AREA SPACE TELESCOPE)

The measurement of dark matter is but one of the many purposes of the GLAST project. The main instrument of the GLAST is called the Large Area Telescope (LAT) and is designed to detect photons in the energy range of 20 MeV to 300 GeV. The energy range of 30 GeV to 300 GeV is a region in which no previous experiments have attempted to detect photons. We believe that we can detect neutralinos (χ) by means of the neutralino annihilation processes occurring in the galactic halo and we will use the

LAT to detect the annihilation processes for M_χ ranging from 50 GeV to ~ 300 GeV.

DarkSUSY SIMULATION

The DarkSUSY code calculates the photon flux Φ_γ that results from neutralino annihilations. This flux depends on the MSSM parameters, the model for the galactic halo density, and the neutralino annihilation cross-section. Figure 3 is a flowchart that summarizes the calculations needed to complete the flux calculation, starting with the random generation of an MSSM model, followed by the intermediate calculations and checks for model exclusion if it does not satisfy constraints, and ending with the calculation of Φ_γ if the model is allowed by constraints. The calculations shown in the flowchart are performed by the DarkSUSY code in the following six stages:

1. Generation of MSSM parameters;
2. calculation of the relic particle density;
3. calculation of the masses of particles introduced by the MSSM;
4. calculation of the photon fluxes for neutralino line processes;
5. calculation of the photon flux for the neutralino continuum process; and
6. calculation of the actual photon spectrum for the neutralino continuum process for each model.

The DarkSUSY code is modular and so each step may be submitted to the CPU or computer servers as a separate job. This is important, for example, if one does not want to tie up a computer network with one large job (the first step of the DarkSUSY simulation alone takes about 12 hours on the SLAC computer farms to generate one million models).

MSSM PARAMETERS GENERATION

We studied the way in which DarkSUSY excludes generated models. In particular we checked the accelerator constraints implementation and found that it is not up to date with the most recent particle physics developments. The code uses values from the Particle Data Group 2000[7] and will have to be updated.
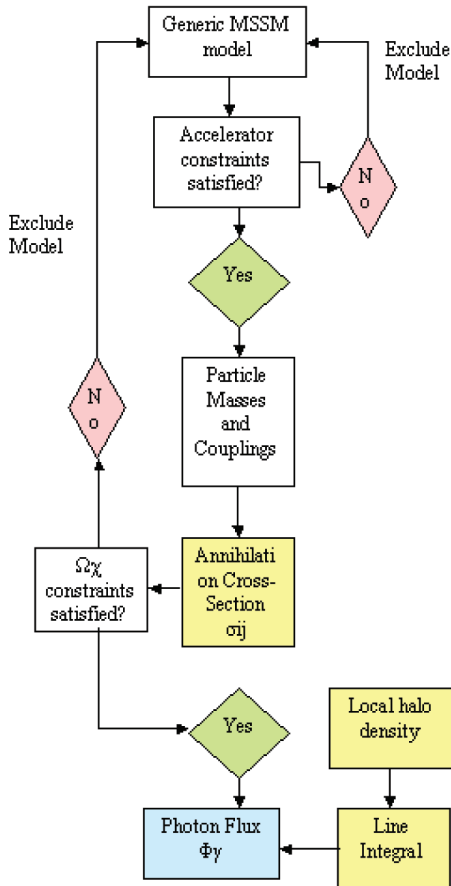
Figure 3. This flowchart summarizes the calculations involved in finding the photon flux due to the neutralino annihilation processes occuring in the galactic halo.
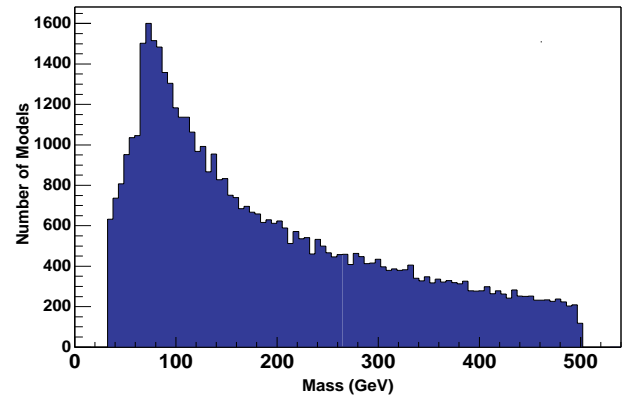
Figure 4. The number of models generated by the DarkSUSY simulation versus the value for the mass of the lightest neutralino χ_1^0 to which the models lead. The dark matter detection searches with GLAST will attempt to detect the annihilation process for 50 GeV $\leq M_\chi \leq$ 300 GeV.

RELIC PARTICLE DENSITY CALCULATION

In the calculation of the relic particle density, this project's task was to understand the connection between the variables in the code and the variables in the physics equations because it was not immediately evident to us to what the variables in the code corresponded. Specifically, we analyzed the use of the Boltzmann equation in calculating $Y = n/s$ where n is the neutralino density and s is the entropy of the halo.[8] The value of Y is needed to calculate the density of relic neutralinos that formed in the galactic halo in primeval times immediately following the Big Bang and whose formation is subsequently frozen-out.

DarkSUSY must calculate the density in the galactic halo because it varies depending on the choice of halo model. We used the output of this stage of the calculation to modify the J integral in stage 4, where the DarkSUSY simulation calculates the flux for the line processes. We previously referred to the calculation of the halo density for different halo models. The following equation determines the choice of a halo model based on the value of (α, β, γ):

$$\rho(r) \propto \frac{\rho_C}{\left(\dfrac{r}{a}\right)^{\gamma}\left[1+\left(\dfrac{r}{a}\right)^{\alpha}\right]^{\frac{(\beta-\gamma)}{\alpha}}} \quad (4)$$

where r is the distance from the center of the halo, a is a parameter related to the core radius of the halo[5], and ρ_C is the local halo density. A plot of the halo density for different halo models appears in Figure 5. The three models used in the DarkSUSY simulation are shown in the figure. The three models are the following: isothermal, $(\alpha, \beta, \gamma) = (2,2,0)$; Navarro-Frenk-White (NFW), $(\alpha, \beta, \gamma) = (1,3,1)$; and Moore, $(\alpha, \beta, \gamma) = (1.5,3,1.5)$.[2,10,11]

MSSM PARTICLE SPECTRA CALCULATION

It was not immediately obvious to us which variables in the code corresponded to what masses of the MSSM particles. As a result, we interpreted the mass variables in the code and documented the names of the variables for future reference.

PHOTON FLUXES FOR LINE PROCESSES

The DarkSUSY simulation calculates the flux of photons from the galactic halo by means of the equation $F \propto \sigma J$, where σ is the cross-section of neutralino annihilations and $J \propto \int_{\text{line-of-sight}} \rho^2(l)dl(\hat{n})$, the line integral of the neutralino density in the galactic halo along the line of sight (i.e., the amount of neutralinos in the galactic halo).[5]

The calculation of flux due to line processes took the J integral averaged over a solid angle rather than as a function of the galactic coordinates and returned an average flux. This project was responsible for altering the code to take J as a function of galactic coordinates and thereby producing flux as a function of galactic coordinates.

PHOTON FLUXES FOR CONTINUUM PROCESSES

The primary objective of this project was to produce the flux of photons from the galactic halo due to neutralino continuum processes in the galactic halo, which is handled in this step of the simulation. We wrote a subroutine that outputs a table of the photon spectrum which we used to plot a histogram (see Figure 5).

INPUT DATA FOR PHYSICS ANALYSIS TOOLS

After one runs all six stages of the DarkSUSY simulation, one obtains six different output files containing output for each stage. For data analysis software such as Root[9], however, it is best to have one large output file that contains all the data that one wishes to plot so that one can apply cuts to the data. We wrote a new program specifically for the DarkSUSY output files that combines the data from all six files into one table. We used this program to plot the histograms of the DarkSUSY data that are found in this paper.

RESULTS

There are about 50 figures that we made using the DarkSUSY simulation that one could show in this section. Here we present a sample of some of the plots generated.

As mentioned above, we are detecting photons that result from neutralino annihilation processes such that $50 \text{ GeV} \leq M_\chi \leq 300 \text{ GeV}$. Accelerator constraints lead us to the lower limit around 40 GeV[7], hence we chose an arbitrary range from 50 GeV to 500 GeV for our generated models. Figure 3 is a plot of the neutralino mass for 50,000 models generated by DarkSUSY.
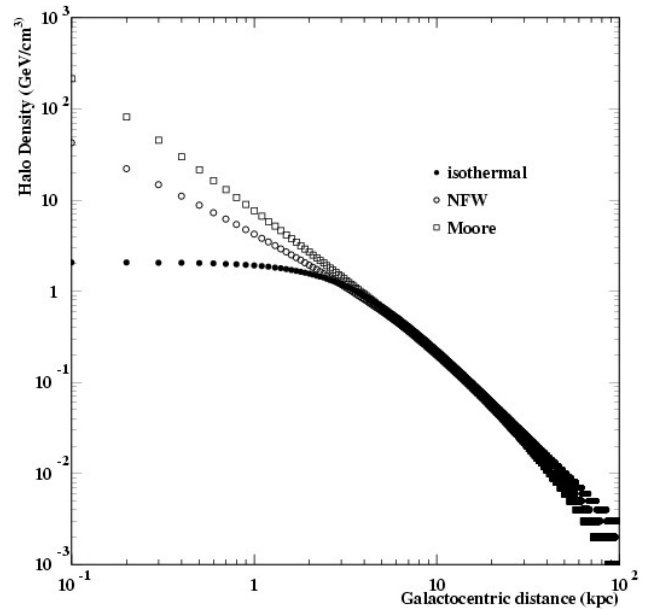
Figure 5. The galactic halo density versus the galactocentric distance for three different halo models since the prediction for the halo density depends on choice of halo model. The three halo models shown here (isothermal, NFW and Moore) are the models used in the DarkSUSY simulation.
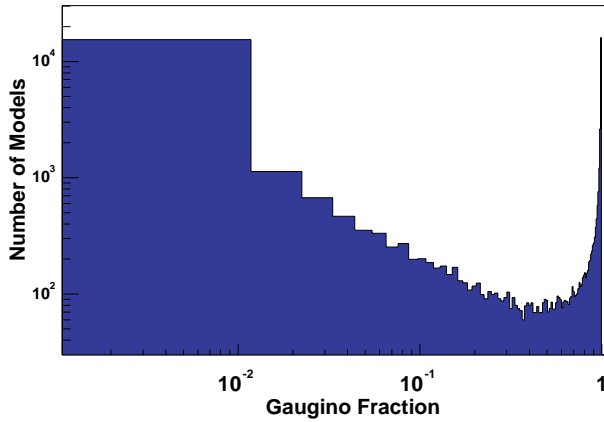
Figure 6. The number of models generated by the DarkSUSY simulation versus the value for the gaugino fraction. The gaugino fraction varies from 0 (Higgsino) to 1 (Gaugino).
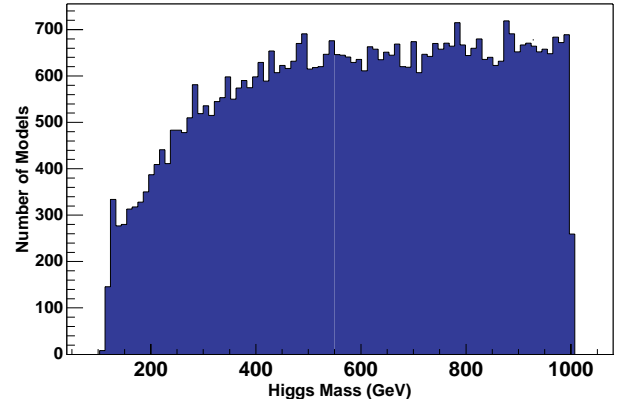
Figure 7. The number of models generated by the DarkSUSY simulation versus the value for the mass of the lightest Higgs boson to which the models lead. There are five Higgs bosons in the MSSM and the lightest one corresponds to the Higgs particle in the Standard Model.
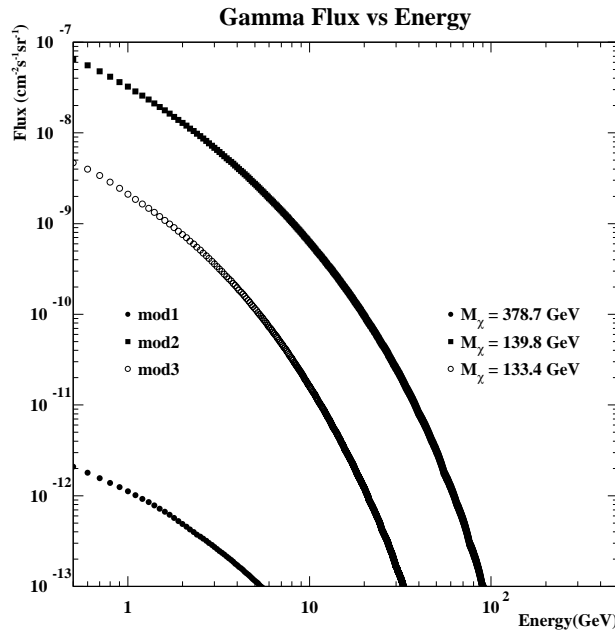
Figure 8. The flux of photons due to the neutralino continuum process in the galactic halo versus the photon energy for three distinct models generated by the DarkSUSY simulation. Shown to the right of the curves is the mass of the lightest neutralino that results from each of the three models shown here.

The gaugino fraction mentioned above, which varies from 0 (Higgsino) to 1 (Gaugino), is shown in Figure 6.

DarkSUSY generates a value for the Higgs mass for which the radiative corrections mentioned above sets an upper limit of 130 GeV.[5] We used DarkSUSY's results for the mass of the lightest Higgs (recall that there are 5 Higgs particles in the MSSM, and the lightest Higgs corresponds to that of the Standard Model) to obtain the plot shown in Figure 7.

The photon flux due to the neutralino continuum process in the galactic halo versus the photon energy is, as mentioned above, the primary objective of this project. We succeeded in creating a

preliminary plot of the continuum photon spectrum for three models generated by DarkSUSY, which is shown in Figure 8. The next step is to analyze the graph shown in this paper and to make graphs that feature more than three models. After that, we will need to simulate the neutralino processes because the continuum process does not result in a definitive signal (since the photon spectrum for the continuum process has the same form as cosmic background radiation). We will detect the continuum process to get a hint of the neutralino's existence and then we will attempt to detect the line processes because its detection is more convincing proof.

CONCLUSION

We made a preliminary histogram that predicts the flux of photons from the galactic halo due to the neutralino continuum process, although we need to verify the values for the flux. Also, we understood and documented around 25% of the DarkSUSY code and began developing a framework under which we can generate the output from DarkSUSY in a useful format. We began estimating the time of execution of the DarkSUSY simulation so that we could develop a framework under which we could run the DarkSUSY simulation on the SLAC computer farms. This project will lead to the calculation of the GLAST sensitivity for the neutralino line and continuum processes.

ACKNOWLEDGMENTS

REFERENCES

1 Gondolo, P et al "DarkSUSY - A Numerical Package for Dark matter Calculations in the MSSM", Proceedings of the 3rd International Workshop on the Identification of Dark Matter", edited by N.J.C. Spooner & V. Kudryavstev. Singapore: World Scientific, 2001, p.318 and http://www.physto.se/~edsjo/darksusy/overview.html

2 Bergstrom, L. 2000, *Rep. Prog. Phys.*, 63, 793-841.

3 Begeman, KG. 1989, *Astron. Astrophys.,* 223, 47-60

4 G. Jungman, M. Kamionkowski, and K. Griest, Phys. Rept. 267:195-373, 1996

5 DiBitonto, Daryl. "Decay Properties of SUSY Particles." In Properties of SUSY Particles. Ed. By Cifarelli and Khoze. Singapore: World Scientific Publishing Co., 1993, 153-170.

6 Feng, Jonathan. *Exploring Electroweak Symmetry Breaking*. Lecture in SLAC Summer Institute, Aug 13 2001.

7 Bartels, J., Haidt, D., and Zichichi, A. eds. *The European Physical Journal C: Particles and Fields*. Heidelburg: Springer-Verlag, 2000.

8 Edsjo, J. and Gondolo, P. 1997, *Phys. Rev.* D56, 1879.

9 http://root.cern.ch

10 Navarro, J. F., Frenk, C. S., & White, S. D. M. 1996, *ApJ*, 462, 563

11 Moore, B., Governato, F., Quinn, T., Stadel, J., & Lake, G. 1998, *ApJ*, 499, L5

EXPLORING THE LIMITS OF THE DIPOLE APPROXIMATION WITH ANGLE-RESOLVED ELECTRON TIME-OF-FLIGHT SPECTROMETRY

Sierra Laidman,[A] Monica Pangilinan,[B] Renaud Guillemin,[C,D] Sung Woo Yu,[C,D] Gunnar Öhrwall,[C,D] Dennis Lindle,[C] and Oliver Hemmers[C]

ABSTRACT

Understanding the electronic structure of atoms and molecules is fundamental in determining their basic properties as well as the interactions that occur with different particles such as light. One such interaction is single photoionization; a process in which a photon collides with an atom or molecule and an electron with a certain kinetic energy is emitted, leaving behind a residual ion. Theoretical models of electronic structures use the dipole approximation to simplify x-ray interactions by assuming that the electromagnetic field of the radiation, expressed as a Taylor-series expansion, can be simplified by using only the first term. It has been known for some time that the dipole approximation becomes inaccurate at high photon energies, but the threshold at which this discrepancy begins is ambiguous. In order to enhance our understanding of these limitations, we measured the electron emissions of nitrogen. Beamline 8.0.1 at the Advanced Light Source was used with an electron Time-of-Flight (TOF) end station, which measures the time required for electrons emitted to travel a fixed distance. Data were collected over a broad range of photon energies (413 - 664 eV) using five analyzers rotated to 15 chamber angles. Preliminary analysis indicates that these results confirm the breakdown of the dipole approximation at photon energies well below 1 keV and that this breakdown is greatly enhanced in molecules just above the core-level ionization threshold. As a result, new theoretical models must be made that use higher order terms that were previously truncated.

INTRODUCTION

Quantum mechanics is used to describe particles on the atomic scale. Quantum mechanics uses wave functions describing electrons in a field of a nucleus. In case of photoionization, wave functions are used to describe discrete orbitals and the emission of photo- or Auger electrons. The famous time-dependent Schrödinger equation is used to find solutions for a given Hamiltonian (the interaction operator) between the bound state and the continuum state. A photon colliding with an atom transfers angular momentum to the outgoing electron during the photoionization process. This free electron can be described by a wave function as a plane wave that is comprised of spherical waves ($e^{i\mathrm{kr}}$). With the help of a Taylor series expansion for $e^{i\mathrm{kr}}$ it is possible to separate the contributions from the spherical waves. If all contributions except for the first ($e^{i\mathrm{kr}}=1$) are truncated, it is termed the Dipole Approximation (DA).

The interaction of x-rays with an atom or molecule is used to probe its electronic structure and the dynamic behavior during photoionization. Using the dipole approximation simplifies theoretical models and neglects all effects resulting from higher-order momenta. As a result, the limits of the dipole approximation must be investigated in order to have more accurate models.[1]

For over three decades nobody had serious doubts about the validity of the DA. In the UV and far-UV photon-energy ranges, the DA for photoionization is grounded in solid physical reasoning. This is because photoelectron velocities following photoemission are extremely small compared to the speed of light, and the wavelength of the light is much larger than the orbitals of the ejected electrons.[2] However, it is widely known that the dipole approximation breaks down completely at the hard-x-ray energy range (hv > 5 keV). On the other hand, the breakdown of the dipole approximation at the intermediate soft-x-ray photon-energy range had not been explored until recently. Higher-order multipole moments (electric quadrupole, electric octupole, and magnetic dipole etc.) show some effect at all photon energies. Thus, it is essential to completely understand at what photon energies the dipole approximation can no longer be used and how important the higher-order Taylor series terms are.

The best way to determine these limits is by measuring the angular distributions of photoelectrons because these are much more sensitive to higher-order effects than the partial cross sections. Electron Time-of-Flight (e-TOF) spectrometry is ideally suited for this task. This technique measures the flight time of electrons between the interaction region and a detector, which

---

A: Bryn Mawr College, Bryn Mawr, PA; B: Cornell University, Ithaca, NY;
C: University of Nevada, Las Vegas, Las Vegas, NV; D: Lawrence Berkeley National Laboratory, Berkeley, CA

can then be used to calculate not only the kinetic energy of the electrons but also the direction of the emitted photoelectrons.[3] Furthermore, the apparatus is able to measure the entire electron energy spectrum simultaneously, eliminating effects due to time fluctuations in beam intensity and sample pressure.

MATERIALS AND METHODS

The experimental setup used was an electron Time-of-Flight end station, which requires an adequate light source. For this experiment, the Advanced Light Source (ALS) at the Lawrence Berkeley National Laboratory was used. Able to produce light in the x-ray and ultraviolet range with light one billion times brighter than the sun, the ALS offers the light needed to study atoms and molecules.

X-rays are emitted from packets of electrons known as bunches, which each have approximately the same diameter as a human hair. The electrons are accelerated to nearly the speed of light, and their energies are increased inside a booster ring. From there, the electrons enter the storage ring and their energy is ramped up to 1.9 GeV. The electrons, maintaining the same energy, change direction with the help of twelve bending magnets in the storage ring. At these twelve positions the electrons produce light because accelerating charged particles, in this case the electrons, give off electromagnetic radiation. When this radiation is emitted, the electrons lose energy, which must be replenished in order to maintain a constant energy. Radio-frequency cavities, which generate an alternating electromagnetic field, give the electrons the same amount of energy that they lost and allow the electrons to maintain their energy. In addition, more light is produced in straight sections of the ring by insertion devices such as wigglers and undulators. Undulators and wigglers are comprised of a series of magnets that produce a spatially alternating magnetic field. When the electron bunches in the storage ring pass through the undulators or wigglers, the electrons are deflected back and forth, thus increasing the amount of radiation emitted along their flight path. By adjusting the undulator or wiggler gap, the maximum number of photons is produced at the appropriate energy for a chosen photon energy. The difference between undulators and wigglers is that undulators produce light that is coherent and in phase whereas the wiggler light is incoherent.

Most of this radiation, which comes in the form of a broad spectrum ranging from infrared to x-rays, leaves the storage ring by tangential ports into beamlines, which are connected to end stations. In the case of this experiment, beamline 8.0.1 was used with an electron Time-of-Flight end station. This end station requires that the ALS operates in 2-bunch mode instead of multibunch mode. The length of each bunch in 2-bunch mode is, on average, 50 picoseconds and the time separation between these two bunches is 328 nanoseconds.

Once the light enters the beamline, a monochromator is used to select a specific wavelength (and thus a specific energy) of photons. In order to do this, a grating diffracts the radiation and a specific wavelength is selected by the exit slit. The monochromator on beamline 8.0.1 has three spherical gratings with radii of 70 m. Each grating is suitable for a different energy range, which is determined by its coating and the number of lines per millimeter.

Various optical devices, such as the entrance and exit slits, are used along the beamline in order to focus, bend, and control the incoming photons. The entrance and exit slits can be varied in slit width and are used in order to adjust the resolution of the monochromator. Directly before the entrance slit, the Vertical Condensing Mirror serves to reduce the height of the beam so that more photons will pass through the entrance slit. Beyond the exit slit, Horizontal and Vertical Refocusing Mirrors are aligned perpendicular to each other in order to achieve maximum horizontal and vertical focusing (Figure 1).

From the beamline, the light enters the vacuum chamber of the electron Time-of-Flight end station (Figure 2). This chamber supports the analyzers and can be rotated about the x-ray beam by 90 degrees while under vacuum. This allows the collection of spectra at many different angles, increasing the accuracy of angular-distribution measurements and allowing for the calculation of additional angular-distribution parameters.

Photons interact with gas that is ejected perpendicular to the photon beam by a needle in a space called the interaction region. There, photoemission occurs due to the collision of the photons from the beam and the gas particles. These electrons can go into an analyzer and must travel a distance of 437.5 mm
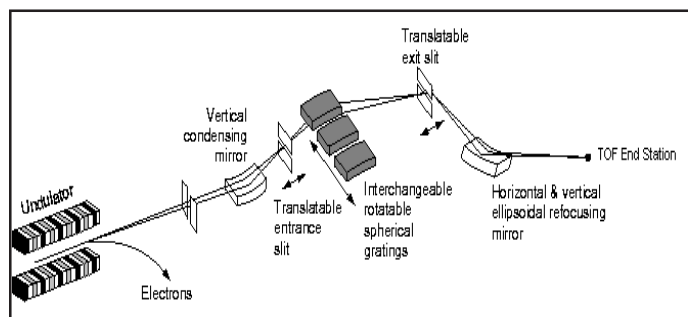
Figure 1. Schematic diagram of Beamline 8.0.1
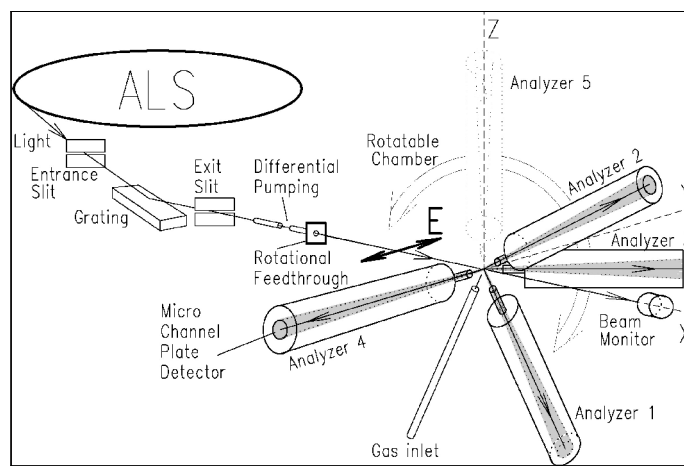
Figure 2. Experimental schematic of the electron Time-of-Flight system. Light from the ALS storage ring passes through beamline optics into a differential-pumping section. The chamber and analyzers can rotate around the photon beam for more accurate electron angular-distribution measurement.

and be within a ± 2.7 degrees cone relative to a straight flight path in order to be detected.

Electrons have to have a minimum kinetic energy of 5 eV to arrive at the detector of any analyzer within the 328 ns time window. Analyzers 2 and 3 are positioned on a cone with a half angle of 54.7 degrees along the photon beam and out of the plane perpendicular to the x-ray beam. For a certain chamber position analyzers 1 and 3 are at the so-called "magic angle." This is the angle at which the dipole parameter disappears from the equation of the differential partial cross section, leaving behind the nondipole parameters. Positioning the analyzers at the "magic angle" allows only nondipolar angular-distribution effects to be studied. Analyzers 1, 4, and 5 are used to measure dipolar angular distributions and cross-section ratios.

Once inside an analyzer, the electrons are detected by two Micro-Channel Plates (MCPs) positioned in a Chevron arrangement. MCPs are thin glass disks with thousands of microscopic tubes. A high voltage is applied across the MCPs and when electrons collide with the walls of the tubes, they produce secondary electrons, which accelerate and cascade down the tubes thus creating even more electrons.

After an electron hits the Micro-Channel Plates, a cloud of electrons is made that hits an anode which charges a capacitor that produces a main pulse each time it discharges. From there, this pulse is amplified. A Constant Fraction Discriminator then inverts the signal, shifts it by less than a nanosecond, and adds the original signal to the inverted and shifted signal. This new signal marks the start time for the time-to-amplitude

converter/biased amplifier while the end time is marked by the ALS Bunch Marker signal that is produced every 328 ns. The time signal is converted into a voltage using an Analog-to-Digital Converter with the different voltages corresponding to specific channel numbers, which are stored as counts in a Multi-Channel-Analyzer. A spectrum is made up of all the counts produced over all the channel numbers with the peaks in the spectrum corresponding to electrons with certain kinetic energies (Figure 3).

For this experiment, the spectra for molecular nitrogen were collected at fifteen different chamber rotation angles. Nitrogen gas was selected because it is a simple molecule with inner and outer shells, and argon gas was used for calibration purposes further explained in the next section. Nitrogen gas spectra were collected at certain photon energies ranging from 413 eV to 664 eV. Each photon energy required adjustments of the undulator gap for optimal resolution and intensities.

DATA ANALYSIS AND RESULTS

Each analyzer produces a separate spectrum that is used to calculate the differential cross section for photoemission processes. This differential cross section describes the angular distribution of ejected photoelectrons from a randomly oriented sample using 100% linearly polarized light. Using the nondipole parameters (δ and γ which can be combined to the single parameter ζ, equivalent to $\gamma + 3\delta$) and the dipole parameter (β), the equation is as follows:

$$\frac{d\sigma_{nl}}{d\Omega} = \frac{\sigma_{nl}}{4\pi}\left[1 + \frac{\beta}{2}\left(3\cos^2\theta - 1\right) + \left(\delta + \gamma\cos^2\theta\right)\sin\theta\cos\phi\right]$$

Each analyzer has a fixed ϕ and θ (Figure 4) that correspond to the angle of the photoemitted electron in regards to the direction of the photon beam and its polarization. σ_{nl} corresponds to the partial cross section of electrons from subshells nl. The equations relating to analyzers 1, 3, and 4 are the only ones needed in order to obtain the dipole and nondipole parameters (β, ζ respectively) (Figure 5).
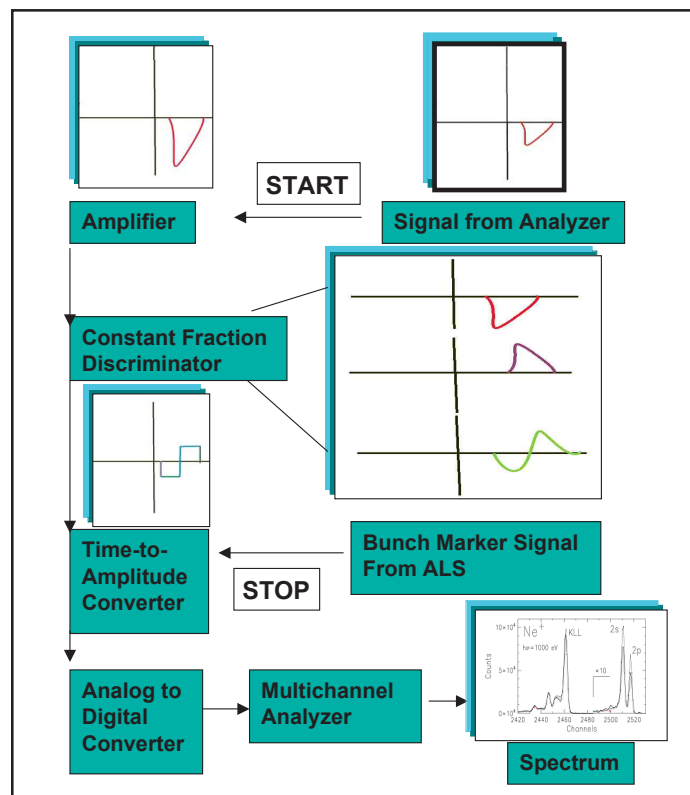
Figure 3. Flow chart of how the signal given by an electron becomes part of a spectrum.
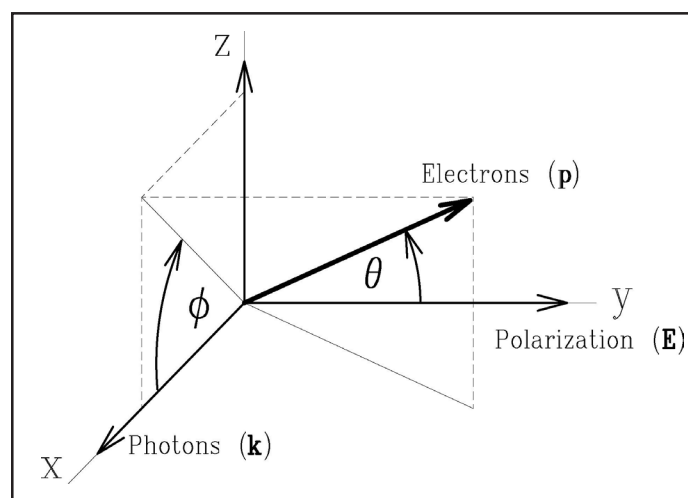
Figure 4. The coordinate system and angles used for the experiment.
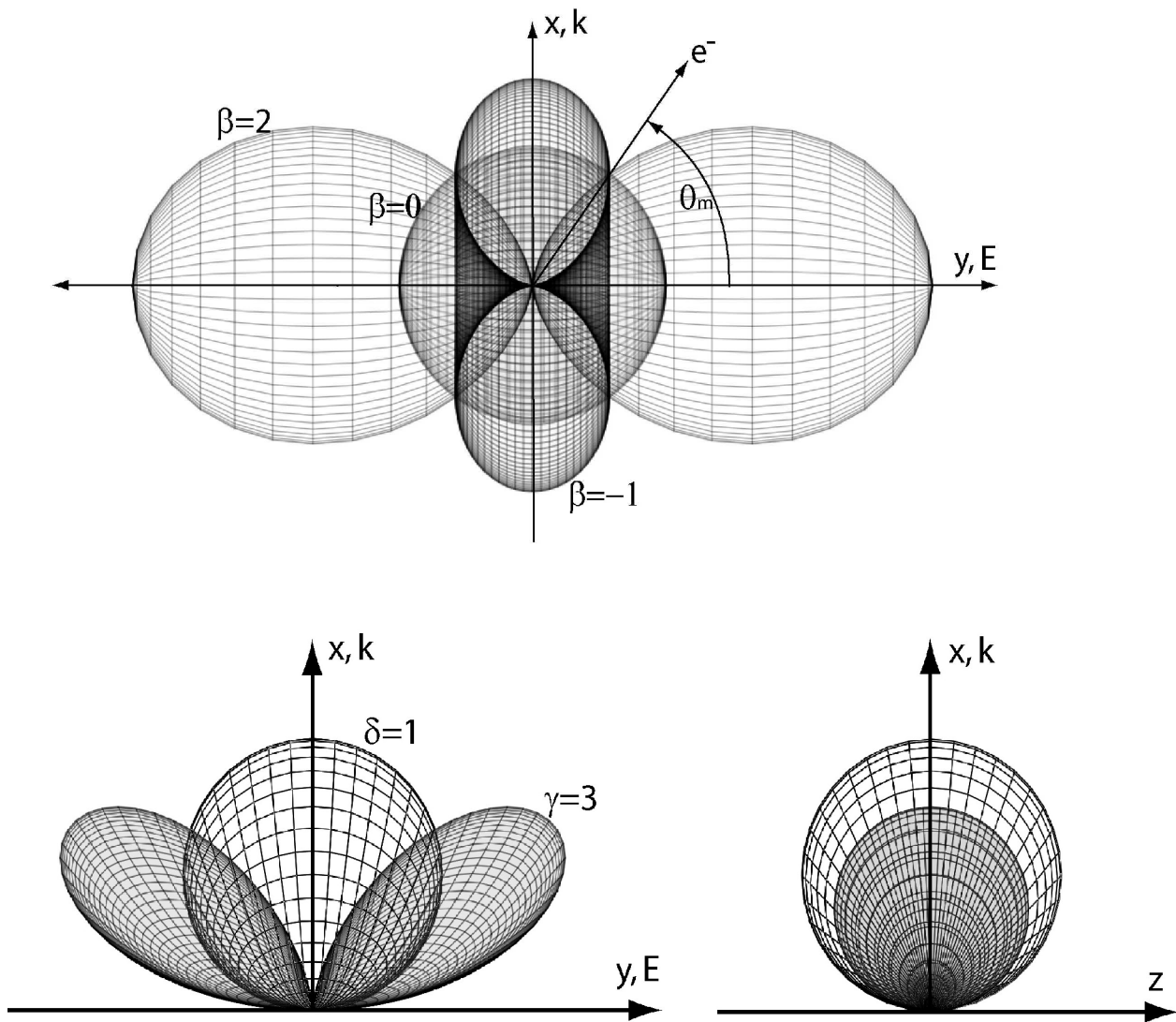
Figure 5. Top - Angular distribution pattern for the dipole parameter β. As β changes values, the angular distribution pattern changes shape. Bottom - The nondipole angular distrubution describing δ and γ. Unlike the dipole angular distrubution pattern, as δ and γ change values, the pattern are scaled accordingly.

$$A_{analyzer\ number}(\theta,\ \phi) = Area$$

$$T_{analyzer\ number} = Electronic\ and\ Detector\ Efficiencies$$

$$A_1\left(54.7^\circ, 90^\circ\right) = \frac{d\sigma}{d\Omega} = \frac{\sigma}{4\pi}\, T_1$$

$$A_3\left(54.7^\circ,\ 0^\circ\right) = \frac{d\sigma}{d\Omega} = \frac{\sigma}{4\pi}\left(1 + \sqrt{\frac{2}{27}}\zeta\right) T_3$$

$$A_4(0^\circ, 90^\circ) = \frac{d\sigma}{d\Omega} = \frac{\sigma}{4\pi}(1 + \beta) T_4$$

The differential cross section is proportional to the area under the N 1s peak for nitrogen gas (Figure 6). By dividing the differential cross sections for analyzers 3 and 4 by that for analyzer 1, it is possible to determine the angular distribution parameters without knowing the partial photoionization cross section.

$$\beta = \left(\frac{T_1}{T_4}\frac{A_4}{A_1}\right) - 1$$

$$\zeta = 3\delta + \gamma = \sqrt{\frac{27}{2}}\left(\frac{T_1}{T_3}\ \frac{A_3}{A_1} - 1\right)$$

Argon gas was used for calibration because all of the dipole and nondipole parameters are known for this element. This way we determine the efficiencies for each analyzer pair.

$$\frac{T_1}{T_4} = (\beta_{Ar} + 1)\frac{A_{1Ar}}{A_{4Ar}}$$

$$\frac{T_1}{T_3} = \left(\sqrt{\frac{27}{2}}\zeta_{Ar} + 1\right)\frac{A_{1Ar}}{A_{3Ar}}$$

Now that all the necessary parameters are known, the nondipole and dipole parameters can be determined for that particular energy. Each of these equations must be solved for each spectrum and from there a graph can be made of the nondipole or dipole parameter over the photon energy.

DISCUSSION AND CONCLUSIONS

Figure 7 shows experimental data of the N_2 N 1s nondipole parameter ζ as filled circles with error bars and theoretical data for molecular nitrogen as a solid line that is in excellent agreement with the data points. The theory for atomic nitrogen is shown as a dot-dashed line. The broad peak centered at about 470 eV photon energy is due to significant contributions of the nondipole parameters in Equation 1.

The theory for atomic nitrogen lacks the resonance-like feature seen in the experimental data, leading to the conclusion that this behavior has a molecular origin despite the largely atomic-like nature of the occupied 1s orbitals in molecular nitrogen. The theory for molecular nitrogen is explained in detail elsewhere.[5]

In short, the magnitude of nondipole effects is dependent on the relation between the photon energy and the size of the orbital. When the photon has a larger wavelength (which corresponds to a lower photon energy) than the orbital, the nondipole effect is small. On the other hand, if the orbital is larger than the photon wavelength, the nondipole effect is large. When comparing N_2 N 1s ionization with atomic nitrogen N 1s ionization, the nondipole effect is more pronounced in molecular nitrogen. This is rather puzzling because the N 1s orbitals are about the same size. Based on theoretical calculations these larger nondipole effects depend on the bond-length distance between the two nitrogen atoms. Therefore, it is necessary to also include the comparison between the wavelength and the bond-length. It has been shown that the nondipole effect is related to the bond-length size to a larger extent than the orbital size and some other molecular contributions.[5] Theory starts to deviate at lower photon energies (410-420 eV). This deviation is attributed to the fact that the theory uses a frozen-core approximation for the calculations and a dynamical potential change needs to be implemented. The observed nondipole effects appear to indicate a universal nondipole characteristic in molecular photoionization, which demands further experimental and theoretical study.

ACKNOWLEDGEMENTS
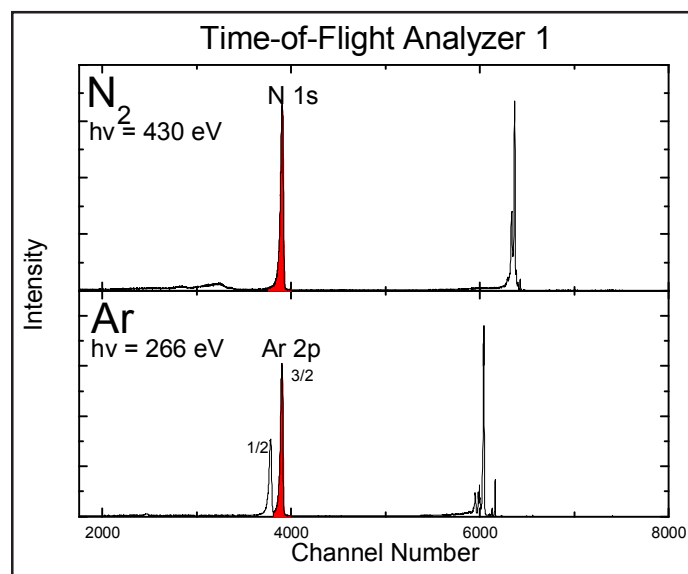
Figure 6. Spectra of nitrogen and argon at a certain photon energy. The colored sections under the graphs indicate which areas were used to calculate the dipole and nondipole parameters.
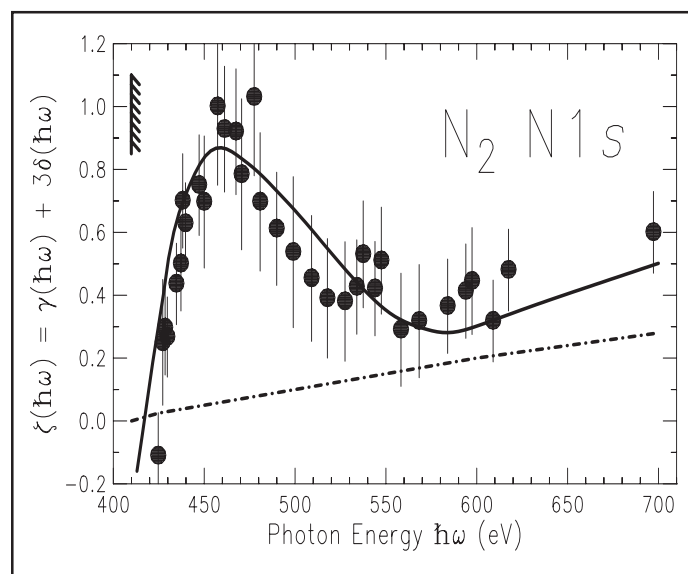
Figure 7. Nondipole parameter ζ for molecular nitrogen. The filled circles with error bars are the data collected as described in the text. The theory for molecular nitrogen is the solid line and the theory for atomic nitrogen is the dot-dashed line.

REFERENCES

1 Derevianko, A., Hemmers, O., Oblad, S., Glans, P., Wang, H., Whitfield, S.B., Wehlitz, R., Sellin, I.A., Johnson, W.R., and Lindle, D.W., "Electric-Octupole and Pure-Electric-Quadrupole Effects in Soft-X-Ray Photoemission," Phys. Rev. Lett. 84, 2116 (2000).

2 Lindle, D. W., Hemmers, O. A. (2000). "Time-of-Flight Photoelectron Spectroscopy of Atoms and Molecules," Proc. of Pan American Advanced Studies Institute. Angra dos Reis, Brazil, April 27 — May 7, 2000 edited by C. Cisneros, H. Bryant, and F. Schlachter.

3 Hemmers, O.A., Lindle, D.W. (2000). "Non-dipolar Effects in Soft-x-ray Photoemission," Proc. of Pan American Advanced Studies Institute. Angra dos Reis, Brazil, April 27 — May 7, 2000 edited by C. Cisneros, H. Bryant, and F. Schlachter.

4 Hemmers, O.A., Whitfield, S.B., Glans, P., Wang, H., Lindle, D.W., Wehlitz, R., and Sellin, I.A., "High-resolution Electron Time-of-Flight Apparatus for the Soft X-ray Region" Review of Scientific Instruments, vol. 69, November 1998. 3809-3817.

5 Hemmers, O.A., Wang, H., Focke, P., Sellin, I.A., Lindle, D.W., Arce, J.C., Sheehy, J.A., Langhoff, P.W., "Large Nondipole Effects in the Angular Distribution of K-Shell Photoelectrons from Molecular Nitrogen", Phys. Rev. Lett. 87, 273003 (2001).

PROCESSING VARIABLES OF ALUMINA SLIPS AND THEIR EFFECTS ON THE DENSITY AND GRAIN SIZE OF THE SINTERED SAMPLE

Ryan Rowley[A] and Henry Chu, Ph.D.[B]

ABSTRACT

High densities and small grain size of alumina ceramic bodies provide high strength and better mechanical properties than lower density and larger grain size bodies. The final sintered density and grain size of slip-cast, alumina samples depends greatly on the processing of the slip and the alumina powder, as well as the sintering schedule. There were many different variables explored that include initial powder particle size, slurry solids percent, amount and type of dispersant used, amount and type of binder used, and sintering schedule. Although the experimentation is not complete, to this point the sample with the highest density and smallest grain size has been a SM8/Nano mixture with Darvan C as the dispersant and Polyvinyl Alcohol (PVA) as the binder, with a solids loading of 70 wt% and a 1500 °C for 2 hours sintering schedule. The resultant density was 98.81% of theoretical and the average grain size was approximately 2.5 μm.

INTRODUCTION

Some of the mechanical properties of ceramics have always been attractive to manufacturers. Their hardness, durability, and ability to operate effectively at high temperatures are unsurpassed by any metal, but their brittleness and difficulty in manufacturing complex shapes have been repelling factors to manufacturers.[1]

Slip-casting of ceramics has made it possible to create complex shapes while maintaining the desirable characteristics of the ceramic. Slip-casting is a relatively simple and inexpensive method used to produce ceramics. The alumina powder is dispersed in an aqueous solution then poured into a gypsum mold. The mold removes the water from the solution leaving the powder in a tightly packed green state. Because of the diversity in the sizes and shapes of the molds, the ceramic can take on any number of shapes. Slip-casting can also yield high densities, small grain sized ceramics. These slip-cast ceramics are very close in density and grain size to hot-pressed ceramics.

If the desired high densities and comparable grain sizes can be achieved through slip-casting, the mechanical properties should be comparable to hot-pressed samples, with the added bonus that complex shapes can be achieved at a greatly reduced cost. To achieve the high densities and grain size needed to obtain the wanted mechanical properties, there are many different processing procedures. The variable ingredients and sintering schedules can be applied in any number of combinations. Our purpose in doing this experiment is to find which combinations of processing, ingredients and sintering schedule provides the highest fired density and smallest grain size for slip-cast alumina bodies.

MATERIALS AND METHODS

The different alumina powders used in the experiment were Baikalox SM8 with a primary particle size of 150 nm, Baikalox CR6 with a primary particle size of 250 nm, and NanoPhase Technologies NanoTek with a primary particle size of 30 nm.[2] The different dispersants used were Darvan C and Darvan 821. The binders used were solid Polyvinyl Alcohol (PVA) and Rhoplex B-60A. The water used was consistent throughout and was de-ionized.

To prepare the slurry, the powder was prepared several different ways. It was used with one, or a combination of several, of the following: out of the bag with no further processing; sieved through a −100 mesh sieve; and heat-treated at 800 °C for 4 hours in air. The sieve was used to break up the soft agglomerates of particles and remove the hard agglomerates, both of which can be detrimental during sintering. The heat treatment was used to remove any impurities that may have been in the as-received powder.

The dispersants were added in quantities ranging between 0.5 wt% of solids and 2.0 wt% of solids. The binders were added according to their recommended dilutions. The PVA was dissolved in water before it could be added to the solution at between 0.1-2.0 wt% of solids. In order to dissolve the PVA, the water had to be heated to approximately 80 °C.

The ingredients were added in the following order: water (with binder if PVA was used), binder, dispersant, then alumina powder. After the wet ingredients are added, solid alumina cylinders are added to the mixture to mix them together. The

---

A: Brigham Young University, Provo, UT; B: Idaho National Engineering and Environmental Laboratory, Idaho Falls, ID

alumina powder is then slowly added allowing for complete wetting of the powder after each small addition of powder. Mixing the powder slowly and allowing saturation of the particles between additions allows faster addition of all the powder.

When all the ingredients are added to the mixture the slurry is allowed to roll mix for several hours. After several hours of roll mixing to allow for complete wetting, the slurry is treated with an ultrasonic horn for 3 minutes. This ultrasonic treatment breaks apart all the soft agglomerates in the slurry allowing for a uniform and tightly packed cast piece. The slurry is then allowed to roll mix at least over night.

The gypsum mold is prepared by using water and plaster of paris at 30 parts plaster to 21 parts water. The molds are prepared in the desired shape and allowed to dry completely before use.

Before the slurry is poured into the mold, it is vacuum treated to remove any air bubbles. It is then poured into the mold and left to dry. After the slurry is completely dry, it is placed in a furnace to sinter according to one of the following sintering schedules:

1. Ramp to 800 ° C, hold for 4 hours, ramp to 1500 °C hold for 2 hours, cool down;
2. ramp to 800 °C, hold for 2 hours, ramp to 1500 °C hold for 1 hour, cool down; and
3. ramp to 800 °C hold for 2 hours, ramp to 1400 °C hold for 2 hours, cool down.

The included 800 °C hold is to burn out the binder in the sample and is ramped at a rate of 10 °C/min. The ramp from 800 °C to the final sintering temperature is between 6 °C/min and 10 ºC/min.

The final sintered densities for each sample were found using Archimedes density principle, provided the density exceeded 92% of the theoretical density.

RESULTS

Our project consisted of making alumina ceramic pieces with the many different combinations of variables. Most of these variables had some effect on the final sintered density of the sample. Table 1 shows the effect of dispersant type on the fired density. Only small differences were observed. However, since Darvan C produced a slightly denser sample, it was used for the remainder of the experiment.

Table 2 shows that the samples with PVA as the binder were ≤ 1 percentage point higher in fired density than samples using B-60A. PVA was used nearly all of the time because of this. However, more complicated shapes held together better with B-60A so it was used in these circumstances.

Table 3 shows that the average particle size of the powder had an impact on the final density of the sample. The CR6 powder was slightly less dense than was the SM8 powder, with the SM8 powder having the smaller initial powder particle size. As with the binder the difference was ≤ 1 percentage point higher in relative theoretical density.

Table 1. Dispersants vs. Density

Sample	Dispersant	% Theoretical Density
Al-PVA-70-C	Darvan C	98.81
Al-PVA-70-821	Darvan 821	98.77

Table 2. Binders vs. Density

Sample	Binder	% Theoretical Density
Al-B60A-0.7	Rhoplex B-60A	97.54
Al-PVA-70-C	PVA	98.81

Table 3. Particle size vs. Density

Sample	Powder	% Theoretical Density
Al-B60A-0.7	CR6	97.54
Al-B60A-SM8-B-15	SM8	98.60

Table 4. Solids wt% vs. Density

Sample	Solids wt%	% Theoretical Density
Al-01-02	50	>92.0
Al-04-0.6	60	96.18
Al-PVA-70-C	70	98.81
Al-B60A-80-C	80	97.74

Table 5. Sintering Schedule vs. Density

Sample	Sintering Temp.	Sintering Time	% Theoretical Density
Al-B60A-SM8-B-14	1400°C	2 hr	95.34
Al-B60A-SM8-B-15	1500°C	1 hr	98.60

Figure 1. Al-B60A-0.7 with an average grain size of ~5.5mm, % theoretical density of 97.54% and CR6 powder.
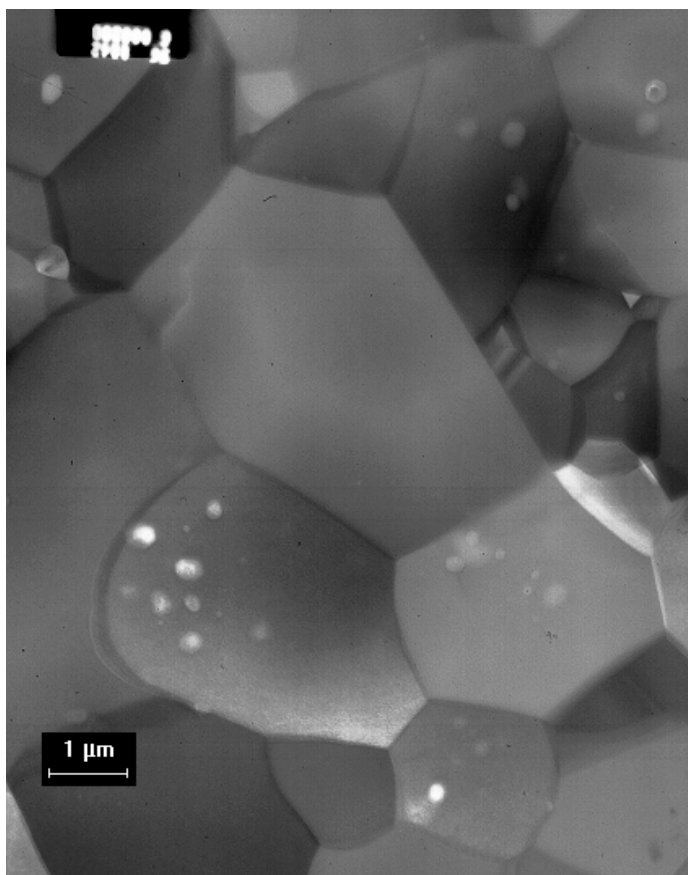
Figure 2. Al-PVA-70-C with an average grain size of ~6mm, % theoretical density of 98.81% and SM8 powder.
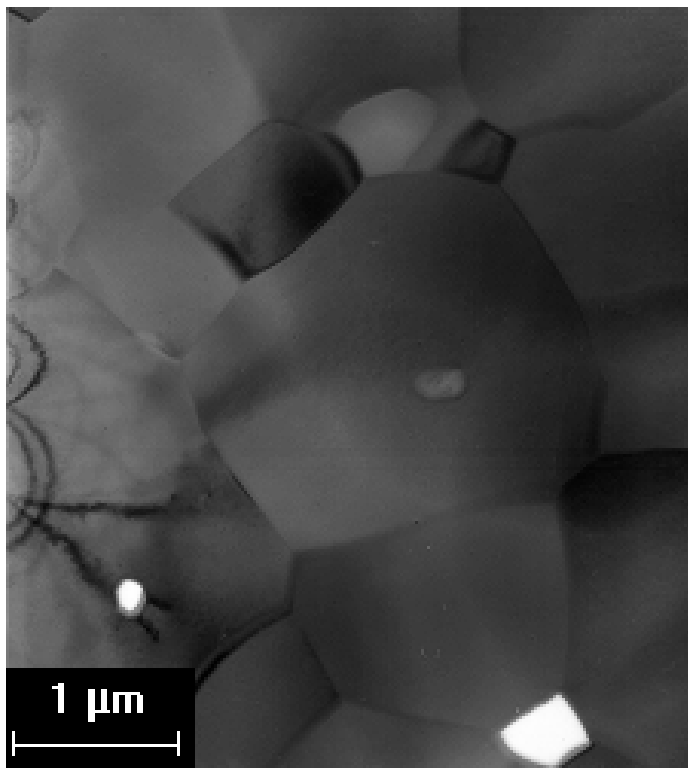
Figure 3. Al-PVA-SMNAN with a % theoretical density of 98.81% and an average grain size of ~2.5 mm.

The slurry solids percent had the greatest impact on the final sintered density of the sample. Table 4 shows that the lower solids percent loading yields a much lower final density, which can be as many as 8 percentage points when the solids loading is dropped to 50 solids wt%. This table also shows that when the solids loading was increased to 80 solids wt% the density dropped ~1 percentage point from 70 solids wt%.

The final variables are the sintering temperature and time. This has an effect on the final density but also has an effect on the sintered grain size. Table 5 shows that the ceramic has a much higher density when sintered at 1500 °C as compared to 1400 °C, the difference being ~3 percentage points of the theoretical value.

The grain size differed between samples, but not enough data has been collected, particularly for the samples in Table 5, to come to any conclusions as to which of the processing variables and sintering schedules provides the smallest average grain size. Several of the discussed samples have been observed through a Transmission Electron Microscope (TEM), and Figures 1 & 2 show their grain structure and average grain size. Also Figure 3 shows a bimodal sample which is the best sample produced to this point in terms of average grain size and density.

The results regarding the heat treatment, sieving, and ultrasonic treatment of the powder showed that these variables produced insignificant effects on the final density.

DISCUSSION AND CONCLUSION

The results of this experiment show that some of the variables make little difference in the final density of the sample, while others make a noticeable difference. Also, some of these differences are easily explained while others are not as clear. The variables that make a difference are the binder used, grain size of the powder, sintering schedule, and solids percent loading. The two dispersants used made very little difference.

From the previously stated results, an optimum processing schedule would be as follows: SM8 aluminum oxide powder at 70 wt% of solids , DI water, Darvan C at 1.5 wt% of solids, PVA at 0.5 wt% of solids , and a sintering temperature of 1500 °C for 1 hour. This schedule would yield the highest density alumina slip-cast sample. Highest density does not necessarily equate to best mechanical qualities, and mechanical testing is on-going to research which of the samples will provide the best mechanical properties.

From the results up to this point, it appears that we will be able to produce high density, small grain size slip-cast alumina ceramics, comparable to hot-pressed alumina samples, and expected to have comparable mechanical qualities. As the research continues, the sintering schedule will be optimized to achieve the needed characteristics and unnecessary processing steps will be eliminated, providing us with a high quality alumina ceramic at a fraction of the cost of hot-pressed alumina ceramics. It will also allow complex shapes to be made, which cannot be made through hot-pressing.

ACKNOWLEDGEMENTS

REFERENCES

1 "Machining of MD & LD Machinable Ceramics." Marketech International, Inc.
   http://www.mkt-intl.com/ceramics/mdld.pdf

2 "Baikowski: Baikalox 99.99% Ultrapure Calcined Alumina Powders." Baikowski. (2002, July 2)
   http://www.baikowski.com/td_baikalox_reg.shtml

INCREASING EFFICIENCY IN PHOTOELECTROCHEMICAL HYDROGEN PRODUCTION

SCOTT WARREN[A] AND JOHN TURNER, PH.D.[B]

ABSTRACT

Photoelectrochemical hydrogen production promises to be a renewable, clean, and efficient way of storing the sun's energy for use in hydrogen-powered fuel cells. We use p-type $Ga_{51}In_{49}P$ semiconductor (henceforth as $GaInP_2$) to absorb solar energy and produce a photocurrent. When the semiconductor is immersed in water, the photocurrent can break down water into hydrogen and oxygen. However, before the $GaInP_2$ can produce hydrogen and oxygen, the conduction band and the Fermi level of the semiconductor must overlap the water redox potentials. In an unmodified system, the conduction band and Fermi level of $GaInP_2$ do not overlap the water redox potentials. When light shines on the semiconductor, electrons build up on the surface, shifting the bandedges and Fermi level further away from overlap of the water redox potentials. We report on surface treatments with metallated porphyrins and transition metals that suppress bandedge migration and allow bandedge overlap to occur. Coating ruthenium octaethylporphyrin carbonyl (RuOEP CO) on the $GaInP_2$ surface shifted bandedges in the positive direction by 270 mV on average, allowing the bandedges to frequently overlap the water redox potentials. Coating the $GaInP_2$ surface with $RuCl_3$ catalyzed charge transfer from the semiconductor to the water, lessening bandedge migration under light irradiation. Future work will focus on the long-term surface stability of these new treatments and quantitative applications of porphyrins.

INTRODUCTION

Current methods of energy production have substantial limitations. The pervasive use of fossil fuels creates large amounts of pollution and poses a threat to both human and ecosystem health. As demonstrated by recent fluctuations in energy prices, the United States has little control over significant portions of its energy supply. Hydrogen fuel is a leading contender to solve these energy problems.

Our work focuses on devising a domestic, renewable, and nonpolluting system for producing hydrogen. The hydrogen-production system consists of a semiconductor working electrode and a platinum counter electrode immersed in an aqueous electrolyte. When the semiconductor is irradiated with light more energetic than its bandgap, electrons in the valence band are excited into the conduction band. The excited electrons generate a photocurrent, splitting water into hydrogen at the semiconductor surface and oxygen at the platinum electrode surface.

For direct photoelectrochemical decomposition of water to occur, the hydrogen-production system must meet several requirements. First, the distance between the conduction band and the Fermi level of the semiconductor must be larger than the redox potential of water. At 25 ºC, the redox potential of water is 1.23 eV. A cathodic overpotential of 24 meV and an anodic overpotential of 96 meV are typical values for water electrolysis at a photocurrent of 20 mA/cm² (Khaselev et al., 2001). Therefore, water has an effective redox potential of 1.3-1.4 eV. The semiconductor must have a bandgap of at least 1.5 eV to split water.

Second, the semiconductor bandedges must overlap the conduction band and the Fermi level. The semiconductor's conduction band must be higher in energy than the water reduction potential so that the reduction of water will be energetically favorable. Similarly, the semiconductor's Fermi level must be lower in energy than the water oxidation potential so that the oxidation of water will be energetically favorable.

Third, charge transfer from the semiconductor surface to the water must occur quickly. If electrons build up on the surface of the semiconductor, they will shift the bandedges and Fermi level in a negative direction. Additionally, charge build-up on the semiconductor surface can destabilize the surface and allow the semiconductor to decay. Methods have been devised to partially catalyze charge transfer (Bansal et al., 2000).

Finally, the semiconductor must be stable during photoelectrolysis conditions in water. Inert semiconductors – such as TiO_2, $KTaO_2$, ZrO_2, and SiC – have too large a bandgap to collect a significant portion of the solar spectrum. Unfortunately, many semiconductors with smaller bandgaps are unstable under photoelectrolysis conditions. Recently, $GaInP_2$ was identified as one of the few semiconductors with an ideal bandgap that is moderately stable during photoelectrolysis (Khaselev et al., 1998).

P-type $GaInP_2$ has a bandgap of 1.8-1.9 eV, ideal for splitting water (Kocha et al., 1994). However, the conduction band and Fermi level are 300-450 meV too negative to overlap the water redox potentials when overpotentials are taken into account. Additionally, $GaInP_2$ does not catalyze charge transfer well. This research focuses on correcting these problems by modifying the inner Helmholtz layer. Previous research has shown that adsorbing organic molecules onto the $GaInP_2$ surface can shift bandedges (Kocha et al., 1995, August), while adsorbing transition metals

A: Whitman College, Walla Walla, WA; B: National Renewable Energy Laboratory, Golden, CO

(particularly Ru and Rh) can partially catalyze charge transfer (Bansal et al., 2000). With the hope of combining these effects, we studied a wide range of metallated porphyrins.

In this paper, we report on our results using capacitance-voltage and current-voltage measurements. We performed kinetics studies to determine charge catalysis on those porphyrins that succeeded in shifting band edges in the positive direction. We also combined porphyrin treatments with transition metals to bolster charge transfer kinetics.

MATERIALS AND METHODS

We used all chemicals as received. The chemicals included H_2SO_4 (J. T. Baker), HNO_3 (J. T. Baker) and dichloroethane (DCE) (Aldrich). The porphyrins used in this study were manufactured by Midcentury and are listed in Table 1. All porphyrins were made to 0.1 mM in DCE. Phthalate buffer and carbonate buffer (pH 4 and 10) (Beckman), Hydrion buffers (pH 2 - 12) (Metrepak) and dilute sulfuric acid were the electrolytes in our three-electrode cell. A 0.010 M $RuCl_3$ (Strem) solution in pH 1.5 HCl was used from a previous study (Bansal et al., 2000). We also used a platinum sol (colloid size ranging from 50 - 100 Å) made by refluxing hydrogen hexachloroplatinate hydrate (Aldrich) with citric acid.

Our materials included zinc-doped 3 μm thick p-type $Ga_{.51}In_{.49}P$ epilayers (henceforth, $GaInP_2$). It was grown by atmospheric-pressure metal organic chemical vapor deposition (MOCVD) epitaxy on zinc-doped GaAs substrates approximately 350 μm thick and misoriented from the (100) surface by 2° toward (110). A growth temperature of 700 °C and growth rate of 4.4 μm/h were used (Kurtz et al., 1992). The carrier concentration in the sulfuric acid-etched $GaInP_2$ layer was (5-7) x 10^{16} cm^{-3}. Electrodes were made from the $GaInP_2$ using a previously published technique (Bansal et al., 2000). Exposed surfaces of the electrodes ranged from 0.02 to 0.13 cm^2. Prior to use, the electrode was etched in concentrated sulfuric acid, rinsed in deionized water, and dried in nitrogen gas. After drying, the electrode surface was chemically modified using the methods discussed below: porphyrin drop evaporation, porphyrin spray application, and metal-ion dip-coating.

Using the porphyrin drop evaporation method, we placed a 50 μL drop of the 0.1 mM porphyrin solution in DCE on the surface of the $GaInP_2$ electrode. The DCE evaporated under a stream of nitrogen gas, leaving a layer of the porphyrin on the electrode surface.

In the porphyrin spray application, we used a chromatography sprayer to apply 0.1 mM porphyrin solutions in DCE to the surface of the $GaInP_2$ electrode. The spraying occurred in half-second pulses to allow the DCE to evaporate before spraying again. The spray time ranged from 5 to 80 seconds.

We performed metal-ion chemisorption using a previously published method (Bansal et al., 2000). Electrodes were immersed in the $RuCl_3$ solution for 60 seconds and in the Pt sol for 1 - 3 hours. In combination treatments of porphyrins with metal ions, the metal ion was adsorbed first. Then, a layer of the porphyrin was adsorbed.

Capacitance-voltage (C-V) and current-voltage (I-V) measurements were performed in a three-electrode cell. The setup consisted of a $GaInP_2$ semiconductor, a platinum mesh counter electrode (~2 cm^2) and a saturated calomel reference electrode (SCE). We irradiated the $GaInP_2$ electrode with a Cole-Parmer 41500-50 Fiber Optic Illuminator housing a 150 W quartz halogen bulb. Data were collected using a Solartron 1286 Electrochemical Interface connected to a Solartron SI 1260 Impedance/Gain-Phase Analyzer. We used ZPlot 2 and ZView 2 software to collect and analyze C-V data and CorrWare 2 and CorrView to collect and analyze I-V data. Measurements were made at a frequency of 10 kHz with a 10 mV rms amplitude. Scan rates ranged from 5 to 10 mV/s. For measurements in the dark, data was collected between –1.0 V and +0.2 V vs. SCE and the current range was automatically selected by ZPlot. For measurements in the light, the negative end of the scan range extended to –2.2 V vs. SCE and the current range was fixed at 0.2 or 2.0 mA, depending on the photocurrent.

In agreement with a previous study, we successfully modeled the $GaInP_2$/water system as a series RC circuit (Kocha et al., 1996). In this model, R_S is the series resistance of the circuit and C_{SC} is the capacitance of the space charge region (see Figure 1). By modeling the space charge layer of the semiconductor in this manner, we were able to determine the flatband potential using Mott-Schottky plots.

RESULTS

Table 1 displays the flatband potentials for drop-evaporated porphyrin treatments and drop-evaporated porphyrins combined with transition metals. The porphyrins were drop-evaporated onto a new $GaInP_2$ electrode after initial characterization and etching
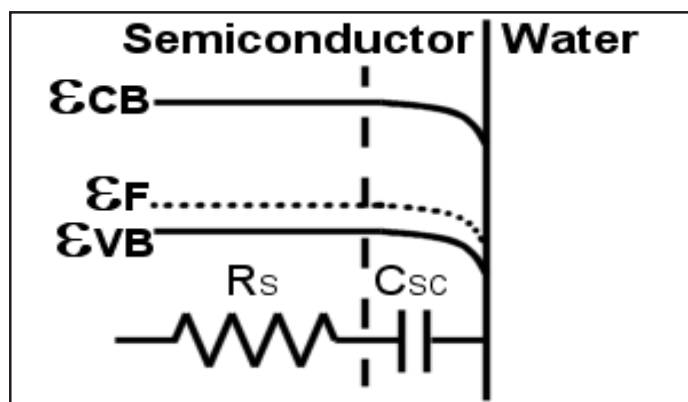
Figure 1. Modeling a p-type semiconductor as a series resistor and capacitor. R_S = System resistance. C_{SC} = Semiconductor capacitance.

Table 1. Results of Mott-Schottky plots in pH 4 buffer.
OEP = Octaethylporphyrin, TPP = Tetraphenylporphyrin.
V_{FB} = Flatband potential, which is a measure of the bandedge positions.

Treatment	V_{FB}	Standard Deviation
CoOEP	0.117	0.017
CoTPP	0.121	0.053
FeOEP Cl	0.102	0.058
FeTPP Cl	0.100	0.043
Pt sol + RuOEP CO	0.481	0.012
RhOEP Cl	0.138	0.082
$RuCl_3$ + RuOEP CO	0.488	0.207
RuOEP CO	0.266	0.182
RuTPP CO	0.161	0.091

with concentrated sulfuric acid. The testing was done in pH 4 buffer. Repeated scans were performed in the cathodic and anodic directions to determine the stability of the surface treatment. The results in Table 1 are the average of all of the scans in both cathodic and anodic directions. All of the porphyrins show a statistically significant shift in flatband potentials, with the ruthenated porphyrins showing the greatest shift. The bandedges shifted into overlap conditions about 20% of the time with the RuOEP CO treatment. Both of the combination treatments of RuOEP CO with either Pt sol or RuCl₃ showed substantial shifts in bandedge position. These combination treatments allowed overlap of the water redox potentials to occur in the dark

Figures 2 and 3 show the results of charge transfer catalysis testing in pH 4 buffer. The porphyrins were applied to new electrodes. At higher light intensities, the potential scan range was shifted negative as the flatband potential shifted negative. Of the molecules tested, only the RuOEP CO shifted the conduction band and Fermi level into the correct positions under light irradiation.

Figure 4 demonstrates the effect of a combined porphyrin-metal ion treatment. Dip-coating a RuOEP CO-treated electrode with $RuCl_3$ vastly improves charge catalysis properties up to a photocurrent of 1 mA/cm². Testing is in pH 4 buffer.

Figure 5 compares the drop-evaporation method with the spray application method. The drop-evaporation method is capable of adsorbing greater amounts of porphyrins on the $GaInP_2$ surface than the spray application method.

Displayed in Figure 6 are the effects of testing in a range of pHs on a treated and untreated electrode. The most substantial shift in flatband potential occurs at pH 4, hence the testing at that pH.

Figure 7 shows the possible desorption of CoTPP in pH 4 buffer over a period of days. The flatband potential decreases by 50 mV after 23 hours and by another 25 mV after another 70 hours.

Table 2 shows the doping densities in an untreated electrode (and hole concentrations in a treated electrode). The combination metal-RuOEP CO treatments show a statistically significant decrease in doping density as compared with untreated electrodes.

Figure 2. Charge transfer catalysis testing under increasing light intensities. Testing performed in pH 4 buffer. V_{FB} = Flatband potential, which is a measure of the bandedge positions.
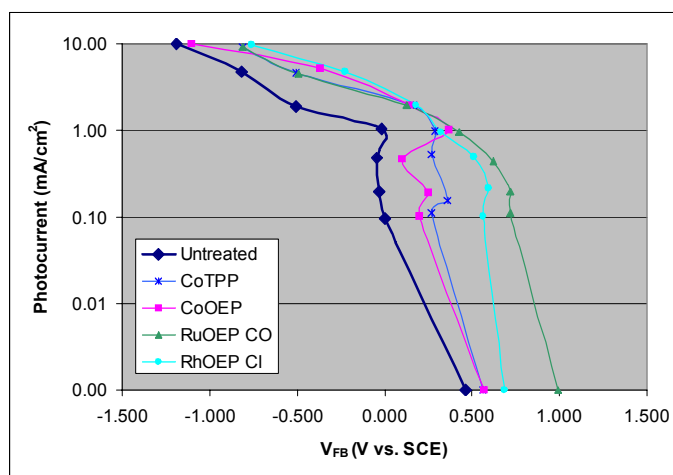
Figure 3. Charge transfer catalysis testing under increasing light intensities. Testing performed in pH 4 buffer.
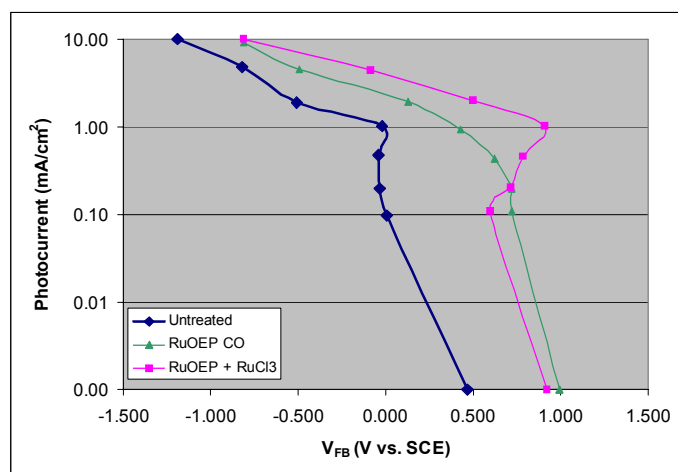
Figure 4. Charge transfer catalysis of various treatments. Testing performed in pH 4 buffer.
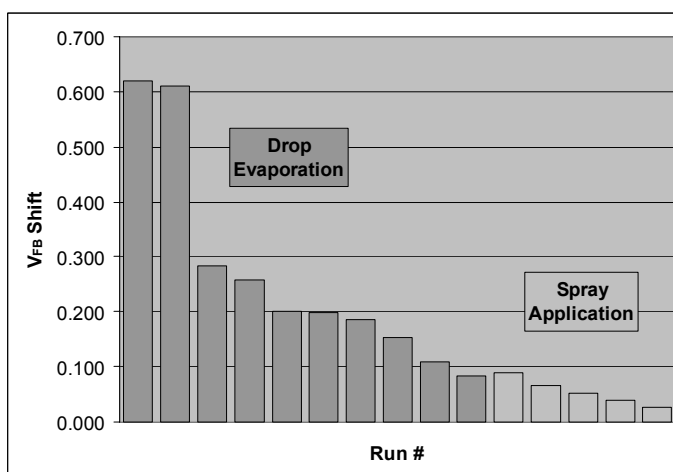
Figure 5. Comparison of drop evaporation and spray application of RuOEP CO. The magnitude of the shift in bandedge position correlates well with the thickness of the RuOEP CO application. V_{FB} Shift is the change in flatband potential between a treated and untreated electrode.

DISCUSSION AND CONCLUSION

In order to photoelectrochemically split water into hydrogen and oxygen, the conduction bandedge must be higher in energy than the water reduction potential and the Fermi level must be lower in energy than the water oxidation potential. Our survey of porphyrins as bandedge-shifting agents showed that RuOEP CO shifts bandedges a substantial amount in the correct direction. When combining the RuOEP CO with a transition metal, such as ruthenium or platinum, the bandedge shift increases.

The large standard deviation in the flatband potential is caused by two factors. The first is the varying application thickness. As we increase the porphyrin application thickness on the $GaInP_2$ surface, the shift in flatband potential increases (see Figure 5). With the RuOEP CO drop-evaporation treatment, the flatband potential shifted as much as 600 mV when a large amount of porphyrin was applied to an electrode with a small surface area. Conversely, the flatband potential shifted as little as 100 mV when a small amount of porphyrin was drop-evaporated onto a larger surface area. The RuOEP spray application applied only minute amounts of the porphyrin to the electrode surface, causing only slight shifts in flatband potentials. The flatband potential shifted as little as 26 mV when we sprayed the electrode for 5 seconds, and as much as 90 mV when we sprayed the electrode for 80 seconds.

The second factor causing a large standard deviation in the flatband potential is the electrode age. After several etchings in concentrated sulfuric acid, the response to porphyrin treatments decays. We hypothesize that the decrease in response is due to the decrease in surface defects (and an increase in the surface smoothness) of the $GaInP_2$ as the electrode is etched more. A previous study showed that the photoluminescence of $GaInP_2$ increases as the etch time increases (Kocha et al., 1995). In fact, the photoluminescence increases the fastest when etched in concentrated sulfuric acid, as compared with the other etchants studied. The increase in photoluminescence is indicative of fewer surface states, suggesting that the $GaInP_2$ has a cleaner surface with fewer defects. As the number of surface states and defects decrease, there is less opportunity for the porphyrin to attach to the surface. Thus, with less porphyrin attached to the surface, the bandedge shift substantially decreases.

We also performed testing with HNO_3 as the etchant. Nitric acid etches the surface at a much faster rate, creating a relatively rough $GaInP_2$ surface. This allows more porphyrin to attach to the surface, regardless of etching time. In accordance with prediction, etching in HNO_3 increased the repeatability of flatband potential measurements and decreased the decay in response as the electrode was used more.

Testing of charge catalysis at the GaInP2 surface showed that the RuOEP CO and the RhOEP Cl catalyze charge transfer up to a photocurrent of 0.2 mA/cm2. However, the conduction band and Fermi level are not in water-splitting position in either of these cases. However, adding a platinum sol or ruthenium metal to the surface substantially increased flatband potential and charge catalysis. A charge catalysis study was performed on an electrode treated with ruthenium metal and RuOEP CO (as shown in Figure 4). This treatment placed bandedges in a water-splitting position up to a photocurrent of 1 mA/cm^2, or about one tenth of the intensity of the sun.

Testing was performed almost entirely in pH 4 buffer because we saw the greatest shifts in flatband potential with porphyrin

Table 2. Doping densities (N_D) for untreated (etched) and treated electrodes.

	Etched	Porphyrins Only	Metals Only	RuOEP CO	RuCl$_3$ + RuOEP	Pt sol + RuOEP
N_D	5.89E+16	5.17E+16	5.56E+16	5.29E+16	4.27E+16	3.36E+16
Std. Dev.	1.39E+16	1.48E+16	1.02E+16	2.08E+16	9.23E+15	1.60E+16
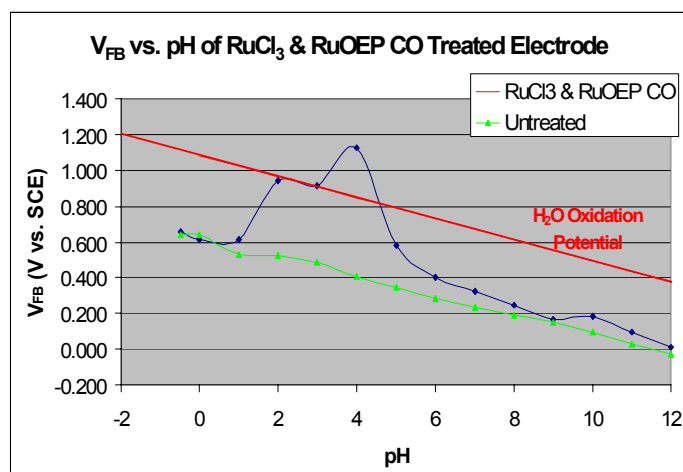
Figure 6. The effect of pH on flatband potential on an untreated and RuCl$_3$ + RuOEP CO-treated electrode.
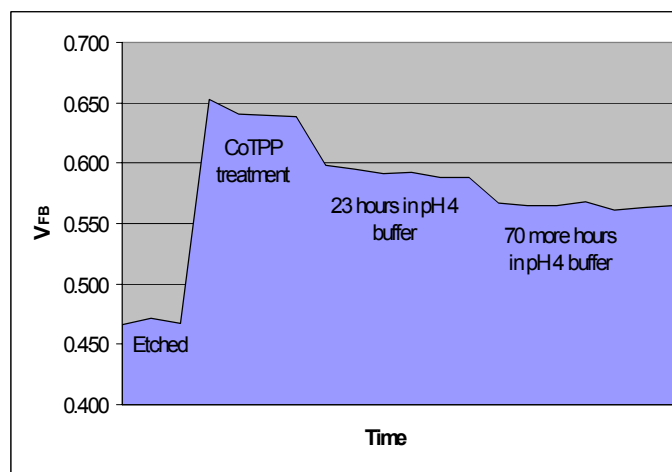
Figure 7. Possible desorption of CoTPP after immersing a CoTPP-modified electrode in pH 4 buffer for extended lengths of time.

treatments at that pH (see Figure 6). However, the short circuit current (SSC) is substantially improved at lower pHs. Further testing will focus on improving porphyrin response at lower pHs so as to improve the photocurrent and water-splitting efficiency.

Another area for improvement is the stability of the porphyrin on the GaInP$_2$ surface. As shown in Figure 7, CoTPP desorbs from surface after extended periods in pH 4 buffer. Further work will be performed on improving the porphyrin stability. Increasing the surface roughness or covalently attaching the porphyrins to the GaInP$_2$ surface are options worth exploring.

An interesting result of the metal-RuOEP CO combination treatments was the decrease in hole concentration in the GaInP$_2$. This suggests that the metal-RuOEP CO treatment donates electrons into the semiconductor. The role of electron donating porphyrins in decreasing the doping density and shifting the flatband potential in a positive direction is yet to be studied.

In this research, we have substantially improved the prospects of GaInP$_2$ for photoelectrochemical hydrogen production. With further work, we will hopefully develop a system capable of splitting water powered by the sun's light. Our research has shifted flatband potentials into water-splitting condition and catalyzed charge transfer. We have the goal of further catalyzing charge transfer to meet our goal of creating a sun-powered hydrogen production system. In this work, we have come closer to our goal of replacing fossil fuels with a clean fuel, decreasing our dependence on foreign energy sources, improving livability within cities, and creating a healthier environment for the earth's ecosystems.

ACKNOWLEDGMENTS

REFERENCES

Bansal, A.; Turner, J. (April 9, 2000). Suppression of band edge migration at the p-GaInP$_2$/H$_2$O interface under illumination via catalysis. Journal of the American Chemical Society, 104, 6591-6598.

Khaselev, O.; Bansal, A.; Turner, J. (2001, February). High-efficiency integrated multijunction photovoltaic/electrolysis systems for hydrogen production. International Journal of Hydrogen Energy, 26, 127-132.

Khaselev, O.; Turner, J. (1998, October). Electrochemical stability of p-GaInP$_2$ in aqueous electrolytes toward photoelectrochemical water splitting. Journal of the Electrochemical Society, 145, 3335-3339.

Kocha, S.; Peterson, Mark W.; Nelson, Art J.; Rosenwaks, Yossi; Arent, Doug J.; Turner, John A. (1995). Investiagtion of wet-etch surface modification of Ga$_{0.5}$In$_{0.5}$P using photoluminesence, x-ray photoelectron spectroscopy, capacitance measurements, and photocurrent-voltage curves. The Journal of Physical Chemistry B, 99, 744-749.

Kocha, S.; Turner, J. (1995, August). Displacement of the bandedges of GaInP$_2$ in aqueous electrolytes induced by surface modification. Journal of the Electrochemical Society, 142, 2625-2630.

Kocha, S.; Turner, J. (1996). Impedance analysis of surface modified Ga$_{0.5}$In$_{0.5}$P – aqueous electrolyte interface. Electrochimica Acta, 41, 1295-1304.

Kocha, S.; Turner, J.; Nozik, A.J. (1994). Study of the Schottky barrier and determination of the energetic positions of band edges at the n- and p-type gallium indium phosphide electrode | electrolyte interface. Journal of Electroanalytical Chemistry, 367, 27-30.

Kurtz, S.R.; Olson, J.M.; Kibbler, A.E.; Bertness, K.A. (1992). Incorporation of zinc in MOCVD growth of Ga$_{0.5}$In$_{0.5}$P. Journal of Crystal Growth, 124, 463-469.

Abstracts

Table of Contents

This 420 ton magnet, part of Brookhaven National Laboratory's Alternating Gradient Synchrotron (AGS), is a high energy accelerator critical to physicists' search for rare decays of short-lived subatomic particles called kaons. The experiment is designed to test a theory of matter known as the Standard Model.

BIOLOGY

The Toxic and Carcinogenic Potential of a 1.6 GHz Wireless Communication Signal: In Vivo Two-Year Bioassay. *SEAN ADHIKARI (University of Washington, Seattle, WA 98195) LYLE B. SASSER (Pacific Northwest National Laboratory, Richland, WA 99352)*

Years ago, the possible carcinogenic effect of radio frequency (RF) radiation from cell phones was brought to the public's attention. It is believed to increase the risk of brain cancer. The purpose of this study was to assess the carcinogenic effects of Motorola's 1.6 GHz Iridium Signal on Fischer 344 rats. Four groups of male and female rats were tested: one cage-control (kept in cages and not loaded and unloaded into exposure chambers), one sham-exposed (loaded into exposure chambers without exposure to the signal), and two fully exposed to the signal at different doses. According to data collected based on statistical analysis, no significant differences existed in survival rates or body weights between the groups of males and females. Also, no significant differences existed in birth performances between the four treatment groups of pregnant females. Therefore, the study has not yet established a clear connection between RF radiation and cancer. Nevertheless, much is left to be completed of this study, including necropsy and histopathology of all animal tissues. Afterwards, it still may not successfully prove the harmful effects of cell phone radiation.

Teaching about Nature in Nature Integrating Field Methods into Biology Classrooms. *JENIFER BERRELLI (U. Mass. Amherst, Amherst, MA 01003) TIMOTHY GREEN (Brookhaven National Laboratory, Upton, NY 11973)*

Presently, most educational curriculums lack active learning and field methods. To enhance learning in high school biology classrooms, it is possible to introduce professional field methods to educators, with hopes that they may integrate more field trips and outdoor activities into their curriculum. This summer's (2001) field program enabled high school students to learn many scientific techniques, skills and concepts. Throughout the summer, the students learned valuable observation skills as they explored numerous nature centers, beaches, dunes, marshes, woodlands, rivers and ponds. Students learned about glacial deposition as a means of land formation, coastal change and development, how to determine history of a coastal, marshland or woodland area given topographical, sediment and/ or vegetation data, how to determine the susceptibility of an area to burn dependent on fuel load, how to determine the difference between areas of natural formation as opposed to areas disturbed by anthropomorphic activities, and how to conduct a vegetation and topographical analysis of a segment of river. They proceeded to choose a specific research topic and use the scientific method to evaluate topic of concern, hypothesize, record data, analyze, and conclude the research followed by the production of research papers, posters and presentations. As parents and teachers observed the students' presentations, it is anticipated that these field methods will be regarded as particularly productive and may influence those educators to include more of this type of teaching methods in their program of study.

Development of Sentra - A Database of Signal Transduction Proteins for 45 Prokaryotic Organisms. *SAURABHA BHATNAGAR (Illinois Institute of Technology, Chicago, IL 60616) NATALIA MALTSEV (Argonne National Laboratory, Argonne, IL 60439)*

Advances in biology and bioinformatics have made a significant contribution to our understanding of biological systems, especially in identification of genes and the functions of their products. Identification of the components of biological systems has progressed significantly, such that new methodologies and techniques can be developed to aid in the understanding of the system as a whole. Reconstructing the sensory process requires understanding the nature of the transmitted signal as well as mechanisms involved in its transduction. Cellular responses to a variety of environmental and internal cellular signals were identified in prokaryotic organisms by experimental studies. However, predicting the nature of a transmitted signal by computational analysis is problematic and should take into account all available information that could assist such functional assignments. We have performed identification of five classes of signal transduction proteins in 45 completely sequenced genomes. In order to provide conjectures about possible mechanisms of their signal transduction processes as well as the nature of transmitted signal it is necessary to analyze the domain composition of the components of the signal transduction

proteins and their participation in conserved chromosomal gene clusters. This can be done within the environment of the new Sentra at: http://www-wit.mcs.anl.gov/sentra. Sentra provides flexible querying capabilities, as well as visualization of not only protein functional domains and similarity searches, but allows the user to examine the contig in which the gene encoding for the protein resides, as well as the genes clusters with the gene in question.

Deletion of hsdR gene from Shewanella oneidensis MR-1 genome. *STEPHANIE CHU (Sacramento City Community College, Sacramento, CA 95822) MARGIE ROMINE (Pacific Northwest National Laboratory, Richland, WA 99352)*

Shewanella oneidensis MR-1 has the ability to respire a large variety of compounds, including radionuclides and metals. Respiration of radionuclides, such as U and Tc, leads to the precipitation of relatively insoluble metal oxides, thereby limiting their mobility in aquifers where they can pose a health risk. MR-1 is poorly receptive to "foreign" DNA and therefore it is more difficult to transfer DNA that has been genetically engineered in E. coli into MR-1. Exclusion of foreign DNA is in part due to the hsdR gene, which is part of a restriction and modification system (RMS). HsdR encodes an enzyme that cleaves unmethylated, "foreign" DNA. By deleting this gene we hope to eliminate the restriction activity, thereby making MR-1 more receptive to genetically engineered DNA. A clone in which DNA flanking either side of the hsdR gene were fused together was generated by PCR. The resulting PCR fragment was cloned into pcrII-TOPO and transformed into E.coli. Preliminary results indicate we were successful in cloning the PCR product. The insert will next be transformed into a suicide vector, which will then be transferred to MR-1 to promote replacement of the genomic region containing hsdR with our genomic segment lacking hsdR via a process known as homologous crossover. Once a strain lacking hsdR is constructed through this approach we can test whether this mutation produces a variant that is more successful in taking up and maintaining DNA isolated from E. coli.

Is Ycf9 the Linchpin of Photosystem II? Heterologous Expression for Structural and Functional Studies. *HELEN CHUNG (Cornell University, Ithaca, NY 14853) GEOFFREY HIND (Brookhaven National Laboratory, Upton, NY 11973)*

One group of ORF's, ycfs (hypothetical chloroplast reading frames), have proven to be highly conserved between species of plants, and are thought to be genuine genes. ycf9 in particular has caught the attention of scientists. It encodes for a 62 amino acid protein that contains two alpha helices that are highly hydrophobic and is found in the PS II thylakoid membrane fractions. Gene knockout experiments have been done to determine the function and importance of this gene while fractionation experiments have been done to locate the whereabouts of its products. But no experiments have been done to isolate the protein in attempt to study its structure. In this experiment, I isolated ycf9 from the leaves of a spinach plant, expressed it in E. coli, and identified it through SDS PAGE. Circular dichroism spectroscopy and polarized infrared spectroscopy will be performed in hopes to unravel one of the many mysteries of photosynthesis: how PSII is put together and/or held together by ycf9.

Structural Classification of the Internal and External Loops Found in Ribosomal RNA. *BRIANA COOK (Southern Utah University, Cedar City, UT 84720) STEPHEN HOLBROOK (Ernest Orlando Lawrence Berkley National Laboratory, Berkley, CA 94720)*

As part of a project to classify RNA structure we have made a preliminary effort to group the internal and external loops of 5S, 16S and 23S RNA. We used a software package, AMIGOS, to calculate pseudo-conformational angles from the coordinates from the overall ribosomal RNA structure. These angles were plotted and common conformations were determined from clusters in the distribution of points. We then used computer graphics to visualize the three-dimensional structure of these conformations. We identified a common motif in which an S-shaped backbone results in base-base interaction on the same strand and forming a three base triple interaction with the opposite strand. We also identified a common structure in external loops consisting of five residues. In this structure the first and fourth residues were hydrogen bonding while the second residue in the loop was perpendicular to the first and the third protruded into solution. These conserved motifs will be utilized in our overall structure of classification of RNA.

Detection of Cardiac Tissue Damage Using a Cantilever-based Biosensor.

LESLIE COOK (Davidson College, Davidson, NC 28036) PANOS DATKSOS (Oak Ridge National Laboratory, Oak Ridge, TN 37831)

Detection of cardiac tissue damage currently involves detection of marker molecules released by the damaged cardiac cells, for example, myoglobin and troponin. The level of marker biomolecules present in the blood stream is usually determined using an antibody-based ELISA (enzyme-linked immunosorbent assay). Recent developments in biosensor research have shown that microcantilever-based sensors have the potential to show greater sensitivity than current ELISA techniques. Greater sensitivity for biomarker detection could result in earlier detection and treatment for cardiac patients. Troponin is a protein cardiac marker that is only released into the bloodstream upon damage to cardiac cells. We propose to develop an assay for troponin molecules by immobilizing monoclonal antibodies to troponin on microcantilevers using a specific orientation approach. Antibodies will be covalently crosslinked to microcantilevers using PDP-Hydrazide, which is reactive towards oxidized sugar and carboxylic acid groups on the Fc region of IgG antibodies. Functionalized cantilevers will then be exposed to varying concentrations of antigen (troponin) under flow conditions. Cantilever deflection (molecular interaction) will be measured using a position sensitive detector. Immobilization chemistry will be checked using contact angle measurements. Microcantilever technology will be important in detecting low levels of biomolecules and will facilitate early detection and early treatment of myocardial infarction. It also has great potential for low-level molecule detection in other areas of medical and environmental research.

Deletion of hsdR gene from Shewanella oneidensis MR-1 genome.

VALERIE CRUSSELLE (University of Utah, SLC, UT 84112) MARGARET ROMINE (Pacific Northwest National Laboratory, Richland, WA 99352)

Shewanella oneidensis MR-1 has the ability to respire a large variety of compounds, including radionuclides and metals. For some radionuclides, such as U and Tc, this respiration leads to the precipitation of relatively insoluble metal oxides, thereby limiting their mobility in aquifers where they can pose a health risk. As the genome of this organism has just been sequenced, much research is being done to determine the pathway of this unique respiration. However, it has been found that S. oneidensis MR-1 is not very receptive to "foreign" DNA, which is a necessary characteristic in order for genetic manipulation of the bacteria. This is due to the hsdR gene, which is part of a restriction and modification system (RMS). The RMS system enables the bacteria to distinguish "foreign" DNA from its own. HsdR codes for a restriction activity which cleaves unmethylated, "foreign" DNA. Therefore, deletion of this gene would eliminate the restriction activity. This deletion is created through a series of techniques, including polymerase chain reaction (PCR), cloning, and homologous crossover. Hypothetically, the deletion of hsdR from the S. oneidensis MR-1 genome would therefore make the bacteria more receptive to DNA from other species of bacteria.

Efficacy of surface coatings in prevention of microbial infection: an in vitro study.

BROOKE DEATHERAGE (Washington State University, Pullman, WA 99163) ALLISON A. CAMPBELL (Pacific Northwest National Laboratory, Richland, WA 99352)

The increasing incidence in the medical field of post-implant infection has prompted further investigation into possible coatings to alleviate this problem. This study explores using a "scaffold" system to carry antimicrobial substances and prevent infection. Hydroxyapatite (HAP; Ca5(PO4)3OH), was used as a protective coating for bone bonding and as a delivery system. Two polymers also explored as delivery systems were PMMA (polymethyl-methacrylate) and PLGA (poly-lactide-glycolide). The two antimicrobial agents analyzed were chlorhexidine and silver nitrate. Chlorhexidine has antimicrobial effects on both gram-positive and gram-negative bacteria with little resistance. Silver nitrate also inhibits growth of a wide range of microorganisms. The surfaces of the metal substrates were coated with HAP-based systems via surface induced mineralization (SIM), and with polymer systems through dip-coating. Fourier transform infrared spectroscopy (FTIR), X-ray diffraction spectroscopy (XRD), and scanning electron microscopy (SEM) were used to characterize the coatings. The efficacy of each coating in inhibiting microbial growth was tested in culture plates inoculated with Staphylococcus aureus, a common cause of the targeted infections. Rods coated with HAP/chlorhexidine and HAP/silver nitrate both showed inhibition of Staphylococcus

aureus, whereas the uncoated rods, HAP-only coated rods, and polymer coated rods exhibited no antimicrobial effects. A coating containing both HAP and chlorhexidine has the most potential for reduction of infection rates due to its in vitro display of the largest zones of inhibition, and would be the best choice for use in medicine.

ALCHEMY: the transmutation of matter.

DOUGLAS DZIUBAN (Allan Hancock College, Santa Maria, CA 93454) TAMAS TOROK (Ernest Orlando Lawrence Berkley National Laboratory, Berkley, CA 94720)

Abstract goals of the research: to identify the ability of microbes to reduce hexavalent chromium to it's less toxic trivalent state. approach: set up and conducted an experiment consisting of 32 trials. The variables for the trials were: organism, hexavalent chromium concentration, and addition of an iron source. Each trial was then sampled regularly for biomass growth and hexavalent chromium reduction and the resulting data was then compiled and analyzed. Results: some key findings of the experiment were that some species of microbes have the ability to reduce hexavalent chromium when the concentrations were low (2ppm), and that some can tolerate hexavalent chromium even at high concentrations (200ppm) though they could not reduce it; leading to the conclusion that the ability to tolerate and the ability to reduce chromium are independent of one another. The experiment took a surprise turn when it became apparent that a contaminant in one of the control trials was adept at reducing chromium. Subsequent secondary experiments supported this microbe's ability, which surpassed the ability of the other microbes used in the experiment.

Monitoring of Groundwater Microbial Community.

ALISON EAKIN (Eastern Washington University, Cheney, WA 99004) HEATHER KOSTANDARITHES (Pacific Northwest National Laboratory, Richland, WA 99352)

This was the initiation of a study for monitoring the groundwater microbial community at the Oyster Site in Virginia. This analysis is only a small part of a more extensive research program for developing a potential remediation strategy for leakage of underground storage. Two groundwater flow cells were installed in which microbial transport experiments have been performed under induced and natural flow-gradients. This study was conducted on samples that came from both within and outside the flow cell. Samples from each location were "static" or under natural flow-gradients, and "post-gradient" came from induced gradients. Samples will continue to be collected and tested in the continued induced current state. Plates were made to test for the presence of total coliforms (including E-coli) and streptococcus. If a sample showed the presence of coliforms it was also tested to see if the coliforms were of fecal descent. The second set of samples (post gradient after time with the induced current) showed that no fecal coliforms were present. The second set of samples also contained fewer samples that showed positive for iron related bacteria and sulfate reducing bacteria. Spread plates of the samples were made to observe the general growth and morphology. A biological assay was done using 31 of the most useful carbon sources for soil and groundwater community analysis. Further studies will be done to compare the continued post-gradient samples to the initial post-gradient and static samples.

Purification of an Adenovirus Proteinase Homolog from the Chlamydia Genome.

CHRISTINE EMIGH (University of California, Santa Cruz, Santa Cruz, CA 95064) WALTER F. MANGEL (Brookhaven National Laboratory, Upton, NY 11973)

Chlamydia are bacterial pathogens whose representatives are widely distributed in nature, and C. trachomatis causes several human diseases of medical significance. This is the most common type of genital tract infection and is one of the most damaging of the venereal diseases (Science 1999). Purification and characterization of such a common and diverse type of virulence factor could lead to discoveries that are applicable to all types of virulence factors. It is essential for a good protocol to be designed for the mass purification of this protein for these studies to be carried out. Diffraction data collected from a crystal of the Chlamydia protein could yield important data for the design of a specifically-targeted drug. Although Chlamydia is treatable by antibiotics, this is an expensive and potentially risky treatment. A specifically targeted molecule could end up much less costly to produce and without the potential risks that come with antibiotics.

Effect of Oxygen on Hydrogen Production in Wild type and Mutant Algae. *SARA FALL (Syracuse University, Syracuse, NY 13210) JAMES W. LEE (Oak Ridge National Laboratory, Oak Ridge, TN 37831)*

As petroleum reserves are depleted at an alarming rate, scientists have realized the need to discover novel sources of renewable energy. Both mutant and wild types of the Chlamydomonas algae may be a novel source of hydrogen for energy purposes. In determining whether or not algae may in fact be used as an energy source, several environmental factors that may affect the photosynthetic pathway of the organism must be considered. Current thinking in photosynthesis supports the theory that oxygen may in fact inhibit the production of hydrogen. Therefore, it is necessary to conduct experiments on the effect of oxygen on hydrogen production. This can be accomplished by monitoring the hydrogen production of various types of algae in a dual flow reactor system. A solution of algae and minimal media is put in to reaction vessels and research grade helium and a helium-oxygen mixture of gases are run through the system by a computer-controlled flow meter. The hydrogen production is then measured. Hydrogen production increased following exposure to oxygen. CO_2 was introduced into the system to test for a possible back mutation. The algae did not fix CO_2. This could mean that RuBisco is not the site where O_2 enters the photosynthetic pathway.

BN-350 Spent Fuel Disposition Storage Project Environmental Assessment. *SHARON FELTS (University of Idaho, Moscow, ID 83843) MAUREEN FINNERTY (Argonne National Laboratory, Argonne, IL 60439)*

In an attempt to curtail proliferation risks, the United States agreed to assist Kazakhstan with the decommissioning of the BN-350 nuclear reactor and with the disposition of the spent fuel from the reactor. The US government is providing Kazakh officials with templates and guidelines based on current United States procedures to help build Kazakhstan's infrastructure as a newly independent country. Specifically, the spent fuel disposition program required characterization and packaging of the fuel within the BN-350 reactor as well as the development of a plan for the interim 50-year storage of this fuel. A dry well interim storage facility to be built at the Baikal-1 nuclear testing site in Kazakhstan was proposed for the second stage of the disposition program. In the United States, an environmental assessment (EA) is used to determine the environmental impacts of a proposed action on the surrounding environment. A template of an environmental assessment for the interim storage of the spent fuel in Kazakhstan was prepared considering the impact of the facility and its operation on the environment surrounding the Baikal-1 site. Due to lack of historical data from Kazakhstan and the Baikal-1 site specifically, some sections of the interim storage facility EA could not be completed but general information about the required data and computations necessary was compiled and included in the template.

CYP1B1 Polymorphisms: Possible Risk Factors for Breast Cancer. *KACEE FUJINAMI (Allan Hancock College, Santa Maria, CA 93454) REGINE GOTH-GOLDSTEIN (Ernest Orlando Lawrence Berkley National Laboratory, Berkley, CA 94720)*

Polycyclic aromatic hydrocarbons (PAHs) are a group of chemicals that contain many carcinogens. PAHs are prevalent in industrialized countries because they are formed during incomplete combustion of hydrocarbons in energy production. PAHs deposit in adipose tissues, such as those in the breast. PAH is altered in a two-phase reaction in order to detoxify and excrete PAH from the body. Phase I of the reaction involves enzymes, particularly Cytochrome P450 1B1 (CYP1B1) in breast tissue, that convert PAH to a water-soluble, carcinogenic intermediate. Phase II involves enzymes that detoxify this intermediate for excretion. Two polymorphisms in exon 3 of the CYP1B1 gene are being investigated for their role in breast cancer risk. One variant, m1, is a single base change at codon 432 and causes Leucine to be substituted for Valine. The second variant, m2, is a single base change at codon 453 and causes Serine to be substituted for Aspargine. Both enzymes show higher oxidation levels of PAH than the wild-type enzyme. Genotypes are examined by isolating DNA from tissue, amplifying the CYP1B1 gene using polymerase chain reaction (PCR), digesting the PCR product with Eco57I (digests m1 variation) and Cac8I (digests m2 variation), and running the products in polyacrylamide gel electrophoresis (PAGE). A comparison of genotypes from tissue samples from reduction mammoplasty patients and mastectomy patients has not yet shown conclusive evidence for a specific genotype increasing breast cancer risk, although only a small sample size of 55 reduction mammoplasties and 97 mastectomies has been tested.

Constructing a Plasmid for the Expression of Arginine Rich Protein. *ABRIL GARCIA (California State University, Fresno, Fresno, CA 93740-8026) JONI MOTT (Ernest Orlando Lawrence Berkley National Laboratory, Berkley, CA 94720)*

The extracellular matrix (ECM) is an organized network of extracellular material made of several types of glycoproteins such as collagen, proteoglycan, and fibronectins found beyond the plasma membrane. The ECM plays a key role in determining cell shape and activity. The ECM is degraded by matrix metalloproteinases (MMP), which are a family of zinc dependant endoproteinases. MMP are important in wound healing, implantation, organ involution, and growth and development. MMP are secreted by mammalian cells and are activated extracellularly by the cysteine switch where cysteine residue in the propeptide becomes uncoordinated with the catalytic zinc ion leaving the active site of MMP available for catalyses. Tissue inhibitors of metalloproteinase (TIMP's) are a family of protein inhibitors that regulate MMP activity. Until recently it was believed that TIMP's were the only inhibitors of MMP, research suggests other MMP inhibitors exist. A fragment of Arginine Rich Protein (ARP) was recently identified as a potential non-TIMP MMP inhibitor. The purpose of this research was to create an expression vector for ARP for its expression in mammalian cells.

Beta-1 Integrin Protein Expression in Differentiating Human Lens Epithelial Cells Following X Irradiation. *MICHAEL GARCIA (Allan Hancock College, Santa Maria, CA 93455) ELEANOR BLAKELY (Ernest Orlando Lawrence Berkley National Laboratory, Berkley, CA 94720)*

B1-Integrin is a cell adhesion molecule which has an essential role in anchorage of cells to the extracellular matrix (ECM). We have preliminary immunofluorescence evidence indicating that ionizing radiation modulates expression of B1-Integrin in differentiating Human Lens Epithelial cells (HLE). In the present study, we compared b1-Integrin levels in protein extracts from x-irradiated and non-irradiated, control HLE. HLE were grown on bovine corneal endothelial cell-derived ECM in medium containing 15% fetal bovine serum and 5 ng/ml FGF-2. HLE at four different stages of differentiation were prepared for experiment: cells in exponential growth, and cells at 5, 10 and 15 days post-confluence. Cultures were irradiated with a 4 Gy, single dose of x-ray (150 kVp). Total protein was harvested from samples at various times (30 minutes to 12 hours) after irradiation, and analyzed by Western analysis using SDS-PAGE (Sodium Dodecyl Sulfate-PolyAcrylamide Gel Electrophoresis). B1-Integrin was detected using a mouse monoclonal antibody. Western analysis revealed that B1-Integrin from HLE produced two distinct protein bands. There was no obvious difference in expression levels of B1-Integrin in exponential HLE after 4 Gy compared to controls. The relative intensities of the two b1-Integrin bands changed during the differentiation of HLE. We will compare the expression of B1-Integrin in HLE observed by Western analysis of extracted protein samples, with results obtained previously by immunofluorescence analysis of fixed cells.

Viscosity Reduction of Heavy Crude's Aided by Microorganisms. ERICA GOODRICH (Community College of Rhode Island, Warwick, RI 02886) MOW LIN (Brookhaven National Laboratory, Upton, NY 11973) .

Eight sandstone cores were prepared and filled with samples of a heavy crude oil. The samples were treated with saltwater-mimic and two different strains of Bacillus species of microorganisms at 60°C. After treatment the following parameters were measured. These were: 1) Quantity of oil extracted, 2) viscosity, and 3) hydrocarbon distribution. The treated samples showed a higher quantity of recovered oil, a reduction in viscosity, and an enhancement of lighter hydrocarbon fractions. A direct comparison of the gas chromatographic data showed that the intensity of the hydrocarbon peaks were higher in the bacteria treated samples as compared to those from the saltwater-mimic sample.

PETRI NET REPRESENTATION OF THE KREB CYCLE. *DEAN GULL (Southern Utah University, Cedar City, UT 84720) JOE OLIVEIRA (Pacific Northwest National Laboratory, Richland, WA 99352)*

We have developed a computational model that accurately depicts

sequences of enzyme-catalyzed reactions as specialized directed graphs. We hypothesize that creation of network models for biochemical systems will allow elucidation and quantification of the system response to a given perturbation. Our model is a first step toward a goal of facilitating manipulation and study of a complete biochemical system. Graphical network models provide a computational framework for identifying key circuits, oscillatory behaviors, and response to biochemical perturbation. The model presented here represents a first approximation of the set of all mass-flux balance conserving pathways or circuits for a given biochemical reaction sequence. The size and complexity of the problem of identifying all such paths and combinations of paths requires enormous computational resources. We have extended previous approaches to this problem by formulating a combinatorial geometric model referred to as an oriented matroid. The interested reader is referred to our previous work and to the Mathematics section of this paper.

High Resolution Imaging with the Soft X-ray Microscope, XM-1.
ADEN HABTEAB (San Jose State University, San Jose, CA 95192) GREG DENBEAUX (Ernest Orlando Lawrence Berkley National Laboratory, Berkley, CA 94720)
Microscopy has taken great strides in its evolution since Aton van Leeuwenhoek assembled simple microscopes and used them to study microorganisms. The Center for X-ray Optics (CXRO) is a major contributor to the advancement of microscopy. It built a new high-resolution, soft X-ray microscope, the XM-1, at the Advanced Light Source (ALS) facility. The XM-1 uses bending magnet radiation from a synchrotron as a light source. The optical set-up for the XM-1 allows for high spatial resolution. The resolution is primarily determined by the outer- most zone width of the fresnel zone plate lens used for imaging. Other components of the XM-1, such as the external visible light microscope (VLM) and a Zeiss Axioplan visible light microscope (ALM), contribute to the precision and the user friendliness of the XM-1. XM-1 has applications in biology, environmental science, material science, and magnetic materials. In addition to these applications, optics testing is continuously conducted on the XM-1 to ensure its efficiency and also to expand its capabilities. Testing of the condenser zone plate's illumination revealed an error in its focusing ability. We replaced the zone plate with a new one. The level of damage to the CCD camera due to high-energy photons was revealed through dark current imaging. Currently, testing on stray light, which reduces the contrast of images, is being conducted. There is now a new interactive slide show for visitors of XM-1 at the beam line. Optics testing is necessary for ensuring the optimal performance of XM-1.

Biochip Manufacturing Quality Control Research (Preparation of Acrylamide Micro-Matrices by Photo-polymerization).
KELLY HAMMAN (Richard J. Daley, Chicago, IL. 60629) GENNADIY YERSHOV (Argonne National Laboratory, Argonne, IL 60439)
Creating a biochip involves a 7-step procedure, beginning with a cleaning step and ending with hybridization of oligonucleotides. Throughout these procedures, background fluctuates thus creating variations in fluorescent intensity. The fluorescent intensity can interfere with the readability of biochips. We have created a research design, using a Bio Imager (aka scanner), to read the Digital Luminescent Units[DLU] and to monitor the variations of background throughout the procedure of manufacturing Biochips. Our goal is to find specific background limits in which Biochips can successfully be manufactured. With our data and the rate of successfully produced Biochips, we can apply standard acceptable background limits to the quality control aspect of the manufacturing of Biochips. Further research is necessary to adjust the parameters in which standard acceptable background limits range and can be applied to the manufacturing protocol of Biochips. Data collection regarding contamination can also be applied to a manufacturing protocol 'problem-solving' design. The use of the ANL biochip will revolutionize the world of science. Our biochips are cost-effective, minimize chemical use, time-efficient and will provide an accurate testing medium for all bioscience areas. The Biochip Manufacturing Quality Control Research is imperative to the further development of quality ANL Biochips. While current methods successfully produce ANL Biochips, we desire to create a more cost and time effective protocol. The Quality Control design is vital to producing an ANL Biochip Manufacture method easily obtained and successfully executed by business.

Cholesterol Management: A workshop for reducing a major risk factor for heart disease.
MIRIAM HERNANDEZ (LaGuardia Community College, Long Island City, NY 11101) MARY WOOD (Brookhaven National Laboratory, Upton, NY 11973)
Heart disease is the major killer of women and men in the United States and cholesterol is one of the major factors for heart disease. Cholesterol is a fat-like substance that, when in high levels, causes the blood vessels to narrow and eventually blocks the flow of blood leading to a heart attack or heart disease. For this reason, a three-month cholesterol workshop (CW) was run for BNL employees in order to control and maintain their cholesterol levels. The CW provided information about cholesterol importance in our body, cholesterol as a risk factor for heart disease, cholesterol types and measurements, cholesterol food sources and cholesterol-lowering treatments. All participants had their lipoprotein profile (cholesterol measurements) at the beginning and end of the CW. Then the two cholesterol measurements of each participant were compared to identify changes in their cholesterol levels. Moreover, each participant completed a final evaluation to determine their lifestyle changes after the CW. Looking at the data of the participants, many became more informed about cholesterol issues and changed their lifestyles. Few participants even reached desirable cholesterol levels. These findings suggest that cholesterol levels can be controlled by correct information and lifestyle changes. In this way, heart disease can be prevented.

Spatially Resolved Single Cell Irradiator to Study Bystander Responses to Low LET Radiation.
BROOKE HOLBEN (Washington State University, Pullman, WA 99163) MARIANNE SOWA RESAT (Pacific Northwest National Laboratory, Richland, WA 99352)
The bystander effect refers to the observation of a biological response in the absence of direct irradiation. To examine this for low LET radiation, we are using a novel single cell irradiation device to deposit energy in a pre-selected subset of cells for which the un-irradiated neighbors can be easily identified. Using this device we investigated the presence of a calcium flux following exposure to ionizing radiation. Transient calcium levels were measured using visible wavelength calcium sensitive dye, Flou 4, which exhibits an increase in green fluorescence upon binding to calcium. This research is on going and control results are presented here. To monitor another aspect of the biological response to ionizing radiation, a p53 reporter system has been developed where CHO and D2XRII cells were transfected with p53 and fluorescence reporter EGFP. Characterizations of this system were made by exposing various cell lines to wide field Gamma radiation. We measured p53 localization within the cell as well as stabilization (accumulation) of p53 after DNA damage. Survival curves were obtained for both wild-type and transfected CHO cells following Cobalt-60 radiation. Transfection of cells had no significant effect on cell survival. Using the western blot technique, we were able to analyze protein expression levels of irradiated D2XRIIp53(15X)EGFP cells. The time response following 5.0 Gy irradiation did not conclusively show an increase in the p53 expression and further experiments are necessary.

Data Analysis for Ecological Risk.
KATHRYN HYLDEN (University of Notre Dame, South Bend, IN 46556) TERRI MILEY (Pacific Northwest National Laboratory, Richland, WA 99352)
For four weeks I have worked at PNNL as an intern on a data analysis team. We run a FORTRAN model to assess the effects of Hanford activities on the local ecology. We use a Visual Basic data extraction program to select the results of interest, and then we put the data into graphs so the project ecologist can determine where trouble spots are both currently and under potential future conditions. The scope of the larger project is to ascertain what cleanup of the nuclear waste still needs to happen and how much of the waste is already below harmful levels. I personally had the opportunity to work with various computer programs and languages to produce these results.

Optimization of the Protocol for Nucleic Acid Sample Preparation.
ANA JUAREZ (Richard J. Daley College, Chicago, IL 60652) SERGEI BAVYKIN (Argonne National Laboratory, Argonne, IL 60439)
Many recent advances in genetics have provided a wealth of information that has facilitated the development of new technologies such as DNA microarray technology at a rapid rate. Because accuracy of the produced results is perhaps the most important goal, the method for sample preparation and labeling of the microarrays must provide quantitative results of the highest quality. Scientists have devised eight

separate experiments where the results will be used to integrate any possible changes in the protocol in order to help miniaturize and eventually automate the procedure. We were able to perform two of the eight experiments, "Minimization of cell disruption time with lysozyme" and "Minimization of silica column volume". Nucleic acid yields after 1-hour of lysozyme treatment were not significantly higher than 5-minute treatment. Different silica column volumes do not greatly affect the yields of nucleic acids. Experiments will have to be repeated in order to ensure the integrity of results.

Do Rare Codons Influence the Expression of Heterologous Proteins in Rhodobacter Sphaeroides? *MATTHEW KELLER (Vanderbilt University, Nashville, TN 37235) PHILIP LAIBLE (Argonne National Laboratory, Argonne, IL 60439)*
Knowledge of soluble proteins far exceeds that of membrane proteins, largely due to the difficulty in purifying and crystallizing membrane-bound proteins. The physiology of Rhodobacter sphaeroides makes it an excellent choice for expression of important membrane proteins from almost any organism through a system currently under development at Argonne. To test the expression of foreign proteins whose genes include codons rare to R. sphaeroides, Quantum Biotechnology's red-shifted Green Fluorescent Protein was used as a reporter gene. An existing vector made in the lab, pBSrsGFP, was used as the template for site-directed mutagenesis in creating a silent mutation near the N-terminus of the rsGFP gene. Another silent mutation had to be made at the adjacent position, however, to create a unique restriction site. A control mutant was also made harboring the restriction site-creating mutation only. These constructs were transformed into Escherichia coli, then cloned into an R. sphaeroides expression vector, and eventually conjugated into R. sphaeroides. The expression of rsGFP was characterized by fluorescence in E. coli, and by absorption after affinity chromatography in R. sphaeroides. Unfortunately, it was discovered late that the original "correct" mutant candidates contained an insertion in the gene that inhibited rsGFP expression. Fortunately, a correct single mutant candidate was discovered on a plate, and a correct double mutant was created by recombining portions of the vector and gene. Results are not final yet, but preliminary findings seem to indicate that the rare codon investigated severely inhibits expression of heterologous proteins in R. sphaeroides.

Isolation of two unknown genes potentially involved in differentiation of the hematopoietic pathway, and studies of spermidine/spermine acetyltransferase regulation. *CATHRYN KUBERA (Cornell University, Ithaca, NY 14853) ELIEZER HUBERMAN (Argonne National Laboratory, Argonne, IL 60439)*
Differential display identified a number of candidate genes involved with growth and differentiation in the human leukemia cell lines HL-60 and HL-525. Two of these genes were previously unknown, and one is the gene for the enzyme spermidine/spermine acetyltransferase (SSAT). One of our objectives is to isolate and sequence the unknown genes, 631A1 and 510C1, in order to characterize them and determine their functions. The other is to determine how SSAT is regulated, and look at how the polyamines that SSAT regulates effect macrophage differentiation. By screening the CEM T-cell DNA library and the fetal brain library, we were able to identify clones that had inserts with homology to the 631A1 cDNA probe sequence. The insert was amplified using the polymerase chain reaction (PCR) and is currently being sent to the University of Chicago for automated sequencing. The library screens for 510C1 are currently underway, but hybridization of the 510C1 cDNA probe with nylon membranes containing CEM library lambda-phage DNA produced strong signal, indicating the gene is there. SSAT experiments identified that the rate-limiting enzyme that marks the polyamines spermidine and spermine for degradation is regulated by PKC-beta and a transcription factor called Nrf2. The knowledge of regulation and function of these genes involved in macrophage differentiation will provide new insight into this cellular process, potentially making it possible to discover the roots of the problems that cause cancerous diseases.

The Process of DNA Sequencing. *CALVIN KWAN (University of California, Riverside, Riverside, CA 92507) KWONG-KWOK WONG (Pacific Northwest National Laboratory, Richland, WA 92352)*
The process for DNA sequencing has improved greatly over the last few years. With the ever-increasing pressure to discover cures to genetic diseases and ailments, one must be able to first determine the

sequence of nucleotides that codes for various genes and proteins. The methods of DNA sequencing have become more efficient, allowing for DNA strands of 500 base pairs to be determined within a matter of hours. Larger fragments of DNA can be elucidated in days. With the process becoming more common, it is important for many researchers, particularly those involved in biosciences to understand the procedures involved in DNA sequencing. It is important that accurate results are achieved during DNA synthesis, as the procedure can be quite costly. However, once a gene sequence has been determined, genes functions can be studied easily.

Construction of BAC Resources for Mapping and Sequencing Mammalian Genes. *MICHAEL LAM (City College of San Francisco, San Francisco, Ca 94112) JAN-FANG CHENG (Ernest Orlando Lawrence Berkley National Laboratory, Berkley, CA 94720)*
Part of the process for mapping and sequencing genes in the complex mammalian genome involves the construction of bacterial artificial chromosome (BAC) resources. An organism's genomic DNA is partially digested with EcoRI and size-fractionated by pulsed-field gel electrophoresis. The DNA fragments (100-200kb) are ligated to the EcoRI cloning site of vector pBACe3.6, which will then be transformed into competent E. coli cells for constructing a genomic library. Once the genomic library is completed, high-density filters are generated for hybridization. Screening each filter by hybridizing probes labeled with radioactive 32P isotopes locates the clones containing segments of the initial genomic DNA encoding the gene of interest. BACs of the positive clones are extracted and digested by restriction enzyme Bst171 to generate smaller size fragments for restriction mapping. Restriction digest can also be used to determine the size distribution of the library using the endonuclease NotI. Advance machineries integrated in the process such as the Genetix QPix for colony picking and the BioGrid for generating filters greatly increase the efficiency in constructing the BAC resources. Ultimately, the information derived from mapping and sequencing other mammalian genes enables scientists and researchers to generate cross-species comparative analysis on human gene sequences acquired from the Human Genome Project. The studies of highly conserved non-coding sequences found in both species increase the understanding of important regulatory elements and roles for gene expression, which ultimately leads to significant medical applications.

Evaluation of Diversity of Butterfly Population in the Fermilab Prairie. *MARISA LANNERT (University of Illinois at Chicago, Chicago, IL 60134) TOM PETERSON (Fermi National Accelerator Laboratory, Batavia, IL 60510)*
Butterfly species diversity is an important aspect of evaluating quality of prairie reconstruction projects. Butterflies are considered an indicator species due to their specific habitat preferences and needs. This study was conducted using an Euler circuit in conjunction with butterfly monitoring methods. The species were identified and counted in various habitats of the prairie. Three different environments were evaluated: the open prairie used by the public, open prairie not used by the public, and the savanna/transition area of the Interpretive Trails section of the Fermilab Prairie Reconstruction Project. Data was collected each afternoon (weather permitting) and the number of butterflies was counted as well as the number of species. After data was collected, it was determined the woods edge/transition area was the habitat that contained the more diverse population of butterflies. The data also indicated that the prairie contained two remnant-dependent species. Those species help describe the quality of the reconstructed prairie. Further research can be done in order to evaluate the changes in the prairie for future years and determine the success or decline of the Fermilab Prairie Reconstruction Project.

Exposure of Aquatic Biota to Uranium Groundwater Contamination. *KYLE LARSON (Columbia Basin College, Pasco, WA 99301) BRETT TILLER (Pacific Northwest National Laboratory, Richland, WA 99352)*
Conclusive results were sought in our field research by attempting to control as many of the experimental variabilities as possible. In past studies, biota was sampled at random in known areas of contamination and tested for possible effects. However, these studies do not accurately represent the natural accumulation of contaminants in biota since they are mobile and probably do not live their entire lives in the contaminated areas. By creating "exposure" cages, we will make crayfish, sculpin, and native cubicula live within known contaminated

areas for a set period of time at several different controlled densities. These cages are constructed of 100% non-toxic materials, thus eliminating the possibility of co-contamination. To date, the cages have been constructed and attached to the river bottom and have 3 different densities of cubicula living in them. Crayfish and sculpin must be tagged with an identification tool (PIT tags and iridescent tabs) so that they are not confused with any others that may enter the cages by accident. All sample biota used in our experiment will be collected from the river near the exposure test site so there is minimal risk of cross-contamination from other possible sites. The success of this experiment will help to determine how aquatic biota accumulate low levels of contamination and will hopefully launch similar experiments with terrestrial biota as well.

Protein Crystallography. *BRIANNE LAWRENCE (Fresno City College, Fresno, CA 93741) THOMAS EARNEST (Ernest Orlando Lawrence Berkley National Laboratory, Berkley, CA 94720)*
The Wnt signaling pathway merits further research because it plays a critical role in determining the final fate of a cell during embryogenesis and the proliferation of cells in adult tissues. (Cell proliferation is the multiplying of cells.) Many proteins are involved in the Wnt pathway. An important protein in the pathway, called beta-catenin, interacts with other proteins in the pathway to continue cell proliferation. A destruction complex, comprised of several proteins, breaks down beta-catenin when proliferation needs to be stopped or slowed. Inappropriate activation of the pathway has been found to play a role in various human cancers. During embryogenesis, inappropriate activation of the pathway causes mutations such as multiple organs and other body parts, or the complete relocation of the growth of a body part. In adult humans, overproduction of proteins can lead to the development of colon cancer and breast cancer. Before developing methods and medications to control the pathway when it is found to be faltering, the function of the proteins in the pathway must be identified. In the study of the Wnt pathway proteins, it is necessary to purify each of the proteins and crystallize them. Once crystallized, the protein's structure can be determined using x-ray diffraction. A computer generates a three-dimensional figure of the protein. Further examination of the protein's structure will lead to a better understanding of its function.

Evaluation of Nanofiber Structures for Molecular Assembly. *LAURA LENN (Presbyterian College, Clinton, SC 29325) MITCH DOKTYCZ (Oak Ridge National Laboratory, Oak Ridge, TN 37831)*
Single-walled carbon nanotubes (SWNTs) and multiwalled carbon nanofibers are exciting molecular wires that exhibit phenomenal electrical and mechanical properties. High quality and high purity SWNTs are grown by pulsed laser ablation and isolated by multiple acid treatments and heating; vertically aligned carbon nanofibers (VACNFs) are grown using a plasma enhanced chemical vapor deposition (PECVD) process using a lithographically defined catalyst to initiate growth. Self-assembly of these structures is key in producing multi-component functional structures for applications in electronics and biomedicine. To address self-assembly, we are applying biomedical approaches and molecular biology tools and procedures in an effort to create complex multi-component structures. Molecular biology techniques, such as chemical labeling, characterization, and functionalization of the SWNTs and VACNFs are being investigated. Immobilization of biomolecules on carbon nanotubes by functionalizing the sidewalls is being pursued. Efforts have focused on attaching biomolecules, such as DNA and proteins, to the sides of the nanotubes and nanofibers. Characterization of these hybrid structures is by gel electrophoresis and fluorescence microscopy.

Herbicide Selection of Transgenic Plants. *SOPHIA LIN (State University of New York at Stony Brook, Stony Brook, NY 11794) JOHN SHANKLIN (Brookhaven National Laboratory, Upton, NY 11973)*
Although herbicides are commonly used to control weeds, they also have excellent potential to be used for the selection of transgenic plants. The PAT gene confers resistance to the herbicide glufosinate ammonium (GLA). Adding the PAT gene to a vector with other genes of interest would allow selection by means of a simple herbicide treatment. Seeds without foreign DNA (the PAT gene) would die; survivors would be successful transgenic recombinants. This project used a commercial glufosinate herbicide for selection of transgenic Arabidopsis thaliana. The gene of interest was the castor hydroxylase

gene that codes for the hydroxylase that converts oleic acid into ricinoleic acid (a novel fatty acid with commercial value). This type of selection yielded many transgenic plants that were both resistant to GLA herbicide and produced novel hydroxy fatty acids.

Partial Purification of a Thermophilic Catalase from Thermus brockianus. *LEANNE MCFARLAND (Knox College, Galesburg, IL 61401) VICKI THOMPSON (Idaho National Engineering and Environmental Laboratory, Idaho Falls, ID 83415)*
Extremozymes are enzymes isolated from microorganisms that thrive in extreme conditions such as: temperatures as high as 100°C to temperatures below 0°C, immense pressures found on the ocean floor, high salt environments like the Great Salt Lake, even acidic condition with pH values less than 2. One of the driving forces behind research on extremozymes is the possibility of application for industrial processing. The enzyme of interest, catalase, catalyzes the breakdown of peroxide protecting cells from its toxic effects. Paper mills often use peroxide to bleach paper, but a normal catalase cannot degrade peroxide at the high temperatures at which the process is run. A catalase enzyme from a thermophilic or "heat-loving" organism would be ideal at such high temperatures. Thermus brockianus, a thermophilic bacterium isolated from Yellowstone National Park was chosen for catalase isolation. Cells were grown up in a rich lactate media, pelleted by centrifugation, and lysed by French Press. The resulting cell extract was run on an ion-exchange column followed by a hydrophobic interaction column and a gel filtration column. The protein has been partially purified from an original specific activity of 24 units/mg to 4,723 units/mg by the three chromatographic steps. Catalase positive fractions from the final column resulted in approximately four proteins of similar size and properties. Future experiments to purify catalase from Thermus brockianus will be conducted on the PerSeptive Biosystems Vision Workstation with new columns. After purification effects of temperature and pH, enzyme kinetics, and metal inhibition will be tested.

Classification of Protein Function from a Global Parameterization of Amino Acid Sequence Using Support Vector Machines. *RICHARD MERAZ (California State University Long Beach, Long Beach, CA 90840) STEPHEN R. HOLBROOK (Ernest Orlando Lawrence Berkley National Laboratory, Berkley, CA 94720)*
The exponential growth of sequence data in protein sequence repositories makes necessary the development of rapid and accurate tools for annotating protein function from amino acid sequence alone. The prevalent techniques for annotating function involve the use of various hybrids of sequence homology comparison algorithms to deduce similarities between newly sequenced proteins and previously annotated entries in the databases. These techniques are unable to detect proteins that may have common functionality but lack sufficient sequence similarity. We investigate the use of machine learning methods for the empirical classification of protein function from appropriately parameterized representations of amino acid sequence. Specifically, we trained support vector machines on sequence databases assembled according to the molecular functions of the Genome Ontology (GO). The current results are for the classification of nucleic acid binding proteins in the radioresistant bacterium *Deinococcus radiodurans*.

Characterization of the Morphology of the Inter-Cytoplasmic Membrane Found in Photosynthetic Mutants of Rhodobacter sphaeroides. *DAVID METS (University of Rochester, Rochester, NY 14627) PHIL LIABLE (Argonne National Laboratory, Argonne, IL 60439)*
Understanding the membrane morphology of R. sphaeroides is an important part in the assessment of a given strain, and its ability to be used in the expression of heterologous protein. R. sphaeroides expresses its photosynthetic apparatus in a specific, easily purifiable membrane invaginations. Therefore understanding the membrane structure in different strains will allow insight into the regulation of this membrane formation and, perhaps, allow heterologous protein expression levels to be increased. The use of transmission electron microscopy is particularly suited to this situation. It allows a visualization of the internal membrane structure of the bacterium. This tech-

nique coupled with a range of strains with known phenotypes and genotypes will allow a greater understanding for what forms the intercytoplasmic membranes (ICMs) that house the photosynthetic protein.

Determining Activation of Epidermal Growth Factor Receptor and Extracellular-Signal Regulated Protein Kinase.

EDWARD MEYER (Pasadena City College, Pasadena, CA 91106) BRIAN D. THRALL (Pacific Northwest National Laboratory, Richland, WA 99352)

Cells communicate extra-cellular signals through activation of protein kinase-signaling cascades. MAP kinase signaling pathways are known to regulate many different cellular responses, such as proliferation and cell death. One class of MAPK pathways is the extra-cellular signal regulated kinase (ERK) pathway, which is commonly activated by growth factors, such as epidermal growth factor (EGF), and is thought to be involved in cell proliferation and pro-survival responses. In the case of EGF, binding of EGF causes phosphorylation of the EGF receptor, which ultimately leads to phosphorylation and activation of the downstream kinases, Raf, MEK and ERK. Phosphorylation of ERK leads to stimulation of its kinase activity, translocation to the nucleus, which results in changes in gene expression. While growth factors such as EGF activate the ERK pathway through specific receptors, many environmental contaminants such as radiation can also activate this pathway. Our ultimate goal is to understand how the MAPK pathways are activated by environmental contaminants

Determination of Microsatellite Marker Polymorphisms on Chromosome Chr) 15 Between C57BL/6J (B6) and 129X1/SvJ Strains of Inbred Mice.

MATTHEW MILLUS (Southwestern Community College, Chula Vista, CA 91915) YUN YOU (Oak Ridge National Laboratory, Oak Ridge, TN 37831)

Microsatellites, known as simple-sequence repeats (SSRs) or simple sequence length polymorphisms (SSLPs), are short, repetitive DNA sequences. They consist of 2 or 4 base pairs repeated 10 to 100 times that are flanked by unique sequences. They have been found throughout the genome of different inbred mouse strains. The most common SSRs found in the mouse genome are comprised of a CA dimer repeated in tandem. They are highly polymorphic in the number of repeating units among different inbred mouse strains, and are useful for genotyping and chromosome mapping. SSR length data exists for many different strains of inbred mice, only scattered data was available for the 129 strains at present. Polymorphisms on Chr 15 from 26.4cM to 55.7cM (centiMogan) were analyzed between B6 and 129X1/SvJ strain of inbred mice utilizing Chr 15 SSR markers. A hybrid F1 (C57BL/6J X 129X1/SvJ) embryonic stem (ES) cell line was used to confirm results and to identify any preferential PCR (polymerase chain reaction) amplification of B6 or 129X1/SvJ DNA. The results of the PCRs were visualized by ethidium bromide following agarose gel electrophoresis. 49 markers were tested, 15 demonstrated polymorphisms between B6 and 129X1/SvJ strains, 2 failed to produce results and the remaining 32 do not indicate polymorphisms on agarose gel. Data will be subsequently used to map deletions on the distal half of mouse Chromosome 15. A DNA targeting vector for the calcium channel beta subunit 3 (Cacnb3, xx cM on Chr 15) was developed to create deletion complexes centered at the Cacnb3 locus on the distal portion of Chr 15. Polymorphic markers tested above will be used to determine the size of deletions.

Expression and Structural Analysis of Membrane Proteins.

ZACHARY MORRIS (Ripon College, Ripon, WI 54971) PHILIP LAIBLE (Argonne National Laboratory, Argonne, IL 60439)

Membrane proteins, while tremendously active in biological processes, are under-represented in scientific understanding as a result of difficulties in completing functional and structural analysis by traditional methods. These difficulties arise from the amphiphilic character of membrane proteins, which provides a tremendous challenge to the maintenance of a native environment and the production of suitable crystal structures for x-ray crystallography. In this paper I discuss research I have conducted this past summer aimed at further developing and understanding a high throughput expression system for the production, purification, and crystallization of membrane proteins from Rhodobacter (R.) sphaeroides. Such research has entailed attempts at such expression and purification, development of protein crystallization techniques from the cubic phase of a lipid solution, and investigation of protease activity in R. sphaeroides.

Development of Cantilever Based Biosensor for Cardiac Marker Detection.

ARNAB MUKHERJEE (George Washington University, Washington, DC 20052) THOMAS THUNDAT (Oak Ridge National Laboratory, Oak Ridge, TN 37831)

IInteractions between biological molecules are of vital interest to many scientific and technological fields. Through the use of gold-coated silicon cantilevers, under flow, both physical mass loading and specific interactions between biological molecules can be detected. Using the highly specific interaction between biotin and neutravidin, a model system was developed for functionalizing the cantilever surfaces. This model was then tested using the cardiac marker myoglobin and myoglobin monoclonal antibodies. Antibodies (biotinylated goat antibody (IgG class); myoglobin antibodies) interact to differing cross-linkers such as DTSSP attached to gold-coated cantilevers; cantilevers are then exposed to neutravidin and myoglobin, respectively, under flow conditions. The specific properties of the cross-linker used can effect the orientation of the antibody and, consequently, the degree of interaction between the immobilized antibody and its antigen. Contact angle measurements were also used as a qualitative technique in the verification of the presence of the cross-linkers and immobilized antibody on the gold surface. Biomolecule interaction is measured as deflection of the cantilever through the use of a position sensitive detector. Interaction of myoglobin with myoglobin monoclonal antibody results in a net negative deflection. Interaction of myoglobin with monoclonal antibody will be quantified in order to achieve a nanogram order of sensitivity. These sensors show great potential for expanding the detection limits of marker biological molecules in both the medical and environmental disciplines.

Determination of the Chemical Structure of 3-Hydroxyisobutyrate Dehydrogenase (HIBADH) from Alcaligenes faecalis (Bacterium).

RAJNESH NARAYAN (Contra Costa College, San Pablo, CA 94804) PAUL ELLIS (Stanford Linear Accelerator Center, Stanford, CA 94025)

3- Hydroxyisobutyrate Dehydrogenase, commonly known as HIBADH, is a ubiquitous enzyme involved in valine catabolism. HIBADH is composed of approximately 300 amino acid residues, and has a molecular weight of 30,000. The organism from which the HIBADH being researched throughout this paper was extracted from a bacterium known as Alcaligenes faecalis. If the level of HIBADH in an organism is changed from its equilibrium, the process of valine catabolism is disturbed. Thus, leading to a fatality in an organism. This disturbance is not genetic. Rather, it is a spontaneous mutation. It would be of clinical and industrial advantage if the chemical structure of HIBADH could be determined. The chemical structure may give an understanding of how to overcome disturbance in the process of valine catabolism. While performing crystallization of an impure sample of Arsenite Oxidase from Alcaligenes faecalis, one HIBADH crystal was grown out of pure luck. Diffraction data was collected using this crystal. An electron density map from the data was calculated. Using the XtalView- Xfit program, amino acid residues making up the HIBADH structure were fit into their corresponding electron densities. The built HIBADH structure was refined for several cycles. Appropriate adjustments were made to the structure. The R factor decreased from a value of 36% to 34%. Because of the use of 2Å data, we would have expected to get a final R factor value of 20%. However, possible errors might have occurred leading towards this very high R factor value after refinement. Considerations might be an error in the unit cell symmetry, or possibly the fact that 1/10 of the structure was not accounted for.

Efficiency of Fatty Acid Extractions.

TESSIE NG (Bowdoin College, Brunswick, ME 04011) TAMAS TOROK (Ernest Orlando Lawrence Berkley National Laboratory, Berkley, CA 94720)

Identification of microorganisms and characterization of microbial communities are often based on fatty acid analysis. Although published extraction protocols have not been systematically compared, it is well understood that these methods extract fatty acids from different cellular domains. It is uncertain whether they are being extracted sufficiently and this consideration becomes critical, especially since different fatty acid composition profiles will lead to inaccurate identification of isolates and imprecise characterization of communities. Here we assessed the extraction efficiency of fatty acid methyl ester (FAME) and phospholipid fatty acid (PLFA) extraction techniques, with and without the use of a pressurized accelerated hot solvent extractor

(DIONEX ASE 200), on isolates. Four bacterial and two fungal isolates were systematically analyzed. Analysis of the profiles was carried out using Sherlock, Microbial Identification System'. The TSBA40 and FUNGI methods of the analysis software were tested for fidelity of positive peak and species identifications of known microbial species (four bacteria and two fungi). The profiles indicate that there is no one technique that is able to extract all the fatty acids present in all three methods. The PLFA/DIONEX technique, however, was faster and able to increase the yield of a representative 16:0 fatty acid when compared to the traditional method of PLFA extractions for all but one of the bacteria.

Development of an Automated DNA Characterization Procedure for Use in DNA Microarray Preparation. *REBECCA PARSLEY (Pellissippi State Technical Community College, Knoxville, TN 37933) MITCH DOKTYCZ (Oak Ridge National Laboratory, Oak Ridge, TN 37831)*
Detection and quantification of small amounts of DNA, such as PCR products, are extremely important in a wide variety of biological applications. A problem frequently encountered while attempting a gene expression analysis or the quantitation of a PCR amplification yield is the unreliable automation of experiments. The inaccurate data occurs because there are often variances in the amounts and/or concentrations of the samples. Therefore, an automated quantitation of probes for use in DNA microarrays was attempted using a Packard MultiPROBE II EX (MPII) robotic liquid handling system and a Perkin Elmer HT Soft 7000 Plus Bio Assay Reader. A standard curve that was comprised of known concentrations of DNA was first obtained through hand pipetting. This standard curve was then prepared using automated procedures on the MPII with a known amount of a fluorescent intercalating dye called picogreen. Precise readings of the liquid's fluorescence yielded a standard curve. Refinement of the procedure produced a reliable standard curve that allows for the determination of PCR product concentrations by correlating the fluorescent readings with those of the standards. This achievement was significant in that the automated quantitation of the PCR amplification yields will allow for the rapid characterization of the large numbers of PCR products needed to prepare high density DNA arrays.

An Electron Microscope Examination of Iron Reducing Bacteria. *PENELOPE POWELL (Truckee Meadows Community College, Reno, NV 89502) YURI GORBY (Pacific Northwest National Laboratory, Richland, WA 99352)*
Dissimilatory metal reducing bacteria couple the oxidation of reduced organic compounds to the reduction of multivalent metals. In natural, anaerobic environments ferric iron, Fe (III), is the most abundant electron acceptor. At typical neutral pH values, Fe (III) is very insoluble and forms ferric oxide minerals. Enzymatic reduction transforms these mineral phases to more soluble Fe (II). Other multivalent metals, such as uranium, technetium, and chromium, can be reduced by metal reducing bacteria. In contrast to iron, these metals are soluble in their oxidized state and poorly soluble in their reduced state. Hence enzymatic reduction of heavy metals and radionuclides provides potential for stopping the migration of these contaminants in groundwater and for removing them from aqueous contained wastes. Demonstrates an electron microscope approach for determining the location and composition of precipitated heavy metals and radionuclides in and around iron reducing bacteria. The work presented here, demonstrates an electron microscope approach for determining the location and composition of precipitated heavy metals and radionuclides in and around iron reducing bacteria.

The Effects of Trifluoroacetic Acid on Mixed Waste Biodegradation. *ANGELA PROCTOR (Southern Utah University, Cedar City, UT 84720) WILLIAM T. STRINGFELLOW (Ernest Orlando Lawrence Berkley National Laboratory, Berkley, CA 94720)*
Mixed wastes generated by the biomedical community contain both hazardous organic compounds and radioactive isotopes. These wastes have high water content (80%) and a high organic content (less than or equal to 20%). Some of the major hazardous organic compounds in these mixed wastes are acetonitrile and trifluoroacetic acid. Due to conflicting disposal regulations, incineration is the only option for disposal of these mixed wastes, creating a problem because incineration releases the radioactive isotopes directly into the environment. We have proposed that biodegradation could be an alternative treatment for the mixed waste stream that would not result in the release of radioactivity during treatment. The purpose of this study was to determine if mixed wastes containing acetonitrile and trifluoroacetic acid could be treated biologically. Previous study has shown that the acetonitrile component of the mixed waste is biodegradable. In this study, we tested the effect of trifluoroacetic acid on acetonitrile degradation. Trifluoroacetic acid is present in the mixed wastes in low concentrations (0.1%) but the chemical was suspected of having a toxic effect on acetonitrile bacteria degradation. An oxygen uptake measurement as a function of trifluoroacetic acid concentration was used to determine the effects of trifluoroacetic acid on the acetonitrile degrading culture. The results of this study demonstrate that trifluoroacetic acid is not toxic to the acetonitrile degradation process and that mixed wastes containing trifluoroacetic acid will be amenable to biological treatment.

Exposure to Environmental Tobacco Smoke. *JANE QI (Contra Costa College, San Pablo, CA 94508) BRETT SINGER (Ernest Orlando Lawrence Berkley National Laboratory, Berkley, CA 94720)*
Environmental tobacco smoke, or "secondhand smoke", is a complex mixture formed from sidestream smoke and the smoke exhaled by the smoker. Sidestream smoke is the escaping smoke of a tobacco product. The health risks of ETS include heart disease, lung cancer, asthma and impaired respiratory function. It is uncertain which components of ETS fine particles, specific vapors, or some combination affect the health outcomes. Quantifying exposures to organic vapors from ETS is challenging. It involves dynamics of organic vapor concentration. Therefore, improving quantitative data on ETS toxic exposure is an initial step to further understand the health impacts on exposed nonsmokers. In our research, we focus on the study of indoor's toxic air contamination from sidestream smoke, which is the major contributor to ETS. The target of this project is to improve methods estimating the organic exposure vapors and particle in ETS and to measure emissions of a range of individual organic vapors. We place special emphasis on nicotine exposure, which is used as a tracer of ETS. It may pose a health risk to nonsmokers. We will compare the emission mass of daily smoking with the non-repeated smoking in 24-hour. The result will tell us the effect of sorption and re-emission on the daily smoking in indoor ETS exposure .The calculated AEFs might estimate a more accurate organic vapor exposure in ETS, when daily smoking is applied in a realistic indoor model.

Toxicity of 2,3,7,8-TCDD, PCB-77, PCB-126 and 1,2,4,5,7,8-HCX to Ictalurus punctatus during ELS testing. *HEATHER ROBINSON (Portland State University, Portland, OR 97207) HEIDA DIEFENDERFER (Pacific Northwest National Laboratory, Richland, WA 99352)*
Battelle's Marine Science Laboratory was contracted to perform early life stage (ELS) tests to observe the toxic effects of 2,3,7,8 TCDD, PCB 77, PCB 126 and 1,2,4,5,7,8-hexachloroxanthene (HCX) on the channel catfish, Ictalurus punctatus. The purpose of the study was to replicate potential exposure at Centredale Manor, a NPL Superfund site in Providence, Rhode Island. TCDD and PCBs, along with VOCs, semivoloatile organic compounds, pesticides and metals, were previously found in the Woonasquatucket River. The fertilized eggs were exposed to the chemicals for 24-hours then allowed to hatch in a flow through system. After a 10-day range-finding test the LC-50 of TCDD was calculated to be 0.01 ng/ml. A second set of concentrations with the same mixtures of TCDD, PCB-77 and PCB-126, included hexachloroxanthene (HCX), a little-studied chemical found in large quantities at the site. The LC-50 for the HCX series was also 0.01 ng/ml. Data including mortality rates, growth rates and physical abnormalities from a 32-day definitive test is currently being analyzed. Noted abnormalities include hemorrhaging, craniofacial skeletal deformities and cardiac and yolk sac edemas.

Satellite Imagery Analysis. *LORENA SANCHEZ (Columbia Basin College, Pasco, WA 99301) JANELLE L. DOWNS (Pacific Northwest National Laboratory, Richland, WA 99352)*
Satellites have become a recent form of technology that has allowed us humans to view the continuous changes of our earth. As a Community College Initiative (CCI) intern with the PNNL Ecology Group, I was allowed the opportunity to use this technology. My projects involved ground truthing or verifying analysis products derived from satellite imagery of the Hanford Site in Eastern Washington and sites

near Grand Junction in Western Colorado. Satellite imagery was used to verify areas on the Hanford Site that burned and did not burn. Collecting and analyzing data at sites on our model were chosen to improve the Hanford Site ash/vegetation index and allow us to improve the calibration of our image and better identify areas of the Hanford Site that did and did not burn. In Colorado, satellite imagery was used to verify areas of high and low vegetation for the Bureau of Land Management (BLM) lands. Remote sensing data provided us with an understanding of vegetation conditions of the areas important for managing grazing lands. Part of this data collection was to identify areas that are anomalous or areas of concern because they did not have the vegetation we expected.

Theoretical Determination of Rate Constants for VOC's + OH: A DFT Study. *NICHOLAS SCAIEF (Washington State University, Pullman, WA 99163) SHAWN KATHMANN (Pacific Northwest National Laboratory, Richland, WA 99352)*

Radical reactions are very important to atmospheric chemistry, but are very difficult to study experimentally and theoretically. In principle, it is possible to determine rate constants for these reactions by ab initio methods. In the present work the reactions of some volatile organic compounds (VOC) with hydroxyl radical were examined. Minimum energy structures and ground state energies for the reactants, transition states, and products of reactions were found at various levels of theory including MP2/cc-pvdz and UCCSD(T) levels, using the Gaussian 98 electronic structure software package. DRDYGAUSS (Direct Dynamics with Gaussian) was used to trace out the minimum energy path along various reaction channels. Variational transition state theory (VTST) was used to obtain a rate constant from the topology of this energy surface. Changes in the level of theory used (selection of basis set and treatment of electron correlation) produce small changes in ground state energies and structures; the resulting potential energy surface becomes altered in the process. It was found that the theoretical rate constant depends exponentially on small variations in the potential energy surface topology. Thus, the level of theory has tremendous effect on the theoretically determined rate constant.

Is Ycf9 the Linchpin of Photosystem II? Heterologous Expression for Structural and Functional Studies. *EMILY SHESTON (Wilkes University, Wilkes-Barre, PA 18766) GEOFFREY HIND (Brookhaven National Laboratory, Upton, NY 11973)*

The ycf9 gene (orf 62) is found in chloroplast genomes of all plants as well as in cyanobacteria. When Ycf9 is phosphorylated by an intrinsic protein kinase (Race & Hind, 1996), it detaches from photosystem II, allowing migration of LHC-II away from the reaction center core diminishing reaction center energy capture. Work done by Ruf et al. (2000) showed that Ycf9 mutants also lacked a mobile chlorophyll a/b protein, CP26, presumably because CP26 could not be assembled into the photosystem. We hypothesize that Ycf9 is a linchpin holding CP26 and LHC-II to the reaction center core of photosystem II. Purification of Ycf9 was attempted using two methods: gel analysis and vector-induced protein expression. Fractions of photosystem II-enriched membrane complexes were run on 16.5% tricine/bis-tris propane acrylamide gels suitable for separating low molecular weight proteins. We designed tricine/bis-tris propane buffer to avoid the complications tris/glycine buffers pose in subsequent protein sequencing. We identified a protein of approximately 6.3 kD in the reaction center cores and photosystem II-enriched subfractions that we suspect to be Ycf9. Chloroplast DNA was prepared from Spinacia oleracea as described by Triboush et al. (1998). PCR was used to amplify the known ycf9 nucleotide sequence and add restriction sites for ligation into the vectors pFLAG-ATS and pFLAG-CTC for expression in E. coli. Low levels of protein were expressed in the periplasm of pFLAG-ATS transformants. Further work will attempt to improve yields of expressed protein and explore other vector systems.

Determining the activation of EGF receptors depending on the availability of the ligand. *MELISSA SILVA (Western Washington University, Bellingham, WA 98225) LEE OPRESKO (Pacific Northwest National Laboratory, Richland, WA 99352)*

Cells communicate in many different ways. One way in particular is through ligands. The ligands in the epidermal growth factor receptor are membrane anchored. The epidermal growth factor (EGF) receptor can be turned on and off by different stimuli in a cell's environment. In our research we are trying to determine which stimuli do just that and

why, how the ligands are regulated, and why these stimuli have different outcomes in a given cell. We also want to look at how the cell signaling pathways are affected. We transfected Chinese hamster ovary cells (CHO cells) with six different chimeras. These chimeras were constructed in blue script and were cut out and put into the expression vector, pIRES puro. The six different chimeras are EGF: amphiregulin (ACT) (CT= cytoplasmic tail), EGF: betacellulin (BCT), EGF: EGF (ECT), EGF: heparin binding (HCT), and EGF: TNFalpha (TCT). Once the chimeras were successfully transfected into the cells, we put the cells into selection using puromyicen and lipofectamine. We then screened these cells using a LC antibody. In doing this we weeded out the cells that were not expressing the ligand. Once we did this, we grew up the positive colonies and froze them down. We will take the frozen cell and quantitate the rate of the release of a particular ligand using an EGF ELISA assay. This will allow us to see how the signaling pathways are affected.

Renovation of the Photovoltaic-Diesel Generator Hybrid System at Natural Bridges National Monument. *BRITTANY WALKER (University of Colorado, Boulder, CO 80309) OTTO VAN GEET (National Renewable Energy Laboratory, Golden, CO 80401)*

IIn 1979 a large 93 kW photovoltaic-diesel generator hybrid system was installed as the only source of power for Natural Bridges National Monument. As the components in the system have aged the performance of the system has declined by more than 50% despite its upgrade in 1992. Natural Bridges has enlisted the help of the Federal Energy Management Program (FEMP) to provide suggestions on how to upgrade the existing hybrid system. A software program called Hybrid Optimization Model for Electric Renewables (HOMER) was used in determining cost-effective measures of upgrading the existing hybrid system at Natural Bridges. Two primary simulations were modeled in HOMER: the existing hybrid system performance and the optimum upgraded system. The model of the existing hybrid system was found to closely match the performance of the actual system. The HOMER simulations determined the optimum upgraded system to have a 40 kW photovoltaic array, a 400 kWh battery bank, a 40 kW inverter, and the current 60 kW generator. Based on knowledge of the condition of the components within the system and HOMER simulations, FEMP made recommendations to maintain the existing 40 kW photovoltaic array as well as the 60 kW generator, replace the existing 500 kWh battery bank with a 400 kWh battery bank, and also to replace the existing 50 kW inverter and existing charge controllers with newer models. If Natural Bridges takes penalties for emissions from diesel fuel into account, then the photovoltaic array should be increased approximately 15 kW to an output of 55 kW.

ULTRAVIOLET A WAVEBANDS INDUCE DIFFERENT DNA DAMAGES IN XIPHOPHORUS MACULATUS SKIN CELLS WITH AND WITHOUT MELANIN. *TSUHAO YEUNG (University of Rochester, Rochester, NY 11953) R.B. SETLOW (Brookhaven National Laboratory, Upton, NY 11973)*

It is known that UVB wavebands (280 - 320 nm) have the capability to induce DNA damages, such as cyclobutane pyrimidine dimers, while the effects of UVA (320 - 400 nm) remain mysterious. If unrepaired, these damages negatively affect the cell's ability to replicate and its homeostatic functions, resulting in cell death and cancerous growth. In our studies, we use UV-endonuclease from Micrococcus luteus and alkaline gel-electrophoresis, to identify occurrences of damage to DNA isolated from black and white skin of Xiphophorus maculatus 163B after exposure to UVA wavelengths over 320 nm. Our preliminary results show that damages due to UVA exposure are readily occurring, especially in skin with melanin, and warrant further investigations.

Design, Construction and Analysis of Single-lesion Containing Shuttle Vectors for Use in Studies of Transcription-Coupled DNA Repair. *JESSICA ZELLHOEFER (Cornell University, Ithaca, NY 14853) PRISCILLA COOPER (Ernest Orlando Lawrence Berkley National Laboratory, Berkley, CA 94720)*

Our goal is to design a shuttle vector that contains a unique, site-specific lesion in order to study transcription-coupled repair of human DNA. In our system, the lesion is introduced by insertion of a synthesized 8-oxoguanine-containing oligomer into a pS189-derived plasmid at either of two locations: within the t-antigen (Tag) intron 400 bases beyond the ATG translation start codon, or at the end of the Tag, after the polyadenylation signal. The pS189 shuttle vector was modified to increase the transcription frequency of the Tag, prevent plasmid replication, and distinguish between Tag derived from SV40-trans-

formed cells and that from the shuttle vector. Initial studies were undertaken to optimize the transfection conditions and also to verify the various plasmid alterations. Preliminary RT-PCR of mRNA harvested 24 hours after plasmid transfection has demonstrated that use of primers tuned to the Tag modifications do successfully distinguish plasmid from cellular RNA. Replication assays using methylation-sensitive endonucleases have verified the competence of engineered mutations in the SV40 ori in achieving preclusion of plasmid replication. RT-PCR has also shown low amplification near the Bgl II site, suggesting its removal during the processing of mature mRNA. It will therefore be necessary to construct a new site for lesion insertion before the poly-adenylation signal. In conclusion, with the competency of the pS189-derived plasmids confirmed by RT-PCR, both the shuttle vector and the transfection protocol have been optimized for TCR studies, and we are ready to insert the 8-oxoG-containing oligomer.

PAHs & Estrogens Effect On Gene CYP1B1 Expression. YILI ZHEN (University of California at Berkeley, Berkeley, CA 94704) REGINE GOTH-GOLDSTEIN (Ernest Orlando Lawrence Berkley National Laboratory, Berkley, CA 94720) .

Polycyclic aromatic hydrocarbons (PAHs) are known carcinogens ubiquitous in the environment. Inhaled or ingested PAHs are metabolically activated to exert their oncogenic effects. Cytochrome P4501 B1, encoded by the gene CYP1B1, is a major activating enzyme involved in PAH metabolism. In previous studies, CYP1B1 was shown to have a high level of expression in breast tissue. The amount of the CYP1B1 enzyme is controlled at the level of transcription by the Ah Receptor. The Ah receptor presents in the cytoplasm is activated by the PAHs (or also dioxin) binding to it. The activated Ah complex binds to regulatory regions of various genes involved in PAH metabolism including the CYP1B1 gene and results in increased transcription of these genes. We compare the efficiency of various PAHs in inducing the CYP1B1 expression through the Ah receptor pathway in cells in culture treated with the PAH by measuring expression by RT-PCR. The compounds to be compared are benzo[a]pyrene, benzo[c]fluorene and coal tar, a mixture of PAHs representative of PAHs occurring in the environment. It is well established that PAHs and dioxin have an antiestrogenic effect and there is a "crosstalk" between Ah receptor and estrogen receptor. So, estrogens, which are also the substrates for CYP1B1, may increase the expression of gene CYP1B1. CYP1B1 expression with PAHs treatments was increased but there were no obvious changes in CYP1B1 expression of the estrogen treatment.

CHEMISTRY

Growth of Carbon Nanotubes, using Chemical Vapor Deposition. TRAVIS ADAMSON (Brigham Young University, Provo, UT 84602) CHRIS AARDAHL (Pacific Northwest National Laboratory, Richland, WA 99352)

Carbon nanotubes (CNT's) are new materials that have yet to be entirely researched. No one has fully realized their potential as a new material for the 21st century. CNT's have many potentially valuable physical properties. CNT's are characterized by their high mechanical strength, adjustable electronic properties, high surface area, and light weight. Our project entails growing CNT's on a variety of substrates using a hotwall furnace and a method known as Chemical Vapor Deposition (CVD). The CVD method calls for us to flow ethylene gas, a hydrocarbon, under extreme temperatures in order to deposit carbon on the chosen substrate. The substrate (usually a silicon wafer) is placed inside a quartz tube that runs through the furnace. Ethylene gas is flowed through the tube when the temperature has reached 700 degrees Celsius. In the future, carbon nanotubes could prove very valuable for their abilities to store hydrogen for fuel cells. They could also be used for aerospace engineering, electronic nano- devices, and any number of tasks which are yet to be discovered.

Chitosan/N-isopropylacrylamide graft copolymers for tissue engineering applications. NATHANIEL BAER (Cornell University, Ithaca, NY 14853) ANNA GUTOWSKA (Pacific Northwest National Laboratory, Richland, WA 99352)

Water-soluble chitosans of assorted molecular weights were grafted to different oligomer chain groups with temperature sensitive properties. The solutions were then cleaned and dried. The resulting polymers displaying both water-soluble and temperature sensitive qualities were tested for a variety of properties. Mw determination was tested using Gel Permeation Chromatography. Success of

grafting was qualitatively analyzed with an IR machine, utilizing thin films, and Quantitatively estimated by titration of HCl. Use of Rheometer compared strength of gel under increasing temperature. Results from four solutions show that oligomer was successfully grafted onto chitosan. The gelling properties appear dependent to both the brand of chitosan, the amount of oligomer and the success of grafting. The polymers cover a wide range of Mw and respond differently to stress at given temperatures. Further testing of these polymers as well as synthesis of different polymers will give insight into the ability of gels to serve as drug delivery systems inside the human body.

Application of MALDI-MS for Environmental Analysis. KATE BOETTCHER (Oregon State University, Corvallis, OR 97331) JAMES A. CAMPBELL (Pacific Northwest National Laboratory, Richland, WA 99352)

The analytical techniques presently used to identify unknown compounds are extremely expensive, time consuming, and labor intensive. Techniques are being explored that will save time and expenses. A potential technique is matrix assisted laser desorption ionization- mass spectrometry (MALDI-MS). MALDI-MS is a much quicker and cost efficient way to analyze an entire mass spectrum with a dramatic reduction in sample amounts and hazardous waste than previous methods such as liquid chromatography/mass spectrometry or gas chromatography/mass spectrometry. MALDI-MS allows a one step process to analyze both positive and negative ion modes with minimal preparation. MALDI-MS was used to analyze various low-molecular weight compounds such as amines, nitrosoamines, aromatic, and chlorinated species. Some particular compounds analyzed were nitrosodiphenylamine, dichlorobenzene, naphthalene, and nitrosodimethylamine. The results yielded promising information to help in future applications. Once tests have been run to produce a mass spectrum, the sample needs to be quantitatively analyzed as well. This will allow practical and beneficial operation when taken onto the field.

Fundamental Process Chemistry at Pacific Northwest National Laboratory. KARLYN BOTT (Whitman College, Walla Walla, WA 99362) JOHN LINEHAN (Pacific Northwest National Laboratory, Richland, WA 99352)

The focus of this appointment was on the carboxylation of alcohols with carbon dioxide to form carbonate salts. Firstly, the solubility of carbon dioxide in methanol was investigated using high-pressure proton and 13C NMR. A linear relationship was found between the pressure of carbon dioxide and the amount solvated. Next, carbon dioxide solubility in methanol with a small amount of water was investigated by the same method. The additional water had no effect on the solubility of carbon dioxide. The carbonate salts were made by bubbling carbon dioxide on room temperature mixture of the alcohol to be carboxylated and a base to act as the cation in the product. This carboxylation was performed using various alcohols, including methanol, ethanol, 1-propanol, 2-propanol, t-butyl alcohol, 1-butanol, 1-pentanol, 2-pentanol, 1-hexanol, 1-octanol, ethylene glycol, 2-chloroethanol, 3-chloropropanol, and phenol. 1,8-Diazabicyclo[5.4.0]undec-7-ene and triethylamine were the bases used. The actual carboxylation of the alcohols was investigated through IR and high-pressure proton and 13C NMR spectroscopy. IR spectroscopy of the salt product showed peaks that were indicative of carbonate. The high-pressure NMR spectra were obtained using a PEEK tube and a carbon dioxide pump.

Quantum Yield Temperature Dependence of the Photodecomposition of Hydrogen Peroxide. AARON BROWN (University of Washington, Seattle, WA 98195) DONALD CAMAIONI (Pacific Northwest National Laboratory, Richland, WA 99352)

In this experiment, samples of hydrogen peroxide were photolyzed with a high-power excimer laser. Several of these trials were tried at different temperatures and relative quantum yields were calculated from these trials. The temperature dependence was then determined from these quantum yields. A computer model of the photodecomposition of hydrogen peroxide was then made, assuming that there was no effect from solvent viscosity. The theoretical quantum yield was found to be 2 in the model because some resultant hydroxyl radicals promoted further reactions with the hydrogen peroxide. The fact that there is a temperature dependence of the quantum yield shows that the solvent viscosity was hampering the mobility of some of the hydroxyl radicals. Therefore, some radicals were unable to escape

the solvent cages and instead collided with each other to reform some hydrogen peroxide, lowering the quantum yield. The temperature dependence of the quantum yield of hydrogen peroxide photodecomposition was found to be linear between 8° C and 35° C.

Thermosensitive hydrogels for medical applications. *MEGAN BRUEMMER (Whitman College, Walla Walla, WA 99362) ANNA GUTOWSKA (Pacific Northwest National Laboratory, Richland, WA 99352)*
Degradable and nondegradable thermosensitive hydrogels were studied for application in drug delivery and tissue engineering. Polymers were titrated with acid or base to determine average molecular weight. Titration was also used to determine the composition of newly synthesized polymers for AAc and oNIPA groups. Characteristics of the polymers were also studied. LCST experiments were conducted on a UV/Visible Spectrometer to determine the clouding point curve and temperature of gelation for pure polymers and polymers grafted with chitosan. Nondegradable thermosensitive hydrogels were tested for drug release. Fluorescein Isothiocyanate-Dextran was used to simulate the molecular size of the drug. Samples were kept in a 37°C water bath to match human body temperature. The Dextran was released into phosphate buffer saline solution over a two-week period. Supernatant samples were taken periodically. A UV/Visible Spectrometer analyzed the sample to calculate the amount of Dextran released from the gel disks. Results showed that even the largest Dextran was effectively released from the gel disks. Nondegradable and degradable gels were tested for tissue culture. The same Dextran was used for this study to simulate the cells' ability to exit the gel disks. Further studies in this area will test biodegradable gels for drug release.

Chemical Inventory and Updating the Chemical Management System. *CARLY CARMODY (University of Illinois, Urbana, IL 61801) CATHY BRESNAHAN (Argonne National Laboratory, Argonne, IL 60439)*
The Chemical Management System at Argonne National Laboratory is a site-wide database which tracks tens of thousands of chemicals and their Material Safety Data Sheets (MSDS). My project was to inventory certain division's chemicals and link a MSDS to chemicals that did not have one. Inventories were done using a laptop computer and a barcode scanner in the laboratories. MSDS sheets were looked up in the system and the number linked to the chemical or obtained using search engines on manufacturer websites. The system was updated quite a bit through this work, but due to its magnitude it will remain an ongoing project in the Environment, Safety & Health Division.

Preparation of New Polymer Coatings for Detection of Pertechnetate Ion. *COLIN CARVER (Columbia Basin College, Pasco, WA 99301) TIM HUBLER (Pacific Northwest National Laboratory, Richland, WA 99352)*
The general aim of this work is the design and implementation of a new sensor technology for analysis of the complex chemical mixtures found at DOE sites nationwide. The specific goal of this research is the development of a sensor for technetium (Tc) that is applicable to characterizing and monitoring the Vadose Zone and associated subsurface water at the Hanford site. The sensor design consists of a basic spectroelectrochemical configuration consisting of a waveguide with an optically transparent electrode that is coated with a thin chemically selective film. The films are being developed for pertechnetate ion analysis. Samples containing pertechnetate ion will partition into the films by electrostatic attraction, then electrochemically converted into a Tc coordination compound that gives a strong optical signal associated with an electrochemical reduction/oxidation process. This presentation focuses on strategies for preparation of the selective sensor films.

Correction of the Dispersed Input Function Produced by the Automated Blood Sampling System. *SARAH CUNNIFF (St. Joseph's College, Patchogue, NY 11772) DAVID SCHLYER (Brookhaven National Laboratory, Upton, NY 11973)*
An automated blood sampling system (ABSS) is often used in congruent with a PET scanner, so that physiological information can be obtained. However, during the process of extracting blood from a patient, the input function is slightly distorted by the ABSS. In order to ascertain the original input function after dispersion, the amount of

dispersion that is occurring has to be calculated and then subtracted from the ABSS input function. In determining the amount of dispersion that is created we conducted a series of experiments using the ABSS and radioactive isotopes. Once we computed the amount of dispersion we mathematically manipulated this data into a matrix form. It was established that the inverse of the new dispersion matrix had to be computed and multiplied by the ABSS input function in order to attain the original input function. A computer program was written to perform matrix inversion, so that the inverse of this new dispersion matrix could be computed and then multiplied by the ABSS input function. By doing this, we were successful in mathematically subtracting the dispersion that had been created from the automated blood sampling system and created a sharpened, more accurate input function.

Isotopic Analysis of Wire Mesh Samples Using Glow Discharge Mass Spectrometry. *GARY DOBBS (University of Central Arkansas, Conway, AR 72035) DOUGLAS C. DUCKWORTH (Oak Ridge National Laboratory, Oak Ridge, TN 37831)*
As part of the Nuclear Nonproliferation Treaty agreement, member state nuclear facilities are commonly surveyed for conformance. The usual sampling and analysis media include cloth and paper swipes. A new methodology employing wire mesh sampling and analysis is now being investigated. This concept is to provide effective surface sampling that can produce measurement samples compatible with a variety of radiological, elemental, and isotopic analytical techniques. The ideal method would produce sensitive, accurate, and precise analyses for each mesh sample in a timely and cost effective manner. Glow discharge mass spectrometry (GDMS) is a solid sampling elemental and isotope analytical technique that provides low parts per billion detection limits. To date, GDMS has given promising results in isotopic analysis for the wire mesh media. The purpose of this project is to extend and improve GDMS analysis of metal mesh and steel wool media. Typical analytical figures of merit will be reported. Once developed, this sampling medium and analytical methodology will result in more timely and cost efficient means of supporting nuclear safeguard activities.

Hartree-Fock and Kohn-Sham orbitals for ionic systems. *CARL FAHLSTROM (Eastern Oregon University, LaGrande, OR 97850) JEFF NICHOLS (Pacific Northwest National Laboratory, Richland, WA 99352)*
Density Functional Theory (DFT) allows chemical properties to be determined directly from the calculated electron density. This theory is useful in molecules with a large number of electrons, N, because it formally scales as $O(N3)$ whereas other methods which include electron correlation scale much worse. Hartree-Fock (HF) theory and four DFT methods were applied to several hydrogen-bonded complexes and ionic systems. Ionic compounds containing Na, Cl, F, Li, and H were studied. The hydrogen-bonded systems studied were the HF dimer, water dimer, and the H2O-HF complex. The DFT methods compared were Local Density Approximation (LDA), Optimized Energy Potential (OEP) SIC perturbative, and the Generalized Gradient Approximation (GGA). The methods used with ionic systems were HF, LDA and GGA. The Highest Occupied Molecular Orbital (HOMO) energies of the ionic systems were found using each of the methods described. The Hartree-Fock results were plotted against the LDA and GGA results. These plots show a linear relationship between the two methods. There is also a phase shift in the functions that is periodic with the electronegativity of the atoms in the compound. Calculating the energy of the dimer system and subtracting the calculated energy of both monomer units determined the interaction energies of the dimer systems. The energy was calculated at several geometries. These geometries varied by the distance between the two molecules in the dimer. This data was used to make Potential energy curves for each system.

Forensic Analysis Of Glass Using Inductively Coupled Plasma Mass Spectrometry. *MEGHAN FINN (Virginia Tech, Blacksburg, VA 24060) DOUGLAS DUCKWORTH (Oak Ridge National Laboratory, Oak Ridge, TN 37831)*
Glass fragments are a common form of evidence in crimes such as burglary, vandalism, and hit and run accidents. Fragments can be recovered from a suspect's clothing and compared to the fragments from the crime scene. Historically refractive index (RI), an optical property, has been used to compare glass samples. Due to improvements in the glass manufacturing process and quality control measures, temporal variation in the refractive index has decreased, reducing the discriminatory power of RI. While the RI will continue as a

mainstay in forensic glass analysis, the lack of discriminatory power has caused forensic scientists to investigate the use of trace elemental analysis. Inductively coupled plasma atomic emission spectrometry (ICP-AES) has been used successfully, and more recently inductively coupled plasma mass spectrometry (ICP-MS) has been investigated as a multielement technique that has lower detection limits than ICP-AES for many elements. A method has been developed using the ICP-MS to measure the concentration of 25Mg, 26Mg, 47Ti, 55Mn, 71Ga, 85Rb, 86Sr, 88Sr, 90Zr, 91Zr, 121Sb, 137Ba, 140Ce, 147Sm, 178Hf, and Pb, some of the most variant elements in glass. This method's variance has been measured within a single laboratory; however, before this method can be validated, the variance between laboratories must be determined. For this purpose, ORNL is participating in a round robin with the four other laboratories. Having this information should increase the judicial merit of glass evidence due to the fact that an accurate strength of association between unknown and known glass samples can be made with confidence.

Permanganate Reaction Kinetics. *AMBER GAUGER (Lewis-Clark State College, Lewiston, ID 83501) RICHARD T. HALLEN (Pacific Northwest National Laboratory, Richland, WA 99352)*
Tank waste on the Hanford Site contains radioactive elements that need to be removed from solution prior to disposal. One effective way to do this is to precipitate the radioactive elements by permanganate oxidation. When added to tank waste, permanganate, Mn(VII), reacts quickly producing manganese(IV) dioxide precipitate. Because of the speed of the reaction it is difficult to tell what is happening. Individual reactions using non-radioactive reductants found in the tanks were done to determine reaction kinetics. In this project sodium formate, sodium gluconate, EDTA, HEDTA, sodium citrate, glycolic acid, and sorbitol were used as reductants in sodium hydroxide solutions with manganese(II) chloride, iron(III) nitrate, iron(II) chloride, neodymium nitrate, and strontium(II) nitrate as complexing agents in various concentrations. It was determined that HEDTA reacted quickest, followed closely by sorbitol and EDTA, then gluconate, formate, glycolic acid, and lastly citrate. When the complexants were added to the reductants, changes in the rates of the reactions occurred. When the complexants were added to gluconate, manganese(II), strontium(II), and neodymium made the reaction go faster, whereas iron(III) and iron(II) appeared to react at the same rate as when no metal ion was in solution. With EDTA, manganese(II) was the only complexant that made the reaction rate increase, while iron(III) was a little slower, and strontium decreased the reaction rate significantly. With HEDTA, iron(III) did not have an effect on the rate of reaction, while strontium slowed it down considerably. These reactions should determine what happens when permanganate is added to a tank.

Sol-gel synthesis of Cs-Zr-Si and Ba-Zr-Si Polymers. *LIBBY HEEB (University of Washington, Seattle, WA 98105) WILLIAM D. SAMUELS (Pacific Northwest National Laboratory, Richland, WA 99352)*
A Cs-Zr-Si waste form is to be used to remove radioactive cesium from tank waste at the Hanford Nuclear Reservation. However, as cesium decays into barium, the waste form's structure deteriorates, causing it to crumble. This is not favorable for waste transportation or storage. A sol-gel process was successfully used to make the Cs-Zr-Si waste form. The same process was used to try to make the same structure with barium instead of cesium. Due to barium's insolubility, this was not successful. However, with more time to complete further research aimed at finding a way to keep barium in solution, it may be possible to first make the barium structure, and then make the structure with some barium and some cesium. These structures could be examined using IR spectroscopy, heated, and then reexamined to determine any structural changes.

Pronghorn 2001: Quantitative Analysis Using Infrared Remote Sensing. *COREY HEITSCHMIDT (Washington State University Tri-Cities, Kennewick, WA 99336) TIM JOHNSON (Pacific Northwest National Laboratory, Richland, WA 99352)*
The development of remote sensing technology to detect chemical plumes is important for environmental and national security purposes and it is thus important to test the sensors and their capabilities under scenarios that represent actual releases of hazardous materials under realistic atmospheric conditions. During the Pronghorn 2001 campaign at the Nevada Test Site HAZMAT Spill Center, PNNL used a passive FTIR remote sensor system to obtain qualitative and quantitative results

from controlled releases. PNNL participated in campaign to improve upon 1) its equipment sensitivity, 2) its abilities for remote identification and quantification of gas atmospheric pollutants, and 3) the software evaluation methods used in the detection. The passive system consisted of a Midac M2400 FTIR equipped with a liquid-N2 cooled MCT detector coupled to a 14" telescope to detect the infrared radiation. Data were gathered by recording an "on-plume" segment looking at the chemical emissions followed by an "off-plume" segment, which was used as a background to subtract from the on-plume spectrum. The spectrometer response was calibrated using a pair of blackbodies. The data collection was successful and ppmV mixing ratios were determined for the analytes methanol, tri-chloroethylene, sulfur hexaflouride, and ammonia. The comparison of release rates from HSC and PNNL's calculations have shown that PNNL estimates are typically low by a factor of 2 to 3, but that the qualitative agreement between calculated and measured spectra are excellent. The PNNL estimated concentrations scaled nicely with calculated mixing ratios for all analytes.

DNA Microarray Technologies: A Novel Approach to Genomic Research. *ROCHELLE HINMAN (Whitworth College, Spokane, WA 99251) BRIAN THRALL (Pacific Northwest National Laboratory, Richland, WA 99352)*
A cDNA microarray allows biologists to examine the expression of thousands of genes simultaneously. Researchers may analyze the complete transcriptional program of an organism in response to specific physiological or developmental conditions. By design, a cDNA microarray is an experiment with many variables and few controls. One question that inevitably arises when working with a cDNA microarray is data reproducibility: How easy is it to confirm mRNA expression patterns? In this paper, a case study involving the treatment of a murine macrophage RAW 264.7 cell line with tumor necrosis alpha (TNF-a) was used to obtain a rough estimate of data reproducibility. Two trials were examined and a list of genes displaying either a > 2-fold or > 4-fold increase in gene expression were compiled. Variations in signal mean ratios between the two slides were observed. We can assume that erring in reproducibility may be compensated by greater inductive levels of similar genes. Steps taken to obtain results included serum starvation of cells before treatment, tests of mRNA for quality/consistency, and data normalization.

Columbia River Recreational Survey 2001. *MATTHEW HOERTKORN (University of Washington, Seattle, WA 98195) JIM BECKER (Pacific Northwest National Laboratory, Richland, WA 99352)*
During World War Two, it was believed that there was only one quick way to end the war and that was with the atom bomb; As a result the Hanford site was created. The production of the bomb created nuclear contamination at the Hanford Site and surrounding areas, which is still present today. To determine the most effective way to clean up the contamination, research must be done to look at several different substances and variables. One important variable is the amount of exposure to people living and visiting this area receive from the contamination. The Columbia River Recreational Survey was designed to give an understanding of how river-based recreation on the Columbia River affects human exposure to nuclear contamination, and how potential future clean up tactics might affect the economy in the Columbia region. One item gathered from this survey is the types of fish being caught at different places. With this knowledge it can be discovered where the sites Northern Pikeminnow, formerly known as Squawfish, a fish with a bounty on it, are being caught.

Development of Physiologically Based Pharmacokinetic Model for Chlorobenzene Exposure. *MELISSA KANIA (University of Washington, Seattle, WA 98195) KARLA THRALL (Pacific Northwest National Laboratory, Richland, WA 99352)*
Chlorobenzene, a volatile chemical, has been historically used in the manufacture of phenol, aniline, DDT, as a solvent for paints, and as a heat transfer medium. Low levels of chlorobenzene are encountered as environmental contaminants at manufacturing plants, and waste sites. The present study focuses on development of a physiologically based pharmacokinetic (PBPK) model to describe the absorption, distribution, metabolism, and elimination of chlorobenzene in rats. Partition coefficients were experimentally determined in rat tissues and blood samples using an in vitro vial equilibration technique. The ratios

indicate that chlorobenzene is highly lipid soluble. Metabolic rate constants were derived from the optimization of a series of in vivo gas uptake curves conducted at various initial chamber concentrations. Pretreatment of animals with pyrazole, an inhibitor of oxidative microsomal metabolism, appeared to inhibit the uptake of chlorobenzene. Studies to evaluate the relationship between chlorophenol (chlorobenzene metabolite) concentration in saliva and urine to chlorobenzene concentration in the blood were conducted. Ultimately this data will be used to develop a PBPK model that could be used to assess chlorobenzene exposures in humans.

Methods Development on the Characterization and Separation of Organic Acids and Chemical Warfare Simulants.

JEREMY LOHMAN (Washington State University, Pullman, WA 99337) JAMES A. CAMPBELL (Pacific Northwest National Laboratory, Richland, WA 99352)

Characterization of tank wastes is an expensive process. New methods need to be developed in order to cut down the cost of characterizing the wastes. Current methods use derivatization and other expensive methods that make relatively large amounts of waste. MALDI MS and capillary electrophoresis are relatively inexpensive ways of characterizing these wastes, without producing more waste because of the small sample sizes. MALDI MS has previously been used to characterize the organic acids in tank waste. MALDI MS also has the potential to be miniaturized for the purpose of analyzing air for chemical warfare compounds. Some of the chemical warfare compounds have the same phosphate backbone as some of the plutonium extracting chemicals. Finding methods of separating the warfare compounds and analyzing by MALDI would also be a step in analyzing the extracting chemicals as well. Developing a method for separating organic acids took some time, because acetate and glycolate coeluted. Finding the right way to analyze the chemical warfare compounds was only impeded because a couple of the compounds fragmented in aqueous solutions. This was overcome by analyzing them without water. The phosphate containing compounds were not affected by water and will possibly be separable by CE. After a method was found for separating acetate and glycolate, the conclusion was made that CE might be better for separating the acids, because it takes two columns to separate them by ion chromatography. A combination of CE and MALDI will be a useful tool for the characterization and separation of components in tank wastes in the future.

In Search of the Elusive Quantum Dot: Using Microcantilevers as a Mask and in Detection Systems.

SOPHIA MCCLAIN (Goerge Mason University, Fairfax, VA 22030) PANOS DATSKOS (Oak Ridge National Laboratory, Oak Ridge, TN 37831)

Nanostructures are currently being used in studies such as quantum electrical systems and biochemical assays. It is important to learn how to make and image the nanostructures used in these systems. To make the nanostructures holes are drilled into the tip of a microcantilever using a Focused Ion Mill. The microcantilevers are then used as a mask as gold is sputtered through the holes creating quantum dots and wires. These dots and wires are then imaged to prove that these structures can be fabricated by this method. Various forms of microscopy were experimented with to find the structures. A Multi-mode III Atomic Force Microscope and a Scanning Electron Microscope were used in the search for the quantum dots and wires.

CO_2 Interaction with Cation-exchanged Zeolites.

DIAN MCKENZIE (York College, Queens, NY 11451) ETSUKO FUJITA and JON HANSON (Brookhaven National Laboratory, Upton, NY 11973)

The emission of carbon dioxide into the atmosphere is one of the most serious problems with regard to the greenhouse effect. The reduction of carbon dioxide is of special interest. One approach to carbon dioxide reduction is the usage of cation-exchanged zeolites. Titanium Y zeolite, cesium Y zeolite, potassium Y zeolite, and lithium Y zeolite were prepared by ion-exchanging commercial sodium Y zeolite for studies by time resolved in-situ synchrotron X-ray powder diffraction. A series of time-resolved powder diffraction patterns were obtained for all the prepared zeolites before and during dehydration, and during and after dosing with CO_2. The powder patterns for the dehydrated zeolites show an increase in the intensity of the lowest order reflection (111) due to less electron density in the supercages. The powder patterns also show a decrease in intensity of the 111 reflections during dosing of CO_2 on all the dehydrated zeolites. The changes to the powder patterns for CO_2 dosed zeolites are consistent with cation migration and CO_2 binding. Difference Fourier electron density map data of dehydrated Ti Y suggest that there is electron density in SI, SI', and SII cation sites. Preliminary analysis of the refinement data in the range 200-376°C indicates less total charges for titanium than expected. However, the charge on titanium is consistent with +4.

Determining the In Vitro Rate of Metabolism of 1,2-Diethylbenzene in Rats.

ANARGIROS MELETIS (Pacific University, Forest Grove, OR 97116) KARLA THRALL (Pacific Northwest National Laboratory, Richland, WA 99352)

The in-vitro metabolism of 1,2-diethylbenzene was studied in liver microsomes prepared from male F344 rats. The substrate, 1,2-diethylbenzene, is a compound commonly used in the production of divinylbenzene and has been found in the drinking water supplies of some cities across the United States. 1,2-diethylbenzene is believed to be metabolized to 1,2-diacetylbenzene, which is neurotoxic in laboratory animals. The ability of the microsomes to metabolize 1,2-diethylbenzene in vitro was studied by observing the disappearance of 1,2-diethylbenzene and appearance of 1,2-diacetylbenzene over time. Reference vials containing heat inactivated enzymes and active sample vials were incubated with a mixture of HEPES and NADPH and kept in a temperature-controlled Vortex evaporator. The substrate, 1,2-diethylbenzene, was added as a liquid at 100 or 500 mg/ml (in 2% DMSO) to the vials and then incubated for time intervals ranging between 5 to 150 min. At the end of the incubation period the reaction was stopped, chlorobenzene was added as an internal standard, and the samples were extracted and analyzed on an HP 5890 Series II GC with a photo-ionization detector. The concentration of 1,2-diethylbenzene was found to be lower in the active samples than in the inactive samples. Some samples were pretreated with pyrazole.

Measurement of the pKa Values of pH Indicators in Solutions and Sol-Gel Matrix.

KERRY-ANN MILLER (Miami-Dade Community College, Miami, Fl. 33167) SHENG DAI (Oak Ridge National Laboratory, Oak Ridge, TN 37831)

Molecular imprinting is a synthesis technique developed to create specific binding sites for individual chemical compounds. Sol-gel based molecular imprinting has many advantages among which are its low temperature, transparency, and its ability to embed indicators into its matrix. By analyzing the absorbance of the indicator solution at different pHs using the UV-VIS spectrometer, it is possible to calculate the pKa shift to be used as a specific indicator. By entrapping the indicator into the matrix with various initial proton concentrations, the gel with various proton concentrations will have a memory of the proton, which will cause the pKa shift of the entrapped indicators. Prior to the measurement of the sol-gel entrapped indicators, it is necessary to measure the pKa of the indicator in the solution. Spectra were taken of each indicator while the pH was adjusted. The pH of each spectrum was recorded for use later on in the experiment. A linear graph is constructed with the pH/ absorbance, and from this graph and using a formula that was composed of using a combination of Beer's Law and the Henderson Hasselbach equation, the pKa can be calculated. Results are pending due to calculation of data.

Wet Synthesis of Transition Metal-Imidazolole Complexes.

MARIO ORTEGA (Fresno City College, Fresno, CA 93662) DALE L. PERRY (Ernest Orlando Lawrence Berkley National Laboratory, Berkley, CA 94720)

The world around us, including medicinal chemistry and electronics, is all intertwined, and new products are created through several scientific processes, one being synthesis. The process of creating new drugs, materials, and semiconductors relies on the reactions of two or more substances to create a more complex one. Understanding the importance of this concept and utilizing are what enable break-throughs to be made in many of these fields. During my time at LBNL, I synthesized various metal-imidazole compounds, all work being performed in a wet chemistry lab as well as an x-ray diffraction facility. The two highlighted chemical systems of my term here were cobalt imidazolate and copper imidazolate; both were created and crystallized utilizing the same process. Previous attempts at producing these complexes as high quality crystals were fruitless. The complex crystals were obtained from the parent compounds by careful adjustment of the reaction conditions. This process produced metal-imidazolate and metal-imidazole complex crystals simultaneously. As the crystals became visible, various heating and cooling cycles were instituted to stimulate growth and purity over several days. In the near

future, these crystals will be structurally analyzed for comparison of their magnetic and physical properties. Imidazole and related compounds constitute the backbone of histamine and many peptides involved in human biological processes. With the data of these types accumulated here, some previously unexplained biological chemistry and related phenomena might one day be explained.

Pilot Plant Design for the Recovery of Computer Housing Plastics.
ADAM OWENS (Salisbury University, Salisbury, MD 21801) JOE POMYKALA JR. (Argonne National Laboratory, Argonne, IL 60439)

The objective of this project is to design a pilot plant that will be used for the recovery of desired plastics from computer housing plastic materials. The desired plastics, acrylo-nitrile-butadiene-styrene (ABS) and polycarbonate (PC), will be separated from some 3-5 other plastics via the froth flotation method. The froth flotation method of separation incorporates the manipulation of surface tension, pH, and density of a solution that inhibits similar density plastics to be either hydrophobic or hydrophilic. The hydrophobic plastics will float were as the hydrophilic plastics will sink. Various experiments were conducted to find the best conditions for separation to produce a high purity product content of ABS and PC. It was found that in order to obtain high purity, a two-stage separation process must be performed. To design a pilot plant that uses this two-stage separation process many technical issues must be addressed. Such issues include flow rates of solution, tank capacities, screw conveyor specifications, and drying capabilities. The research led to a design for a test pilot plant for the recovery of ABS and PC from computer housing plastics, which may lead to the design and production of a commercial plant in the future.

Xylose Metabolism Pathway of a Thermotolerant Yeast.
ELISABETH PETIT-FOND (Miami-Dade Community College, Miami, FL 33167) JOHN NGHIEM (Oak Ridge National Laboratory, Oak Ridge, TN 37831)

Xylose metabolism of Kluyveromyces marxianus ATCC 36907, a thermotolerant yeast, was verified and studied under both aerobic and anaerobic conditions. The yeast was grown on LB medium supplemented with glucose and xylose. With initial xylose concentration of 5 g/L and glucose concentrations of 1,2,and 5 g/L, 55% of xylose was consumed over a period of 6 days under aerobic conditions. Under anaerobic conditions and over the same period, the percentage of xylose utilized increased from 6 to 18% as the glucose concentrations were increased from 1 to 5 g/L. The results indicated that the K. marxianus strain studied has a xylose metabolism pathway that can be enhanced by glucose.

Thermolysis of Substituted Benzyl Alcohols.
JULIE PIGZA (Allegheny College, Meadville, PA 16335) PHILLIP F. BRITT (Oak Ridge National Laboratory, Oak Ridge, TN 37831)

Lignin, the second most abundant biopolymer found in woody biomass, is an under-utilized resource of aromatic chemicals and fuel. However, the thermal degradation of lignin is poorly known. Previous pyrolysis studies on lignin model compounds, such as PhCH(OH)CH2OPh and PhCH(OH)CH(CH2OH)OPh, have found substituted benzyl alcohols as products but the degradation of these products is not known since both free radical and ionic reaction pathways are possible. The current work focuses on the reactivity of these substituted benzyl alcohols under pyrolysis conditions. Starting materials were first purified to >99.9% before pyrolysis. The pyrolysis reactions were carried out at 345°C for either thirty or ninety minutes. Specific features that were investigated were the influence of substituents on the reactivity. Scouting experiments have shown the reactivity of the molecules as follows: 4-hydroxybenzyl alcohol ~ 4-methoxy-alpha-methylbenzyl alcohol > 4-methoxybenzyl alcohol >> 3-hydroxybenzyl alcohol. The most likely decomposition mechanism contains both ionic and radical pathways, with ionic dominating, as determined by the products formed (identified by GC-FID and GC-MS). Establishing the reaction mechanisms of lignin model compounds can then provide insight into optimization of the pyrolysis process.

THE APPLICABILITY OF 3M BRAND MEMBRANE TECHNOLOGY TO RADIOCHEMICAL ANALYSIS AT ARGONNE NATIONAL LABORATORY-WEST.
MEGAN PLUMLEE (Pacific University, Forest Grove, OR 97116) JACQUELINE FONNESBECK (Argonne National Laboratory, Argonne, IL 60439)

EmporeTM Rad Disks, commercially available ion-specific membranes, are designed for large-scale separation and quantification of isotopes in water samples at environmental levels. The membranes were tested for their applicability to samples of higher levels of radioactivity, typical of the analytical work occurring at Argonne-West. The sample water contained high concentrations of a variety of radionuclides. Three membranes were studied: Strontium, Cesium, and Technetium Rad Disks. Following separation, the disks were analyzed by liquid scintillation or gamma spectroscopy. The strontium and cesium disks were successful at isotope separation, although with recovery levels of 80% to 90%, somewhat lower than the success associated with the environmental disk separations. The technetium disks were not found to be compatible with the samples of higher levels of radioactivity used in this study, as they achieved low recovery levels of the target isotope and also retained isotopes other than technetium.

Preparation of Carbonate Salts from Alcohols, Carbon Dioxide, and Tertiary Amines.
MAIRIN ROONEY (Sacramento City College, Sacramento, CA 95822) JOHN LINEHAN (Pacific Northwest National Laboratory, Richland, WA 99352)

Historically, carbon dioxide(CO_2)has not been regarded as a useful monomer, yet as environmental concerns grow and CO_2 remains an abundant industrial byproduct, research and industry have looked toward CO_2 for utilization as an inexpensive carbon feedstock. Synthetic applications of alkyl- and polycarbonates exist including pharmaceuticals, and fuels. Typically these items are synthesized using phosgene or organometallic catalysts. Safer and less expensive methods of carbonate alkylation have been explored, yet few methods are practical on an industrial scale. Various alcohols and polyalcohols were dissolved and reacted with a tertiary amine. CO_2 was bubbled through the carbonate salt precipitating out of solution. The salts were washed, filtered, and allowed to dry. Yields were calculated and salts were characterized using Infrared (IR) spectroscopy, 13C and solid state Nuclear Magnetic Resonance (NMR). The salts were observed by IR with strong bands at wavelengths between 1640 and 1650 cm-1. NMR analysis displayed mole fractions of CO_2 to alcohol as increasing proportional to CO_2 pressure, indicating carbonate salt formation. Yields varied depending upon the alcohol ranging from 11% - 79%. Salts formed from polyalcohols yielded conversion > 100% due to suspected bicarbonate production verified by solid state NMR. Data suggest alcohol and tertiary amines under CO_2 form organic salts of alkyl carbonates via a hemi-acid salt and form in greater yield as CO_2 pressure increases. Less hindered alcohols or alcohols with strong electron withdrawing groups seem to form carbonate salts in greatest yield with salts formed from polyalcohols requiring further study.

Construction of a Protein Crystallographic Calculator.
PREETI SHANBHAG (Bethune-Cookman College, Holly Hill, FL 32117) ANA GONZALEZ (Stanford Linear Accelerator Center, Stanford, CA 94025)

The architecture of macromolecules can be determined by the diffraction of x-rays over the protein crystals. Crystals have a very high degree of internal order, and are composed of repeating groups of the same arrangements of atoms and molecules, which are called cells. After obtaining a perfect crystal, its reflection, which is arranged in a precise diffraction pattern, is obtained by directing an X-ray beam onto a crystal. The intensity corresponds to the reflection of the X-rays, and has a characteristic interplanar spacing 'd'. The 'd' is related to the angle of the X-ray scattering, ‰, by Bragg's law. The Bragg's equation is: n‰ = 2d sin ‰, where ‰ is the wavelength of the radiation. Using this information, a program has been created that will calculate the maximum and minimum resolution, as well as the maximum cell dimension and wavelength. This program is written in Tcl/Tk (Tool Command Language, with it's graphical counterpart, Toolkit).

Synthesis of Materials for New Selective Oxidation of Catalysts: Polyoxometallate Clusters Supported in Mesoporous Oxides.
REBECCA SOINSKI (Bryn Mawr College, Bryn Mawr, PA 19010) LENNOX E. ITON (Argonne National Laboratory, Argonne, IL 60439)

New materials have been formulated for testing as heterogeneous catalysts in the direct selective oxidation of benzene to phenol. Mesoporous silica materials with various structures have been synthesized as supports. Several V/W, V/Mo and Cu/W polyoxometalate compounds have been synthesized as oxidative catalysts. Catalyst materials were prepared by impregnation of the

anionic polyoxometalate clusters into the pores of the silicas. Novel catalyst compositions have been based on SBA-11 mesoporous silica with a cubic cage structure and 25 Å average pore diameter. Syntheses of mesoporous silicas in the form of transparent films, fibers, and monoliths were also accomplished. These materials are useful for spectroscopic characterizations and as host materials in applications unrelated to catalysis. The mesoporous silicas were analyzed using TGA, pore size distributions, and in situ SAXS.

Synthesis and 13C NMR Spectroscopy of Steryl Ferulates and Coumarates in Corn Oil. *NICOLE STAIR (Whitman College, Walla Walla, WA 99362) JAMES A. FRANZ (Pacific Northwest National Laboratory, Richland, WA 99352)*
The objective of this study was to synthesize authentic samples of coumarate esters of sterols thought to be found in corn oil. In this study, a fraction of corn oil derived form corn hulls potentially could contain steryl cinnamic acid derivatives of both ferulic and coumaric acid. Two important representatives of corn oil derived sterols, stigmasterol and stigmastanol, and one structurally similar coumarate, that of cholesterol, were synthesized in order to determine and compare their 13C NMR spectroscopic properties to those observed for extracts of corn fiber. In addition, chromatographic techniques were employed to resolve steryl esters in corn oil. The study revealed that steryl ferulates are present in significant yields in the corn oil, but steryl coumarates were determined to be present in the corn oils at concentrations less than 10% of the ferulates.

Correlation of Algal H2 Production with PSI Content: An Experimental Verification of the Z-Scheme Model. *JEFFREY STEILL (University of Tennessee, Knoxville, TN 37901) JAMES WEIFU LEE (Oak Ridge National Laboratory, Oak Ridge, TN 37831)*
A rigorous experimental verification of the 'Z-scheme' hypothesis for the molecular basis of photosynthesis is undertaken by a precise quantification of both the components and products of the process. The model postulates a coordinated action of two photo-systems, PSI and PSII, within the chloroplast membrane. In this model PSII is solely responsible for O2 production and contributes reductive potential to PSI. The anaerobic activity of the algae Chlamydomonas is used to isolate the contribution of each process. Under anaerobic conditions, a reductive pathway to the Hydrogenase enzyme produces H2 gas. Under light-saturated, single-pulse conditions, the predictions of the model are tested by measurement of both H2 gas per mg Chlorophyll per light pulse and total PSI within the sample. A variety of genetically modified mutants, with predictable variation in the ratio of PSII to PSI, are used as samples. The H2 output is quantified as an increase in potential across an O22- selective membrane as the combustion of hydrogen decreases the O2 concentration. The detector response is calibrated by water electrolysis. Initial results show reasonable reproducibility of H2 measurement and demonstrate a correlation with PSI content roughly consistent with the model. The wild-type CC-125 shows about 1.1 (10%) nanomoles H2 produced per mg chlorophyll per flash and the PSI-deficient mutants: Duke 1047 and LM Fud 26 show considerably less H2 output (by a factor of about 2). Positive or negative verification of the model is not yet possible, but improvements in measurement precision and direct spectophotometric PSI quantification will lead to more conclusive determinations.

Hydroxyapatite-SN15 Binding as a Model For Protein-Mineral Interactions. *DANIEL STEVENS (University of Washington, Seattle, WA 98195) XIAOHONG, LI (Pacific Northwest National Laboratory, Richland, WA 99352)*
Past research has found that quantities as small as 0.1% (by weight) of proteins in solution with minerals can drastically alter crystal growth and morphology. This research focused on the interaction of hydroxyapatite (HAP), and the 15 N-terminus amino acids of the statherin protein (SN15). Statherin inhibits mineral deposition on teeth by keeping saliva supersaturated with respect to calcium phosphate. HAP is the phase of calcium phosphate that makes up enamel and parts of bone. One of the primary goals of this research was to determine the secondary structure of SN15 when it is bound to HAP, which could be used to model other mineral-protein interactions. The SN15 peptide was isotopically labeled at L8G12. The peptide was then adsorbed onto HAP. The samples were then analyzed using solid state NMR (peptide structure), fluorometery (peptide coverage), CCK (kinetics), and were also run through zeta potential experiments (charge

interactions). A calibration curve was constructed using a fluorometer on samples with known peptide concentrations. The curve was then applied to solutions prior to and after adsorption isotherms to determine coverage. CCK and zeta potential experiments are expected to demonstrate that electrostatic interactions are the primary initiator of HAP-statherin binding, as opposed to crystal face specific sites. Solid State NMR is expected to show that the region of interest on the protein becomes highly helical after binding.

LiFePO4 as a Cathode for Rechargeable Lithium Batteries. *HEATHER SWINGER (Taylor University, Upland, IN 46989-1001) JOHN T. VAUGHEY (Argonne National Laboratory, Argonne, IL 60439)*
Rechargeable lithium batteries are used for a wide variety of consumer electronics. The cathode materials currently in use are LiCoO2, LiNiO2, and KiMn2O4. A new material is being sought which is cheaper and less toxic than those currently in use. LiFePO4 is an excellent candidate because it has comparable theoretical capacity and fits the two criteria given previously. This paper investigates the effects of baking temperature and carbon addition on the capacity of a LiFePO4 sample.

Preparation of New Polymer Coatings for Detection of Pertechnetate Ion. *MATTHEW THORNTON (Columbia Basin College, Pasco, WA 99301) TIM HUBLER (Pacific Northwest National Laboratory, Richland, WA 99352)*
The general aim of this work is the design and implementation of a new sensor technology for analysis of the complex chemical mixtures found at DOE sites nationwide. The specific goal of this research is the development of a sensor for technetium (Tc) that is applicable to characterizing and monitoring the Vadose Zone and associated subsurface water at the Hanford site. The sensor design consists of a basic spectroelectrochemical configuration consisting of a waveguide with an optically transparent electrode that is coated with a thin chemically selective film. The films are being developed for pertechnetate ion analysis. Samples containing pertechnetate ion will partition into the films by electrostatic attraction, then electrochemically converted into a Tc coordination compound that gives a strong optical signal associated with an electrochemical reduction/oxidation process. This presentation focuses on strategies for preparation of the selective sensor films.

Protein Mineral Interactions as they Influence Final System Conformation. *LINDSEY VANSCHOIACK (Rose-Hulman Institute of Technology, Terre Haute, IN 47803) ALLISON CAMPBELL (Pacific Northwest National Laboratory, Richland, WA 99352)*
Literature evidence suggests that proteins in solution with growing minerals can greatly affect the mineral's morphology. As little as 0.1% wt/wt protein in solution can cause the crystal's size and morphology to be drastically altered. Understanding a protein's secondary structure after formation on a biologically derived mineral would contribute greatly to the current understanding of biomineralization. As a model system to study tooth and bone biominerals, this research focuses on the relationship between structure and surface coverage of a peptide derived from the N terminal 15 amino acids (SN15) of statherin and its biologically relevant mineral calcium phosphate. Statherin inhibits calcium phosphate deposition from supersaturated saliva onto teeth. Our work involved the SN15 peptide, isotopically labeled at L8G12 for NMR studies. The peptide was adsorbed on hydroxyapatite (HAP) crystals, and fluorometry, solid state NMR, constant composition kinetics, and zeta potential experiments were used to observe coverage, structure, kinetics and electrostatic charge respectively. Fluorometry measurements yielded a calibration curve to allow quantification of surface coverage based on the Langmuir model. Results to date include CCK and SSNMR data at monolayer coverage. CCK results suggest that charge interactions, rather than crystal face specific sites, induce bonding. Zeta potential measurements will provide additional support for this theory if they show a significant change in charge for bound vs. free HAP crystals. SSNMR results suggest a largely helical conformation in the region of interest, both on the surface and as a lyophilized powder.

Implementation of Gel Electrolytes in Rechargeable Lithium-ion Batteries. *JENNIFER WADE (University of Iowa, Iowa City, IA 52240) KATHRYN STRIEBEL (Ernest Orlando Lawrence Berkley National Laboratory, Berkley, CA 94720)*

The use of a polymer gel electrolyte in a rechargeable lithium ion battery will help provide a mechanically stable and compact structure connecting positive and negative electrodes via a thin ion conducting layer of gel polymer. The properties of a successful gel electrolyte will create stable interfaces with the electrodes have an ionic conductivity of 1 mS/cm at ambient temperatures. Specifically, lithium ion conductivity, electrolyte uptake (swelling) and binding to electrode materials were investigated for commercial microporous polyolefin membranes (Celgard). With the aid of a poly (vinylidene fluoride) (PVdF) coating on the Celgard samples, bonding between the separator and the electrodes was possible. Moreover, the microporous character of the membrane allowed for a much greater swelling of electrolyte than predicted (=100% by mass). The conductivity obtained varied based on the composition of the membrane and whether the membrane was coated with the PVdF polymer host.

Increasing Efficiency in Photoelectrochemical Hydrogen Production. *SCOTT WARREN (Whitman College, Walla Walla, WA 99362) JOHN TURNER (National Renewable Energy Laboratory, Golden, CO 80401)*

Photoelectrochemical hydrogen production promises to be a renewable, clean, and efficient way of storing the sun's energy for use in hydrogen-powered fuel cells. We use p-type Ga.51In.49P semiconductor (henceforth as GaInP2) to absorb solar energy and produce a photocurrent. When the semiconductor is immersed in water, the photocurrent can break down water into hydrogen and oxygen. However, before the GaInP2 can produce hydrogen and oxygen, the conduction band and the Fermi level of the semiconductor must overlap the water redox potentials. In an unmodified system, the conduction band and Fermi level of GaInP2 do not overlap the water redox potentials. When light shines on the semiconductor, electrons build up on the surface, shifting the bandedges and Fermi level further away from overlap of the water redox potentials. We report on surface treatments with metallated porphyrins and transition metals that suppress bandedge migration and allow bandedge overlap to occur. Coating ruthenium octaethylporphyrin carbonyl (RuOEP CO) on the GaInP2 surface shifted bandedges in the positive direction by 270 mV on average, allowing the bandedges to frequently overlap the water redox potentials. Coating the GaInP2 surface with RuCl3 catalyzed charge transfer from the semiconductor to the water, lessening bandedge migration under light irradiation. Future work will focus on the long-term surface stability of these new treatments and quantitative applications of porphyrins.

Evaluation of sample preparation techniques to decrease alkali metal interference by inductively coupled plasma optical emission spectrometry in an axial torch position, particularly in a fusion matrix. *SARAH WARRINER (Washington State University, Richland, WA 99352) LMP (MAY-LIN) THOMAS (Pacific Northwest National Laboratory, Richland, WA 99352)*

IIn research, efficiency and reliability of sample analysis are vital. The inductively coupled plasma optical emission spectrometer (ICP) has the ability to simultaneously analyze multi-analyte samples. However, interferences have been found when analyzing for alkali metals (K, Li, Na) in fused glasses. In this study, two sample preparation parameters have been varied to find a sample preparation technique that will reduce the alkali interference. Test 1 varies the HNO3 concentration from 0% to 4%, and test 2 varies the Cs concentration from 0ppm to 1000ppm. In both tests, the samples were spiked with 0.5ppm of Li, 1.0ppm Na, and 2.5ppm K. In addition, test 1 samples were spiked with 300ppm Cs and test 2 samples were prepared in 2% HNO3 matrix following the current procedure. The results were surprising. Instead of seeing a rising response that leveled off after a particular Cs concentration, the response continued to increase as the concentration increased. The results also showed that the HNO3 concentration was the most stable at 2%. By reviewing previous ICP alkali data, it was discovered that about 200ppm of Na or K are added during the fusion process. The standards used to standardize the ICP instrument, like the samples, are all spiked with only a 300ppm Cs spike. Therefore to accurately standardize the ICP for a glass sample matrix, the standards need to be spiked with a 500ppm Cs spike to increase the standard's salt concentration to match the sample's total salt concen-

tration. Future research could test the effect of salt concentrations at higher levels during ICP analysis to determine if a response limit can be reached.

Proton Imprinting Via Sol-Gel Captivated pH Indicators. *MICHAEL WEAVER (Pellissippi State Technical Community College, Knoxville, TN 37933) SHENG DAI (Oak Ridge National Laboratory, Oak Ridge, TN 37831)*

The various properties of sol-gel chemistry present many opportunities for nanoscale isolation and investigation. The encapsulation permitted by sol-gel chemistry has generated an interest in molecular imprinting. A fundamental experiment was conducted involving proton embedding in the sol-gel matrix. Several indicators, whose color varied with pH, were protonated (or deprotonated) in situ during sol-gel synthesis with acid (or base) catalysts. After the gel dried, with the indicator encapsulated, the gel was subjected to an analysis of visible light absorption as pH varied. An equation was derived from Beer's law and the Henderson-Hasselbach equation; this equation allowed straightforward determination of the equilibrium constant values for the proton gain or loss in the subject, embedded indicators. This analysis provided a direct comparison between established indicator equilibrium constant values in solution versus experimental sol-gel embedded indicator equilibrium constant values. Results indicate the sol-gel matrix confers protection to ionic species when free from extended aqueous storage, and subsequent chemical modification of the gel's surface with functional groups resulted in larger protection of the indicator. This experiment demonstrated the sol-gel's efficacy in surrounding and shielding charged ionic species on the molecular level.

Applications of Synchrotron Based Technologies to the Forensic Examination of Ink and Paper. *TOMMY WILKINSON (Fresno City College, Fresno, CA 93705) D.L. PERRY (Ernest Orlando Lawrence Berkley National Laboratory, Berkley, CA 94720)*

Synchrotron-based technologies, including Fourier Transform Infrared Spectromicroscopy (FTIR-SM) and XRay Fluorescence Microprobe (XFM), can be used for direct and rapid evaluation, characterization and identification of writing inks. These techniques can be used for the direct nondestructive analysis of inks on paper and other materials, without any mechanical or chemical destruction of the paper, and without having to extract or separate the inks. These techniques allow for very small sample size (less than 10 microns) and with very low quantities (less than 10 femtograms). These methods may also be useful in other areas of ink analysis, including, but not limited to, qualitative and quantitative analysis of the primary ink components, verification of the identical nature of several inks, and potentially determination of the age of the ink relative to the paper.

High Precision Control System for an Acoustic Cavity Resonance Spectrometer. *CARL WILLIS (Guilford College, Greensboro, NC 27410) DEBRA BOSTICK (Oak Ridge National Laboratory, Oak Ridge, TN 37831)*

Acoustic cavity resonance spectroscopy (ACRS) is a powerful new technique for measuring properties of fluid samples (critical points, for example) with unprecedented accuracy, precision, and rapidity. By tracking acoustic resonant frequencies in a sample-filled cavity, ACRS takes advantage of the sensitivity of the speed of sound to changes in the sample's density and elastic properties. The pressure, volume, and temperature of the sample must be precisely known when the acoustic measurements are taken, in order to realize the precision of which ACRS measurement is capable. Furthermore, temperature and volume should be user controllable so that measurements can be taken in a particular range of interest. We have developed a computerized volume and temperature control / measurement system, based on LabVIEW programming, for the ACRS housed at ORNL. A PID (proportional-integral-differential) algorithm drives the cavity oven for heating and a liquid nitrogen proportional valve for cooling. Sample temperature can be held constant or swept at a user-defined rate, with a deviation of less than 0.004 Celsius degrees, within the range of 20°C - 120°C. Resonator volume, adjustable between 0 and 8 mL by a stepper-motor-driven piston, is measured by a linear variable differential transformer (LVDT); volume changes are known to one microliter. Some challenges remain to be addressed in future work, primarily water condensation in electronics at low temperature, and inefficiency of the cooling mechanism. In further developments we expect to extend the lower temperature limit to -40°C. We also plan to verify the ACRS system's accuracy with CO2 critical point measurements.

COMPUTER SCIENCE

Mass Spectrometry Using the Scan Function Editor. *KISSIE ANDERSON (Southern University, Baton Rouge, LA 70813) IRENE ROBBINS (Oak Ridge National Laboratory, Oak Ridge, TN 37831)*
Mass spectrometry provides valuable information to a wide range of professionals. Mass spectrometry is used to monitor the breath of patients by anesthesiologists during surgery, determine how drugs are used by the body, and to analyze environmental pollutants, to name a few. Mass spectrometry is a powerful, analytical technique that is used to identify unknown compounds, to quantify known materials, and to elucidate the structural and chemical properties of molecules. The Chemical Biological Mass Spectrometer Block II is a new and improved system for the detection and identification of chemical and biological warfare agents for the United States Army. The Scan Function Editor (SFE) software is intended to provide tools for an expert user to conduct mass spectrometer experiments and collect mass spectral data. The basic objective was to provide user documentation for the Scan Function Editor software. This software is still under development, but provides mechanisms for development of scan functions, setting and monitoring of instrument parameters, and collection of mass spectral data in graphical displays, ITS40-format files, and textual files.

Motion Control of the 0.8-m Telescope at Rattlesnake Mountain Observatory. *CULLEN ANDREWS (Eastern Washington University, Cheney, WA 99004) KEN SWANSON (Pacific Northwest National Laboratory, Richland, WA 99352)*
Rattlesnake Mountain Observatory is an astronomical observatory that is not currently used for research. Located on top of Rattlesnake Mountain northwest of Richland, WA, it is not a very accessible place. Work is now being done to automate the 0.8-m telescope and dome, so that local high school students will eventually have remote access to it via the Internet. Gaining adequate motion control of the telescope is currently the most immediate goal. Optical encoders on the hour angle and declination axes were used to measure output velocities over a range of input velocities sent to the control unit of the two servomotors. It was found that the velocity resolution—the smallest increment by which velocity can be changed—was 0.225 arc seconds per second. It turns out that this is because motor velocities are limited to integer values of motor encoder counts per second. This is insufficient for tracking stars during a prolonged photographic exposure. Velocity resolution of 10^-3 arc seconds per second or better is needed. A program is needed that will change motor velocity over time in order to stay within 1 arc second of the target. Increasing the gear ratio between the servomotors and telescope would improve velocity resolution, but not enough to completely solve the problem. Future projects at the observatory include calibration of the axis encoders and communication between the main computer and the dome control units.

Optical properties of the metal-film-on-silicon system. *DIMITRY AVERIN (New York City Technical College, Brooklyn, NY 11201) MYRON STRONGIN (Brookhaven National Laboratory, Upton, NY 11973)*
The main focus of this research was to workout equations for the transmission of light through a thin metallic film on a dielectric substrate. There are approximate equations theoretically developed by R. E. Glover and M. Tinkham; however their precision is limited. The goal of this investigation was to confirm and possibly improve the accuracy and validity of the existing methods. Maxwell's equations and the electromagnetic wave equations were used as the basis for the computations. The main tool utilized in this research was the mathematical software MathCAD 7. It was used to perform complex computation and graphically represent obtained equations. In order to verify the accuracy of the developed equations their outputs were compared with the experimentally gained data. As a result some of the developed equations now can be programmed on a PC this would allow the exploration of a greater variety of cases.

Evaluation of the use and maintenance of E.P.I.C.S. extension tools at the Stanford Linear Accelerator Center. *ROGER BAKER (California State University, Bakersfield, Bakersfield, CA 93301) RON CHESTNUT (Stanford Linear Accelerator Center, Stanford, CA 94025)*
Industrial control software development and maintenance at DOE High

Energy Physics Laboratories understandably consumes a vast amount of man-hours. Many of these Laboratories have a number of systems in common with each other, and even with industry. For this reason, the EPICS collaboration was born, to reduce the amount of duplicate work being done at various research centers. The base distribution of EPICS has been thoroughly evaluated and critiqued, but the particulars of the maintenance cycle, specifically for the extensions, or add-on tools, has barely been addressed. This project has addressed the specific issues related to installation, maintenance, and upgrade of small, but extremely useful, extensions to the EPICS distribution. We concerned ourselves mainly with use testing, code modification, and software compatibility issues in a collaborative software development environment. Finally, it is our hope, that we have shown the effectiveness of such a development environment, and illustrated ways in which it may be improved, and used as a template for future cooperation.

Computing Resource Inventory Database. *DON BIBLE II (Pellissippi State Community College, Knoxville, TN 37933) TERRY HEATHERLY (Oak Ridge National Laboratory, Oak Ridge, TN 37831)*
Organizational computing resources are critical cost elements for most businesses. Within the Engineering Technology Division (ETD) at Oak Ridge National Laboratory, employees use approximately four hundred desktop computing systems to support their diverse research activities. Management desired an automated tool to better assist them in managing their numerous computing resources on a daily basis. The Computer Resource Inventory database was developed to provide the capability to perform routine cross-cut and roll-up types of analyses that will supply (1) system administrators with the specific technical data of the systems in operation, (2) managers a snapshot of when systems may need to be replaced, and (3) an estimated value of the collection of computing resources being utilized. The database will employ detailed information for specific system capabilities, their owners, their locations, and will assist managers and technical administrators to perform a variety of analyses. In addition, the database will provide a basis for continual updates as new resources are procured and older resources are retired. The development and implementation of this database should improve ETD's organizational management of its numerous computing resources.

Evaluation of Understanding Processes for the Visualization Theatre. *NATHAN BOWER (Jamestown Community College, Jamestown, NY 14701) MICHAEL MCGUIGAN (Brookhaven National Laboratory, Upton, NY 11973)*
The knowledge of using the software of the three-dimensional visualization theatre was one of our project's main goals. The software that was used ranged from open source programs from the Internet to package software that came with the Silicon Graphics computers. Some of these software programs include Data Explorer, image viewer, and Image Magick. We learned the process of converting images and models through the Data Explorer program and using the models in the three dimensional projection theatre. Some of the data that was processed included condensed matter data. The images produced were of an iron atom with its outer electrons. This information was important because it was used to help determine why metals such as iron have magnetic capabilities. The other data that was used was Quantum Chromodynamics (QCD) related data. This dealt with the theoretical possibilities of subatomic particles such as fermions and gluons. Another important aspect of our project's study was learning how to use some of the hardware equipment in the theatre. The main goal of this project is to learn how to use the visualization theatre, install successfully at our home campus, and stimulate interest in the project from our community.

An Autonomous Robotic Scheme for Visual Tracking and Pursuit. *HUNTER BROWN (North Carolina State University, Raleigh, NC 27607) LYNNE PARKER (Oak Ridge National Laboratory, Oak Ridge, TN 37831)*
In autonomous mobile robotic formation, it is often essential for robots to know the position of other robots. This project involves studying a team of mobile robots, called Emperor robots, to enable them to achieve "follow-the-leader" formations. Solutions to this problem use data from various sources including GPS, laser range finders, sonar and visual tracking. In this research, machine vision is being studied to provide position information. This paper describes a set of algorithms that have been developed that enable robot team members to analyze

images to locate the robot within its field of vision, and to estimate its distance. These algorithms work by first acquiring an image via the pan-tilt-zoom vision system with an image frame grabber through the manufacturer-included Mobility software interface and then applying several algorithms on it. The image is then color segmented, averaged, run through an object detection and assignment scheme, and then a position and distance estimation algorithm. The output of these algorithms is the centroid of the robot (if one exists within the image) and an estimated distance, which is then used in locomotion routines. Results are presented that illustrate the effectiveness of our algorithms on the Emperor robots. These results include real-time processing of an average 14 frames per second, high precision, accurate position information, and distance estimation. The findings show that the algorithms, in place with the current control scheme, provide an excellent solution for indoor and outdoor machine vision tracking and pursuit capabilities.

Developing a High Speed Subnet for Testing Windows 2000 Server and LINUX Red Hat 7.1 operating systems.

MARK CARPENAY (Queens College, Flushing, NY 11367) EVERETT HARVEY (Ernest Orlando Lawrence Berkley National Laboratory, Berkley, CA 94720)

The goal of our project was to test the Windows 2000 server and the Linux Red Hat 7.1 operating systems for stability and reliability, using an isolated subnet. The subnet was configured using four PCs. The first machine was configured as a server to boot the Windows 2000 Server and Linux Red Hat 7.1 operating systems. The second PC was configured to be a LINUX server and the other two machines were configured to be windows 98 clients. The clients were used to test the various features that were installed on the on the servers. Some of the features installed and tested on the servers were Domain Name Services and Routing. The Windows 2000 server was configured to be a Domain Controller and Active Directory, enabled to test the latest securities and scalability features of Windows 2000. This machine was also configured to be a DNS server and a Router. DNS servers are used to maintain records for domains they host and respond to queries for a given host name with the IP address stored in the DNS database for that host. This machine was also configured to be a router to link our subnet to the Lawrence Berkeley Laboratory Network. The design and building of subnets are important for maintaining large efficient networks, of which the current largest network being the Internet. In conclusion we found the LINUX operating system to be more stable and reliable than Windows 2000 Server and thus better suited for high-end networks with greater traffic.

Coding a Water Budget Model in C++.

STEVEN CERVENY (Case Western Reserve University, Cleveland, OH 44106) PHIL MEYER (Pacific Northwest National Laboratory, Richland, WA 99352)

The near-surface water budget is useful for estimating groundwater recharge and contaminant transport from soil contamination. Solution of the time-dependent water budget under a set of simplifying simulations has been completed. This code is currently written in a combination of Fortran and MathCAD, but was desired in C++ to provide wider distribution and improve its ease of use. Other benefits include substantially quicker runtime, a standalone executable, greatly expanded graphing abilities, ability to read-in constants from file, enhanced error checking, increased modularization of code, and software evolution towards a completely command-line operated Monte Carlo simulation version. Recoding and testing was completed with sufficient time remaining to develop a Windows-based GUI (graphical user interface) yielding a professional software package that can be widely used for a broad range of implementations.

Software Version Control For Multi-Collaboration Software Project.

CHIN CHAN (Pellissippi State Technical Community College, Knoxville, TN 37933) ERNEST L. WILLIAMS JR. and DELPHY NYPAVER (Oak Ridge National Laboratory, Oak Ridge, TN 37831)

Implementing a software version control system for software application development is one of the primary objectives for the Spallation Neutron Source (SNS) Control Systems Group. In a multi-collaborative software development environment, integrating software efforts from different departments and developers from different locations is important. Failure to integrate software efforts would not only create confusion and increase development and labor costs but

would also cause project delay. Currently SNS is using Concurrent Version System (CVS) as version control, remote users are accessing the CVS repository via secure shell. However, CVS is not very user friendly since it is command-line based. The goal of this project is to implement an easy to use interface that allows the remote developers and software managers to access the CVS repository with respect to version control. By using a web based CVS, the SNS Control Systems Group is able to provide a user-friendly, convenient and secure software development environment. Developers have more flexibility and a more convenient means to safeguard, develop, debug and test new software.

Development of A XAS Utilities Resource Page Using The JavaScript Programming Language.

TIMOTHY CHEERS (Morehouse College, Atlanta, GA 30314-3773) MATTHEW LATIMER (Stanford Linear Accelerator Center, Stanford, CA 94025)

Researchers performing X-ray Absorption Spectroscopic experiments have an allotted amount of time to collect their data. Most of this time is consumed from having to convert the analyzed data from a photoelectron wave vector (k) to energy (eV) in order to collect this information. Since a k to eV calculator is not readily available, researchers must work endlessly converting the data in order to check for the various other elements that may be found in a sample. Also, the VAX software used in collecting data is incompatible with general PCs. Coding the program to allow compatibility with general PCs may suffer from too many errors. JavaScript, which is a web based programming code integrated into HTML (Hypertext Mark-Up Language), has the ability of being viewable in web browsers enabled with JavaScript software. It is possible to use the JavaScript programming code to construct an X-ray Absorption Spectroscopic Web Resource Page that would be applicable through all computers.

Using Java to Process Streams of Performance Event Data.

JENNY YJ CHUU (Las Positas College, Livermore, CA 94550) DAN GUNTER (Ernest Orlando Lawrence Berkley National Laboratory, Berkley, CA 94720)

I have participated the summer project at the Data Intensive Distributed Computing (DIDC) Group, Distributed Systems Department at NERSC, LBNL. The DIDC group has begun to develop an archive for performance monitoring data, such as application logs from NetLogger or ping and netstat data from JAMM (Java Agents for Monitoring and Management) or Enable. The DIDC group is also working on a language-independent publish/subscribe protocol to access this data that can perform real-time filtering on high-throughput streams. The main focus of my summer project is to learn Java I/O coding related to the monitoring network performance. Examples of using java.io package and the File, OutputStream, InputStream, Writer, Reader classes for stream input/output operations and processing files are described. Also demonstrate how to use java exceptions when try and catch blocks signal some particularly unusual events in the program that deserves special attention. In addition, the potential interests of this technology to the biological applications are discussed.

Modeling and Simulation of the Equilibrium Compositions of Chemical Species.

SCOTT CLARK (University of Tennessee, Knoxville, TN 37996) JUAN FERRADA (Oak Ridge National Laboratory, Oak Ridge, TN 37831)

In today's chemical industries, the costs of construction and maintenance of facilities are high. Similarly, attempts to improve production and disposal of chemicals come with high costs and safety risks. For years, chemical engineers have sought better ways to design and operate plants where chemical and physical changes take place in materials. Computer simulation has been implemented to study how chemical species are affected by condition changes that cannot be easily or safely applied in real life. Software, such as FLOW and HSC4 Chemistry 4.1, has been developed to make simulation easier. These modeling tools have been linked by an object-oriented interface. This interface is designed to model the conversion of chemical species, percentage mass flow rates, temperature and pressure modeled by FLOW into a format that can be used by HSC4 Chemistry to calculate equilibrium composition data. This new data is then converted back into a format that can be used by FLOW. In addition, Microsoft Excel has also been interfaced so that graphical representations of equilibrium compositions can easily be visualized. This new interface will help

FLOW users to have access to better chemical models at a lower cost. Thus allowing engineers a safer, more cost efficient way to study behaviors of chemical species in response to condition changes.

Exploitation of Obstacles to Increase Strength in a Highly Redundant Manipulator. *AREL CORDERO (University of Oregon, Eugene, OR 97403) WARREN DIXON (Oak Ridge National Laboratory, Oak Ridge, TN 37831)*
A highly redundant manipulator has a greater variety of motions available in the case of obstacle avoidance. Some of these cases may require long extensions of the manipulator arm, thus necessitating a stronger and larger structure. One idea for increasing the working strength, thereby reducing the necessary size of the robot is to allow contact with obstacles to provide leverage for the manipulator arm. Computer simulation provides a basis on which to study this capability. However, two limitations impeded demonstrating this constraint: the need to extend the existing simulation program to support robots with a high degree of redundancy (DOR), and to create and implement a suitable manipulator arm. The latter, involves determination of the highly non-linear forward kinematic equations and Jacobian matrix. To overcome these problems, the source code for the simulator was studied and modified to allow for arbitrary serial-linked manipulators while maintaining backward compatibility. Next, new software was developed to generalize the calculation of the forward kinematics and Jacobian. An object-oriented approach in Java was chosen. As a result, it is now trivial to create new manipulators or fine tune existing models for the simulator. With the new capabilities in place, the future goals of this project involve demonstrating new constraints and criteria to advance motion planning of an end-effector. From this, the creation of smaller, stealthier and more capable robots is facilitated.

Material Balance and Heat Transfer Calculations for 237Np Targets. *APRIL COX (Fayetteville State University, Fayetteville, NC 28301) ROBERT WHAM (Oak Ridge National Laboratory, Oak Ridge, TN 37831)*
The Department of Energy supplies NASA with long-life portable heat for use in remote locations such as deep space. To perform this task DOE provides a special isotope, 238Pu produced from reactor irradiation of 237Np targets and subsequent post-irradiation chemical processing. The Radiochemical Engineering Development Center (REDC) at ORNL has been selected to carry out this project. As part of the planning studies, the REDC fabricated 237Np targets for irradiation and processed those targets to recover and purify the 238Pu. Once processing was finished, the data was analyzed using a spreadsheet format (Microsoft Excel). Material balance flow sheets were constructed for understanding product recovered, waste products, and analysis of the 236Pu impurity. The results will aide in determining future 237Np target design. Also detailed calculations of the heat transfer and temperature profiles across a neptunium oxide-aluminum target rod were performed based on calculation techniques using a previous model for a curium oxide-aluminum target rod.

Developing An SAP Web Transaction for United Way Deductions. *JUSTIN CRANSHAW (Skidmore College, Saratoga Springs, NY 12866) DAVID BROUGHTON (Oak Ridge National Laboratory, Oak Ridge, TN 37831)*
Oak Ridge National Laboratory (ORNL) currently uses the SAP enterprise system for a wide range of business and administrative applications. With the planned system upgrade to version 4.6, SAP offers additional capability in providing web-based access to system functionality. Among other advantages, such a web interface bypasses the need to have the SAP graphical user interface installed on a client's computer. Research was conducted into the various ways of developing an SAP Internet application through communication with the SAP Internet Transaction Server (ITS). After consulting with the Payroll customer, a prototype Internet Application Component (IAC) Web Transaction was created to aid in future SAP web development. This prototype, if ever put into effect, would allow ORNL employees to modify their monthly/weekly contributions to their United Way agency of choice. Under the current method, contact is needed between the employee and an SAP administrator, who manually updates the necessary information within the SAP R/3 system. Using a Web Transaction, when the employee makes changes to her United Way accounts from the web, she seamlessly passes her modifications to the ITS, which then communicates the information to SAP. The underlying SAP system then interprets and records the data, automati-

cally making a recurring deduction, which is then routed to the chosen United Way agency. SAP also returns these changes to the web for output. Not only will this method far more efficient than the manual one, it also makes the employee an active part in the distribution of her pay. This change could yield future increase in ONRL United Way contributions.

MUSTPAC. *KRISTI DRAGOO (University of Washington, Seattle, WA 98105) LAURA MS CURTIS (Pacific Northwest National Laboratory, Richland, WA 99352)*
MUSTPAC stands for Medical UltraSound Three-dimensional, Portable with Advanced Communications. The MUSTPAC system was designed to expand ultrasound data into a 3-dimensional image, which can be transmitted to another location for diagnosis. Any ultrasound technician that has knowledge of basic anatomy can use the MUSTPAC system. It is entailed of attaching the MUSTPAC system to any standard ultrasound machine, sweeping the probe over the area to be scanned, and the MUSTPAC system will produce a three-dimensional image that can be stored on the system. This scan can then be transmitted to another location anywhere in the world in a matter of minutes for diagnosis purposes. This summer, I performed various tests on the MUSTPAC system as well as prepared the data to submit for FDA 510(k) approval. My tests included, calculating the percentage error from the image produced by the MUSTPAC system. I did this by scanning a calibration phantom, took measurements from the 3-dimensional image produced and compared the measurement to what the actual figure should have been. My data came out to have a percentage error of less than 5% in each category. In addition, I wrote supporting documents that included a flowchart and hardware outline. I also designed and implemented the creation of the MUSTPAC web page by using the program Macromedia Dreamweaver 4. The web page consists of MUSTPAC's general information, its history and current trial runs, as well as a short movie that shows how MUSTPAC works. This web page will be available to our clients as well as the general public at http://aims.pnl.gov:2080/mustpac/.

A Program for Analysis of Similarity Tables Generated by ARB for Use in Microbial Genomic Analysis. *ROSHITHA DUNSTAN (Washington University, Saint Louis, MO 63105) JIZHONG ZHOU (Oak Ridge National Laboratory, Oak Ridge, TN 37831)*
In today's world of high-speed sequencing, analysis of genomic information can take longer than the initial sequencing. It is due to this fact that researchers have been relying on computers for high-speed data analysis. In some cases, they have written their own programs to accomplish this task (i.e. Phrap). In microbial genomics, it is sometimes necessary to compare the similarity of the genomic sequence of different clones or organisms. While programs such as ARB will do such analysis, the resulting data can be enormous. ARB will create a similarity matrix showing the percentage match (of bases) between the organisms. The creation of groups of organisms that are 95 percent alike, for example, can be extremely tedious. In a "group", each member must match every other organism in the group by at least the filter value (i.e. 95 percent). In matrices with few members (20-40) this is not a very large problem. However, when there are 400-500 different members, this analysis can take hours or days. In order to solve this problem, a program was developed using the C++ programming language on a Unix platform. Instead of taking hours to analyze a data set, analysis can be done in minutes. Due to the nature of the coding, it is very easily portable to other platforms and has already been compiled and tested in a DOS environment.

Efficient Data Distribution Among Cluster Systems. *DOUGLAS FULLER (Iowa State University, Ames, IA 50010) STEPHEN SCOTT (Oak Ridge National Laboratory, Oak Ridge, TN 37831)*
Cluster computing has come into its own as an effective, affordable means of achieving supercomputer-class computing power. Still, practical, useful administration software has yet to become widely available. An essential part of any cluster administration software is a convenient utility for inventory and distribution of files. In large and multiple cluster environments, simple one-to-many distribution techniques are inefficient when participating network interfaces lack multicast capability. Therefore, a scalable mechanism must be devised for data transmission. Such a mechanism implies the participation of all cluster nodes in the distribution. Two methods lend themselves to this mechanism, with significantly different optimization characteristics. These methods and their probable optimization characteristics were

studied, and sample codes were produced. A test suite was then coded to study various optimization characteristics of the two methods. Optimization relative to file size, working size, and number of participating cluster nodes will be studied using this method. The study of these optimization characteristics will permit inclusion of intelligent file distribution methods in the Cluster Command and Control ("C3") suite, a cluster configuration and administration utility under development at Oak Ridge National Laboratory.

Development of collaborative software tools, to be used in conjunction with current software on the Access Grid. . NEIL GAEDE (*Kenai Peninsula College, UAA, Soldotna, AK 99669*) BOB OLSON (*Argonne National Laboratory, Argonne, IL 60439*)
The Access Grid is a relatively new concept and is still under development at the Argonne National Laboratory. Exploration is underway to determine the set of software tools that best matches the Access Grid environment. Hardware platforms are also a factor when evaluating new software tools. Microsoft PowerPoint has proven to be a simple and effective way of conducting presentations in a non-distributed environment. Conducting presentations over the access grid is another matter entirely. The Java Shared Data Toolkit, and the Java Software Development Kit were chosen to provide a solution to this challenge. Developing software applications can be done in several ways, especially on Windows systems. The objective of a code- once, run-anywhere program is easier said than done. Microsoft Visual J++ 6.0 was chosen as an IDE for the Windows portion of the project. Emacs was chosen as the "IDE" for the UNIX portion of the project. Many hours and revisions later, several applications were in operation that proved that the JDK and JSDT were indeed capable of providing an adequate solution to the problem.

Analysis, and Implementation of an Online Research Document Management System. *GIRISH GHATIKAR (California State University, Hayward, Hayward, CA 94542) JAMES MCMAHON (Ernest Orlando Lawrence Berkley National Laboratory, Berkley, CA 94720)*
The research project involves coming up with a solution for a web-based (online) document management system that lets you easily store, access, and search the Energy Efficiency Standards Groups' Research documents collected for twenty years in a secure work environment, both at micro and macro level. This also allows a designated user on any system to post and retrieve information in certain commonly used format(s). Text, scanned images, Microsoft Office documents, web links, etc. can be managed over the Web. Users have the power of the information access, ease of use, and electronic storage on the Web at their disposal. The most suitable implementation was assessed after a thorough investigation and analysis pertaining to vendors. The existing infrastructure of the division formed the crux of the problem, and thus to come up with an answer that is viable and cost effective as well. With this solution, sharing information is as easy as storing it on a hard drive of a computer, and finding it is as easy as browsing the Web, where one has the access from virtually anywhere. This becomes very important, considering the future energy analysis and comparisons based on the former research and analysis.

BaBar Database Monitoring and Java. *MICHAEL GHEBREBRHAN (Florida A&M University, Tallahassee, FL 32307) ADEYEMI ADESANYA (Stanford Linear Accelerator Center, Stanford, CA 94025)*
Knowing BaBar's database growth rate would be of use to collaborators around the world which is why a program to display the data was written. The graph displayed the size of the database in real time, plotting the size in terabytes as a function of time. Using Java, a platform-independent language suited for the Internet, a visual can be constructed allowing researchers around the world to view the growth of the databases. Java was chosen because executables written in it are platform independent requiring only its Runtime Environment. Since Java is an object-oriented language the approach used was to split important functions into classes with the top most class displaying the graph. At first, though, the solution was considered to be to write a separate application to format the data in a useable way and then have an applet call the application to run when needed and obtain the formatted data. This failed because security restrictions posed on applets prevent them from running executables over a host computer. The second and successful approach was to create objects that when fitted together produced a graph. Though a program was written to display the graph, the rigorous security,

especially in browsers, features makes it difficult to implement classes in a variety of ways. Future programs may include more detailed information of the databases such as information distribution.

Three-Dimensional Galerkin Boundary Integral Analysis for Anisotropic Elasticity. *ADAM GRIFFITH (Rice University, Houston, TX 77005) LEONARD J. GRAY (Oak Ridge National Laboratory, Oak Ridge, TN 37831)*
Elastic analysis using the Boundary Integral Method requires treating the integral equations for surface displacement and surface traction. The primary requirement in the numerical implementation is correct evaluation of the singular (displacement equation) and hypersingular (traction equation) integrals. For anisotropic materials, the singular integration is further complicated by the fact that the Green's function is not known in closed form. A boundary integral code implementing a Galerkin approximation of the anisotropic displacement equation has been developed. The integrals are evaluated numerically for the non-singular case and by a combination of analytic and numeric integration for the singular contributions. The singular integrals are defined in terms of a limit-to-boundary, which, by choosing the limit direction appropriately, can be carried out. Symbolic computation is employed to significantly ease the algebraic work required to develop the appropriate analytic integration formulas. The traction equation is essential for the very important topic of fracture analysis, and the extension of these techniques to treat the more difficult hypersingular integrations appears to be feasible. This is currently being investigated.

Parallel MPEG Playback Using a Scalable Display Wall System. *CRAIG GRUBE (Purdue University, West Lafayette, In 47906) SCOTT KLASKY (Princeton Plasma Physics Laboratory, Princeton, NJ 08543)*
The Princeton Plasma Physics Laboratory High Resolution Display Wall project utilizes commodity components to create an immersive, high quality large-format display that is competitive with custom-designed, high cost graphics machines. Currently, the display is comprised of a 3 x 3 array of LCD projectors that project onto an 8' x 15' rear-projection screen. The display wall can be controlled by a cluster of nine machines running Linux, or by one machine with three quad-headed graphics cards running Windows NT 4.0. Prior to the development of a parallel MPEG player, all videos were played on the single machine. Unfortunately, due to limitations with the bandwidth on the 32-bit PCI bus, videos often cannot be played back at their full frame rates. With synchronizing playback in the nine-machine cluster, videos may be played on the display at their full frame rates.

Design and Development of Chemical Engineering Process Simulation Software using Visual Basic. *JOSHUA HOWARD (Coahoma Community College, Clarksdale, MS 38614) JUAN FERRADA (Oak Ridge National Laboratory, Oak Ridge, TN 37831)*
Although chemical process simulation software already exists, software designers can never be complacent. Improvements and upgrades must be made continuously in order to keep customers satisfied. The chemical process simulation software currently in use runs from a DOS environment. The goal of this project is to develop new simulation software similar to the current ORNL DOS version, but run from a Windows TM environment that provides for a more user-friendly interface. Visual Basic is the tool being used to satisfy this goal. There are several Phases in developing this new software. Phase I allows the user to view a form, drag, drop, and connect icons onto the form. This phase has been completed. The second phase should allow the user to save the icons and connecting lines and load them in the same position in which they were saved. The second phase should also allow the execution of a chemical process. Phase II is now under construction. Icons can successfully be saved and opened in the correct positions. Although this software is yet in the early stages of development, it shows promise as a powerful tool for the future.

Monitoring of the data acquisition of BaBar to search for sources of dead time problems. *ANNA HURST (Union College, Schenectady, NY 12308) STEFFEN LUITZ (Stanford Linear Accelerator Center, Stanford, CA 94025)*
There is sometimes unexplained dead time in the data acquisition system of BaBar. It is important to identify the source of this dead time in order to eliminate the problem and avoid loss of data. Some areas of the data acquisition system are already well monitored, but one area

that is not is the logging manager. Two programs were developed using Portable Channel Access (PCA). One monitored the amount of network traffic entering and leaving the logging manager. The other monitored the status of the logging manager. Preliminary runs of the programs showed that they could run for periods of several days without crashing and that the results they gave corresponded with the same data retrieved with other system monitoring methods. At this time, no unexplained dead time has occurred and therefore no conclusions about the sources of the dead time can be drawn. The programs will be in continued use to search for the source should a dead time problem occur.

Computer Hardware and Software Support. *ANTHONY IGBOKWE (Bronx Community College, Bronx, NY 10458) TODD CORSA (Brookhaven National Laboratory, Upton, NY 11973)*
Today, with computer or network related applications pervading more and more of our lives at work and at home, good support infrastructure has become a major factor in many organizations. Computers break and have problems as it being used during a period of time, one way or the other there is need support and maintenance services. The PC Deskside support group in BNL provides PC hardware and software support for thousands of it's end-users. Many approaches are used to solving computer mishaps. They include defining users computing requirements, specifying appropriate computer hardware and software, identifying sources for equipment and software, ordering necessary materials, receiving and staging computer hardware and software, and installing PC hardware and software and configuring it as required.

Computer Network Guide: Topologies and Network Media Types. *TEJASKUMAR JAGANI (Hudson County Community College, Jersey City, NJ 07306) KENNETH TERRY (Brookhaven National Laboratory, Upton, NY 11973)*
Computer networking has brought the world closer than ever. About 10 years ago Internet technology was under development. Since then the Internet has become popular all over the world. At home, business, school or bank we can find computer networks everywhere now a days. The Media is a term that largely refers to the cable or wires connecting together the various computing devices that make up a LAN (Local Area Network). There are many different media types in use today in LANs. They are twisted pair, unshielded twisted pair, coaxial and fiber optic cables. There has been much improvement in media cables through out these years. They can carry signals on higher speed than before. LAN topologies define the manner in which network devices are connected. Three most common topologies exist: bus, ring and star.

Transfer of Data in a Fully Connected Network with Broadcast Trees. *MICHAEL JANSSEN (University of Northern Iowa, Cedar Falls, IA 50613) STEPHEN SCOTT (Oak Ridge National Laboratory, Oak Ridge, TN 37831)*
Cluster computing is a growing field in computer science, allowing for supercomputer-like resources at fractions of the cost of a normal supercomputer. In order to make cluster computing viable for research, tools need to be created in order to make this paradigm of computing resources work as well as it has in the past. One of the problems introduced by the cluster computing is the movement of data within the cluster. While clusters are fully connected, speed of distribution of data is still limited by the network hardware. In order to overcome this problem, techniques were developed that would increase the speed of data distribution. One technique, using a lopsided tree called a broadcast tree, is presented and discussed in detail. One implementation of a broadcast tree written in C using a client-server model over TCP was developed and tested. Basic concepts behind broadcast trees are discussed in full detail, as well as the protocol used and disclosing the implementation's successes and downfalls. Comparisons between the broadcast tree method and other methods for accomplishing the same goal including structures based on rings, normal binary trees, and conventional fan-out methods are presented. Methods that should prove to be more effective than broadcast trees are also discussed including broadcasting and multicasting. A flexible framework in C is presented, allowing the test of various methods of distribution in a fully connected network.

Using a unidirectional ring to connect several clusters, distributed control for the Harness distributed virtual machine. *SIMON KANAAN (Westminster College, New Wilmington, PA 16172) STEPHEN L. SCOTT (Oak Ridge National Laboratory, Oak Ridge, TN 37831)*
Parallel processing, the method of cutting down a large computational problem into small tasks, which are solved in parallel, is a field of increasing importance in science. Parallel processing is used to simulate real world problems such as the human genome research. Distributed computing converts single workstations into heterogeneous clusters, increasing the performance of general-purpose hardware solutions. Some of the current solutions are Parallel Virtual Machine (PVM) and Message Passing Interface (MPI). This work aims to develop a distributed control algorithm for the Harness distributed virtual machine that avoids single point (or set of points) of failure for distributed heterogeneous system architecture, which is one of the weaknesses of PVM and MPI. The distributed control needs to automatically detect and recover from faults and failures and cascaded faults and failures. The control messages will be sent in a unidirectional ring to help update the head nodes in the clusters. Nodes can be assigned or removed from this ring at any time. An algorithm already exists and I will be using the C programming language and PVM to simulate this distributed control.

Database Programming. *JASON KILSDONK (The University of Chicago, Chicago, IL 60637) THOMAS FANNING (Argonne National Laboratory, Argonne, IL 60439)*
Radionuclide release modeling for Argonne National Laboratory's Ceramic Waste Form radionuclide release modeling is being performed so that this waste form can be evaluated for acceptance into the proposed Yucca Mountain repository. In order to analyze the experimental data in a more effective manner, it is being compiled into a database. This makes comparison of tests performed under similar test conditions much easier, and values that are calculated or derived from experimental data would no longer have to be updated every time a new set of data was obtained. With an Oracle database and the SQL database language, queries on the database are made very simple. Only the necessary data is entered in the database, thus taking up the smallest amount of computer storage space possible. However, with virtual tables called views, automated calculations can be performed on the information in the database provided that it matches the programmed constraints. With the PERL DBI programming interface, information from the database can be passed to web pages so that authorized personnel can query the database and easily compare test information. Although the online database is not yet finalized, it will be very cohesive, with standard links on each page so that one can easily navigate and compare information for the same grouping of tests.

Enhancement of Data Acquisition Computer Program for Mockup Cooling Unit. *BERESFORD KIRTON III (New York City Technical College, BROOKLYN, NY 11201) HELIO TAKAI (Brookhaven National Laboratory, Upton, NY 11973)*
This project is part of the ATLAS (A Toroidal Liquid Hardon Collider ApparatuS) experiment being built at CERN. CERN is the European Organization for Nuclear Research, the world's largest particle physics center. The particular part of the project covered in this document addresses the activities in Brookhaven National Laboratory (BNL) regarding the integration issues of the liquid argon calorimeter front-end electronics. The mechanical setup in BNL is a mockup of one of the ends of the Barrel Electromagnetic Cryostat. The mechanical assembly will be used to evaluate space problems for cable routing, sensors positioning, power cable positioning, and ease of use and maintenance. The electronics performance is the important part of this project. An important aspect of the ATLAS project is the evaluation of the electronics being built for the liquid argon calorimeter. We will make use of the mockup at BNL to run a series of tests on several electronics boards being built by other ATLAS institutions. For this purpose we will assemble a small data acquisition system. The DAQ is comprised of a personal computer, VME crates, CAMAC crates and custom electronics in ATLAS liquid argon board sizes. My project is to update and enhance the Data Acquisition (GENIE) Computer Program. An attempt will also be made to meliorate the Control System (Adam) and integrate a Laser Compact Vision (fault detection) Alarm System (VESDA) to these data acquisition control devices.

Construction of a Cold Fusion interface and Java Map to Improve the Presentation and Maintenance of the AmeriFlux Website.

THOMAS KOLLAR (University of Rochester, Rochester, NY 14627) TOM BODEN (Oak Ridge National Laboratory, Oak Ridge, TN 37831)

ORNL serves as the data archive for continuous measurements made by roughly 50 sites comprising the AmeriFlux network. The World Wide Web (WWW) serves as the primary means used by ORNL to make AmeriFlux data and information available to users worldwide. The primary tasks of this project were to assemble clear, informative, and easily maintainable WWW pages for sites in the AmeriFlux network and to create a map of all the AmeriFlux sites. To begin to complete the first of these tasks, a Microsoft Access database had been created to store much of the information about the AmeriFlux sites. The current project used that database to dynamically post information on the AmeriFlux website using a markup language and software provided by Cold Fusion. Because of Cold Fusion's ability to make dynamic web pages, 50 html pages could be made into one Cold Fusion page. Thus, the time needed to be spent updating and changing the web pages was reduced. Also, having one web page as opposed to 50 allowed for the easy creation of a template. Thereby, the information on the website has become clearer, more accessible, and more informative, completing the first of the tasks. To complete the second of the tasks, a dynamic map of the AmeriFlux sites was made using Java and Cold Fusion. The dynamic nature of this map allows for a more easily accessible and updateable web site.

Construction of a Wrapper Class Using the CDEV Data Structure.

BRUCE KOVALENKO (Fordham University, Bronx, NY 11367) TED D'OTTAVIO (Brookhaven National Laboratory, Upton, NY 11973)

The data transmitted from the accelerators at the laboratory is packaged and analyzed by various data structures before being distributed to the various applications. The efficiency, modifiability, and handling of the data structure are very important for faultless data transmission. The data structure that was wrapped was the Value class structure due to the cumbersome instance variable mutability of the Value class instance variables. The CDEV data structure was utilized as a data member of the Value class to allow for easier access to class instances after initial instantiation using the Value class constructor. The project consisted of two phases. In phase one, the methods of the Value class were searched through out the VOBS(versioned object bases) database to figure out which methods were used. This phase required the use of some text processing programs written in C++. The second phase consisted of writing the methods for the new and modified Value class using an instance of the CDEV class data member.

Characterizing Beam Losses and Irradiation of Beam Line Components for SLAC Experiment E158.

JUANITA LEE (North Carolina Agricultural and Technical State University, Greensboro, NC 27411) MIKE WOODS (Stanford Linear Accelerator Center, Stanford, CA 94025)

Experiment E158 will make the first measurement of parity violation in Moller scattering. The experiment is a fixed target experiment in End Station A. The experiment operates with very intense electron beams and is attempting to measure a small (10-7) physics asymmetry. It is important to minimize beam losses and this paper makes a study of such losses in a recent engineering run. Some recommendations are made for preparing for the physics run in 2002.

Database Design for the Stabilization/Solidification of Wastes Using Microsoft Access 2000.

TRACY LOFTIS (Tennessee Technological University, Cookeville, TN 38505) ROGER SPENCE (Oak Ridge National Laboratory, Oak Ridge, TN 37831)

Experimental data on the stabilization/solidification of wastes is abundantly available but unorganized. There are various waste compositions and, in turn, various treatments. Organization of data is a key factor in reducing the amount of time and money involved in research. Currently, an individual wanting to obtain information on the stabilization and solidification of waste must perform literature searches either electronically or manually and then decipher the information given. With the aid of a database development tool such as Microsoft Access this data can be organized in a logical and useful manner. The hopes are that this database will someday be obtainable electronically. Therefore, generators having a particular composition of waste will see at a glance what has worked, and failed, for others. These individuals may choose to analyze this data using statistical controls, which will aid in their decision of an optimal approach for treatment.

Connectivity Detection and Routing in Wireless and Wireline Networks.

ARUL MANICKAM (Carnegie Mellon University, Pittsburgh, PA 15213) NAGESWARA S. V. RAO (Oak Ridge National Laboratory, Oak Ridge, TN 37831)

This project deals with the implementation and testing of networking modules that enable message transport between the nodes of ad hoc networks consisting of wireless mobile and wireline units. The design involves the detection of single and multiple hop connectivity and also the transport level routing of the messages. Three components have been implemented and tested. First, the setup modules detect the immediate neighboring nodes in an ad hoc network consisting of wireless mobile and wireline nodes. Second, the path computation modules compute shortest paths from a source node to all reachable destinations via single and multiple hops. Third, routing modules transport messages between various nodes and are developed for two scenarios. For the static scenario, messages are routed via the network nodes without buffering. In the dynamic case, messages are suitably buffered to account for the changes in connectivity, i.e. messages are buffered at intermediate nodes for specified amounts of time if the destination is not reachable. The modules are implemented in C programming language using the sockets interface under Linux operating system.

An Individual Based Model for a Tall Grass Prairie Containing Oil Wells.

BRIAN MASKARINEC (University of Georgia, Athens, GA 30609) YETTA JAGER (Oak Ridge National Laboratory, Oak Ridge, TN 37831)

The need and understanding of how to take care of the planet is an issue of importance to us all. One way to predict how certain actions will affect a habitat is through computer simulation. For our program we are choosing to simulate a grassland prairie in Oklahoma that contains several oil wells. Using the data collected over the past 10 years about this certain prairie, such as species of flora and fauna living there, information about the oil equipment such as failure rate, and other occurrences like fire we are able to create a computer program this particular prairie for future possibilities. This allows us to see what will happen to the prairie if nothing more was done, more wells were added, or if clean up was attempted.

Adapting a Nonlinear Equation Solver to Scale the Residual Functions Dynamically.

MEGAN MCCLEAN (University of California, Berkeley, Berkeley, CA 94709) DAVID LORENZETTI (Ernest Orlando Lawrence Berkley National Laboratory, Berkley, CA 94720)

Newton-Raphson is an iterative method for solving nonlinear problems. It begins with an initial guess at the solution, and then generates a sequence of points that step increasingly close to the real solution. When the initial guess is far from the solution, the Newton-Raphson method may diverge. Descent methods are used to control divergence. A descent method requires that each step reduce some measure of residual magnitude, commonly the sum of the squared residuals. Preliminary numerical tests show that the global convergence of the Newton-Raphson method can be improved by weighting the residuals with weights that incorporate sufficient information from the residual models at each iteration. The goal of our research was to reproduce these results by modifying an existing nonlinear equation solver to dynamically scale the residuals using the five weighting formulas employed in the previous study. We modified TENSOLVE to update the weights for the residual functions at each iteration. The algorithm was tested on 14 problems, with and without the weighting. Weighting the residuals neither improved the number of problems solved, nor decreased the number of Jacobian evaluations required to solve problems. Our results are inconsistent with those of the previous study. The previous study showed a reduction in the number of Jacobian evaluations for all five weighting formulas, and an increase in the number of problems solved successfully for four of the five weighing formulas. Future research will investigate why results from the previous study, and our study using the modified TENSOLVE algorithm, do not agree.

Columbia River Recreational Survey 2001: Human Health Risk Assessment. *FRANCES MELENDEZ (Columbia Basin College, Richland, WA 99352) AMORET BUNN (Pacific Northwest National Laboratory, Richland, WA 99352)*

The United States Department of Energy (DOE) has become concerned about the environment and resultant effect on human health near the Columbia River. DOE scientists have relied on the principles of risk assessment in their evaluation of its surroundings and the affects on individual and community health. One way to help evaluate their concerns for the environment is by collecting information using recreational surveys. The aims of these surveys are to help describe the potential threat that toxic contaminants may have on both the environment and human health. Remedial solutions, such as facilitating future clean up and the prevention of toxic contaminants from affecting the Columbia River, can be maintained using the risk-based information form these surveys.

Network-Enabled Automatic Differentiation. *SHANNON MELFI (University of Illinois, Urbana-Champaign, Urbana-Champaign, IL 61801) BOYANA NORRIS (Argonne National Laboratory, Argonne, IL 60439)*

Computer code can often be effectively thought of as a mathematical function. And, like any mathematical function, computer code can be differentiated. ADIC, a system developed in the MCS division at Argonne National Laboratory, automatically generates derivative codes for computing the first and second derivatives. The creation of the ADIC Application Server provides access to the benefits of automatic differentiation through the World Wide Web. Users of the server can upload ANSI-C code, manage files remotely, apply ADIC to selected functions, make use of advanced options using control scripts generated with user specifications, and download derivative codes. Soon, users will also be able to save time by using an automated driver generator instead of writing their own.

PHENIX Web Communicator: Design and Function. *HILARY MERCER (Cumberland University, Lebanon, TN 37087) BRANT JOHNSON (Brookhaven National Laboratory, Upton, NY 11973)*

The PHENIX Web Communicator is intended to provide a better way to interact with information in various databases. The PHENIX Web Communicator will help keep the collaborators up to date. To get the project started PHENIX information was worked on first. This included participant documents: Analysis Notes, Draft Physics Papers, Draft Technical Papers and Internal Talks. Other categories available to the general public, which include International Talks, National Meeting Talks, Physics Papers, Technical Notes, Technical Papers, Conference Proceedings, Workshop and Review Talks and Colloquia and Seminars. The PHENIX Web Communicator is a highly anticipated way to interact with databases. It will be able to help with processing new employees, keep up with when they are on-site, and when they are at their home institution and what their home institution is. The PHENIX Web Communicator is based on Perl scripts, which create an html file on the fly. This makes it very easy to have one main file that calls other files, instead of having many different files to create one html page.

Modeling the Escherichia coli Bacteria cell in a virtual interactive environment. *ALYSSA MIGRALA (Elmhurst College, Elmhurst, IL 60106) MIKE PAPKA (Argonne National Laboratory, Argonne, IL 60439)*

Rendering the e.coli cell in a virtual environment where one can interact with it for scientific study is critical to understanding the impact of this bacterium and can only aid in finding its complete prevention and cure as well as more of an understanding of bacteria in general. Detailed and attentive modeling requires a comprehensive knowledge of the anatomy of the cell and the various components that contribute to its growth and reproduction. Once a full understanding of the biology is obtained, a graphics program with sufficient memory is required to hold the textures and mapping that is required of a biological specimen. Detail of vast proportions outweighs any attempt at reducing memory space because of the experimentation that may be required of it and the advantage of realistic models. Transport of cell model into the virtual environment poses problems of an interesting kind. To get accuracy in the portrayal, we must add to our cell incredible detail and information. This than is interpreted in its literal form in the virtual environment, which means that all polygonal "extras" are inferred in that environment as literals which ends up looking

jagged and course. After some analysis the author is impressed with results from various mathematical algorithms that present themselves to be more in sync with nature itself.

Upgrading the Framework for Risk Analysis in Multimedia Environmental Systems (FRAMES). *JEANNE NOWLIN (Big Bend Community College, Moses Lake, WA 98837) MITCHELL PELTON (Pacific Northwest National Laboratory, Richland, WA 99352)*

The U.S. Department of Energy (DOE) and the U.S. Environmental Protection Agency (EPA) have regulatory programs pertaining to potential-risk environmental contaminants. They demand sound scientific methods of performing in-depth assessments over a variety of conditions. Many computer tools being similar, DOE and EPA logically concluded to collaborate in the development of computer applications that could mesh their software and experience towards standardization. Early efforts were difficult to modify and were concerned with a single medium. Battelle staff at Pacific Northwest National Laboratory (PNNL) undertook the challenge to create a platform that would allow users to input data in their own format and to link that data to other modules (such as receptors), and thus came about Framework for Risk Analysis in Multimedia Environmental Systems (FRAMES). FRAMES has a user-friendly interface. It deals only with how data is transferred between modules and, therefore, the user can track contaminants through different media of the environment and view textually or graphically the results of exposure in time and concentration as well as human health risks. FRAMES utilizes established stand-alone programs such as Multimedia Environmental Pollutant Assessment System (MEPAS), a physics-based modeler. Its numerous versions demonstrate the necessity of any computer application to either undergo constant upgrading or become obsolete, as well as reflecting sensitivity to user feedback and requirements. FRAMES is presently undergoing tremendous coding changes that will radically alter the way it handles information, as well as opening itself to a broader spectrum of users.

Simulating Reality Using OpenGL. *MICHAEL PAGLIOROLA (Rutgers University, New Brunswick, NJ 08854) SCOTT KLASKY (Princeton Plasma Physics Laboratory, Princeton, NJ 08543)*

As part of the visualization department of the Computational Plasma Physics Group of Princeton Plasma Physics Laboratory, working under Scott Klasky, Ph. D. my task was to create a virtual walkthrough of the National Spherical Torus Experiment (NSTX) for use on the high-resolution display wall. The original idea for this was to create a walkthrough using pure OpenGL computer code and modeling each object in the room in order to make it seem like one is actually in the real test cell room. However, a better solution was found using the Unreal Tournament game engine, which utilizes OpenGL to render its objects. By using the editing software and partial source code that comes packaged with Unreal Tournament an immersive walkthrough is being constructed with greater detail, in less time, and with more elements of the real world.

Document Control and Records Management - Collaboration among six laboratories. *TOSCHA PEYTON (Robeson Community College, Lumberton, NC 28358) BECKY LAWSON (Oak Ridge National Laboratory, Oak Ridge, TN 37831)*

The Document Control and Records Management (DCRM) Program is integral to the successful construction of the Spallation Neutron Source Project (SNS). The SNS is an accelerator-based neutron source, a one-of-a-kind facility. The SNS is being built by a partnership of six DOE laboratories, Arogonne, Brookhaven, Lawrence Berkeley, Los Alamos, and Oak Ridge and Thomas Jefferson National Accelerator Facility. The research site will be located on the Oak Ridge Reservation in Tennessee. While the DCRM group is responsible for providing comprehensive and compliant records management and document control support as well as guidance for the project, the SNS Document Control Center (DCC) serves as the central archive for the project's record documentation and is tasked with ensuring that SNS documentation is captured and managed to provide long term accessibility. The two web-based systems that support this effect are the Information Manager (iMAN), a Product Data Management (PDM) tool by Unigraphics, and the Engineering Design and Information System (EDIS), an in house developed system which issues and tracks document and drawing number schemes. The iMAN system ensures access to the latest released/approved version of project documenta-

tion and provides a central location for storing and managing released/approved documentation in a variety of electronic formats. Support provided by iMAN and EDIS will be discussed.

AN INTEGRATED MODELING SYSTEM TO STUDY THE IMPACTS OF CLIMATE VARIABILITY ON WATER RESOURCES IN THE SAN JOAQUIN BASIN, CALIFORNIA. *PALLAVI RAMARAJU (Contra Costa College, San Pablo, CA 94806) NIGEL W.T. QUINN (Ernest Orlando Lawrence Berkley National Laboratory, Berkley, CA 94720)*
Water resource planners need to develop contingency plans to deal with the potential impacts of climate variability and changes in the frequency and magnitude of extreme weather events in the San Joaquin Basin. Studies suggest that warmer winter storms, earlier runoff from the Sierra snow pack, and reduced summertime flow in the tributary streams could adversely affect the water supply, water quality and agriculture production. Planning studies involving suites of complex mathematical models are often compromised owing to the inordinate amount of time devoted to data processing as the output from model is manipulated to become the input to the next in sequence. Hence the objective of this research is to develop an integrated modeling system using Object User Interface (OUI), a software package developed by the U.S. Geological Survey. OUI, a map based interface, provides an environment for efficient database/model integration, aids in map-based communication with databases, and offers controls for model execution. OUI also has tools that provide for the graphical and statistical analysis of the results. Successful linkages of various water resource management models, newly developed within State and Federal water agencies can assist in the management of water quality, water supply and agriculture production in the San Joaquin Basin and Bay-Delta. The model system will also aid analysts in performing vulnerability analysis and suggesting management strategies for mitigating the impacts of increased climate variability and more frequent extreme weather conditions hence reducing the vulnerability of the existing system to permanent damage.

Remote Sensing and Circulation Modeling: Willapa Bay, WA. *BENJAMIN ROONEY (Central Washington University, Ellensburg, WA 98926) KAREN STEINMAUS (Pacific Northwest National Laboratory, Richland, WA 99352)*
The purpose of this study is to investigate the coupling of high resolution remotely sensed images with circulation and transport modeling in the marine environment. The transport of carbon-containing material from the river environment to the coastal environment may be a critical component of Earth's carbon cycle and may also be significantly impacted by subtle long-term changes in the regional climate.

Interactive Volume Rendering on Standard PC Graphics Hardware using Multi-Textures and Multi-Stage Rasterization on Linux. *TETSUYA SAKASHITA (University of Illinois, Urbana-Champaign, Urbana Champaign, IL 601820) MIKE PAPKA (Argonne National Laboratory, Argonne, IL 60439)*
The work done in this paper is largely due to the work of C. Rezk-Salama, K. Engel, M. Bauer, G. Greiner and T. Ertl. Their paper Interactive Volume Rendering on Standard PC Graphics Hardware using Multi-Texturing and Multi-Stage Rasterization was the basis for this work. We will elaborate their algorithm in detail and methods for interactive volume rendering. Their algorithm exploits NVidia's Geforce graphics processors and the performance is comparable to high-end graphics workstations. The Linux version of the volume render was created for its use in the Active Mural, which is a high-resolution tile display.

Security on the Web. *BARBARA SIMON (Suffolk County Community College, Upton, NY 11973) KEITH LALLY (Brookhaven National Laboratory, Upton, NY 11973)*
Web Security is a major concern for any company or organization that has a network system. Systems and software have many known vulnerabilities that can be exploited by hackers. It is important for a system administrator to be extremely familiar with the utilities, tools, and methods a hacker uses to infiltrate a network. In fact, these same methods are used to test a system for weaknesses in order to prevent a hacker from gaining access to it. System administrators must constantly keep abreast of software patches, fixes and bug notifications. The network traffic must also be constantly monitored to detect

suspicious activity. A well-trained staff and the proper tools are essential for this process. By eliminating holes that allow unrestricted access to and from the Internet, the perimeter's ability to screen or conceal the internal resources is restored, maintaining the integrity of the physical network, the network software, any other network resources, and the organization's reputation. The organization's internal resources are blocked from the general public and only accessible to the organization's associates. Network strategies of the internal and external pages of the site are very important to prevent exposing internal information to the outside, while not restricting the open scientific environment where the free exchange of ideas is encouraged.

Investigation of Self-Organized Criticality in Packet-Based Communications Networks. *NATHANIEL SIZEMORE (Westminster College, New Wilmington, PA 16172-0001) VICKIE E. LYNCH (Oak Ridge National Laboratory, Oak Ridge, TN 37831)*
A system is governed by self-organized criticality if it is a driven system that self-organizes to be close to some critical point. Communication systems have been shown to have a critical point where the system goes from continuous flow of information to a jammed state. Here we have examined the possibility of self-organization as a competition between information demand and congestion control. An object-oriented computer simulation was written in C++ to examine the self-organization properties in packet-based communication networks. Various congestion control methods were examined after confirming previously published results that did not include these methods. These included a simplified choke packet technique, congested signaling, backpressure, and dropping packets. Impacts of these schemes on self-organization were compared using a variety of diagnostics including throughput, average time traveled by packets, and probability distribution functions from time and distance traveled by packets. Studying the properties of self-organization can help better understand the macroscopic trends and properties such as throughput in large packet-based networks ranging from corporate LANs and WANs to the global Internet.

Computer Modeling of Belief Formation. *JAMES SLOUGHTER (Gonzaga University, Spokane, WA 99258) A. LYNN FRANKLIN (Pacific Northwest National Laboratory, Richland, WA 99352)*
The theory of explanatory coherence as put forth by Paul Thagard has the potential to be widened in scope so as to be useful as a predictor of public opinion and response. A computer model of the theory, similar in function to Thagard's ECHO program, was begun with the potential to be modified to allow for additional factors unaccounted for in Thagard's model. The scope of who could be modeled was expanded. Plans were made to model factors such as existing biases, order of information presentation, and emphasis of information. Strategies were developed to isolate the influences of individual propositions within a belief system. Once completed, the new program could be a useful tool in predicting public response to information without needing to present the information to the public. This could allow for improved public relations, and could provide a means for the user to be more immediately responsive to the public's needs and concerns.

Design of an Orbit Control Graphic User Interface in MATLAB. *SABRINA TURNER (University of Maryland, Baltimore County, Baltimore, MD 21250) JEFF CORBETT (Stanford Linear Accelerator Center, Stanford, CA 94025)*
The research done by the SSRL part of SLAC deals with the radiation produced by the electrons that are traveling in the storage ring SPEAR. SPEAR is a large electron storage ring that is 234 meters in circumference. This electron beam needs to be steered somehow. So, as the electron beam travels along the ring, Beam Position Monitors (BPMs) detect the position of the beam and Corrector Magnets are used to deflect the beam so it travels in a circle around the ring. When the electron beam makes contact with a magnet, the electron beam emits high-frequency radiation that turns out to be quite useful for scientific purposes. The intense x-ray radiation can be used by chemists, biologists, geologists and other scientists to x-ray materials. Currently there is a program written in FORTRAN that controls the electron beam. A new program had been written in MATLAB to control the electron. This software has many advantages over the older program including a graphical user interface to control the position of the

electron beam. The graphical interface and linear algebra behind it will make it easier for the scientists using the beam to do their research. In order to make this program efficient, flow charts were made for all of the functions and function calls in the program so that multiple unnecessary calls to a function are not made. The graphic user interface was re-worked and additional functional graphical elements were added.

The New Linux Image Distribution Software for the RHIC Computing Facility. *THERON WEIMER (Iowa State University, Ames, IA 50010) ANTONIO CHAN (Brookhaven National Laboratory, Upton, NY 11973)*

In this paper we describe a new Linux image distribution system for the RHIC Computing Facility (RCF) that works well with hundreds of computers. The basis for the image distribution system is a software package called SystemImager. Both the old and new systems are described, including benefits and drawbacks of each. A description of the testing procedure and the difficulties overcome during implementation of the new software system is also given.

Visualization of Rocket Thruster Models and Experiments. *KATHERINE WHITE (University of Tennessee, Knoxville, Knoxville, TN 37916) MARK D. CARTER (Oak Ridge National Laboratory, Oak Ridge, TN 37831)*

Visualization is an important factor in the use of computer codes to model scientific experiments. The EMIR codes are used to model the mini-RFTF experiment at ORNL that is used to test ion propulsion for NASA's Variable Specific Impulse Magnetoplasma Rocket. IBM Data Explorer provides an effective way to check the correctness of the models and to analyze information provided by the codes. A Fortran module was written to put the output of these codes into native Data Explorer format. The module contains several subroutines that are used to output different types of data including scalars, vectors, and complex fields. The module converts data into a binary format, using less memory than that of an ASCII or text file. Data explorer networks and macros were developed to read and visualize the data using the isosurface, glyph, and plot modules. IBM Data Explorer was found to be a worthwhile open source software package and documentation was created to enable future users to learn to use the Fortran module and Data Explorer applications.

Software to Detect Interactive Traffic in Real-time. *ALEXANDER WITHERS (Gonzaga University, Spokane, WA 99258) LIZ FAULTERSACK (Idaho National Engineering and Environmental Laboratory, Idaho Falls, ID 83415)*

One of the goals of Intrusion Detection systems is to find backdoors being placed on systems or previously placed backdoors. The usual method for finding these backdoors is to look at the content of the traffic. A paper recently published by V. Paxson and Y. Zhang entitled "Detecting Backdoors" lays out some general algorithms for determining if traffic is interactive. Software was written that implements these algorithms as a Snort preprocessor. The software can be used to find backdoors by looking at TCP connections that are both interactive and uncharacteristic of the network.

Development of an Automated Microfluidic System for DNA Collection, Amplification, and Detection. *BRIAN YOXALL (Harvey Mudd College, Claremont, CA 91711) CINDY BRUCKNER-LEA (Pacific Northwest National Laboratory, Richland, WA 99352)*

The project was focused on developing and testing software for an automated Pathogen Detection System. The Pathogen Detection System has three primary components. The cell concentration component captures bacterial cells onto magnetic beads. The cell lysis and DNA amplification component consists of a temperature-controlled chamber for lysing cells (during heating) and amplifying DNA using polymerase chain reaction (PCR) or strand displacement amplification (SDA). The DNA detection component consists of laser induced florescence detection. The three components create a flexible platform that can be used for pathogen detection in liquid samples, in applications from health monitoring to laboratory research. Recent development of the system has included creating software for controlling the components and developing procedures to automate processes on the system. Software was created in "C" using Labwindows/CVI from National Instruments and provides independent process strings to prevent data loss and instrument interference. Additionally, it is easily adaptable to different types of instruments and different component configurations, and it provides real-time data output in graphs and

numbers. Future developments of the system will include on-line DNA detection during DNA amplification and improved capture and release methods for the magnetic beads during cell concentration.

Creating a High Speed Subnet Behind Firewalls. *CHAKAMEH ZAHEDKARGARAN (Contra Costa College, San Pablo, CA 94806) EVERETT HARVEY (Ernest Orlando Lawrence Berkley National Laboratory, Berkley, CA 94720)*

The recent surge of viruses and hacker attacks has increased the necessity for making the computers at Lawrence Berkeley lab more secure. The goal of my group was to design and implement a firewall scheme that improves the system security. For this purpose we chose to use both Linux and Windows 2000 server operating systems. Since our experiment had to be isolated from the LBL domain, we created our own private subnet. We configured both a Linux and a Windows 2000 machine to serve as a DNS (Domain Name System) server and a router and later we implemented our firewall scheme on them. However, the Linux operating system was preferred for this project because of its flexibility and the unlimited authority it provides for the administrator. The Domain Name Services (DNS) is a distributed Internet directory service. DNS is used mostly to translate between domain names and IP addresses, and to control Internet email delivery. If DNS fails, web sites cannot be located and email delivery stalls. A routing configuration allows the packages from the Local Area Network (LAN) to be forwarded to the Internet depending on the firewall permissions. To enable routing and firewalls on Linux machine, I updated and recompiled the kernel with the packet filtering and routing options enabled. Then I wrote a script of appropriate IPCHAINS commands that contains the permission and denial of package forwarding between different domains and ports, and create barriers in order to prevent unauthorized access to our network.

Peoplesoft Financial Development. *NIKUNJ ZALAVADIA (Hudson County Community College, Jersey City, NJ 07306) GREGORY MACK (Brookhaven National Laboratory, Upton, NY 11973)*

All of Brookhaven National Laboratory's departments require Budget Reports. These reports are extremely valuable to the lab, as they exhibit the current state of funding allocation. After analyzing these reports, business office personnel are able to advise Principle Investigators, whom are responsible for the distribution of funding. Since these reports are crucial, there is a continuous demand for these reports to provide more powerful methods of data selection, manipulation, and presentation. BNL's budget data is managed by an Oracle RDBMS (Relational DataBase Management System), which end-users interface with through PeopleSoft, a popular business application. The lab's Business System Division has developed a budgeting system using Peoplesoft, which consists of three major components: budget execution, budget submission, and personnel forecasting. These components are divided into many complex units of allocation, some hierarchical, others independently related. SQR (Structured Query Report Writer) is Peoplesoft's chosen programming language for generating reports. In addition to printing reports on paper, SQR can be used to generate delimited flat files, which Microsoft Excel is able to convert into spreadsheets. These spreadsheets are used for manual data manipulation. My assignment has been to modify the output of existing reports. This was accomplished by using Peoplesoft's Query Tool, to rapidly generate SQL (Structured Query Report Language) and then import the code into SQR programs, thereby altering the selected data. After this, the code necessary to generate the aforementioned spreadsheets had to be written.

ENGINEERING

Realizing a Biorefinery by Expanding the Sugar Platform: Monosaccharide Separation. *PAUL ALBERTUS (University of Michigan, Ann Arbor, MI 48109) KEITH NEEVES (National Renewable Energy Laboratory, Golden, CO 80401)*

The development of a biorefinery'a plant fed only by biomass and capable of producing multiple products, from fuels to plastics to pharmaceuticals represents an important step toward the transformation to a sustainable society. The monosaccharides of biomass, glucose, xylose, mannose, galactose, and arabinose may serve as the basis for a renewable chemicals industry. In order to take advantage of each monosaccharide's unique structure they must be separated from each other and the other components of biomass. Simulated moving bed (SMB) chromatography is one method for industrial scale

sugar separations. Its complexity requires that a computer model be used to predict flow rates and switching times. Therefore, batch chromatography was used to determine the values of the parameters needed to construct a computer model of a SMB system. Pure component isotherms for each of the five monosaccharides at various concentrations, and competitive isotherms, in which multiple monosaccharides were included in a single pulse, were gathered. Flow rate and column length was varied to determine their effect on elution profiles. From these isotherms, it was clear that for monosaccharide concentrations similar to that from a slipstream of hydrolysate from a bioethanol process, elution time is independent of monosaccharide concentration and the presence of multiple monosaccharides. Increasing residence time only modestly improved the separation. The computer model generates theoretical elution profiles that can be matched to the experimental ones by varying flow parameters. The correct parameters will be used by the model to aid in a full-scale experimental verification of the separation.

Evaluation of the EMI Heat Pump Water Heater impact on the residential climate control system.

GUSTAVO ARAMAYO (Iowa State University, Ames, IA 50013) JJ TOMLINSON (Oak Ridge National Laboratory, Oak Ridge, TN 37831)
Rather than strictly using electric energy, a heat pump water heater utilizes the ambient heat, producing hot water and cooled, dehumidified air. By utilizing ambient heat, the heat pump water heater requires much less energy than the conventional electric resistance water heater. However, since the evaporator of the heat pump relies on ambient heat to function, the overall performance of the unit depends on its location, namely if in a conditioned (such as a closet) or unconditioned (such as a garage) environment. To evaluate the overall impact of a heat pump water heater's location, an experiment was set up and is being conducted in an unoccupied house near Oak Ridge. An actuated valve was placed in the hot water line and programmed to regularly make water draws similar to those of a typical family. Sensors were placed on and around the water heater to determine the impact of the heat pump water heater on the heating and cooling loads of the house. Data was gathered to characterize the room the unit was located in as well as the water heater's performance itself. From this data, an assessment of the impact of the heat pump water heater on the space conditioning loads was performed.

Cascading of Ansoft High Frequency Structure Simulator S-matrices.

ERIN AYLWARD (Harvard University, Cambridge, MA 02138) VALERY DOLGASHEV (Stanford Linear Accelerator Center, Stanford, CA 94025)
Design of modern microwave networks and junctions includes extensive use of sophisticated computer simulations. Although some networks or junctions are too complex for direct computer simulation in their entirety, they can be decomposed into simpler subcomponents. Modeling of the entire system can then be reconstructed by cascading S-matrices obtained from the subcomponent simulations. High Frequency Structure Simulator (HFSS) is a commercial program by Ansoft that can be used to characterize passive microwave devices. It uses the finite element method and advanced techniques such as automatic adaptive mesh generation and refinement to calculate S-parameters and full-wave fields for arbitrarily shaped 3D passive structures. Subcomponent models of wave guide pieces containing inductive irises and also subcomponent models of cells of linear accelerator structures were modeled in HFSS. The software calculated their S-parameters. Then the S-matrix of a larger network built form these subcomponent S-matrices was computed. This was accomplished by performing scattering matrix cascading on the subcomponent S-matrices. It was found that the S-matrix of a network, which was virtually built from coupled subcomponents modeled by HFSS, could be accurately calculated this way and was representative of the entire network.

Microsorption Systems for CO_2 Capture and Compression.

DUSTIN CALDWELL (Washington State University, Pullman, WA 99163) SCOT RASSAT (Pacific Northwest National Laboratory, Richland, WA 99352)
CO_2 adsorption (a solid sorbent media) and absorption (a liquid sorbent media) are both standard gas purification methods used today in industry. By utilizing microtechnology to improve mass transport and thermal transfer these system have increased efficiency. These systems have potential uses for DOE, DOD, NASA and industry. NASA applications include CO_2 collection and compression for fuel processing during a Mars robotic sample return mission. Carbon management of exhaust gases from automobiles, factories, and electrical power plants are all possible applications for microsorption systems. Currently, we are designing a one-eighth scale adsorption system for the NASA Micro-ISPP project and testing a microscale absorption apparatus.

Construction of the Anode Testing Facility for the Discovery of Inert Anodes Used in Aluminum Electrolysis.

MATTHEW CASTELEIN (University of Illinois, Urbana, IL 61801) GREG KRUMDICK (Argonne National Laboratory, Argonne, IL 60439)
The production of aluminum by electrolysis is an inefficient as well as an environmentally unfriendly process due to the use of carbon anodes. These anodes break down by oxidation during electrolysis, releasing greenhouse gases and increasing energy requirements. It has been observed that anodes made of certain metal alloys form a thin outer film that protects the anodes from disintegration. The use of these alloys as anodes in aluminum electrolysis could save energy as well as eliminate greenhouse gas emissions due to the inert nature of the alloys with the electrolysis bath. However, further research focusing on oxidation rates at the anode surface is necessary to select the most successful anode material. Therefore, an anode testing facility has been designed and constructed to test different anode materials. Various measurement equipment has been installed and calibrated, and a data acquisition program has been written to collect data during anode testing. With the completion of the anode testing facility, the selection of an inert anode for aluminum electrolysis can now begin at Argonne.

Theoretical and computer study of electrons (both individual and in bunches) interacting with both static and dynamic electromagnetic fields.

JOHN CASTRO II (Oklahoma State University, Stillwater, OK 74075) ROMAN (Stanford Linear Accelerator Center, Stanford, CA 94025)
The purpose behind our project is to study how the energy of an electron is modulated by interactions with electric and magnetic fields, both static and dynamic. The dynamic fields that we will be concerned with are radiation fields. This is done to see if practical techniques can be developed to generate electron pulses that are in the atto-second range. The reason this can be explored now is because of the availability of low-emittance electron beams from laser driven photocathode RF guns. This technology has been developed to a sufficiently high level only within the last few years. The approach we are studying will be applicable to electron beams in linear accelerators rather than storage rings. We will simulate both the electron beams and the fields they interact with in mathematical form using the FORTRAN programming language. We will use the Lorenz Force law to describe and simulate the effects that these fields will have on an electron bunch and determine if the effects will allow the compression of sub-intervals of the electron bunch to atto-second lengths. So far, we have developed a program that defines the initial conditions for each electron in an electron pulse. These initial conditions define the coordinates of the bunch in real and momentum space. The program in its finished form will be able to completely simulate the interactions between the electrons and the fields to see if new designs for electron bunch compression are possible. If so, such designs might be implemented into future linear accelerators here at SLAC.

Cost and Performance Analysis of Evaporative Cooling Enhancement for Condensers at Empire Energy Geothermal Plant.

DAVID COSTENARO (Washington University, St. Louis, MO 63105) CHUCK KUTSCHER (National Renewable Energy Laboratory, Golden, CO 80401)
Many of today's geothermal power plants are located in arid climates. With water at a premium, air-cooled condensers are often used instead of wet-cooling towers. During the hottest times of the day, plant performance suffers as the "cold sink" (the ambient air) rises in temperature. For summer peaking utilities, these are also the times when grid power demand is highest. To boost the performance of a particular plant in Empire Nevada during these problematic peak hours, we have explored four methods for enhancing air cooling using evaporative means: 1) spray cooling, 2) Munters packing media-cooling, 3) deluge cooling, and 4) a hybrid combination of spray and Munters. A detailed Microsoft Excel spreadsheet is used to evaluate the performance and cost characteristics of each system operating in

the Empire environment. It is concluded that the deluge cooling system, despite potential scaling on the condenser tubes, is the most economical way to optimize the plant's performance. The danger of scaling is dealt with by adding a purified water rinse to wash away new-forming scale whenever the deluge system shuts down.

Phase Stability of the Main Drive Line at Stanford Linear.

BENJAMIN COTTS (University of Portland, Portland, OR 97203) RON AKRE (Stanford Linear Accelerator Center, Stanford, CA 94025)
The Linac Coherent Light Source (LCLS) project at SLAC has higher RF phase stability requirements than the presently running system. Currently there is no way to directly measure the RF stability of the Main Drive Line (MDL) to the desired precision. There is a point at each sector of 8 klystron stations, called a head-tail monitor where phase measurements are taken. This point is the intersection of two signals, which both originated on the MDL and then took different paths to the same place. Though part of one of these paths is on the MDL, the phase measurements include more variation than is on the MDL alone. In order to determine the phase stability of the MDL, it was necessary to build an interferometer. Because of time limitations, data extraction was not possible. The design and testing of the interferometer, and predicted results are discussed.

BEARS Diagnostics.

AARON DAVIS (Southwestern College, Chula Vista, CA 91910) PEGGY MCMAHAN (Ernest Orlando Lawrence Berkley National Laboratory, Berkley, CA 94720)
A diagnostic device was created for use with BEARS—Berkeley Experiments with Accelerated Radioactive Species. The diagnostic device will take the place of phosphors, which are useful at the low beam intensities used in BEARS. The diagnostic device consists of a positively charged carbon foil, two strong permanent magnets, and a 25mm micro channel plate.

Applications of Modified Microcantilever Tips.

MATTHEW DELGADO (University of Texas, Austin, Austin, TX 78723) PANOS. G. DATSKOS (Oak Ridge National Laboratory, Oak Ridge, TN 37831)
The atomic force microscope (AFM) has mainly been used to image a variety of substrates using common tipped cantilevers with a small radius of curvature (typically 20-60 nm). Tipped cantilevers consist of a pyramid like structure extending normally from the cantilever plane. Variations from tip to tip causes uncertainty in the dimensions of the tip, therefore microspheres are attached, at the tip of the cantilever, whose radius is well known. The microspheres are Kromasil and have an average diameter around 10•m. The spheres are made out of high purity silicon and a various concentrations of carbon. The spheres are attached by using an optical fiber to pick up a sphere and a human eyebrow hair to apply the epoxy to the cantilever tip. The optical fiber and the eyebrow have tips that are approximately 10•m in width. This makes eyebrow and optical fiber the correct order of magnitude to pick up the spheres and apply the glue. The epoxy must be workable for at least five minutes order to have enough time to attach the sphere. After attachment the spherical tip can be used in the AFM to create a liquid bridge between the sphere and the surface. By having a spherical tip of a known radius, one can use the Kelvin equation, which has been verified for this order of magnitude, to measure the surface tension of a liquid bridge. This surface tension is measured by observing the deflection of the cantilever, as it comes in contact with the surface to when it releases. Then force vs. distance curves can be constructed. Furthermore, the tips can be used to measure the friction of the substrate by operating the AFM in contact mode.

Exploring The Concept of Fault Analysis.

MONIQUE DELMAR (Suffolk County Community College, Brentwood, NY 11717) VINCENT CASTILLO (Brookhaven National Laboratory, Upton, NY 11973)
Today one of the principal means of physics research is preformed through the use of particle accelerators. Research using these accelerators has given us the ability to study topics such as symmetry theories or the nature of the universe just after the big bang. However, this manipulation of high-energy particles has its drawbacks. There are some potentially harmful aspects, not only to the environment but also to the individuals working within the accelerators. One of the major hazards in working with the accelerators is exposure to radiation. A high enough dose of radiation within a given period can lead to physical side effects, some minor like headaches or nausea, and others as severe as death. To measure the levels of radiation, there are safety devices that are used within the accelerators, one of which is called a chipmunk. The chipmunks are stationed at multiple points around the accelerators and give a visual and audio display using lights, meters, and sounds so workers can easily check and confirm that radiation levels are within a safe range. Therefore, it is essential to keep these chipmunks operational at all times. A protocol must be designed to quickly identify and repair any faults that may occur within these devices. By building a working model of the chipmunk's circuitry, various fault conditions can be simulated to ensure proper operation. By manipulating the components of the circuitry we can effectively troubleshoot potential problems, develop a contingency plan for when problems arise, and cut down on repair time.

Model Validation for Computational Fluid Dynamics Simulations of Restricted Jet Configurations.

MICHAEL ECKERT (Hudson County Community College, Jersey City, NJ 07306) THOMAS BUTCHER (Brookhaven National Laboratory, Upton, NY 11973)
The behavior of confined jets in regions of entrainment, turbulence and boundary layers is difficult to study directly. The introduction of too much instrumentation changes the behavior of the system, but turbulence, recirculation and other fluid phenomena occur on a very small scale and can be missed entirely if too broad a net of sensors is cast. Regions of turbulence and entrainment in confined jets can display rapid variation in pressure, fluid velocity, and direction of flow, which are difficult to detect and interpret accurately. The current project, which is a part of ongoing research on jets and combustion in the Energy Science and Technology Department at Brookhaven National Laboratory centers on devising a method of model validation for Computational Fluid Dynamics Simulations of the inner workings of certain configurations of confined jets to be used in experimental ASTM #2 heating fuel combustion systems. The behavior of jets in restriction is of great interest to the Oil Heat Research Program as it pertains to performance of combustion equipment with flame tube assemblies. The current work will serve as elementary model validation and testing for eventual predictive studies on more complex configurations.

The Effects of Electrical Current and Ion Exchange Resin Mixture Ratios on Continuous Electrodeionization.

SUSAN FERNANDEZ (University of Maryland, College Park, MD 20742) PAULA MOON (Argonne National Laboratory, Argonne, IL 60439)
Continuous electrodeionization (EDI) is a process involving ion permeable membranes and ion exchange resin and requires the application of an electrical current. EDI allows for the transfer of ions from aqueous salt solutions or sugar solutions. These solutions may then be recycled more easily. In this study, current and ion exchange resin ratios were varied to determine their effectiveness in the transfer of sodium and chloride ions from a sodium chloride solution. In the course of the study, EDI runs were performed in a resin mixture of 65% anion exchange resin, 35% cation exchange resin as well as a resin mixture of 75% anion exchange resin, 25% cation exchange resin. Current levels tested were 0.59 and 1.20 amps. Conductivity and pH measurements were taken over the course of each EDI run, as well as samples for ion chromatography. It was found that current utilization was smaller for 1.20 amps; reduced current utilization is desirable. It was found that ion chromatography was the best process for determining sodium transfer from EDI feed solutions. In future work, various ratios will be tested. They are as follows, in terms of (% anion exchange resin, % cation exchange resin): (50%, 50%); (25%, 75%).

Containment Testing of the Berkeley Fume Hood.

MATTHEW FISHER (Augustana College, Rock Island, IL 61201) GEOFFREY C. BELL (Ernest Orlando Lawrence Berkley National Laboratory, Berkley, CA 94720)
This summer's research was dedicated to preparing a Berkeley Fume Hood for installation at San Diego State University, a future demonstration site. The Berkeley Hood introduces room air at the face thus reducing the air volume drawn from the room needed for hood containment. Reducing exhaust results in large energy savings while still meeting containment standards. Preparation of the hood entailed sealing leaks in the hood, obtaining an even velocity distribution out of each supply plenum, and testing the hood for containment. The hood's fittings and joints were sealed with silicone caulk to prevent leakage of fumes. The initial configuration of the lower supply plenum yielded a range of velocities from 31 FPM to 107 FPM. By manipulating the construction of the plenum and streamlining the air intake of the fan, we obtained a more even velocity distribution ranging between 77 FPM and 89 FPM. Throughout the United States the most accepted test for

fume hoods is the ANSI/ASHRAE Standard 110-1995 test. It is a three-part test that offers qualitative and quantitative means to testing the performance of fume hoods. The Berkeley Hood was tested according to the ASHRAE Standard 110-1995 protocol using two recognized detectors: the ITI Qualitek Leakmeter "120" and the Foxboro Miran 1A Gas Analyzer. At 30% the exhaust of a conventional hood, we successfully passed the ASHRAE tracer gas test by meeting the specific requirement of 4.0 AI 0.1, set by the American National Standard Institute.

Developing New Technology for High Gradient Induction Accelerators. *CARMEN FRIAS (East Los Angeles College, Monterey Park, Ca 91754) STEVE LIDIA (Ernest Orlando Lawrence Berkley National Laboratory, Berkley, CA 94720)*
The high-energy physics world uses high-energy colliders to probe into the structure of matter. Current technology limits the high-energy scale to 100-200 GeV. High-energy physicists believe that they will find important information on the structure of matter at a 500 GeV-1 TeV scale. To achieve such a high scale a higher-power more efficient power source is needed. The RTA group is currently developing this kind of technology. Their current linear induction accelerator uses Ferrite cores, which have a magnetic flux swing (DB) of 0.5-0.6 Tesla. By replacing the Ferrite cores with MetGlas DB is increased to 2.5 Tesla or greater. This is an improvement of a factor of five. Before being able to replace the Ferrite with MetGlas, the MetGlas cores must first be tested to make sure that they are within specifications. To do this I set-up a tabletop experiment to find the value of DB for individual MetGlas cores. I then wrote a LabVIEW program that does the following: 1. Acquires data from the oscilloscope 2. Plots the graph of the Magnetic Field (H) 3. Plots the graph of the Magnetic Induction (B) 3. Plots the graph of B vs. H (Hysteresis Curve) and 4. Plots the graph of the Integral of B*H (Energy Losses). From the Hysteresis curve we obtain the value of DB. The value of DB for the cores that I tested ranged from 3.0-3.3 Tesla, which is well above the specifications.

Fabrication and Testing of Bi-metallic Micro and Nano Tweezers using the Focused Ion Mill and Evaporator. *BRENT GEORGE (Tennessee Technological University, Cookeville, TN 38505) PANOS DATSKOS (Oak Ridge National Laboratory, Oak Ridge, TN 37831)*
The manipulation of objects on the micro and nano scales is a very challenging process. To manipulate these structures, especially free standing structures, special tweezers need to be fabricated with various tips to minutely move and orient these structures as needed. The tweezers are fabricated using the focused ion mill. Each edge is cut away from either an undoped piece of silicon or a silicon nitride cantilever. Next, the milled tweezers are put in the evaporator to apply chromium (5nm) and gold (0.1ìm). By applying a potential of opposite polarity across the bi-metallic tweezers they will attract to one another due to elastic deformation of the legs. Once the tweezers make contact, electrostatics keep them together. An insulating layer between the legs is needed to prevent them from connecting electrically. Tips for the tweezers can be made into any shape that is desired for the given task, however since the tip is part of the tweezers a new set of tweezers must be made for every given tip. By expanding the number of various tips and tweezers an arsenal of tweezers can be constructed and be readily available the next time the same task presents itself. Mounting the tweezers is also a difficult task. Since the tweezers themselves are made of thin fragile materials like that of which you are trying to manipulate special care must be made in the mounting harness. The design envisioned in this process would give forward and backwards motion as well as a 90° rotational factor. Using this harness and the tweezers that can be constructed, manipulating micro and nano structures is simplified to an extent not possible with the bare hand.

The Application of Microcantilevers in an Aqueous-based Chemical Detection System. *KATHLEEN GIESFELDT (University of Texas at Dallas, Richardson, TX 75083) PANOS DATSKOS (Oak Ridge National Laboratory, Oak Ridge, TN 37831)*
Many chemicals can cause serious injury or death at level well below the ppm range. Many chemical detection systems have been developed to identify airborne and water-borne contaminants. However, numerous chemical warfare agents and some industrial chemicals are hazardous well below the detection limits of most commercially available instruments. In previous research in this laboratory, it has been determined that commercially available microcantilevers, similar to those used in atomic force microscopy, can be used to detect single elements or chemical compounds at ppb range in the gas phase. In this work, chemical detection in an aqueous solution with microcantilever-based optical detection systems is demonstrated. The deflection of microcantilever was observed using a low-power diode laser operating and a four-element silicon photodiode (quadcell) when different concentrations of saline, ethanol, and isopropanol were flowed at 1 ml min-1 into a sample cell. The output of the quadcell was connected to an oscilloscope. The microcantilever deflections, which were detected, were recorded as a function of time using a lock-in amplifier. Microcantilever-based optical detection systems appear to be very sensitive in the detection of contaminants in aqueous solutions as was in the case with gas phase contaminants.

Monte Carlo N-Particle Modeling of the Shielded Measurement System and the Prompt Gamma Neutron Activation Analysis System at ANL-W. *CATHERINE GOFF (Massachusetts Institute of Technology, Cambridge, MA 02139) BILL RUSS (Argonne National Laboratory, Argonne, IL 60439)*
The particle transport code MCNP, a computer code developed at Los Alamos National Laboratory that utilizes the Monte Carlo method, was used to evaluate two specific experiments being developed and carried out at the Argonne West INEEL site. The first of these experiments evaluated was the proposed Prompt Gamma Neutron Activation Analysis (PGNAA) system to be installed at ANL-W for nondestructive drum inspection. The MCNP model, which included realistic modeling of the neutron source, shielding, and layout of the experimental area, served the purpose of determining the radiation (a combination of both neutron and photon) doses delivered to personnel working in the proximity of the PGNAA system. The dose rates obtained through this model were used to write an Engineering Analysis for the ANL-W ALARA Regulatory Committee. In the second half of this project, the Shielded Measurement System (SMS) developed by Argonne West was modeled using MCNP. The SMS is a versatile measuring device for the characterization of spent fuel in dry storage. Part of the SMS is a Shielded Instrument Ring, which contains numerous ports capable of accommodating a wide variety of radiation measuring instruments. This project focused on determining the optimal width of a variable collimator designed to aid in the detection of gamma rays emitted from an EBR-II blanket subassembly.

Development of an Automated Microfluidic System for DNA Collection, Amplification, and Detection of Pathogens. *BETHANY HAGAN (Washington State University, Pullman, WA 99163) CYNTHIA BRUCKNER-LEA (Pacific Northwest National Laboratory, Richland, WA 99352)*
This project was focused on developing and testing automated routines for a microfluidic Pathogen Detection System. The basic pathogen detection routine has three primary components: cell concentration, DNA amplification, and detection. In cell concentration, magnetic beads are held in a flow cell by an electromagnet. Sample liquid is passed through the flow cell and bacterial cells attach to the beads. These beads are then released into a small volume of fluid and delivered to the peltier device for cell lysis and DNA amplification. The cells are lysed during initial heating in the peltier device, and the released DNA is amplified using polymerase chain reaction (PCR) or strand displacement amplification (SDA). Once amplified, the DNA is then delivered to a laser induced fluorescence detection unit in which the sample is detected. These three components create a flexible platform that can be used for pathogen detection in liquid and sediment samples. Future developments of the system will include on-line DNA detection during DNA amplification and improved capture and release methods for the magnetic beads during cell concentration.

Evaluation and Development of RF Source for Cryomodule Testing. *RYAN HALE (Tennessee Technological University, Cookeville, TN 38501) RAY FUJA (Oak Ridge National Laboratory, Oak Ridge, TN 37831)*
In the near future, Jefferson National Laboratory (JLab) will be conducting cryomodule cavity tests for the Spallation Neutron Source (SNS) project, and Oak Ridge National Laboratory (ORNL) and Los Alamos National Laboratory (LANL) are pooling their resources to provide JLab with the necessary facilities. One of the tasks of the SNS Accelerator Systems Division at ORNL is to provide JLab with a 1MW peak RF source that will include a power supply, energy storage, and fault protection (crowbar) system. An industry-built power supply was ordered to provide the ~100 kVDC necessary to operate the transmit-

ter klystron. A crowbar cabinet, originally used in the Continuous Wave Deuterium Demonstrator (CWDD), was received from Argonne National Laboratory. This system implements a thyratron tube and is designed to protect the klystron in the event of a high voltage fault. The system is currently being evaluated and will soon be tested in the SNS Receiving/Acceptance/Testing/Storage (RATS) building. This evaluation includes circuit diagram generation and component testing. Following the testing and any necessary modifications, the system will be shipped to JLab for their testing.

Biochip Reader. *SUSAN HAMMOND (Bismarck State College, Bismarck, ND 58501) GENNADIY YERSHOV (Argonne National Laboratory, Argonne, IL 60439)*
A Biochip is a microchip that contains a set of immobile oligonucleotides used for DNA sequencing. Once these chips are manufactured, they need to be read to ensure they will work. The purpose of reading the Biochips is for quality control as well as determining the DNA of a certain sample. After the oligonucleotide probes have been attached and a sample has been run, the reader will test them by measuring the intensity of the fluorescent dye on the target DNA. The Biochip is read by illuminating the Biochip with a laser light and capturing the image with a CCD camera. The image and all other data are sent to the computer and analyzed further. This device is in its preliminary stages of development. Once completely assemble, the reader will be re-designed until all mistakes have been eliminated.

Characterization and Analysis of a Typical T8 Luminaire for the Development of a Flexible Computer Based Control System. *BRYAN HILSON (Central Piedmont Community College, Charlotte, NC 28235) J.D. MUHS (Oak Ridge National Laboratory, Oak Ridge, TN 37831)*
Energy efficiency is a common concern in today's economy. The Hybrid Lighting Project combines energy conscience technologies like solar collection and remote source lighting. A hybrid luminaire blends both natural visible light with artificial fluorescent light. This requires a control system to maintain a constant total illumination by increasing and decreasing fluorescent light to inversely match the decrease and increase in natural light. Proper design of a hybrid luminaire control system required the characterization and analysis of a general purpose Lithonia Model 2GT8 luminaire, four Sylvania 4100k Octron fluorescent lamps, and two controllable rapid-start electronic ballasts from Advanced Transformer Company. A system-level evaluation of two potential hybrid luminaires was used to establish a base of knowledge for the development of an effective control system. A photosensor that utilizes transient signal analysis to distinguish between the fluorescent and natural light was used to develop the transfer equation that is the heart of the control system. A prototype hybrid luminaire was developed complete with fixture, fluorescent lamps, dimmable ballasts, photosensors, and software driven control system. With this prototype the control system can be further developed and future more efficient hybrid luminaires can be developed.

Temperature Control of Beam Line Mirrors. *LINDSAY HOPKINS (Spelman College, Atlanta, GA 30314) JOHN BAGNASCO (Stanford Linear Accelerator Center, Stanford, CA 94025)*
Researchers have noticed that the beam position had been drifting vertically, causing it to miss their research samples. It is believed that this is caused by temperature changes in the mirror water-cooling system. These changes cause the mirrors to pitch, moving the position of the beam. This is due to the differences in silicon and copper thermal expansion coefficients. To alleviate this problem, the group will install temperature-controlling equipment to maintain the water temperature to within $0.01°C$ from the operating temperature of the water-cooling system of $30°C$, which would be an improvement from the current fluctuations of $\pm 0.2°C$. The two choices are water mixing valve temperature control system and a direct heating temperature control system. The group decided to use the water mixing valve temperature control system because it is more accurate. This system should allow the beam line group to regulate the water-cooling temperature within the desired range. The system would monitor whether or not the current temperature is at the desired level. Based on the result, the cooling system will mix hot water into the water flow. The cooling system reads voltages so it does not recognize the temperature readings from the temperature detectors. This leads to the need of a medium to translate the temperature readings to voltages that can be understood by the cooling system. My project is to create

the medium that will be installed into the system. Hopefully, this should end the instability problem with the water-cooling system of the apparatus.

Remotely Operated Nondestructive Examination System for Double Shell Tank Inspection. *LINDSEY JOHNSON (Stanford University, Palo Alto, CA 94309) TODD SAMUEL (Pacific Northwest National Laboratory, Richland, WA 99352)*
It is required by the WA State Dept. of Ecology that all 28 double shell tanks built at the Hanford Site between 1968 and 1986 be inspected for any pitting or cracking of the walls that would threaten their integrity. To achieve this, a project was begun in FY-1999 whose purpose was to develop and construct a system that will allow detection, localization, and sizing of flaws and cracks in Hanford's Double Shell Waste Tanks (DST's). Prefabricated systems are not available for this type of examination because they cannot reach the highest stress region of the tank, the lower corner, or knuckle region. The system built utilizes a two-step method in which the operator will use Pulse Echo imaging with ultrasonic waves to detect and localize flaws in the knuckle region. The data acquired is sent through the SAFT, or Synthetic Aperture Focusing Technique, which focuses it and enables the operator to find the appropriate area to scan for additional information about the flaw. Next, Tandem scanning, which involves two transducers moving simultaneously, is used to size the flaw. The testing done so far has proven the concept to be a valid one and the project is in the prototype stage but future testing is still necessary to perfect the process and to troubleshoot the system until it is ready for use in the field.

Design of Software for Motor Control Center for water pumps used in cooling water loops. *THOMAS JUSTICE (Tennessee Technological University, Cookeville, TN 37845) JOHN HAINES (Oak Ridge National Laboratory, Oak Ridge, TN 37831)*
The neutron-scattering research that will be conducted at the Spallation Neutron Source (SNS) when completed is expected to benefit all areas of scientific research. Neutron scattering will take place in the mercury target when an intense proton beam bombards the target. Because the spallation process produces heat, various systems must be cooled down using cooling water loops. The target has five cooling water loops, four in the target building and one in the ring injection dump. This paper describes the control system, which is designed to operate the two pumps and four block valves in each cooling water loop. The control system provides the target operator with the ability to start the system through automatic procedures or manual procedures, as well as giving the operator valuable diagnostic information at the touch of a graphic interface button. The motor is controlled using a programmable logic controller (PLC) and the Experimental Physics and Industrial Control System (EPICS), which provides the graphical user interface. EPICS is the development tool used to access all the process variables. In conjunction with an input/output controller (IOC), EPICS communicates between the PLC and the user interface. The PLC allows EPICS to communicate with the motor starter over DeviceNet, which is standardized communication software and hardware.

Analysis of Vadose Zone Contaminant Releases at Hanford Site Using VZGRAB Data Extractor. *SHARON KARLESKY (Oregon State University, Corvallis, OR 97330) WILLIAM NICHOLS (Pacific Northwest National Laboratory, Richland, WA 99352)*
The Hanford Site was established in 1944 to produce plutonium for use in nuclear weapons. A byproduct of the production process was the release of radioactive and chemically toxic waste to the environment. Since plutonium production ceased in 1988, the Department of Energy (DOE) has pursued a waste management and cleanup mission at the Hanford Site. In 1997, DOE established the Groundwater/Vadose Zone Integration Project, a project that includes development of the System Assessment Capability (SAC) software. This software represents a first-ever attempt to model environmental migration and subsequent impacts for all waste inventories at the Hanford Site. The SAC simulates the transport of contaminants from release at hundreds of locations, through environmental pathways in the vadose zone, the groundwater aquifer, and the Columbia River for the years 1944 to 3050. Moreover, this is done in a stochastic framework, representing uncertainty in results due to uncertainty in input parameters. A data extraction tool, VZGRAB, was developed to efficiently examine the overwhelming quantity of data produced in the vadose zone portion of

the SAC. VZGRAB provides the analyst the means to efficiently analyze the vadose zone results with respect to specific site(s), contaminant(s), realization(s), or any combinations thereof. By correlating the results with similar SAC data extractors for other components, the impacts of residual waste can be assessed. This information may be used to guide future waste management and cleanup decisions.

Savannah River Site Mixer Pump Operational Improvement.
JAMES KARNESKY (Rensselaer Polytechnic Institute, Troy, NY 12180) FADEL F. ERIAN (Pacific Northwest National Laboratory, Richland, WA 99352)
Waste mobilization through the use of mixer pumps faces severe challenges to operational efficiency in the storage tanks used on the Savannah River Site. Among these is the possibility that the bottom wall of the tank interferes with the mixing jets, which contributes to the degradation of these jets, and thus the inability of the mixing jets to mobilize waste at outer portions of the tank nearest the floor. This effect, however, is not well understood, and it was the goal of the project enumerated herein to investigate this phenomenon and determine the maximum depths to which the jets are still effective. Both an experimental setup and CFD analysis were applied, and the results obtained were analyzed with the intent of applying them to the mobilization problems of the Savannah River Site.

Portable System for Calibrating Power Losses in NLCTA Components.
CATHERINE KEALHOFER (Princeton University, Princeton, NJ 08544) JOSEF FRISCH (Stanford Linear Accelerator Center, Stanford, CA 94025)
A simple technique for monitoring electric fields in the accelerator structures of the NLCTA (Next Linear Collider Test Accelerator) involves picking off some of the microwave power sent to these structures and measuring it. In this context, the calibration of power losses in the relevant components is an important problem. This paper describes the use of a Gunn oscillator in a portable calibration system. Measurements of the oscillator's frequency and amplitude variations with temperature and operating voltage are also presented. In addition, upper limits placed on the oscillator's phase noise indicate other potential applications for these oscillators, for instance in measuring the phase of the RF sent to the accelerator structures.

Magnetic Levitation of Small Objects.
RYAN KEREKES (University of Tennessee, Knoxville, TN 37916) PANOS G. DATSKOS (Oak Ridge National Laboratory, Oak Ridge, TN 37831)
Infrared detection is important in many applications such as thermal imaging, industrial process control, and chemical sensing. Using thermal MEMS (microelectromechanical systems) devices, IR detection can be accomplished. Thermal isolation of the micromechanical sensing element is very important in such applications because small amounts of heat energy must be detected by the sensor. Magnetic levitation provides a means of achieving thermal isolation. A magnetic levitation system can be used to "float" an unattached magnetically coated MEMS structure at a fixed position to achieve bending responses to infrared photons. An electromagnet connected to an active feedback circuit is necessary to keep the hovering MEMS in place. The circuit uses a pair of photodiodes and a laser to detect the position of the floating object, and it adjusts the strength of the magnetic field accordingly by varying the current through the electromagnet. Such a system could lead to new possibilities in precision and accuracy for IR detection applications.

Memory Device Program Authentication.
SAMUEL KORSLUND (Blue Mountain Community College, Pendleton, OR 98632) JIM SKORPIK (Pacific Northwest National Laboratory, Richland, WA 99352)
There are several different types of electronic memory devices, each having their own unique characteristics. Some are one-time-programmable while others can be erased and re-programmed a number of times. Combinations of these different memory devices can be found inside of other electronic components such as microcontrollers, which can also save a program and have that program erased and re-written. These devices are very important in the operation of the circuit in which they are installed, making any error or alteration to the original program greatly effect the resulting operation of the circuit. Therefore, a method of authenticating a microcontroller program is very neces-

sary. One method of performing an authentication is to remove the device from the circuit and place it into a device programmer. The programmer is then interfaced with a computer, and the program is read and displayed on the monitor. From there it can be saved to a file or printed out and compared to an original copy of the program. Any errors or alterations can then be detected and repaired. This method is fairly simple in its procedures, but does require certain pieces of hardware. Most importantly, the programmer and computer, but also equipment is needed to remove the component without doing any damage to it.

Indoor Environmental Quality of Relocatable Classrooms: Preparation of Active Sampling Instruments.
SHAWNA LIFF (Northeastern University, Boston, MA 02118) MICHAEL G. APTE (Ernest Orlando Lawrence Berkley National Laboratory, Berkley, CA 94720)
Dr. Apte and associates from the Indoor Environment Department are attempting to establish new relocatable classroom (RC) designs that simultaneously provide higher energy efficiency and better indoor environmental quality (IEQ) in California. It is thought that RC occupants will benefit from improved IEQ through increased health and performance. The incorporation of a new HVAC system and the implementation of lower emitting materials in RCs will be evaluated using samples of volatile organic compounds (VOCs), aldehydes (ALDs), and carbon dioxide (CO_2), counts of various sized particles, and temperature and relative humidity measurements. Before sampling each instrument was prepared for field installation and its functionality and accuracy evaluated at the laboratory. Evaluation consisted of a month of continual operation during which data was collected to monitor instrument performance. The CO_2 sampler's calibration measurements and the ALD and VOC sampler's flow rates proved to be consistent and no operational glitches were observed. One particle counter experienced a fatal error while the other seven counters tracked well but did not display the 5% error the manufacturer guaranteed. Consequently, two of the seven counters were sent back to the manufacturer for re-calibration. The humidity sensors displayed compatibility, however the 2% error guaranteed by the manufacturer was exceeded. All the instruments are ready for fieldwork and the VOC, ALD, and CO_2 samplers display minimal performance degradation, while the error of the humidity sensors and particle counters exceed that specified by their manufacturers and will be significant in the analysis of field data.

Evaluation of Variable Speed Drive Technologies.
MICHAEL MULKERIN (American River College, Sacramento, CA 95841) STEVEN A. PARKER (Pacific Northwest National Laboratory, Richland, WA 99352)
Variable speed drives are more efficient than dampers and bypass loops. Rather than restricting flow or bypassing a heat exchanger, variable speed drives vary the speed of the output fan shaft in order to reach a desired flow. Some of the more popular variable speed drives include, two types of magnetically-coupled variable speed drives and the variable frequency drive. The efficiencies of these drive systems were measured using a dynamometer at the Oregon State University Motor Testing Laboratory. Motors were run according to a theoretical pump and fan curve in order to quantify the efficiency of each drive. The data show that the variable frequency drive is up to eight times more efficient than the magnetically-coupled variable speed drives at the extreme low end of the pump and fan curve and overall more efficient over a wide array of data.

Chemical ionization in ion traps.
MATTHEW NEWBURN (Walla Walla Community College, Walla Walla, WA 99362) ALEXANDER, MICHAEL L (Pacific Northwest National Laboratory, Richland, WA 99352)
There are inherent amounts of hydrogen peroxide, water vapor, nitrogen, dioxide, and other low mass gases in an ion trap. These chemical species often react with other molecules in ion traps before the mass spectrum can be taken. These reactions can reduce the number of critical ions in the spectrum or they can be used to boost ion concentrations of certain molecules. To be able to optimize the RF voltage in the ring electrode, to allow time for these reactions to occur, one would need to know the reaction constants of these reactions. The productions or reductions of three of the most common ambient ions were chosen for this experiment. In particular, O_2^+ and H_3O^+ ions

will ionize many other neutral molecules. H_3O^+ was used as a chemical ionization (CI) agent and the reaction constant measured.

Electron Beam Ion Source Interlock Circuit. *OLUSOLA OLAODE (Monroe Community College, Rochester, NY 14623) OMAR GOULD (Brookhaven National Laboratory, Upton, NY 11973)*
The EBIS Research facility produces heavy ions (ions with large molecular mass) such Gold and Cesium. It is intended to be used as a Heavy Ion Injector for high-energy physics research. The Anode and Collector Power Supplies in the EBIS require sequential operation. The Anode Power Supply (APS) is used to initiate the acceleration of electrons. The Collector Power Supply (CPS) is used to accelerate the electrons. The Anode power supply should not be in the on state unless the Collector power supply is itself in the on state. Otherwise, the electrons will not be accelerated to the collector device. The purpose of this project is to: Design a circuit that ensures APS does not turn on before the CPS. Design a circuit that shuts off all other EBIS power supplies upon a fault condition. These objectives are accomplished using mechanical switches, analog electronic switches, logic gates and Flip-flops.

HANDSS-55. *SAMUEL PETERSON (Brigham Young University, Provo, UT 84602) ROD SHURTLIFF (Idaho National Engineering and Environmental Laboratory, Idaho Falls, ID 83415)*
DOE facilities around the nation have in their possession low-level nuclear waste or transuranic waste (TRU-waste). This TRU-waste is stored in thousands of 55-gallon drums. DOE facilities have been or are going to store TRU-waste into the Waste Isolation Pilot Plant (WIPP), an underground repository licensed to safely and permanently dispose of transuranic radioactive waste left from the research and production of nuclear weapons. To prepare 55-gallon drums of TRU-waste manually is dangerous, timely, and costly. The Handling and Segregating System for 55-gallon Drums (HANDSS-55) provides an automated technology to process TRU-waste and mixed TRU-waste. HANDSS-55 opens 55-gallon drums and liners and prepares the waste inside these drums for shipment to WIPP. The technology incorporated in the HANDSS-55 is both automated and modular, allowing individual modules to be used with a multitude of other applications. The HANDSS-55 system performs four main processes: Automated Drum and Liner Opening (AD&LO), Process Waste Reduction (PWR), Waste Sorting, and TRU-Waste Repackaging. The system is still being developed and has not reached final stages. The AD&LO has been completed and tested very well. Testing on other sub-systems have also been done and led to many changes and enhancements, due to errors that occurred. Nevertheless, HANDSS-55 is doing well and is right on course to be deployed and functional in 2003.

The use of Waterjets for Coating Removal. *TRENT ROTH (Bismarck State College, Bismarck, ND 58501) MICHAEL RINKER (Pacific Northwest National Laboratory, Richland, WA 99352)*
This abstract lacks detail due to business sensitive technologies. High-pressure waterjets are used to clean surfaces in industry. However, surfaces with protective coatings must be cleaned without removing the coatings. High-pressure waterjets were used to find the threshold of steel carbon plates coated with paint. Tests were conducted at various pressures, standoff distances, and traverse rates to determine the proper setting to remove debris while keeping the coatings intact. Results showed that as long as the pressures stayed below 4000 pounds per square inch, the standoff distances and traverse rates did not adversely affect the coatings.

Processing Variables of Alumina Slips and their Effects on the Density and Grain Size of the Sintered Sample. *RYAN ROWLEY (Brigham Young University, Provo, UT 84602) HENRY CHU (Idaho National Engineering and Environmental Laboratory, Idaho Falls, ID 83415)*
High densities and small grain size of alumina ceramic bodies provide high strength and better mechanical properties than lower density and larger grain size bodies. The final sintered density and grain size of slip-cast, alumina samples depends greatly on the processing of the slip and the alumina powder, as well as the sintering schedule. There were many different variables explored which include initial powder particle size, slurry solids percent, amount and type of dispersant used, amount and type of binder used, and sintering schedule. Although the experimentation is not complete, to this point the sample with the highest density and smallest grain size has been a SM8/Nano mixture with Darvan C as the dispersant and Polyvinyl Alcohol (PVA) as the binder, with a solids loading of 70 wt% and a 1500° C for 2

hours sintering schedule. The resultant density was 98.81% of theoretical and the average grain size was approximately 2.5×10^{-6}m.

Handling and Segregating System for 55-gallon Drums. *SHARON ROWLEY (Brigham Young University, Provo, UT 84602) MICHAEL GIFFORD (Idaho National Engineering and Environmental Laboratory, Idaho Falls, ID 83415)*
The Waste Isolation Pilot Plant (WIPP) is a permanent storage facility for transuranic waste resulting from Department of Energy (DOE) nuclear research and development. Several DOE facilities will be and have been sending WIPP acceptable transuranic waste to WIPP. This waste is radioactive and thus a dangerous and slow process for humans to handle, so it is desirable to have a machine to semi-automatically prepare and sort WIPP compliant items. The machine being built to do this is the Handling and Segregating System for 55-gallons Drums (HANDSS-55). HANDSS-55 is a remotely operated and remotely maintained system that will open 55-gallon drums, including liners, and prepare the waste inside the drums for shipment to WIPP. HANDSS-55 will perform four main processes: drum and liner opening, waste sorting, waste repackaging, and process waste reduction. The numerous components of HANDSS-55 are in different stages of development and testing, and so far HANDSS-55 has been able to accomplish the desired tasks. The drum and liner opening system has completed testing and is ready to operate as part of the system. The fabricated waste sorting components have generally performed well, but enhancements are still being made. The repackaging system is scheduled for testing. The process waste reduction system is in the final design process. Any negative test results have been addressed and improved, or are in the process of being improved. The system is performing well, on schedule, and expected to be operational in 2003.

Density and Densification of the Pressureless Consolidated Ceramic Waste Form. *MAY SATTERFIELD (Yale University, New Haven, CT 06520) KENNETH J. BATEMAN (Argonne National Laboratory, Argonne, IL 60439)*
Abstract Density and Densification of the Pressureless Consolidated Ceramic Waste Form. Barclay Satterfield (Yale University, New Haven CT 06520) Kenneth Bateman (Argonne National Laboratory, Idaho Falls, Idaho, 83403). As Argonne National Laboratory continues research and scale-up of the Ceramic Waste Form, it has become important to determine the material's density during firing, especially over long firing cycles. In this research a formula for volume as a function of height is developed for the canisters used and then applied in order to determine the material's density during firing with a linear potentiometer. The material's densification pattern is found to be a logarithmically increasing curve, even over long firing cycles, and final bulk densities range from 1.7 g/ml to 1.97 g/ml. Methods for further increasing the ease and accuracy of height monitoring are also investigated.

Renewable hydrogen. *MALENE SAVAGE (Clark Atlanta University, Atlanta, GA 30314) BOB EVANS (National Renewable Energy Laboratory, Golden, CO 80401)*
Many efforts have been made to produce a competitive alternative to natural gas. Natural gas lowers the pollution but it is expensive and limited. One leading idea is that of renewable hydrogen. Renewable hydrogen has the potential of being cost effective and environmental friendly. The strategy is based on producing hydrogen from biomass pyrolysis using a co-product strategy to reduce the cost of hydrogen. During the first steps slow pyrolysis is used to maximize the yield of charcoal using densified peanut shells. Results were produced using the molecular beam mass spectrometer and the differential scanning calorimeter. MBMS produced kinetic data analysis that will help in predicting time and temperature requirements. The DSC produced information needed for heat requirements. All of the data gained from this summer will be used in the planning of the project.

Prototype Performance Evaluation for the Federal Bureau of Investigation Portable Supercritical Fluid Extractor. *ANTHONY SCOTT (Eastern Oregon University, La Grande, OR 97850) THOMAS S. ZEMANIAN (Pacific Northwest National Laboratory, Richland, WA 99352)*
The substitution of traditional solvents with supercritical fluids for extraction is an area of many possibilities. While some research has been performed, more is needed to fully investigate the utility of supercritical fluids. The need was expressed for a functional, durable, and smaller portable unit to perform supercritical fluid extraction (SFE)

in the field utilizing CO_2 as the solvent. Previous generations of portable SFE's have achieved manageable portability, but a smaller unit was requested. The unit was designed and manufactured. The tasks for this project were to run the machine through its paces and test its systems to assure that they operated as designed. From initial testing, it was seen that target pressures were reached in approximately 25-40 minutes, depending on the fill achieved and target pressure. The extractor systems (electronic, Booster/ Generator, and restrictor/ recovery) were tested (by stopwatch, thermocouple, observation, and instrument readout) and were functioning as designed. System cool down took between 1½ -2 hrs. Multiple runs through with the extractor showed that it was functioning as designed. The main problem that occurred was minor in scope. Improvements such as a Generator dump valve would be useful, in bleeding the gas off for a better liquid fill and for dumping the CO_2 after use. This work contributed to the design process of the extractor. Implications of this work include further study of system perfor- mances, simple design modifications, and an overall operation view for the end user, the FBI.

Digital Imaging of Diesel Sprays.
JONATHAN SHIH (Duke University, Durham, NC 27708) RAJ SEKAR (Argonne National Laboratory, Argonne, IL 60439)
Diesel powered locomotives are one of the largest consumers of diesel fuel in the country, so emissions and fuel efficiency are central concerns of the industry. One area where more scientific understand- ing could yield better fuel efficiency and decreased emissions is the fuel injection process. Poorly designed injection can significantly hamper a diesel engine's performance. Using high speed digital imaging, two geometric properties, penetration length and cone angle, were determined by varying different variables such as diesel injector, chamber pressure, cam shaft speed, pulse width and time. Images were taken, and then analyzed programmatically using LabView. Mathematical correlations were then determined for both penetration length and cone angle.

Re-Design of a Hydraulic Oil Delivery System for Wind Turbine Blade Fatigue Testing.
JAMES STACK (Bucknell University, Lewisburg, PA 17837) WALTER MUSIAL (National Renewable Energy Laboratory, Golden, CO 80401)
The advancement of the wind energy industry is very much dependant on the ability to test the equipment being used in order to learn about their properties and make improvements in future designs. One type of test commonly performed is a fatigue test, which involves using hydraulic actuators to simulate the cumulative loading a blade will experience during its lifetime. Currently, new larger wind turbines are being produced with rotor blades spanning over 80 m and are stretching the testing capabilities of many test facilities. The Industrial User Facility at the National Wind Technology Center in Colorado is the premier wind turbine structural testing facility in the country and has just received a set of these new large-scale blades to test. But in order to maintain the speed at which these tests can be performed, the oil-pumping capacity of the hydraulic delivery system must be upgraded substantially, from the current rate of about 150 GPM up to 280 GPM. This paper focuses on the re-design of the hydraulics delivery system at the IUF, which involves combining two large pumps to operate in parallel, as well as the installation of a new oil cooler and larger piping to deliver the increased oil flow to the actuators in the test section.

Pitch-based carbon foams.
SHAUN STINTON (University of Tennessee, Knoxville, TN 37996) JAMES KLETT (Oak Ridge National Laboratory, Oak Ridge, TN 37831)
Pitch-based carbon foams with high thermal conductivity are being researched for thermal applications. Foam is currently produced using a batch method that requires several different steps, and is costly. The objective of this project is to determine whether the foam can be made with extrusion in a continuous manner, which will decrease the cost. The extrusion is done through a series of chambers that forms a continuous tube. Pellets of mesophase pitch are ground up and melted in the screw extruder that contains several heating zones that create the proper molten phase. Molten pitch enters the metering pump, which controls the flow rate into the chambers after the pump, and the temperature is raised high enough for the pitch to foam and start solidifying. The pitch is cooled and exits through the die head. Testing relies on the heating profile of the extruder since chamber tempera-

tures affect how the pitch foams. Different heating profiles have been tried, and the last run seemed to be close to what is needed. The testing showed that there was a problem in the design of the extruder, which caused the pressure to rise and flow to be affected. The problem was probably due to the change in shape of the chambers after the pump. Parts of the extruder were redesigned in order to have a continuous shape through the last several chambers. The samples taken from the first extruder runs were examined under a SEM, and the results were encouraging. Similar open celled porosity was found in both types of foam. The next step is to obtain better-extruded foam samples so the properties of the extruded foam can be tested and compared to properties of foam made by the batch method.

Energy Efficient Lighting.
EVAN STONE (Santa Barbara City College, Santa Barbara, CA 93109) MICHAEL SIMINOVITCH (Ernest Orlando Lawrence Berkley National Laboratory, Berkly, CA 94720)
Lawrence Berkeley Laboratory has developed an energy efficient lamp named the Berkeley Lamp. The lamp is applicable in both home and office settings, and is bright enough to light up any room. The Berkeley lamp consists of two compact fluorescent lamps that are separated with a reflective dish designed to direct light a particular direction. From the upper lamp, light is directed upward toward the ceiling, and thereby illuminating the room with an indirect source. When using the lower lamp, light is directed downward and illuminates the task area. The Berkeley Lamp's two compact fluorescent lamps use about 115 Watts at full power, while typical overhead lighting in one office uses about 250 Watts. The lamp has potential for large energy savings, but the evidence must be concrete. I was thereby able to develop methods that could measure energy savings and could determine the full impact that the Berkeley Lamp would have in an office. Certain characteristics of offices can have a big influence on the collected data. Issues such as day lighting, occupancy sensors, double occupancy offices, and a recent effort to conserve energy, all need to be included in the data analysis. So far, I have deployed an initial set of light loggers in LBL offices, visited sites that might work well for collecting data, and determined the connected load to numerous offices. Soon we will be able to accurately state how much energy the Berkeley Lamp can save.

Evaluation of the Smithsonian Environmental Research Center Two-Story Visiting Scientist Housing Designs Using Energy-10.
RAINA STRICKLAN (Colorado State University, Fort Collins, CO 80523) ANDY WALKER (National Renewable Energy Laboratory, Golden, CO 80401)
The Smithsonian Environmental Research Center (SERC) is located in Edgewater, Maryland. Plans to build visiting scientist housing have been submitted to the Federal Energy Management Program for energy analysis using Energy-10. Energy-10 is a software program that conducts annual hourly evaluations of a building's energy use. It uses thirteen energy efficient strategies to apply to a building to analyze energy efficiency. Modifications had to be made to the program since Energy-10 was designed to be used before the building design process, and the SERC blueprints were already drawn up. Insulation, air leakage control, high efficiency HVAC, and duct leakage strategies were considered for the SERC housing. Additional modifications were made to simulate a ground source heat pump, a wastewater heat recovery system, and a solar water heater. Each strategy was analyzed separately, showing insulation and a wastewater heat recovery system paired with a solar water heater to offer the greatest energy savings. Strategies were also combined to account for synergistic effects. By implementing a PV system, additional energy would be saved, generating 64% annual energy use savings over the SERC housing as planned. Implementation costs were not estimated as part of this study.

A Superconducting Undulator.
SAI-WANG TAM (Pasadena City College, Pasadena, CA 91770) SHLOMO CASPI (Ernest Orlando Lawrence Berkley National Laboratory, Berkly, CA 94720)
Superconducting Undulator is an important device for generating Synchrotron Radiation. An Undulator magnet is a device consisting of a sequence of dipole magnets with alternating polarity. Superconducting coils generate the magnetic field and the resultant field of y component is sinusoidal oscillation. When the electron bean pass through the magnetic field, the electron will oscillate in the horizontal plane due to the Lorenz forces. Because electron accelerates during oscillating, polarized synchrotron radiation is emitted. In order to analysis the

magnetic generating from the Undulator, a C program was written to model the geometry coil. The geometry of the coil was described by considering each wire segment as a rectangular box of eight corners. All the coordinates of each corner was calculated through out to a real winding situation. Then the resultant geometry displayed in the AutoCAD, 3D Exploring and ProEngineering. After the entire geometry of coil completed, the magnetic field was calculated by using numerical method of Biot-Savart Law. Since the geometry of coil divided into many small boxes, the total magnetic field summed up from all contribution of each box. There were two important advantages of this geometry. First, the magnetic field of y component is uniform across the beam. Second, the magnetic field of x and z component are zero along the coil center.

Ammonia-Scrubbing Technology for Removal of Industrial CO_2 Emissions. *ROBERT TOWNSEND (Tennessee Technological University, Cookeville, TN 38505) JAMES WEIFU LEE (Oak Ridge National Laboratory, Oak Ridge, TN 37831)*

A potential way in which to achieve 22% reduction in the emission of CO_2 as outlined in the Kyoto Treaty is to use a method by which flue gas (15% CO_2 by volume) from coal burning power plants is passed through a reaction chamber while a fine spray of ammonium hydroxide (NH_4OH) is concurrently introduced to the resulting flue gas cloud. Theoretically, a reaction then occurs by which ammonium bicarbonate (NH_4HCO_3), a useful fertilizer, is formed from NH_4OH and CO_2. This product precipitates out as tiny white particles or aggregates of particles in the form of snow. In order to prove this reaction occurs, a bench scale model of this reactor was designed. Upon spraying by means of an electric field, it was found that particles did not form instantly, but instead only formed along the walls of the reactor where the NH_4OH coalesced as it was sprayed. This product was harvested and analyzed using NMR analysis techniques. The product created was pure NH_4HCO_3, substantiating the concept behind this method. The mechanism by which the bicarbonate product forms turns out to be two phase. Ammonium carbamate is initially formed followed by a slower, second reaction where the carbamate is transformed into bicarbonate. In actuality the bicarbonate may have been forming, but due to the excess of water in the hydroxide solution and the high solubility of NH_4HCO_3, the particles were being absorbed into the water phase. This was demonstrated using a bubble tank that used NH_4OH as the constant phase while bubbling pure CO_2 through the fluid bed. Particles only precipitated out after the solution became saturated, thus showing an excess of water in the hydroxide solution.

Development of a Weather Correction Model for Outdoor Vehicle Testing. *DANIEL TUHUS-DUBROW (Brown University, Providence, RI 02912) ROM MCGUFFIN (National Renewable Energy Laboratory, Golden, CO 80401)*

When a vehicle sits all day in the sun, its cabin air temperature can reach as high as 80°C, and the dash temperature can reach 120°C. This requires a great deal of air-conditioning power for the initial cool-down of the vehicle. The National Renewable Energy Laboratory is currently looking into methods for reducing peak solar loads in vehicles, examining such technologies as solar reflective glazings, improved thermal insulation, and ambient venting systems. Two Lincoln Navigators are being tested outside the Thermal Test Facility for this purpose. One problem with outdoor testing of any kind is that the weather is always changing, and this could have an important effect on the results of the test. For example, if one technology was tested on a cloudy day, and another one on a sunny day, comparing the results would be meaningless. In order to account for these variations, a weather correction model has been developed. This is a two-node model that predicts the temperature rise in the cabin air and the cabin mass. "Standard" weather conditions are then chosen, and the measured data are normalized to these standard conditions so that different tests can be meaningfully compared. Results from the model are promising, but more testing must be done before the weather corrector can be put into use.

Mechanical Designs for a Support Structure and Header Plate of a Nb3Sn Superconducting Magnet. *DANIEL VALENTINE (Christian Brothers University, Memphis, TN 38119) RAY HAFALA (Ernest Orlando Lawrence Berkley National Laboratory, Berkley, CA 94720)*

The quality of superconducting magnets serves great importance to particle accelerators. Through engineering design and extensive

testing of these superconducting magnets, greater magnetic fields can be reached to push materials to their mechanical limits. This would help engineers to define the properties that are required to go even harder. With magnet design changing so must the objects and mechanisms used to test it change. This is the case with the 32-inch header piece off of the cryostat unit used in testing these superconducting magnets. A special cut had to be made through this plate so that proper measurements of the superconducting magnet's field could be made with the probing unit. Slight modifications also had to be implemented to the probing unit so that the orientation of the transversing mechanism would be directly over the magnet borehole. With cost efficiency in mind, the superconducting magnet group has come up with the idea to reduce their testing magnet to a 1/3-size scale. This would reduce the amount of material used and therefore the overall cost. Now, modifications have to be implemented for a smaller cryostat unit to be placed where the full sized unit was. The new support structure for the 1/3-scale superconducting magnet has been designed using a four-point structure. From each pole protrudes an arm that connects to the cryostat to suspend it approximately 2 inches above the ground.

Measurement of Uniform Irradiation Responses of The 120º Neutron Detector. *MICHAEL VIRDONE (University at Buffalo, Buffalo, NY 14261) GRAHAM SMITH (Brookhaven National Laboratory, Upton, NY 11973)*

This paper describes the principle of operation of a new two-dimensional thermal neutron detector, which has been designed and built at Brookhaven National Laboratory. Its application is for protein crystallography at Los Alamos National Laboratory, for which it will provide unprecedented resolution, linearity, and rate capability. Significant new features have been incorporated into the new detector system. In particular the hardware of the detector, and the software for data acquisition have been specifically developed so that the eight segments constituting the device possess "seamless" position readout. My particular contribution to the project involved software development and data analysis to ensure that this advanced feature is working correctly. A comprehensive description is given of the linearity measurements carried out at BNL during summer 2001.

Effects of Continuous Ventilation on Indoor Air Quality (IAQ). *JACOB WEMPEN (Utah State University, Logan, UT 84321) CRAIG WRAY (Ernest Orlando Lawrence Berkley National Laboratory, Berkley, CA 94720)*

Space-conditioning system operation affects energy use and indoor air quality (IAQ) in houses. This study assesses the IAQ implications of continuous versus cyclic system operation with and without whole-house ventilation, in support of ASHRAE Standard 62.2P. A calibrated multizone airflow and contaminant transport model of a Fresno, CA house was constructed and used to evaluate the effectiveness of six system operation and ventilation schemes for controlling distributed and point source contaminants over a day with cooling and a day with heating. The whole-house ventilation schemes considered were: infiltration with unintentional ventilation due to duct leakage, infiltration with continuous single-point central exhaust ventilation, and infiltration with cyclic multi-point supply ventilation. The multizone simulations show that continuous air-handler operation can significantly lower both the peak and average concentrations for both point source and distributed source contaminants, and can reduce room-to-room variability, regardless of mechanical ventilation strategy. Mechanical ventilation with cyclic air-handler operation can also lower the average concentration of both point source and distributed source contaminants, but can still produce unacceptably high peak concentrations from point sources. Further research is necessary to evaluate these issues over a wider range of residential floor plans, ventilation system configurations, and weather. Research to create a tool that can evaluate the simultaneous IAQ and energy implications of coupled space-conditioning system operation and ventilation is needed.

Enhancing the Design Guide for Energy Efficient Research Laboratories. *JONATHAN WINKLER (James Madison University, Harrisonburg, VA 22807) GEOFFREY BELL (Ernest Orlando Lawrence Berkley National Laboratory, Berkley, CA 94720)*

Laboratory facilities consume extreme quantities of energy to provide conditions required for adequate research, and to ensure a high level of worker safety. In a world where energy is a limited supply, laboratories must be designed to operate as efficiently as possible. Through the "Design Guide for Energy-Efficient Research Laborato-

ries" designers can discover where and how energy savings can be made. When originally written in 1996 the design guide was viewed as a useful tool in aiding in the design of efficient labs. With the addition of pictures, diagrams, drawings, and Internet links to outside sources, the Design Guide will prove to be a more effective design tool. These pictures and diagrams being added to the Design Guide were found by conducting a search of related Internet web pages. Power Point presentations used in training by the creators of the Design Guide also contained various pictures and diagrams that will be incorporated into the Design Guide. Drawings were made when a required diagram could not be found and these were constructed using Auto CAD software. The additions made to the Design Guide will be implemented in September 2001. The effectiveness of the design guide is expected to increase.

Developing User Documentation for Human Engineering Design Review Software. *PA-YI JACKIE WU (State University of New York, Stony Brook, Stony Brook, NY 11790) WILLIAM S. BROWN (Brookhaven National Laboratory, Upton, NY 11973)*
User documentation is an essential part of a software program. However, it is often an afterthought for various reasons. Writing user documentation is not a simple task. A careful product analysis and user population definition can help to increase the usability of the user documentation. Conventions need to be adapted or formulated, in a cumulative fashion, and have to be used consistently throughout the documentation. It helps the users to learn and adapt to the user documentation. Conventions also help to speed up the process of information seeking and problem solving for the documentation users. In this project, literature on the design of user documentation was reviewed. Among the types of user documentation considered were reference manuals, job performance aids, and tutorials. Conventions have been categorized into three different levels: Document-level organizations of user documentation including the title and headings give users a clear and straightforward view about the content of the documentation; Page-level organizations including margin and justification of paragraph helps document users to focus; and Line-level organizations like typography provide users cues/patterns while they are tracking down the desired information. The information developed in this research will be the basis for user documentation that will accompany a computer program to support human engineering design reviews. This documentation, along with a short tutorial, will help users of the review guideline to learn about the program, master the different functions, and navigate within the program effectively.

Measurement of NST Superconducting Tapes in the Presence of an Applied Magnetic Field. *MARCUS YOUNG II (University of Tennessee, Knoxville, Knoxville, TN 37996) JONATHAN DEMKO (Oak Ridge National Laboratory, Oak Ridge, TN 37831)*
The ability of high temperature superconductors (HTS) to maintain superconducting properties in the presence of a magnetic field must be known for their use in present and future HTS applications. Although the critical current differs according to the manufacturing process, the critical current of HTS tapes generally degrade as the applied magnetic field increases. NST (Nordic Superconductor Technologies) superconducting tapes were constructed from a silver-metal alloy consisting of BSCCO-2223. V-I measurements of these tapes were performed at the Oak Ridge National Laboratory at 77K under DC operating conditions while in the presence of an applied magnetic field. A superconducting cryogenically-cooled magnet was used to achieve the desired magnetic field, and the orientation of the magnetic field was set by the position of the superconducting tape within magnet. V-I curves were taken for both the perpendicular and parallel magnetic field orientations. The critical currents where then calculated and plotted versus magnetic field.

ENVIRONMENTAL SCIENCE

Evaluations of Sagebrush Die-Off on the Hanford Site. *SHELLEY ALONGI (Washington State University, Tri-Cities, Richland, WA 99352) JANELLE L. DOWNS (Pacific Northwest National Laboratory, Richland, WA 99352)*
In 1993, Hanford Site biologists noticed extensive areas where Wyoming Big Sagebrush (Artemisia tridentata ssp wyomingensis) plants were dying. Big sagebrush is a vital component of the shrub-steppe plant community with many animals relying on if for food and shelter. Six monitoring transects were installed in early 1997 with 5

inside the effected area and one control plot. In December 1997, seedlings raised in-house were transplanted inside and outside the effected area. In March 2001, a direct seed trial was started. The monitoring transects and the transplanted sagebrush have been monitored every year since 1997. Analysis of the data for both of these trials indicates the affected area is still in decline. The area of decline may also be spreading, as the control transect for the monitoring trial has been declining in a similar pattern to the other five transects. The direct seeding trial had no seedlings emerge. This could be due to the drought this year. It is not clear that seedlings cannot germinate within the effected area. Further monitoring of the seeding trial is necessary to determine the potential for sagebrush germination, recruitment and establishment. The analysis results indicate that a new control plot for the monitoring trial maybe needed, and that a new map of the affected area might show patterns and direction of spread of the die off.

Determination of LC50 in Medaka Fish, Oryzias latipes. *YAHAIRA ARROYO (University of Puerto Rico, Cayey, Cayey, Puerto Rico 00731) RICHARD SETLOW (Brookhaven National Laboratory, Upton, NY 11973)*
It is hypothesized that pesticides can cause mutagenesis in living organisms. The purpose of this experiment was to determine the LC50 of pesticide Acetochlor for Medaka fish (Oryzias laptipes) at different times. Thirty adults fish Medaka HNI were separated equally into five, 400 mL beakers. Two hundred milliliters of filtered aquarium water were used at 4 different concentrations of Acetochlor (2.50mg/L, 12.50mg/L, 25.00mg/L, 50.00 mg/L). After placing the fish in each one of the beakers with different concentrations, the number of fish was counted at selected times (30 minutes, 15 hours, 24 hours, 40 hours, 48 hours, 72 hours, 96 hours, 120 hours). The time in which each fish died is used to determine the LC50 that is the lethal concentration of Acetochlor in which 50% of the fish died at a given time. Medaka fish will survive in concentration of up to 2 mg/L Acetochlor for 72-96 hours or 20 mg/L for 15 hours.

Usage of Infrared LED and DataLogger as an Air Sampling Device. *ANGELA AYON (Yakima Valley Community College, Yakima, WA 98902) RANDY R. KIRKHAM (Pacific Northwest National Laboratory, Richland, WA 99352)*
An air sampler is used to measure the concentration of a certain substance in the air. Examples of two that are used at the Yakima Training Center by Randy R. Kirkham are the mini-vol and sequential sampler. These samplers are set up at various locations with various natural surroundings. My mentor and I prepared an air-sampling device with equipment that was readily available in hopes of producing an inexpensive and accurate road dust monitor sampler. The equipment we used consisted of the following: 1 Campbell Scientific data ram, 2 infra-red Light Emitting Diodes that were mounted on tri-pod stands, 1 Kodak PC 290 digital camera, and 1 Sony digital motion camera. The experiment setup occurred on a fairly dusty road just out of canton-ment at the Yakima Training Center. Infrared eyes were positioned on opposite sides and several feet away from the road. The sender was wired to the DataLogger and Kodak digital camera. The receiver was connected to a 12-volt power source. The program that ran from the DataLogger logged data whenever the signal was broken and took a picture at that exact moment. Located inside the vehicle were two DataRams of PM size 10 and 2.5. The DataLogger recorded time the signal was tripped, time the signal came back on, and the voltage difference between the two eyes. After viewing the results, several factors affecting accuracy were distinguished. The results of this experiment proved the setup to be an inexpensive dust sampler that will be used in future research.

Land Use/Land Cover Map of the Central Facility of ARM Program in the Southern Great Plains using DOE's Multispectral Thermal Imager (MTI) Satellite Images. *SUSAN BAEZ-CAZULL (University of Puerto Rico, Rio Piedres, San Juan, Puerto Rico 00931) ALICE CIALELLA (Brookhaven National Laboratory, Upton, NY 11973)*
Scientists studying global climate change collect and analyze data from a large array of instruments to study the effects and interactions of sunlight, radiant energy, and clouds on temperatures, weather and climate. Land Use/Land Cover maps provide information about soil moisture, land surface, and plant growth. This information can be used as ancillary data for instruments measuring energy balance, for

studies in soil moisture and research on carbon fluxes affected by the vegetation. In this project, three satellite images from DOE's Multispectral Thermal Imager (MTI) taken in different seasons of 2000 provided the information to create a Land Use/Land Cover Map of the Central Facility of ARM site in the Southern Great Plains. Vegetation indices (NDVI) and Principal Components Analysis (PCA), along with ancillary data including Digital Orthophoto Quarter Quadrangles (DOQQs), other land maps, personal communications, and harvest tables were used to label the classes to create the final Land Use/Land Cover map. The 14 classes map, which represent a seasonal land cover, was created using a combined Multitemporal plus NDVI plus PCA image. The classes that are static (forest and water) were easily determined by their strong spectral and spatial characteristics in the NDVI, PCA, Near Infrared (NIR) and true color images. While the classes that change over the season (pasture/grass/hay, bare soil/buildings, and fallow) were the classes with the most confusion, due to their similar spectral characteristics. To improve this Land Use/Land Cover map additional ground truth data for 2000 will be needed.

Effects of Soil Particle Size Distribution on Post Fire Vegetation.
SARAH BAKER (University of Washington, Seattle, WA 98105) MICHAEL SACKSCHEWSKY (Pacific Northwest National Laboratory, Richland, WA 99352)
The 2000 Hanford wildfire greatly altered the vegetation on much of the Hanford site. Vegetation re-growth has shown interesting patterns in some areas. One such site, which is west of the 200 W Area, has intermingled patches of distinctive vegetation types. Several of these patches are dominated by cheatgrass (Bromus tectorum), others by Russian thistle (Salsola kali), while others have little vegetation besides scattered Russian thistle and bur ragweed (Ambrosia acanthicarpa). Since the particle size distribution of a soil, especially the percent fines, can influence plant communities, this study was conducted to determine if the soil texture differed under the various vegetation types and if similar vegetation types shared similar soil. To do so, soil samples were collected and particle size analysis performed. Vegetative canopy coverage of each area was also determined. It was shown that the patches dominated by Russian thistle had significantly higher percent fines in the soil than the other vegetation areas. The other areas had little difference in their particle size analyses. Thus, the results are somewhat inconclusive. It appears that while soil texture may have influenced vegetation patterns on this site, other factors probably influenced it as well.

Development of Educational Materials for Fuel Economy Website.
REBECCA BROCKWELL (Florida State University, Tallahassee, FL 32306) DAVID L. GREENE (Oak Ridge National Laboratory, Oak Ridge, TN 37831)
The Internet is becoming a more popular resource for educators. One of the biggest challenges for those using the Internet in the classroom is the lack of easily accessible curriculum that utilizes the current data available on the web. Science Educators are being encouraged by the National Science Education Standards to encourage students to consider science as a part of the larger society and as a means to consider societal problems. As a result of this new thrust, more schools are adding environmental studies as a part of the science curriculum. A website, fueleconomy.gov has been developed by DOE to provide up to date information for consumers about vehicle energy use and greenhouse gas and pollutant emissions. The site allows consumers to research the fuel economy of cars from model year 1985 to present. An educational module including a lab activity was developed for the website to encourage students to consider the impact personal vehicle choices have on the production of greenhouse gasses. The students calculate the greenhouse gasses produced by their own vehicle. They then move outside the classroom to examine vehicle exhaust. By collecting exhaust in a plastic bag and using the collected gases to extinguish a candle, students are able to visualize the vast quantities of oxygen-depleted gasses vehicles produce. Students are encouraged to consider the impact of personal and group choices on the environment. The webpages will be monitored to determine the popularity of the new materials.

Evaluation of Fuji Prescale Pressure Sensitive Film for Assessing Damage to Fish from Turbine Passage.
JESSICA BUSEY (Middle Tennessee State University, Murfreesboro, TN 37132) GLENN CADA (Oak Ridge National Laboratory, Oak Ridge, TN 37831)

The passage of fish through hydroelectric turbines is a very important issue to energy production. As a fish passes through a turbine it can experience several different kinds of injury mechanisms (strike, grinding, shear, and pressure changes) and the magnitude of these forces is often unknown. Fuji Prescale Pressure Sensitive Film (PSF) can make an accurate and permanent record of pressures applied to the surface. By sending the PSF through the turbine, the pressures and forces experienced by the fish could be estimated, specifically those related to strike. The PSF must be put in a waterproof package due to the effect of water on the film. The Fuji Prescale Pressure Sensitive Film comes in various weights, enabling it to measure a wide range of pressures. By stacking the film, it can measure a wider range of pressures and better assess the pressures the turbine exerts on the fish. It was found that LLW and LW Fuji Prescale Pressure Sensitive Films were not significantly affected by the waterproof packaging or by stacking several layers of film on top of each other. Fuji Prescale Pressure Sensitive Film is sensitive to temperature and humidity; however, due to the difference in slope the Analysis of Covariance (ANCOVA) could not detect a difference in temperatures. Because humidity can be controlled and recorded during the waterproof packaging of the PSF it is not perceived as a problem. Fuji Prescale Pressure Sensitive Film will work well to test the pressures experienced by turbine passed fish and may aid in development of more fish friendly turbines.

Understanding Computed Microtomography.
RYAN BUTRYN (Jamestown Community College, Jamestown, NY 14701) KEITH W. JONES (Brookhaven National Laboratory, Upton, NY 11973)
The discovery of the X-ray and its ability to pass through opaque objects without damage has led to many important biological discoveries in the last century. Using the high intensity X-ray beam generated by the National Synchrotron Light Source at Brookhaven National Laboratory coupled with imaging computers, microtomography allows the viewing of previously unexplored microstructures. This technology proves useful in areas of geology, oceanography, and environmental biology with current research involved in analyzing porosity of sandstone samples. The recently developed stereographic viewing technology compliments computed microtomography producing stunning images that seemingly jump off the screen. Collecting microtomographic data suitable for visualization is a learned process involving control of beam energy in relation to sample density. Experimenting with instrument capabilities deepened understanding of synchrotron light and imaging technology. Computed Microtomography offers itself as a tool capable of supporting the three-dimensional data visualization field.

The DeltaQ Project: Quantifying Duct Leakage.
BRIAN CARROLL (University of Texas, Austin, Austin, TX 78704) DARRYL DICKERHOFF (Ernest Orlando Lawrence Berkley National Laboratory, Berkley, CA 94720)
Existing HVAC duct systems in residential buildings are currently only 50 - 75% efficient due to air leakage to the outside environment. The recent mismatch of energy supply and demand has created an insurgence to increase the efficiency of such systems. The DeltaQ test measures the change in airflow through duct leaks (holes, cracks, poor construction) as the pressure across the leaks is varied in a controlled manner. With the HVAC system off, the house is pressurized using an apparatus called a Blower Door. Pressure transducers are placed at the inlet of the fan so that the pressure drop across the device can be measured. The fan is calibrated to produce a particular airflow rate for a given pressure drop. The fan speed is varied using computer software and pressure/flow data points are recorded. The test is then repeated with the HVAC system on. Analytical methods are then employed to curve fit the data with the least possible error. The resulting equation will determine the zero pressure point, which corresponds to the airflow out of the system's ductwork into the outside environment. My work focused on the precision of the test. My objective was to determine the repeatability and accuracy of DeltaQ test method. This was accomplished by installing various known leaks on an existing system located at an on-site testing facility. Numerous tests were performed and the results were compared to the expected leakage values. Results showed the test to be highly repeatable and accuracy was generally within 10% of the known value. The test has

recently been proposed as a new ASTM standard for duct leakage measurements.

Cleanroom Energy Benchmarking. *ZHONGNING CHEN (Cosumnes River College, Sacramento, CA 95823) TENGFANG (TIM) XU (Ernest Orlando Lawrence Berkley National Laboratory, Berkley, CA 94720)*
Cleanrooms are used in a wide range of industries, universities, and government facilities nowadays. Electronics and biotechnology industries, which are important to the economy of California, are heavily dependent upon energy-intensive cleanroom environments for their research and manufacturing. Energy use for environmental systems in these cleanrooms is high, as is the energy use for processes within cleanrooms. Pacific Gas and Electric Company (PG&E) and Lawrence Berkeley National Laboratory (LBNL) have been collecting energy use benchmarking data for energy intensive cleanroom facilities. The purpose is to provide useful energy metrics and measured data to building operators to enable them to assess their building systems performance. Meanwhile best practice information is expected to emerge which will provide awareness of the opportunities for continual improvement. Once data is collected, it is entered into a database for further evaluation and analysis. My summer research project mainly focuses on evaluation and analysis of the benchmarking data, which includes: 1) evaluate the completeness and accuracy of the benchmarking data; 2) improve the integrity of the benchmarking database; 3) conduct analysis on energy performance of environmental systems by generating charts for major metrics; 4) automate mass data analysis by using Microsoft Visual Basic; 5) document work progress & suggestions for further data analysis.

Ozonation of Produced Water from the Oil Industry. *MICHELE DINSMORE (Tennessee Technological University, Cookeville, TN 38505) COSTAS TSOURIS (Oak Ridge National Laboratory, Oak Ridge, TN 37831)*
The oil industry, in the process of pumping oil from wells, generates "produced water" which is usually seawater contaminated with various organic substances. Before produced water is returned to the environment, it needs to be treated for organics. One method to eliminate organic substances from produced water is oxidation, using ozone. Several experiments have been conducted in this study to investigate the effectiveness of ozone in oxidizing organic substances in real produced water from two oil companies. In these experiments, ozone was produced by a corona-discharge ozone generator and flushed through a large batch reactor containing a stir bar. Produced water was then injected in the reactor with 50-mL syringes to a total volume of 200 mL. Gas and water samples were taken at varying intervals from 0 to approximately 1600 minutes. Sampling events were adjusted depending upon the disappearance of ozone in the gas phase. Samples were analyzed for concentration of CO_2, extractable organics, ozone, and organic acids. In some experiments, the produced water was heated to 80 degrees C to attempt to increase the removal of extractables. Results show that organic compounds can be successfully removed from produced water with the use of ozone. Heating the produced water improved the rate of removal. This information will be used for preliminary design and cost estimation.

Salt-Balance in California's San Joaquin Valley. *DAVID FOLLETTE (Princeton University, Princeton, NJ 08544) NIGEL QUINN (Ernest Orlando Lawrence Berkley National Laboratory, Berkley, CA 94720)*
The San Joaquin Valley is known for its fertile soil and highly productive farmland. However, with little rainfall, much of the agriculture is supported by groundwater pumping and federal and state surface water deliveries. Although the water from the Sierra Nevada snowmelt carries relatively little salt, large volumes of water use, coupled with little drainage outflow, create a serious salt balance problem. As salt accumulates in the soil, it becomes less fertile, crop yields decrease, and eventually the land is no longer economic to use. We approached the problem with a two-part solution. First, we set up and upgraded water quality monitoring stations on some of the smaller tributaries of the San Joaquin River. With a number of sensors at each site, water and salt flows are calculated. With this data, it will be easier to discriminate between the saline water sources, and work to minimize those discharges. Some of these sites required the design and construction of broad-crested weirs to act as water measurement control structures. Second, the stations were set up with modems and telephone connections for remote access to the data. In turn, with a computer and a modem, I set up a real-time system that automatically gathers data from each of the individual remote stations, creates graphs, and posts the data to the Internet. Agricultural users, bound to monthly load targets, can now monitor their discharges in real-time and ensure that they meet environmental standards. As this project continues to gather data, the salt-balance problem will be better understood and more easily solved.

In-situ X-ray Absorption Spectroscopy on Mn-Oxide based Lithium Battery Electrodes. *ALISON FOWLKS (University of Michigan, Ann Arbor, MI 48104) ARTUR BRAUN (Ernest Orlando Lawrence Berkley National Laboratory, Berkley, CA 94720)*
In-situ X-ray Absorption Spectroscopy was performed to investigate structural changes in Lithium Manganese Oxide, a lithium battery electrode material during electrochemical lithiation. Various spectroscopy techniques, such as XANES and EXAFS, were employed to monitor the changes in the electronic and crystallographic structure during the deep discharge process. XANES was used to quantitatively study the chemical shift of the spectra and to determine the average manganese oxidation state before and after discharge. EXAFS data provided such information as the inter-atomic distances and coordination numbers. Analysis of the EXAFS spectra showed the occurrence of a crystal phase transition from a cubic lattice to one of lower symmetry.

Air Pollution Impacts and Prevention. *STACI GARCIA (Southwestern Oklahoma State University, Weatherford, OK 73096) ROYA STANLEY (National Renewable Energy Laboratory, Golden, CO 80401)*
The quality of our air is of utmost concern. Increasing uses of fossil fuels has caused increased levels of air pollutant emissions. The notion that consumers share responsibility for this pollution has been widely accepted. Fossil fuel emissions are responsible for adverse health effects common in children, the elderly and athletes. Studies were collected that have detailed the relationship between harmful air pollutants and negative health effects. The results of the studies, presented in this paper, have provided conclusive evidence of the link between air pollution and adverse health. Energy efficiency strategies and renewable energy technologies provide possible solutions to lowering pollutant emissions. Studies presented here show that wind and solar technologies are cost competitive with traditional energy sources and will have a positive impact on the future of humans and the environment. These renewable energy sources are continually replenished and are free to consumers after an initial investment. Further work is required to implement more stringent emission standards. Added research in renewable technologies is also warranted. These efforts will benefit the well being of humans, the environment and our natural resources.

Woodlands at Brookhaven National Laboratory. *JOSE GOMEZ (University of Puerto Rico, San Juan, Puerto Rico 00931) TIMOTHY GREEN (Brookhaven National Laboratory, Upton, NY 11973)*
The recent wildfires in New Mexico have highlighted the need to assess the fire potential of woodlands. In order to address this need data was collected at Brookhaven National Laboratory during the summer of 2001. The data included leaf litter, ladder fuel, hour fuels, and living vegetation. The woodlands analyzed included white pine, pine/oak, and oak/pine forests. A Rapid Environmental Assessment was carried out in each BNL sites in order to establish the factors necessary to determine fire potential. These factors include a consideration of both internal (ladder fuel, leaf litter, and duff) and external variables (temperature, wind speed, wind direction, and moisture). Although not considered here, terrain and canopy should be evaluated. Quadrants were established and random points sampled within each quadrant in all study sites. Fuel load was determined and the percentage of each component (pine needles, oak leaves, twigs etc.) noted. The understory was determined and the percentage of live vegetation was noted as a fire inhibitor. The depth of the duff was measured. Ladder fuel was determined as well as the percentage of one, ten, and one hundred hour fuels. The data indicates that there are distinct differences in the fire potential of each of these woodlands. This data has been used to prepare a predictive equation, which has

the potential for accurately predicting the potential for fire in various woodland communities.

Reducing Boron Toxicity by Microbial Sequestration.
TRACY HAZEN (University of California, Davis, Davis, CA 94533) TOMMY J. PHELPS (Oak Ridge National Laboratory, Oak Ridge, TN 37831)
While electricity is a clean source of energy, methods of electricity-production, such as the use of coal-fired power plants, often result in significant environmental damage. Coal-fired electrical power plants produce air pollution, while contaminating ground water and soils by build-up of Boron, which enters surrounding areas through leachate. Increasingly high levels of Boron in soils eventually overcome Boron tolerance levels in plants and trees resulting in toxicity. Formation of insoluble Boron precipitates, mediated by mineral-precipitating bacteria, may sequester Boron into more stable forms less available or toxic to vegetation. Results have provided evidence of microbially-facilitated sequestration of Boron into insoluble mineral precipitates. Analyses of water samples taken from ponds with high Boron concentrations showed algae present contained 3-5 times more Boron. Boron sequestration may also be facilitated by the incorporation of Boron within algal cells. Experiments examining Boron sequestration by algae are in progress. In bacterial experiments with added ferric citrate, the reduction of iron by the bacteria resulted in an iron-carbonate precipitate containing Boron. An apparent color change showing the reduction of amorphous iron, and the precipitation of Boron with iron, were more favorable at higher pH. Analysis of precipitates by x-ray diffraction, scanning electron microscopy, and inductively coupled plasma mass spectroscopy revealed mineralogical composition and biologically-mediated accumulation of Boron precipitates in test tube experiments.

A Study of Genetic Diversity Due to Spatial and Temporal Differences Among Southern "Alamo" Switchgrass (Panicum virgatum L.) Sites.
ERIN HOTCHKISS (Oxford College of Emory University, Oxford, GA 30054) LEE E. GUNTER (Oak Ridge National Laboratory, Oak Ridge, TN 37831)
As environmental concerns continue to surface due to the pollution caused by (and the depletion of) fossil fuels, scientists are looking more and more toward renewable energy sources. Switchgrass (Panicum virgatum L.) is one of the most important potential sources of ethanol fuel, which burns much cleaner than fossil fuels. However, the conversion of switchgrass material into ethanol is still not cheap or efficient enough to compete with the non-renewable energy sources that we use today. We need to better understand the genetic make-up of switchgrass in order to enhance positive switchgrass characteristics needed for quicker ethanol conversion and also to find and manipulate genetic traits that allow for quicker growth and higher crop yields. The purpose of this experiment is to identify 1) whether spatial and temporal changes in gene frequencies are occurring in switchgrass plantings, and ultimately 2) whether a marked differentiation in gene frequencies is having a positive or negative effect on productivity in "Alamo", a switchgrass cultivar that has been adapted to the southern states. Using random amplified polymorphic DNA (RAPD) markers, changes will be assessed in marker frequencies among "Alamo" genotypes collected from four plots at five different research sites (Virginia Tech [2 sites], VA; Lexington, KY; Knoxville, TN; and Jackson; TN) in the southeast over a seven year period. Genetic differences within and among populations and an assessment of changes in gene frequencies will be discussed.

Global Change and Forest Physiology Impacts of Elevated Atmospheric CO_2 on Photosynthesis in the Low Light Environment of the Forest Understory.
REBEKAH HUTTON (University of Tennessee, Knoxville, TN 37916) CARLA GUNDERSON (Oak Ridge National Laboratory, Oak Ridge, TN 37831)
The effects of increased atmospheric CO_2 in the forest understory have been studied very little in comparison to the effects in high light environments. It is, however, important to look at the effects because plants in the understory depend on their ability to carry out photosynthesis both when there is very limited light and when there is direct sunlight. Elevated CO_2 might have a bigger impact on photosynthesis at low light because it could cause plants to make better use of limited light availability. This hypothesis was tested in five forest plots, three under ambient conditions, and two with elevated CO_2 provided by a free-air CO_2 enrichment facility. The impact of elevated CO_2 exposure was measured in seedlings of Acer negundo (boxelder) and Lindera benzoin (spicebush). Measurements of photosynthesis and stomatal

conductance at multiple light levels were taken from six different trees of each species in each plot. In elevated CO_2, light saturated photosynthesis was 22.5% and 41% higher than it was in ambient CO_2 seedlings in A. negundo and L. benzoin, respectively. Increases in low light were similar to those at light saturation, ranging from 27.5% to 39%. High CO_2 still reduced stomatal conductance in low light by approximately 9.9% to 11%. However, most of these differences were not statistically significant. Thus, impacts of increasing atmospheric CO_2 may be minimal for the forest understory.

Bioprocess with Filamentous Fungi.
SHANA LACROSSE (Pima Community College, Tucson, AZ 85730) ROBERT A. ROMINE (Pacific Northwest National Laboratory, Richland, WA 99352)
The goal of this project is to achieve the ability to use filamentous fungi for the production of new chemical products. The metabolic versatility of fungi is not well exploited by the fermentation industry. It is used on a limited basis to produce organic acids, industrial enzymes and antibiotics. There is a need to develop fermentation strategies using filamentous fungi for the production of new products. This research involves manipulating filamentous fungi at an early stage (in shake flask experiments) and later in bench top fermentors. This work is targeted at maximizing the production of specific organic acids that can be used as a feedstock to catalytic conversion processes to produce specialty chemicals of interest to industry.

Sorption of Cesium on the Upper and Lower Sands of the Upper Ringold Formation and the Plio-Pleistocene.
JENNIFER LADD (Tennessee Technological University, Cookville, TN 38505) PHILIP M. JARDINE (Oak Ridge National Laboratory, Oak Ridge, TN 37831)
Large amounts of radioactive, chemical and mixed wastes were generated for decades at the Department of Energy Hanford reservation located in Richland, Washington. Underground waste tanks were utilized to dispose of a variety of radionuclides and mixed wastes in concentrated sodium nitrate. Leaks have resulted in discharge of radionuclides to the surrounding vadose zone, and 137Cs have been detected at more than 38m in depth and more than 30m from the source. Samples of the Miocene age upper Ringold formation and the Plio-Pleistocene caliche layer were taken from an area near the Hanford site. Both disturbed and undisturbed samples were obtained in order to quantify the coupled hydrologic and geochemical mechanisms contributing to contaminant mobility. The goal of this study was to quantify Cs^+ sorption onto each solid phase. Isotherms were determined using batch techniques for initial Cs^+ concentrations ranging from 0-20 ppm. The effects of background ionic strength were investigated by performing experiments at two ionic strengths, 0.02M and 0.2M. The effects of background cation on Cs^+ sorption were investigated using two different matrices, Ca(NO3)$_2$ and NaNO$_3$. The overall distribution coefficients (K_d) follow the trend: 0.02MNa>0.02MCa>0.2MCa>0.2MNa. Overall K_d's reflect 2:1 ratio that would be expected based on the charge of the matrix cation. This enables the prediction of Cs^+ sorption as a function of ionic strength. The 0.2M ionic strength Ca^{2+} matrix is best for transport experiments based on analytical difficulties with Na^+ and similarities of results. These results now make it possible to predict transport times through the large undisturbed cores.

Dissolution Kinetics of LAWA44, a Candidate Low Activity Waste Glass, In Relation to Solution pH.
SUZIE LANCASTER (Truckee Meadows Community College, Reno, NV 89557) JONATHAN ICENHOWER (Pacific Northwest National Laboratory, Richland, WA 99352)
Secure storage of radioactive waste from the Cold War atomic defense legacy is a pressing environmental concern. Current Hanford remediation plans call for vitrification of the low activity portion of liquid waste and subsequent repository emplacement. Corrosion resistance of Immobilized Low Activity Waste (ILAW) Glass has been tested for varying environmental factors; our focus was the range of potential interstitial pore water pH. We used a single-pass flow through apparatus to measure dissolution rates for LAWA44, a candidate waste form, using a range of solutions from pH 7 to 11. Analysis of effluent samples indicates that the power law coefficient, eta, for the dependence of the rate on solution pH is 0.43. Therefore, the constant temperature rate in dilute solution can be written as rate = $k_o(aH^+)^{0.43}$, where k_o is the intrinsic rate constant and aH^+ is the activity of the hydronium ion. The value of eta is identical to that of other silicate

glasses and minerals. These results imply that the dissolution mechanism is the same for all silicate materials, regardless of crystalline structure and Si-O bond length or angle.

Modification of an Individual-Based Model for Use in Biodiversity Studies. *ALLEN MCBRIDE (Swarthmore College, Swarthmore, PA 19081) MICHAEL HUSTON (Oak Ridge National Laboratory, Oak Ridge, TN 37831)*
The study of the effects of species diversity on ecosystem processes has been controversial among ecologists in recent years. Several studies designed to manipulate species number have focused on herbaceous plant growth over periods of a few years. However, critical ecosystem issues involve large trees over periods of centuries. Such experiments are difficult to conduct, and will not produce results for decades or longer. Computer modeling can broaden the study of biodiversity by simulating the growth of mixed-species forests over periods of several centuries. An individual-based model of forest growth developed at ORNL, called LINKAGES, was modified for simulation of biodiversity experiments to investigate the ecosystem effects of different numbers and types of trees. Some modifications were made with the aim of improving the accuracy of the model generally, such as the reformulation of growth rates for tree species based on tree-ring data. Other modifications were made specifically to facilitate biodiversity studies, such as an option to grow several forests of one species each. It is hoped that this modified forest model can be used to explore unanswered questions about the long-term effects of biodiversity.

Analysis of the current state of sediment and chemical erosion as compared to the pre-agricultural state of the Silver Creek Watershed in Green Lake County, Wisconsin. *ERIN MCCANDLESS (Michigan State University, East Lansing, MI 48825) GUSTAVIOUS P. WILLIAMS (Argonne National Laboratory, Argonne, IL 60439)*
The EPA has become increasingly interested in watershed issues. The Silver Creek watershed in southern Wisconsin is one of the highest priority watershed restoration projects in the state. In this study 10 years worth of data for rainfall and erosion events were modeled and analyzed for sediment, erosion, and chemical content with both temporal and spatial group analysis. This watershed was studied to not only benefit its lake and streams, but also to serve as a model for future restoration projects. The results from the temporal group show that as the amount of agricultural land use increases, there is an increase for all types of erosion and an increase in the number of large-scale erosion events. The spatial analysis showed that the location of agricultural land within the watershed had no substantial influence on the sediment and nutrient loads flowing into the creek and lake. This study shows that the current agricultural practices are not adequate in preventing erosion.

A Transition from Tango to Java. *MONG KON MO (Fresno City College, Fresno, CA 93741) JONATHAN KOOMEY (Ernest Orlando Lawrence Berkley National Laboratory, Berkley, CA 94720)*
The End-Use Forecasting Group has developed a number of web applications (i.e. Home Energy Saver and Home Improvement Tool) using Tango. However, the group came to a decision that they wanted to port their Tango applications to Java for deployment on a Java Application Server because of the Java platform's increased stability, portability, and performance. Since the group does not have any Java programmers, they are consulting a private contractor, who will develop the Java applications. As an intermediate step in the transition from Tango to Java, a development Java Application Server (Orion) was setup and a connection between Orion and the group's Oracle database was verified with a sample Java 2 Enterprise Edition (J2EE) compliant application. As the Java applications are developed by the private contractor, the development server can be used to verify that the applications are functioning properly before being deployed on a production server.

Microencapsulation of Volatile Atmospheric Particles. *NATHAN MOORE (University of Washington, Seattle, WA 98195) JAMES P. COWIN (Pacific Northwest National Laboratory, Richland, WA 99352)*
Volatile aerosols, such as ammonium nitrate, sulfuric acid, and tarry organic particles, are known to comprise a large portion the total airborne particulates in certain polluted areas, such as Houston, and yet are difficult to study due to their short shelf-life and high volatility

under typical operating conditions of SEM/EDX and other laboratory analyses. This work aims to improve the method of field particle collection used by Laskin, et al, by encapsulating collected particles within a thin film to substantially reduce their rate of evaporation, thereby allowing more accurate determination of particle size, composition, and number using SEM/EDX laboratory analysis. Several methods of encapsulation are screened, including passive and electrostatic vapor deposition, and evaporation of a solvent carrier. Each is presented as feasible with future refinements.

Indiana Harbor Canal Dredging Project and East Chicago High School. *JAMES O'SHAUGHNESSY (Harry S. Truman College, Chicago, IL 60639) GUS P. WILLIAMS (Argonne National Laboratory, Argonne, IL 60439)*
Education today is insufficient in teaching students basic skills in how to make informed decisions about issues that affect their daily lives. There are alternative methodologies that can address this shortfall in the traditional teaching methods, however there are significant barriers to implementing these methodologies, one of the barriers being time intensification of teaching. One alternative methodology is constructivism. This methodology involves teachers and students working together collaboratively to seek information pertaining to issues, evaluating the information for validity and forming and defending decisions based on the information. This allows for students to learn how to find and evaluate information and then make informed decisions about issues that they will face in their everyday lives. Constructivism is not, at present, widely used in classroom, but more and more curriculums should be written using this proven methodology.

Columbia River Recreational Survey 2001 - General Overview. *RACHEL PARKHILL (Eastern Washington University, Cheney, WA 99004) AMORET BUNN (Pacific Northwest National Laboratory, Richland, WA 99352)*
PNNL is conducting a research study for the U.S. Department of Energy. The Columbia River Recreational Survey was designed to determine the type of recreational activities conducted on the Columbia River. It is also to estimate the impact of recreational activities on the regional economy. Survey teams visited 25 sites and conducted interviews and observations. The survey aspect of our research helped us determine the number of hours and day's people spend on the river and also their recreational activities on or around the river. The observational aspect of our project aided us in determining which sites are most popular with out-of-state and in-state individuals and the activities that were engaged in at each site. All the critical information gathered by our survey team may be used in both human health risk assessment and the economic impact predictions at the U.S Department of Energy's Hanford site.

Physiological and Kinetic Characterization of Octane-Degrading Bacteria. *NICOLE PORTLEY (Boston College, Chestnut Hill, MA 02467) WILLIAM T. STRINGFELLOW (Ernest Orlando Lawrence Berkley National Laboratory, Berkley, CA 94720)*
Several bacteria capable of degrading n-alkanes have been isolated. These bacteria were grown in mixed cultures derived from enrichments of Mission Valley, California, soil. Several strains can use octane as a carbon source. Studies have focused on the physiology of these octane-degrading bacteria. Growth curve analysis allowed for differentiation between bacteria types, because log phase growth rates are unique for each strain. Respirometry analysis measured oxygen uptake by cells, which directly correlates with octane metabolism. Kinetic constants were measured for each organism, including the Ks (maximum growth rate) and Vmax (maximum enzyme activity under saturated conditions). Respirometry results demonstrated differences in efficiency among the enzymes, and this variance may indicate the presence of diverse enzymatic pathways. This research will be integrated with genetic analyses (16S rDNA gene and alkB gene) and Fatty Acid Methyl Ester analyses in order to identify and characterize these bacteria. These bacteria are being developed for use in industrial chemical production.

Which Soil is the Better Water Filter? *MIGUEL ROSARIO (Recinto Universitario de Magaguez, Magaguez, Puerto Rico 00681) TERRY SULLIVAN (Brookhaven National Laboratory, Upton, NY 11973)*
The Brookhaven Graphite Research Reactor, the world's first nuclear reactor dedicated to the peaceful exploration, is currently on an

accelerated decommissioning schedule consisting in combining characterization with removal action for various systems and structures. If the characterization can provide enough information, then the canal's concrete structures and most of the soil around it can remain in place. Using the Environmental Visualization System to create three-dimensional images that visualize levels of soil contamination below the underground structures provides an effective tool to show with high confidence the locations where the hot spots (soils beneath the structures contain contaminant concentration above the regulatory clean-ups levels) of contamination are. Visualizations from the canal house and pile display some high concentration of soil contamination. Whereas it is likely that most of the canal soil were not contaminated above the regulatory clean-up levels. A tie-up process including three-dimensional visualization, risk assessments and others characterizations techniques will support an easier planning process including decisions that affect the extent removal and waste designation. With this the Decommissioning Project will have significant savings and reduced waste volumes for off-site disposal.

Development of Entries and Updates to CDIAC Trends Online.
DARIA SCOTT (St. Cloud State University, St. Cloud, MN 56301)
DALE KAISER (Oak Ridge National Laboratory, Oak Ridge, TN 37831)
In the study of global climate change, the scientific community's access to global data is crucial. To accurately gauge trends in global temperature, data must be shared between countries and then made available to the scientists who need to study it. Three sets of data were added to CDIAC's electronic publication, Trends Online. The first is by Russian scientist A.M. Sterin. The second and third were updates to data sets by Jones et al. and Lugina, et al. These data sets were compiled from either stations reporting surface temperature or from radiosonde data. The data were received at CDIAC in raw format. Calculations were done for seasonal and global means. The data sets were formatted and put into data files and graphs. The were then put on web pages with accompanying background information and made accessible via Trends Online. This enables everyone in the world to use this very important data.

Synthesis and Detection of Hydrogen Peroxide and Methyl and Hydroxymethyl Peroxides. *LUKE SHANNON (Dordt College, Sioux Center, IA 51250) JUDY LLOYD (Brookhaven National Laboratory, Upton, NY 11973)*
Knowledge of the concentrations of peroxides in the atmosphere is of interest to the atmospheric chemist. Hydrogen peroxide and organic peroxides are oxidants in their own right, and can also be used as a test of the oxidative capacity of the atmosphere. Several methods of detection were used in our laboratory. One method involves a continuous analyzer that used different reagents and different pH's to identify individual peroxides. Another method involves HPLC separation followed by fluorescence detection of the respective hydroperoxides. The measurements of ambient air indicated the presence of H_2O_2, methyl hydroperoxide, and hydroxymethyl hydroperoxide. In this project, we used both methods to analyze laboratory standards of these peroxides. Due to their explosive nature when pure, a dilute aqueous solution of organic peroxides was desirable. A Co-60 source of γ-radiation was used to provide a dilute aqueous solution of methylhydroperoxide and H_2O_2. Hydroxymethyl hydroperoxide was synthesized in an equilibrium reaction involving HCHO and H_2O_2. These solutions were analyzed after separation by HPLC using fluorescence detection. The same samples were analyzed using the field instrument. Chromatograms from the HPLC method consistently and reproducibly showed the presence of the desired peroxides with adequate separation. The field instrument gave data that indicated the presence of an interfering factor. Elimination of this interference should prove to be relatively forthright. Future study into the HPLC method shows promise as a way to evaluate currently used field equipment and may be a feasible method of field data collection itself.

The Effects of Land Use on Midsummer Soil Respiration in Selected Crop Groups of the Southern Great Plains. *NICOLE STALEY (Modesto Junior College, Modesto, CA 95350) MARC FISCHER (Ernest Orlando Lawrence Berkley National Laboratory, Berkley, CA 94720)*
Land use and management practices have significant impacts on the cycles of carbon in managed ecosystems. In order to understand and predict the effects of current and future land use I measured the soil respiration in plots that represent dominant land use types for the

Southern Great Plains. I used an infrared gas analyzer (Li-Cor 6400), thermocouples, and soil moisture sensors. I used a simple respiration model in which, soil respiration is dependent on the soil temperature, soil organic matter, root biomass, and moisture content of the soil. The laboratory tests confirmed that there are temperature and moisture dependences. The field measurements showed that at this time of year the lack of soil moisture limits respiration to constant low levels, the temperature has less effect, and plant matter (AGB-above ground biomass) increases the respiration level.

Development of a Web-Based Exposure Factors Database for Use in Modeling Contaminant Uptake by Wildlife. *PETIA TONTCHEVA (Wilbur Wright College, Chicago, IL 60634) IHOR HLOHOWSKYJ (Argonne National Laboratory, Argonne, IL 60439)*
Screening level ecological risk assessment provides a rapid but conservative analysis to determine whether a chemical waste poses significant risk to ecological resources at hazardous waste sites. Such assessment typically involves estimating chemical exposure to representative wildlife species. However, one difficulty that risk assessors often encounter is the identification of appropriate species-specific exposure factors for wildlife models. While the Environmental Protection Agency has developed a handbook of exposure factors for wildlife species common to the United States, the handbook lacks wildlife species specifically for the arid environments of North America. In order to provide more accurate and realistic exposure factors for wildlife in arid ecosystems, a database has been developed. This database identifies species-specific exposure factors such as body weight, home range, diet composition, food, water, and soil ingestion rates. Data for 28 wildlife species are obtained from a variety of peer-reviewed publications, books, and agency reports and are incorporated into the database. Additionally, the database has environmental data fields such as location, ecological region, age, sex, season, and habitat, associated with each exposure parameter. Allometric estimators are also incorporated into the database in case of absence of field or laboratory measured data. A web-based user interface has been developed using Cold Fusion@ to provide access of this database to the Internet community. Future development of this web-based tool will include the addition of more wildlife species and the improvement of user interface.

Evaluation of the Success of Bluebird Boxes at Fermilab.
MARIA TORRES (University of Illinois, Chicago, Chicago, IL 60607) ROD WALTON (Fermi National Accelerator Laboratory, Batavia, IL 60510)
At Fermi National Accelerator Laboratory, in Batavia, Illinois, bluebird boxes are posted in various areas around the facility. The key to a successful increase of the bluebird population, with the use of bluebird boxes, is continued monitoring. Along with monitoring, location of the bluebird boxes and the proper design of the box are needed. This research was conducted by using an Euler circuit. Certain bluebird boxes were visited three times a week over a ten-week period. The bluebird boxes that were monitored throughout this research were in four different sections. One was in the Main Ring, another in the Interpretive Trails, another along Road C, and the last one was near Site 38 at Fermilab. Information that was noted from observing the boxes was to see if they are successfully being used by bluebirds. After the data was recorded and analyzed, the outcome was that these bluebird boxes were not successful. Many of the data give different reason why they may have not been successful. Some reasons may have been because the boxes have not been steadily monitored until the research was started, the location of the box and its surroundings, and most of the boxes were not correctly built according to the proper design. Since this is the start of a continuing research, monitoring must be continued in order to maintain and increase the bluebird population.

Columbia River Recreation Survey 2001:Geographic Distribution of Recreational Activities. *KATHLEEN TRUJILLO (Montana State University-Northern, Havre, MT 59501) KENNETH HAM (Pacific Northwest National Laboratory, Richland, WA 99352)*
Although the importance of river-based recreation is acknowledged, little specific information is available about geographic distribution of these recreational activities. This information is needed to assess potential risks to human health, as well as impacts on the local economy of future remediation plans for the Hanford site. The Columbia River Recreation Survey 2001 was designed in response to these needs. Survey teams visited 25 sites and conducted interviews

as well as doing 15-minute observations. The observational part of the survey was intended to supplement the interview questionnaires by quantifying the number of recreationists observed during a 15-minute period at each site. This was to correct for the recreationists who declined to participate (or were inaccessible) in the survey, ensuring the total number of river users is not under-represented. In addition, the observations were used to determine which sites are most popular with out-of-state visitors and which activities are prevalent at each site. Preliminary analysis with Microsoft Excel shows Howard Amon Park had the most out-of-state vehicles (mean =3.5 vehicles), while Columbia Point had the most Washington State vehicles (mean = 50.7 vehicles). Water-based activities such as swimming and boating were the most common forms of recreational activity (mean = 15.7 persons), while shore-based activities such as picnics and walking were less popular (mean = 12.8 persons) and less evenly distributed among the locations. This information may be used in both the human health risk assessment and the economic impact predictions at the U.S. Department of Energy's Hanford Site.

Solubility of Chloromethane in Aqueous Systems Containing High Levels of Biomass. *CHRISTOPHER VODRASKA (Whitman College, Walla Walla, WA 99362) JOHN W. BARTON (Oak Ridge National Laboratory, Oak Ridge, TN 37831)*
Chloromethane, also known as methyl chloride, is a common environmental pollutant in landfills and waste sites due to its use in the production of silicones, butyl rubber, methyl cellulose and agricultural chemicals. Although various health effects are associated with chloromethane even at low concentrations, very little data exist for the solubility of chloromethane in systems other than pure water. Reaction vessels were constructed containing varying concentrations of yeast. Chloromethane was injected into the headspace of these reactors and given time to equilibrate between the headspace and the aqueous phase. The headspace was then sampled and tested by gas chromatography to measure the amount of chloromethane present. These data were used to calculate Henry's Law constants for each reactor system as a function of biomass/yeast concentration. Constants were then compared to literature and experimental values for the solubility of methyl chloride in water. Preliminary results show that the solubility of chloromethane in water is increased by the presence of biomass.

Genetic Regulation of Selenium Detoxification in Bacillus subtilis. *GENEVIEVE WALDEN (Fresno City College, Fresno, CA 93722) TERRANCE LEIGHTON (Ernest Orlando Lawrence Berkley National Laboratory, Berkley, CA 94720)*
Selenium contamination is a major environmental problem in California, appearing as discharge from oil refineries in the Bay Area and as agricultural runoff in the Central Valley of California. The soil bacteria Bacillus subtilis has been shown to detoxify selenium by biotransforming the toxic, water-soluble selenite to the insoluble, less toxic elemental selenium, and depositing the selenium between the cell wall and the plasma membrane. Since the exact mechanism of the detoxification pathway is still unclear, our project involved the use of sodium azide to stop the production of ATP during the detoxification process to see if the detoxification pathway was energy dependent. The main focus, however, was to knock out genes that had been identified through genome wide expression arrays as being over-expressed during detoxification. To characterize these genes, mutants were exposed to selenium stress in physiology experiments. At certain time points, samples were taken to assess cell viability counts and selenium detoxification.

Understanding Computed Microtomography. *DANIEL WESTFALL (Alfred State College, Alfred, NY 14802) KEITH W. JONES (Brookhaven National Laboratory, Upton, NY 11973)*
The discovery of the X-ray and its ability to pass through opaque objects without damage has led to many important biological discoveries in the last century. Using the high intensity X-ray beam generated by the National Synchrotron Light Source at Brookhaven National Laboratory coupled with imaging computers, microtomography allows the viewing of previously unexplored microstructures. This technology proves useful in areas of geology, oceanography, and environmental biology with current research involved in analyzing porosity of sandstone samples. The recently developed stereographic viewing technology compliments computed microtomography producing stunning images that seemingly jump off the screen. Collecting microtomographic data suitable for visualization is a learned process involving control of beam energy in relation to sample density. Experimenting with instrument capabilities deepened understanding of

synchrotron light and imaging technology. Computed Microtomography offers itself as a tool capable of supporting the three-dimensional data visualization field.

Analysis of Technology Cooperation Agreement Pilot Project Impacts. *WYATT WILCOX (Washington State University, Pullman, WA 99163) JEANNIE RENNE (National Renewable Energy Laboratory, Golden, CO 80401)*
The Technology Cooperation Agreement Pilot Project (TCAPP), initiated as a result of the United Nations Framework Convention on Climate Change (UNFCCC) Article 4.5, has been working to create sustainable markets for clean energy technologies in developing countries. Recent work by TCAPP staff at the National Renewable Energy Laboratory (NREL) has yielded quantifiable evidence towards the progress of the program. Most outstanding achievements include 20 actions to remove market barriers, facilitation of 13 clean energy business projects, engagement of 400 international business donors as well as10 bilateral and multilateral donors, business investment of $117 million, and greenhouse gas (GHG) emission reductions equivalent to 670,000 tons of carbon per year. Anticipated achievements by the year 2004 include leveraging over $40 million dollars of donor support, $135 million of investment by partners in clean energy technologies and carbon equivalent reductions of up to 774,000 tons of carbon per year. The support for current initiatives suggests that TCAPP will remain a leading model for international clean energy technology transfer.

Biochemical Conversion of Heavy Crude Oil. *ELISHA WILLIAMS (Holyoke Community College, Holyoke, MA 01040) MOW LIN (Brookhaven National Laboratory, Upton, NY 11973)*
Petroleum will continue to play a major role as a transportation fuel in the coming decades. But, petroleum contains sulfur as one of its components. Burning sulfur results in an oxidized sulfur species that causes acid rain. Environmental regulations require that the sulfur be removed from the field prior to burning. Indeed, the EPA has established the cleaner fuels and vehicles program, finalized in December 1999, which requires the sulfur content of diesel to be reduced by up to 90 percent. Conventional methods of removing sulfur include hydrodesulfurization, distillation, and hydrocracking. These methods of sulfur removal are costly and a search is underway to provide a method of sulfur removal that is more cost-efficient. Biochemical conversion of petroleum is one such method. In this method, natural bacteria are used to remove sulfur. In the biochemical conversion process, the bacteria reside in an aqueous phase that is mixed with a nonpolar hydrocarbon phase. In this case, the reaction occurs at the aqueous-hydrocarbon interface. During this process, the bacteria attack the sulfur containing aromatic rings and metabolize the sulfur. The goal of my research project was to evaluate a particular strain of bacteria for sulfur removal from a sample of heavy crude oil. In this study, the treated oil showed a marked decrease in the heavy fractions with a marked increase in the gasoline fractions over the untreated oil. If a bacterial strain is identified that will break up heavy fractions and metabolize sulfur in these heavy crudes, it could reduce the amount of money the refineries use in current conventional methods.

GENERAL SCIENCES

Viscometric Screening of Deicing Fluids for Military Aircraft Application. *KIMBERLY JOHNSON (Montana State University, Billings, Billings, MT 59101-0298) KEVIN SIMMONS (Pacific Northwest National Laboratory, Richland, WA 99352)*
The US Air Force funded a proposal investigating biofriendly de-icing fluids for military aircraft. Ethylene glycol and propylene glycol are the currents choices for deicing. The current deicing fluids are harmful to the environment because of their mammalian toxicity and high biological oxygen demand. The project investigated the chemical and physical properties of six different solutions. Various testing was completed on these solutions to find the optimal solution. The solutions "C" and "E" were chosen for further offsite because they met freezing point and viscosity requirements. This additional testing will look at the corrosiveness, thermal stability and adhesion to aircraft wings under airflow.

Registration of satellite images. *MICHAEL LOW (Truckee Meadows Community College, Reno, NV 89436) GEORGE HE (Pacific Northwest National Laboratory, Richland, WA 99352)*
Registration of imagery is critical to national missions; i.e., national security and resource exploration. The process of registration is used to spatially line up satellite images with one another. Registration of different sensors with different scales is a new challenge. We

examined the manual registration process to understand the factors involved and to facilitate automatic image registration.

Effective Communication Tools. *KATHERINE SHOWALTER (James Madison, Harrisonburg, VA 22807) LINDA WARE (Thomas Jefferson National Accelerator Facility, Newport News, VA 23606)*
A discussion defining the process of communication, using different formats of printed media to enhance the success of transmittal and understanding. The medium chosen to convey a message is sometimes not understandable. As quoted by researcher Harold Lasswell, " Who says what, on which channel to whom, with what effect'" gives insight into the process of communication. It is the senders' responsibility to get the idea concept or point conveyed well in a form that is understandable. The form of the message is involved in the process very intimately. Individuals who possess limited understanding of the spoken language may find pictures helpful when used to communicate important places, such as hospitals, or pictures to designate what to do, or where to go in an emergency situation. Therefore solidifying the bridge between communicator and recipient is a process that involves a holistic approach. Most all the physical senses are involved either in tandem with each other or in a solo capacity. It is this process that will be explored. The development of a pictorial display using text, pictures and color will be used to illustrate the importance of differing mediums of communication. The educational atmosphere at Jefferson Lab serves not only the scientific community but seeks to foster an open door policy with the community. A text pamphlet will explain, define the educational programs that were developed in harmony with Jefferson Lab's role as a community communicator, educator, and business partner.

MATERIALS SCIENCES

CRYSTAL LATTICE INTERFACE ANALYSIS OF SRTIO3/SI USING ION BEAM TECHNIQUES. *EVAN ADAMS (Whitman College, Walla Walla, WA 99362) THEVA THEVUTHASAN (Pacific Northwest National Laboratory, Richland, WA 99352)*
The understanding of metal oxides has become increasingly more important in recent years because silicon dioxide (SiO_2) will soon reach its operational limit in the semiconductor industry. Strontium titanate ($SrTiO_3$) is considered a strong candidate in the search for SiO_2's replacement due to the similar high dielectric properties it shares with SiO_2. Single crystal $SrTiO_3$ (100) was grown in Motorola labs and the stability of the film was studied with respect to temperature. $SrTiO_3$/Si was annealed in three different environments: vacuum, oxygen, and hydrogen. The film's crystalline structure was analyzed with Rutherford backscattering spectroscopy (RBS) including channeling, nuclear reaction analysis (NRA), and X-ray photoelectron spectroscopy (XPS) at Pacific Northwest National Laboratory (PNNL). The channeling measurements discovered a disordering of crystal at the interface between the film and substrate. This corresponds with the reported idea that an amorphous silicate layer was produced at the intersection of the two layers. When the sample is annealed in either a vacuum or hydrogen environments the interface seems to become more disordered as oxygen migrates through the sample. But when heated in an oxygen environment overall crystalline quality seems to improve and the interface becomes more ordered. This suggests that the silicate layer is more thermodynamically stable than the $SrTiO_3$ film and that oxygen will diffuse to the interface. This diffusion creates an oxygen deficiency that disrupts the rest of the film, unless the oxygen is supplied in the environment.

Initial Characterization of a Silicon-Based System (Gubka) for the Treatment and Disposal of Aqueous Waste. *ANN BAKER (Washington State University, Tri-Cities, WA 99352) NANCY FOSTER-MILLS (Pacific Northwest National Laboratory, Richland, WA 99352)*
Russian scientists have developed a new porous material called gubka, which is produced using the hollow glass microspheres recovered from fly ash, a waste product of coal combustion. Russian researchers have reported using gubka to treat and immobilize hazardous wastes as well as using it as a catalyst for methane oxidation. The purpose of our research was to determine if gubka could be used to increase the evaporation rate of water, to determine how temperature affects the evaporation rate of water (with and without gubka), and to determine the feasibility of using gubka as a platform to store and/or treat waste. Measured rates based on the

exposed geometric surface area (g/sec/mm²) showed no significant difference between samples with and without gubka. Evaporation rates of water increased with increasing temperature with no significant difference in the rates between samples with and without gubka. Salt loading studies were designed to determine the feasibility of using gubka as a platform for waste storage. Gubka was etched with hot acid to form holes in the microspheres. After the gubka was etched, it held 5-10% of its weight in salt, which is lower than published values. Improvements in the etching procedure should lead to improvements in the storage capacity of gubka.

Electro-Spark Deposition. *TIMOTHY CHIN (University of Washington, Seattle, WA 98195) ROGER N. JOHNSON (Pacific Northwest National Laboratory, Richland, WA 99352)*
Electro Spark Deposition, or ESD, is a pulsed-arc microwelding process. ESD can be used between virtually any electrically conductive materials. It creates a metallurgically bonded coating of an electrode material on a substrate material. Coatings of Stellite 21 on 4340 steel were sent for evaluation from Advanced Surfaces and Processes, Inc. (Forest Grove, OR). Microhardness testing was conducted on the raw electrode materials and coatings to see if there was any effect of the ESD process on the hardness of a material. Microhardness testing on the substrate was conducted to determine if there was a heat-affected zone (HAZ) present, and, if there was, how much it affected the hardness and what the depth of the HAZ was. HAZ's were present in most coatings. The HAZ's only lowered the hardness by 50 to 100HK and did not extend much further than 10mm from the coating/substrate interface.

Experimentation on the Uptake and Release of Sodium Lactate by Silica - based Mesoporous Colloids. *DAWN DECHAND (Kansas State University, Topeka, KS 66614) GLENN MOORE (Idaho National Engineering and Environmental Laboratory, Idaho Falls, ID 83415)*
In sites contaminated with trichloroethylene (TCE), native microbial cultures can degrade TCE if provided with the proper nutrients, such as lactate. The research focuses on developing silica-based colloids and characterizing their ability to transport and release lactate through the subsurface. Specifically, this paper discusses the analysis of colloids synthesized with F127 surfactant and tetra methyl ortho-silicate (TMOS) and the quantification of their uptake and release of lactate. This synthesis produces hexagonally templated, mesoporous colloids with mobility and zeta potential less than that of soil colloids. Due to the mutual negative charges associated with both lactate and silicon oxide tetrahedrals, forcing the colloids to uptake lactate required experimentation with multiple physical methods and chemical environments. It was found that mixing the colloids with lactate together, then immersing in hexane, and finally oven-drying at 100°C while using methanol as a rinse and transfer agent was the best method of preparation; these colloids slowly released lactate for more than one week. However, further studies are being completed to better quantify this release, perfect the method of colloid synthesis, model the transport of these particles through the subsurface, and analyze the ability of microbes to consume the lactate contained in the colloids.

Calibration and Testing of an Infrared Thermometer for Sub-Scale Brake Testing. *DELIA DUMITRESCU (University of Michigan, Ann Arbor, MI 48152) PETER J. BLAU (Oak Ridge National Laboratory, Oak Ridge, TN 37831)*
This experiment investigated the optimal setup of an Infrared Thermometer for measurements at the interface of the brake pad and the disc in sub-scale brake testing. It determined the required input of the emissivities of two different materials, the angle placement of the sensor, and the reflection of the surrounding environment into the field of view. Measurements were taken using various setups and temperatures for the cast-iron disc and brake pad. The sensor readings were compared to thermocouple readings and the emissivity of materials was found to increase with increasing temperature for the cast-iron disc, and to decrease with increasing temperature for the brake pad. It is recommended that an emissivity value of 0.27 and 0.65 be used for the cast-iron and break-pad, respectively, as these correspond to the values for the predicted temperature ranges to be reached during the brake testing. The variations in temperature due to sensor angle should be minimized by aiming the camera at a zero angle to the material or, in cases when this is not possible, by using a first

surface mirror at a 45-degree angle to reflect the heat radiation. That setup is optimal because it minimizes the reflectivity of the surroundings.

Low Temperature Synthesis of Silicon and Titanium Nitrides & Thin Film Deposition on Silicon Wafers.

ELIZABETH FRANZ (Whitman College, Walla Walla, WA 99362) JEROME BIRNBAUM (Pacific Northwest National Laboratory, Richland, WA 99352)

Due to its physical and chemical inertness, silicon nitride is ideal for such applications as catalyst and sensor support. In this experiment, low temperature nitride synthesis by photolysis was attempted on $(CH_3)_3SiN_3$, $[(CH_3)_2N]_2Si(CH_3)_2$, $[(C_2H_5)_2N]_4Zr$, $[(C_2H_5)_2N]_4Ti$, and $[(CH_3)_2N]_4Ti$. UV-vis spectra were taken for each of the chemicals, and their extinction coefficients at 254 and 300 nm were determined. The chemicals were then photolysed under 254 nm light for at least 15 hours. 1H and 13C NMR showed significant consumption of each of the chemicals. The products of photolysis have yet to be determined. A carbon chain is usually present between a silicon wafer and the functional group when a film is deposited on a wafer. In this experiment we attempted to attach a thin film of ($-CF_3$) groups to silicon wafers. The wafers were hydroxylated and soaked in 0.5% $(CF_3CO)_2O$. The thickness and contact angle were then recorded. Wafers were the photolysed for 30 minutes under 254 nm light, their thickness and contact angle measured, and XPS was performed on the wafers. XPS showed a low content of fluorine, in agreement with low contact angle and thickness measurements to indicate that the film deposition was unsuccessful.

Synthesis of CdS Nanocrystals in Surfactants.

CHRISTINA FREYMAN (Georgia Tech, Atlanta, GA 30332) S.K. SUNDARAM (Pacific Northwest National Laboratory, Richland, WA 99352)

CdS nanocrystals were prepared in the micelle of two surfactants, a hydroxylated poly(syrene-b-butifiene-b-syrene) [SBS] and a commercially produced surfactant, Igepal in three different chain lengths. The synthesis of the SBS was difficult demonstrating the need for a surfactant that can be used as is. The surfactants were dissolved in toluene and hexane to produce micelles formed by the insoluble ends of the molecule. Then these solutions were loaded with Cd^{2+} and S^{2-} ions both in an aqueous method and an anhydrous method to produce CdS nanocrystals in the micelles. The solutions produced were analyzed with FTIR, UV-vis, and TEM. The anhydrous loading of the solution produced more uniform solutions. FTIR confirmed the hydroxylation of the SBS and the interaction between the OH function groups and the Cd^{2+} ions. TEM confirmed UV-vis adsorption edge particle size calculation of about 4 nanometers in both the hydroxylated SBS solution and the Igepal solutions.

Precipitation of Barium Tantalates From Borosilicate Glass.

DOUG GLINIAK (University of Washington, Seattle, WA 98125) S.K. SUNDARAM (Pacific Northwest National Laboratory, Richland, WA 99352)

Barium tantalates are typically materials used for microwave applications as dielectric resonators. $BaMg_{1/3}Ta_{2/3}O_3$ is particularly attractive as a possible material to be used in the millimeter wave frequency range due to a combination of suitable dielectric constant [e=10], and low tangential loss [tan(d)=1.00 x 10^{-4}], which can theoretically outperform alumina as the current leader according to the fundamental attenuation equation in the 30-300GHz frequency range. Many variables are yet to be uncovered and these results are only a preliminary indication of possible low heat formation precipitation of the barium tantalite family from a borosilicate glass. Current results have successfully precipitated out $Ba_{1/2}TaO_3$ and $BaTa_2O_6$, both having perovskite crystal structures belonging respectively to tetragonal and orthorhombic systems. $Ba(Mg_{1/3}Ta_{2/3})O_3$ precipitation did not form within the borosilicate glass with stoichiometric concentrations up to 70mol%, indicating possible thermodynamic stability problems with $Ba_{1/2}TaO_3$ and $BaTa_2O_6$ forming prematurely to exclude Mg within the growth of the perovskite structure.

Ruthenium Partitioning Between Simulated Waste Glass and Spinel.

JEREMY HOLBROOK (Western Washington University, Bellingham, WA 98225) S.K. SUNDARAM (Pacific Northwest National Laboratory, Richland, WA 99352)

Extensive research has led to the consensus opinion of vitrification as the best suited technology for the disposal of nuclear wastes. Crystals such as spinel ($MgAl_2O_4$) form in the glass melts. These crystals settle at the bottom of electrically heated melter. Noble metals present in the waste will also precipitate from the melt and settle. These elements dissolve into the spinel lattice, forming a conductive layer and short-circuiting the electrodes, leading to potential failure. The main objectives of this study are: 1) study the interaction of Ruthenium with spinel and 2) evaluate Tungsten as a noble metals surrogate. Ruthenium was chosen because it is a commonly observed end product in melter tests. A simulated Hanford waste glass, MS-7, was used. Spinels were cut into pieces and a hole of 3 mm diameter and 2 mm depth was drilled into them. The basic glass was melted and ground into a powder. Then, 5 wt.% each of Ru, RuO_2, W and WO_3 was added to make four testing glasses. The test glass powder was packed into the hole in the spinel. Test temperatures were 900 and 1000ºC. Test durations were: 7, 15, 19, and 23 hours. The samples were then cut at the melt line, polished, and used for Scanning Electron Microscopy (SEM) and Energy Dispersive Spectrometer (EDS). Results obtained were as follows: 1) There was significant interaction between the spinel and the melt. 2) An interfacial region exists between the melt and the spinel. 3) Interfacial region was populated by crystals of the dopants (Ru and W). Future work proposed includes: 1) quantitative testing of interfacial kinetics and 2) effect of the chemical composition and the spinel stoichiometry.

Evaluation of Nucleation Enhancement Methods for the Growth of Nanocrystalline Diamond Films.

ADAM HOPKINS (Florida State University, Tallahassee, FL 32306) ROBERT SHAW (Oak Ridge National Laboratory, Oak Ridge, TN 37831)

The growth of diamond films using a hot filament deposition reactor proceeds by means of nucleation, which occurs preferentially at damage sites on the substrate. It is anticipated that a greater number of nucleation sites will yield a smaller grain size in the film, with the target being the growth of a nanocrystalline diamond film (NCDF). Previous work used silicon substrates, which were abraded with diamond particles by hand to enhance the nucleation density. Here, other methods of enhancing the nucleation density were studied in addition to hand abrasion. Substrate abrasion in an ultrasonic bath, chemical etching of the substrate and chemically etching the substrate after abrasion in an ultrasonic bath have been examined. The substrates and films have been examined using scanning electron microscopy (SEM), atomic force microscopy (AFM), stylus profilometry, and micro-Raman spectroscopy. The samples that have been examined showed large amounts of debris on the surfaces, most of which was invisible to the SEM; the elimination of debris will be critical to the growth of high quality films. The films grown in this work were not NCDF's as the nucleation densities were too low. It is hoped that future investigations will lead to high enough nucleation densities for the production of a NCDF.

Preliminary Investigation into Optical Fibers for Elastic Optical Scattering from Ceramic Components.

LEONARDO MELO (Richard Daley College, Chicago, IL 60652) WILLIAM ELLINGSON (Argonne National Laboratory, Argonne, IL 60439)

Laser scattering is a nondestructive method of finding subsurface flaws on materials through a change in optical power. A plane polarized laser beam illuminates the test sample and optical power detector measures how much light is being back scattered. Fiber optic cables can be used to deliver the laser light to the sample and the back-scattered light to the detector. Polarization-maintaining cables would have to be used to deliver the light to the sample and maintain the polarization of the laser light. Light back scattered from a subsurface defect will not have the same polarization as the light that illuminated the defect, so the it will have to be measured and compared to the polarization of the illuminating light. Cables that do not maintain polarization are being used for now to make sure the other parts of the setup work.

Microstructural Analysis of the Mechanisms for Intergranular Stress Corrosion Cracking in Austenitic Type 304 Stainless Steels.

ANTONIO NISSEN (Sacramento City College, Sacramento, CA 95822) STEPHEN M. BRUEMMER (Pacific Northwest National Laboratory, Richland, WA 99352)

The phenomena of Intergranular Stress Corrosion Cracking (IGSCC) is believed to be caused by one of two very distinct mechanisms: slip dissolution (oxidation) or hydrogen embrittlement. Two different tests are being performed on Type 304 SS: one using a statically loaded U-bend sample in corrosive solutions of 100 ppm NaF, 100 ppm NaCl, and

100 ppm $Na_2S_2O_3$ and the other using a statically loaded U-bend sample electrochemically polarized, in a solution of H_2SO_4 to isolate anodic (dissolution) or cathodic (hydrogen) reactions. The purpose is to produce "classic cracks" for each IGSCC mechanism and to assess solution impurity effects. Resulting IGSCC crack characteristics will be recorded using optical metallography, scanning electron microscopy (SEM), and finally transmission electron microscopy (TEM) of cross-section samples. The Type 304 SS metal was heated to create a "sensitized" microstructure causing carbide precipitates and chromium depletion to form at internal grain boundaries. This microstructure is very susceptible to IGSCC. As of the printing of this paper, IGSCC tests are still in progress. Cracks have initiated on the NaCl solution samples with others showing signs of advanced pitting and surface degradation. Completion, of these tests, is expected to require another 2-4 weeks with a journal publication planned after characterization work is complete.

Burst Strength Testing and Pressure Fatigue Analysis of Silicon Wafers as Hibachi Foil.

ABBY OELKER (Lehigh University, Bethlehem, PA 18015) PAUL LAMARCHE (Princeton Plasma Physics Laboratory, Princeton, NJ 08543)
To enable inertial confinement fusion with krypton fluoride lasers, it is necessary to develop a material boundary that will maximize transmission efficiency of electrons into the laser gas and withstand more than one hundred million electron beam shots. Silicon wafers - chosen for their effectiveness in transmitting electrons and relative ease of manufacture were to be analyzed for burst strength and durability. Burst strength was determined by manual hydrostatic testing. It was found that wafers with one side polished had an average burst strength of 148.57 psi and wafers with both sides polished had an average burst strength of 257.71 psi. The discrepancy in burst strengths for single side and double side polished wafers was attributed to imperfections in the unpolished surfaces of the single side polished wafers. Due to hardware problems and time constraints, no durability (pressure fatigue) testing was completed. Future research will include adapting the wafers for operation in an environment of hydrostatic shock, fluorine, x-rays, ultra violet light, low energy electrons, and hydrofluoric acid.

In-situ Electrochemical Experiments at the Synchrotron: Applications in Battery Research.

BOPAMO OSAISAI (San Francisco State University, San Francisco, CA 94564) ARTUR BRAUN (Ernest Orlando Lawrence Berkley National Laboratory, Berkley, CA 94720)
Synchrotron radiation is more and more used nowadays to study advanced materials, including battery electrodes. We are investigating the fundamental mechanisms of battery failure using electrochemical and X-ray techniques at synchrotron radiation sources. Techniques used in this project include battery cycling (the charging and discharging of batteries at a constant current), and X-ray absorption spectroscopy. X-ray absorption spectroscopy is the probing of electrodes with X-rays of various wavelengths to obtain an entire spectrum of Manganese (Mn), a major constituent studied in our battery electrodes. From these spectra we can observe the chemical shift in Mn during battery operation (oxidation state) and determine the changes in the bonding lengths and coordination of atoms in manganese oxide. From battery cycling, we can determine the capacity and power density of the batteries, cycle life of the batteries, and degradation of the electrodes in the batteries. To assign structural and electronic changes in the electrodes as obtained by the X-ray techniques and to the charge and discharge conditions, experiments have to be made under strict potential control by an accurate data acquisition system. A computer controlled portable data acquisition system was built entirely for this purpose with LabVIEW. This research is an ongoing process and as of now, we are at the stage of establishing novel techniques.

Biodegradable De-icing Fluid for the U.S. Air Force.

ANNA OSTERGAARD (Columbia Basin College, Pasco, WA 99301) KEVIN SIMMONS (Pacific Northwest National Laboratory, Richland, WA 99352)
De-icing fluid is a very important necessity for flying airplanes in unfair weather conditions. These fluids, which are mostly composed of a chemical called glycol, are sprayed onto the airplanes wings to increase airflow across the wings and decrease the level of ice that forms from the cold air. During the winter months, when weather conditions are more frequent, there is a high demand for de-icing fluid. Right now, the present de-icing fluid is harmful to the environment, especially in the amounts they are used. This project is geared towards finding a more economical and environment-friendly fluid that performs the exactly same way as the present de-icer.

Development of Divalent-Doped Barium Zirconate Proton Conductors.

DAVID PALMER (City Colleges of Chicago—Harold Washington, Chicago, IL 60637) TAE H. LEE (Argonne National Laboratory, Argonne, IL 60439)
Among perovskite-type oxides demonstrating high-temperature protonic conduction, $BaCe_{1-x}Y_xO_3-$ (BCY) has shown the highest overall conductivity. However, BCY exhibits poor mechanical properties, and is chemically unstable under conditions relevant to technological application as a solid electrolyte in fuel cells or in a hydrogen-separation membrane (i.e., exposure to CO_2 and H_2O). The development of a high-temperature solid proton conductor with an overall electrical conductivity comparable to that of BCY but with superior mechanical properties and chemical stability is therefore highly desirable. This paper details investigations into a divalent-doped barium zirconate system. A divalent-doped barium zirconate was prepared at dopant concentrations from 5 mol% to 40 mol%. The system was found to be unstable at dopant concentrations 20 mol%. Sintered disks prepared at these dopant concentrations were found to collapse on exposure to air. Investigation into the cause of the collapse, including x-ray characterization of the collapsed disks, is ongoing.

Superconductivity: Long Length Critical Current Measuring System.

FRANK PARTICA (Juniata College, Huntingdon, PA 16652) . (Oak Ridge National Laboratory, Oak Ridge, TN 37831)
The ability to measure the critical current, I_c, of superconducting tapes is important in the design of long length superconducting wires. To this end, a long length I_c system was created to characterize tapes over eight meters long. This system has the ability to pinpoint nonhomogeneous current sections in the wires within any 2-cm section along its length. Two unique probe attachments have been designed for this system of measurement. One is used to analyze the I_c every 32 cm along the length of a tape for a six-meter period. The other measures I_c every 16 cm over a 3-meter period. This system has been tested using a commercially available nonhomogeneous superconducting BiSCCO (Bi-Sr-Ca-Cu-O) wire 2.6 meters long. It successfully ran tests measuring the critical current every 32.06 cm and 16.03 cm over the whole length of the tape, and found the end-to-end I_c of the tape. The design of the system and attachments are easily expandable for characterization of both longer and wider superconducting wires.

Investigation of the Superconductivity of YBa2Cu3O7 Deposited on an ISD-MgO Substrate.

DAVID PETERSEN (North Park University, Chicago, IL 60625) PETER BERGHUIS (Argonne National Laboratory, Argonne, IL 60439)
Superconductivity is a fast growing area of research. High Temperature Superconductors have opened the door to many more commercial uses for superconductors. Manufacturing effective and cost-efficient super-conductors has become a concern for many researchers. Transport measurements of current through the superconductor in various temperatures and fields demonstrate the effectiveness of a sample. Understanding the properties of superconductors will lead to the production of useful samples. Inclined Substrate Deposition is one method that is being investigated that might lead to a cost-efficient superconductor that has a high critical current density. It is clear that further study of the Inclined Substrate Deposition method is necessary in order to produce an effective and cost-efficient superconductor.

Comparative Study of Cicadellidae Utilizing Optical and Electron Microscopy: Practical Considerations.

AMY REDELL (Washington State University, Tri-Cities, Richland, WA 99352) JAMES S. YOUNG (Pacific Northwest National Laboratory, Richland, WA 99352)
The invention of the light microscope in 1590 opened the door to the microscopic world. This microscope magnified objects up to 30 times their original size. In the 1930's another prospect began to open: the submicroscopic world as viewed by the electron microscope. The electron microscope utilized the much shorter wavelength of the electron. Using the electron microscope, another thousand-fold increase in magnification was made possible, accompanied by a parallel increase in resolution. There are benefits and limitations to all methods of microscopy. Resolution, depth of field, contrast formation, and illumination source are just four areas of concern. Using a

compound, stereoscopic, and scanning electron microscope, micrographs were compared to illustrate these four attributes. The micrographs show the depth of field limitation characteristic of lighted microscopy. At 50x magnification, both microscopes displayed problems with depth of field and resolution. The SEM, however, demonstrated clear depth of field at 20,000x magnification. These results show that there is a strong need for all areas of microscopy. No single technique is without limitations. However, the future of electron microscopy is promising. It is a future goal to have the routine capability of imaging living systems at high resolution. Electron microscopy is expected to continue to meet the submicroscopic imaging needs of science and medicine.

Evolution of Microstructure and Magnetic Structure of Epitaxial CoPt L10 Films.
KAREEN RIVIERE (Brown University, Providence, RI 02912) LAURA H. LEWIS (Brookhaven National Laboratory, Upton, NY 11973)

CoPt films are under consideration as the next-generation high-density magnetic recording media. To evaluate the suitability of this material, the microstructure and magnetic domain configurations of crystallo-graphically ordered (L1o-type) CoPt thin films of 50 nm thicknesses were characterized using atomic force microscopy (AFM) and magnetic force microscopy (MFM). These CoPt films were epitaxially grown at Carnegie Mellon University by low-rate DC sputtering on MgO substrates that were heated during deposition at temperatures ranging from 400 °C-750 °C. AFM images demonstrated that grain size and the tendency to grain cluster increased with increasing substrate temperature. The magnetic domain attributes progressed from long maze-like domains to concentric fingerprint-like domains and then changed to discontinuous domains with increased substrate heating temperature. The evolution of the microstructure and magnetic domain character is attributed to the thermal energy available to the film during growth. The results indicate that the microstructure and magnetic domain structure are most uniform and continuous at intermediate substrate temperatures.

Characterization of Self-Organized Criticality During Fracture of Carbon Fiber Reinforced Composite Materials.
THOMAS ROGERS (University of Tennessee, Knoxville, TN 37919) SRDAN SIMUNOVIC (Oak Ridge National Laboratory, Oak Ridge, TN 37831)

Self-organized critical (SOC) behavior is exhibited by systems ranging from earthquakes to fluctuations in the stock market and is character-ized by critical events occurring on all time and length scales after some critical state has been established. Classifying a phenomenon as SOC gives scientists a better foundation for describing and under-standing many of the underlying principles of the process. The field of Self-Organized Criticality theory has led to insights in many areas of research. Based on the original theories of Bak, Tang, and Wiesenfeld, and expanded by numerous other studies, SOC models have given researchers valuable tools for exploring the behavior of complex systems. The work presented here explores the SOC behavior of the fracture properties of carbon fiber reinforced composite materials. Materials with randomly oriented fibers and materials with braided carbon fibers were subjected to laboratory tests (crushing) and the results were analyzed for possible SOC behavior patterns. In both types of materials evidence has been found to suggest that the progressive fracture follow SOC patterns. Establishing an SOC pattern of behavior in material fracture is an important step toward our goal of developing predictive stochastic finite element models.

The Effect of Cr Content and H2O Vapor on High Temperature Oxidation of Fe-Cr Model Alloys.
JESSICA SCHENNING (Univer-sity of South Florida, Tampa, FL 33620) BRUCA PINT (Oak Ridge National Laboratory, Oak Ridge, TN 37831)

The oxidation behavior of most stainless steels is a function of their chromium (Cr) content. In order to improve gas turbine engine efficiency these alloys are being used at higher operating tempera-tures and in more aggressive oxidizing environments. The oxidation performance of model Fe-Cr alloys was examined to determine the effect of water vapor (found in exhaust gas) on the minimum Cr content necessary to form a protective, Cr-rich external oxide scale. Samples of Fe with 10%-20% by wt. of Cr were exposed to tempera-tures from 700ºC to 900ºC and were oxidized in both dry air and air + 10% H_2O. The experiments were conducted in 100h cycles, up to 500h, as well as in one-hour cycles, up to 100h. It was found that H_2O

greatly accelerates oxidation attack. Higher Cr levels were required to form the protective surface in air + H_2O than in dry air.

Growth of Epitaxial Gd2O3 Buffer Layers On Nickel Substrates Using a New Metal-Organic Solution Deposition Route for Superconducting YBCO Coated Conductors.
MICHAEL SHANK (Indiana University of Pennsylvania, Indiana, PA 15701) M. PARANS PARANTHAMAN (Oak Ridge National Laboratory, Oak Ridge, TN 37831)

Textured buffer layers are important to fabricate a high current Yttrium Barium Copper Oxide (YBCO) superconducting tape. The RABiTS (Rolling Assisted Biaxially Textured Substrates) process developed at Oak Ridge was used to make textured nickel substrates. The process-ing of YBCO superconductors is usually carried out under oxidizing atmospheres. The nickel substrate oxidizes in this process and forms nickel oxide with a different crystal structure. Therefore, the texture of the YBCO is destroyed and the superconductor carries very low currents. By adding a suitable buffer layer between the nickel substrate and the YBCO, this problem is solved. A metal-organic sol-gel deposition route was developed at Oak Ridge to fabricate thin films on nickel substrate. The problem with the sol-gel solution is that it becomes unstable when it is exposed to humid air. The method developed here is also a metal-organic route, but the solution is stable in air. The precursor solution is very easily made in seconds by mixing chemicals in a bottle and shaking. The precursors solutions are then spin-coated onto textured nickel substrates and heat-treated in a controlled atmosphere to produce Gd_2O_3 films with the right orientation. It has been called the "shake and bake" method. The results of the initial testing show hope that this process will work as well as the sol-gel route. The variables used were furnace temperature, residence time in furnace, and the concentration of the solution. The films grown are textured nicely and they show high degree of crystalline alignment with the nickel. The films made were Gd_2O_3, but this method will be used to process other buffer layers.

A Facile Wet Synthesis of Litharge, the Tetragonal Form of PbO.
ERIK SPILLER (Fresno City College, Fresno, CA 93741) DALE L. PERRY (Ernest Orlando Lawrence Berkley National Laboratory, Berkley, CA 94720)

Lead(II) oxide exists in several structural polymorphs. The phase being produced by previous synthetic techniques is dependent on experi-mental parameters such as temperature, pH, and concentration of the lead(II) starting solution. Additionally, micro structural phase changes that are different from the two principal phases normally reported result as a consequence of the synthetic route used to prepare the material. The resulting phase is also highly dependent on contaminant species of various other elements present in the reaction solution in addition to the lead(II) ion itself. In the present work, the red, tetragonal form of PbO, litharge, has been synthesized by a quick and easy reaction sequence using water as the reaction medium by which, unlike previously reported syntheses, the litharge phase is repeatably produced with no major side products or contaminating phases. The product was characterized by powder x-ray diffraction and compared to published data. Experimental parameters are discussed that lead to both other PbO forms being produced in the wet syntheses and to micro structural alterations of both the litharge and other phases. Motivations for working in the chemistry and technology of PbO include scintillator, thin-film, large crystal, and powder technology applications.

Friction Stir Welding of Aluminum Metal Matrix Composites.
DANIEL STORJOHANN (South Dakota School of Mines, Rapid City, SD 57701) STAN DAVID (Oak Ridge National Laboratory, Oak Ridge, TN 37831)

Friction Stir Welding is a new non-fusion welding technique that has gained a lot of attention recently. The focus of this research was to compare the microstructure evolution in metal-matrix composites (Al-MMC's) during the fusion welding processes with that of the friction stir welding process. The fusion welding processes include gas tungsten arc (GTA), electron beam (EB) and laser welding. Aluminum alloy 6061 reinforced with Al2O3 and aluminum alloy 2124 reinforced SiC were used in this investigation. The welds were characterized with optical microscopy and hardness measurements. Phase stability in these alloys were also calculated using thermodynamic software. Fusion welding led to the decomposition of the reinforcing phases. However in the friction stir welds the reinforcing phases were

retained. Thermodynamic calculations support the phase evolution in fusion welds.

Effect of Magnetic Impurities on Superconductive Properties of Bulk MgB$_2$. *THOMAS THERSLEFF (University of Wisconsin, Madison, Madison, WI 53706) M. PARANS PARANTHAMAN (Oak Ridge National Laboratory, Oak Ridge, TN 37831)*
The discovery of MgB$_2$ as a superconducting material by Ahimitsu et al. in January 2001 has stimulated the interest of the research community in hopes of finding a cheap superconductor with strong superconductive properties. MgB$_2$ becomes superconducting at a transition temperature (referred to as Tc) of 39K, which is relatively high for a non-oxide superconductor. The critical current density (J$_c$) and the critical field (H$_c$) for MgB$_2$, however, are relatively low when compared to other high temperature superconductors. In this paper, the effect of magnetic impurities on these superconductive properties is analyzed in bulk MgB$_2$ samples. The magnetic impurities used are Gadolinium, Iron, Nickel, and Manganese. Samples were prepared by mixing MgB$_2$ powder with the dopant of choice, placed in a tantalum tube, and reacted for 15 minutes in a flowing Ar4%H$_2$ furnace at 880ºC. X-Ray diffraction (XRD) data indicated that the Nickel and Manganese are soluble in MgB$_2$ up to 5%. As the Mn content increases, the lattice parameters a decreased and c increased up to 5%. Detailed measurements were done on Manganese doped samples. Data collected on a DC SQUID magnetometer indicate that the Tc of Mn-doped MgB$_2$ remains constant around 38.3 K. Detailed magnetic hysteresis data are reported. These results will help the scientific community to better understand the mechanics behind MgB$_2$ and how to use it in the future.

Studies Toward Solid/Solid Interaction. *BRIAN TRUE (Washington State University, Pullman, WA 99163) KEVIN SIMMONS (Pacific Northwest National Laboratory, Richland, WA 99352)*
Laser light is a concern in the military today due to it potentially being hazardous to the eyes of military personnel and equipment. In an effort to eliminate this problem a number of separate attempts have been made to refract laser light in a medium. One attempt was using a polymer/solvent pair and the other using a solid/solvent pair. The polymer/solvent pair was synthesized using a polyphosphazene polymer with a specific index. The solid/solvent pair used two different plastics with known refractive indices, Methacrylate-Styrene Copolymer and Styrene-Acrylonitrile, dissolved in trichloroethane. The optical limiting concept is based upon the Christiansen-Shelyubskii filter. The idea is to match the indices of the two materials to the fourth decimal place. If the refractive indices of these materials do match the laser light will be negated.

X-Ray Diffraction on Paper mill tubes. *KARINA ULLOA (University of Texas, Brownsville, Brownsville, TX 78520) JAMES KEISER (Oak Ridge National Laboratory, Oak Ridge, TN 37831)*
The work presented in this paper is a subset of a much larger project. It is a collaboration between ORNL, IPST, PAPRICAN, and Pulp and Paper industry. Industry investigates cracking in composite tubes used in Kraft recovery boilers. The focus of the larger project is to understand why cracking occurs in stainless steel clad carbon steel tubes. The focus of this paper is to investigate the residual stresses in the stainless steel clad layer and how commonly used tube cleaning processes affect residual stresses. Specifically x-ray diffraction will be used to measure residual stresses in stainless steel cladding for each of the following conditions: as removed from the boiler; after being cleaned with a wire wheel; and after being cleaned using a flapper wheel. This data will be analyzed to help determine why cracking occurs and how to prevent cracking in future tubes.

Precision Electrolytic Nanofabrication. *KENT WILCHER (University of Tennessee, Knoxville, TN 37919) JAMES W. LEE (Oak Ridge National Laboratory, Oak Ridge, TN 37831)*
The ability to manipulate individual molecules is of fundamental importance in the development of the next generation of nanoscale devices. One of the major difficulties encountered in the fabrication of such devices is the creation of the interface between macroscopic structures and individual molecules. This project involved the fabrication of nanoelectrodes by precise electrolytic deposition of metal onto a substrate. The substrate consisted of two gold electrodes separated by a distance of approximately one micron, fabricated using electron beam lithography. Metal was then deposited on the tip of one of the electrodes by applying a potential across the gap using a programmable pulse current source while under an electrolytic solution containing metal compounds. The focused electric field generated across the gap between the two electrodes theoretically allows for deposition of metal only at the tip of the negative electrode. The amount and location of the deposition was monitored in situ using an Atomic Force Microscope (AFM). The goal of this project was to demonstrate the ability to create a nanometer-scale gap suitable for molecular applications.

Development of Ductile Cr Alloys for Use in Molten Salt Environments. *JESUS ZAMORANO (University of Texas, Brownsville, Brownsville, TX 78520) JAMES KEISER (Oak Ridge National Laboratory, Oak Ridge, TN 37831)*
Chromium offers a highly desirable combination of high melting point, good high-temperature mechanical properties, and excellent high-temperature corrosion resistance in many environments. However, inadequate ductility at room temperature has severely limited its use as a structural alloy. Work by Scruggs in the 1960's indicated that the room-temperature ductility of Cr could be significantly improved by the addition of MgO. We have succeeded in replicating this work and are developing this class of alloys for possible use as structural alloys or overlay coatings in the aggressive molten salt environments encountered in the paper and pulp industry. This poster will present room-tensile characterization data for the developmental alloy Cr-6MgO-0.5Ti-0.3La$_2$O$_3$ (weight percent) consolidated from blended or blended and ball milled Cr, MgO, Ti, and La$_2$O$_3$ powders. Preliminary results of the corrosion behavior of this alloy in molten smelt (alkali salt byproduct of the Kraft pulping process; material collected at a commercial paper mill) at 975°C will be presented.

MEDICAL & HEALTH SCIENCES

Mechanical Wall Stress in an Idealized Computer Model of Human Abdominal Aortic Aneurysm Following Endovascular Repair. *WILLIAM JENKINS (University of Tennessee, Knoxville, TN 37996) KARA L. KRUSE (Oak Ridge National Laboratory, Oak Ridge, TN 37831)*
Rupture of an abdominal aortic aneurysm (AAA) is thought to occur when the mechanical stress in the aneurismal wall is greater than the strength of wall tissue. Because AAA rupture is a concern even after endovascular repair with a stent-graft, it is important to understand physiological factors that affect wall stress in post-operative AAAs. Upon generating an idealized AAA computer model, various cases of the model were studied including the aneurismal wall, intraluminal thrombus (ILT), and/or a stent-graft excluding the aneurismal sac. Additionally, a type I endoleak was simulated by creating a gap at the proximal attachment site of the stent-graft. Using commercial software, the wall stress was computed for each case following the application of physiologic intraluminal pressure. The highest wall stress occurred in the case of the wall by itself. Inclusion of the ILT lining reduced the wall stress significantly, and inclusion of the stent-graft reduced wall stress even further. In the simulated endoleak, with the aneurismal sac completely filled with ILT, no increase in the peak wall stress was observed. The results indicate that the ILT has a cushioning effect in the reduction of wall stress. Further, the stent-graft bears most of the pressure load with part of the load being transmitted to the wall due to stent-graft deformation. For wall stress to increase due to type I endoleak, we hypothesize that unclotted blood in addition to or in place of ILT must be present in the aneurismal sac to transmit the pressure load.

Evaluation of the *in vivo* and *ex vivo* Binding of Novel CB1 Cannabinoid Receptor Radiotracers. *ASHLEY MILLER (University of Connecticut, Storrs, CT 06269) JOHN GATLEY (Brookhaven National Laboratory, Upton, NY 11973)*
The primary active ingredient of marijuana, 9-tetrahydrocannabinol, exerts its psychoactive effects by binding to cannabinoid CB1 receptors. These receptors are found throughout the brain with high concentrations in the hippocampus and cerebellum. The current study was conducted to evaluate the binding of a newly developed putative cannabinoid antagonist, AM630, and a classical cannabinoid 8-tetrahydrocannabinaol as potential PET and/or SPECT imaging agents for brain CB1 receptors. For both of these ligands *in vivo* and *ex vivo* studies in mice were conducted. AM630 showed good overall brain uptake (as measure by %IA/g) and a moderately rapid clearance from

the brain with a half-clearance time of approximately 30 minutes. However, AM630 did not show selective binding to CB1 cannabinoid receptors. *Ex vivo* autoradiography supported the lack of selective binding seen in the *in vivo* study. Similar to AM630, 8-tetrahydrocanibol also failed to show selective binding to CB1 receptor rich brain areas. The 8-tetrahydrocanibol showed moderate overall brain uptake and relatively slow brain clearance as compared to AM630. Further studies were done with AM2233, a cannabinoid ligand with a similar structure as AM630. These studies were done to develop an *ex vivo* binding assay to quantify the displacement of [131I]AM2233 binding by other ligands in Swiss-Webster and CB1 receptor knockout mice. By developing this assay we hoped to determine the identity of an unknown binding site for AM2233 present in the hippocampus of CB1 knockout mice.

Lack of Potentiation of Boron Neutron Capture by Gadolinium Neutron Capture. *NINA NAMI (Binghamton University, Binghamton, NY 13902) LOUIS A. PEÑA (Brookhaven National Laboratory, Upton, NY 11973)*
DNA damage is central to research in many fields, especially cancer research and toxicology. In this experiment we used normal endothelial cells (HAEC) and a tumor cell line (9L GS) to compare the atomic neutron capture reactions by boron-10, gadolinium-157, and by the combination of both. Cell death/DNA damage was measured by clonogenic survival assays and with single cell gel electrophoresis, also known as the comet assay. The clonogenic assay measures the cell's ability to divide and form colonies after exposure to irradiation. Whereas in the comet assay, electrophoresis causes broken DNA to move from the nucleus towards the anode forming an image resembling the tail of a comet, with the greater the extent of damage, the greater the tail. Our results indicate that the gadolinium-157 containing compound, Gd-DTPA, does not potentiate in the clonogenic assay or in the comet assay. The presence of Gd-DTPA in combination with the boron-10 containing, BPA, attenuated the biological effect of BPA in both HAEC and 9L cell types.

The Effect of Endogenous Serotonin on the *in vivo* Binding of Radiotracers of the 5-HT Receptors in Mice. *ADENIKE OLAODE (Monroe Community College, Rochester, NY 14621) ANDREW GIFFORD (Brookhaven National Laboratory, Upton, NY 11973)*
Serotonin is a group of chemical messenger, which is also known as neurotransmitters. Different radiotracers examined in previous studies showed insensitivity to changes in endogenous Serotonin. The importance of this study is to reveal the relationship between radiotracer used in PET and endogenous Serotonin level in brain. Numerous studies have suggested that some neurotransmitters (i.e., dopamine) are able to have competition on certain radiotracers binding on the receptors. This phenomenon is a critical issue in PET that uses those radiotracers on the study of brain function. In order to more fully understand the role of neurotransmitters on radiotracer binding *in vivo*, the present project was designed to investigate the changes of binding of [3H]WAY 100635 and [3H]NMS in mice brains that had the depletion of Serotonin by 5,7-dihydroxytryptamine (5,7-DHT, i.c.v. 5mg/kg) and p-chlorophenylalanine (PCPA, i.p. 150mg/kg twice/day for 4 days). Our results indicated that the Serotonin level has decreased approximately more than 50% and 80% by 5, 7-DHT alone and 5, 7-DHT with PCPA respectively in both front cortex and hippocampus of mice brain. However, there were no significant changes of radiotracers binding in mice that had these decreases of Serotonin in brain. Thus, our results suggest that the depletion of Serotonin in brain has no significant effect on *in vivo* binding of radiotracers of both 5-HT1A and 5-HT2A receptors in mice.

Developing a Ribonuclease Protection Assay to Evaluate Peptide Nucleic Acids for use in Antisense Research. *JORDAN PLIESKATT (George Washington University, Washington, DC 20052) ANDREW GIFFORD (Brookhaven National Laboratory, Upton, NY 11973)*
In an effort to continue to expand the ability to treat and detect different diseases, researchers have turned to antisense technology. Traditional drugs bind to the targeted protein and block its action. Antisense agents differ from traditional drugs by stopping the protein from ever being translated by binding to the transcribed mRNA. Such technology can be used both in therapeutic applications to stop destructive proteins and also in gene specific imaging. Peptide nucleic

acids (PNA) are ideal antisense probes due to their high cellular uptake and resistance to cellular nucleases. In this study, mRNA for the glial fibrillary acidic protein was used as the antisense target because of its high content in glial cells and because the mRNA expression can be readily regulated both *in vivo* and *in vitro*. Various 15mer PNA GFAP antisense probes were created including 131I labeled versions, which were tested in their ability to bind to complimentary GFAP mRNA. A ribonuclease protection assay, employing radiolabeled peptide nucleic acids rather than conventional radiolabeled cDNA probes, was developed to test, isolate and visualize these hybridized PNA/RNA duplexes on a native polyacrylamide gel. In conclusion, this study confirmed that peptide nucleic acids can hybridize to mRNA and protect it from RNase digestion *in vitro*.

Microbeam Radiation Therapy Cancer Research. *ALLISON SAWCHUK (University of Michigan, Ann Arbor, MI 48109) AVRAHAM DILMANIAN (Brookhaven National Laboratory, Upton, NY 11973)*
High-grade malignant gliomas currently represent 60% of all primary brain tumors, at an incidence of over 8000 cases per year. However, these highly malignant tumors of the delicate central nervous system are difficult to treat, and alarmingly, very few viable treatment modalities are currently available. X-ray radiotherapy, XRT, has been the leading treatment method, used in adjunction to chemotherapy and surgery. However, XRT offers little, if any hope for these highly malignant tumors of the central nervous system, such as a glioblastoma multiforme. Conventional x-ray therapy is a potentially palliative and incomplete treatment prescribed for these highly malignant cancers. It often causes more harm than good in its destruction of both mutagenic cancer tissues and the normal brain tissues. Therefore, the novel technique referred to as microbeam radiation therapy, MRT, provides medical researchers with a fresh perspective on these difficult cancers. Current research on rats and mice suggests that this treatment preferentially destroys malignant gliomas while leaving the healthy tissues relatively unharmed. This phenomenon may support the "endothelial replacement" hypothesis, a possible explanation of the biological mechanism motivating this effective tumor ablation. Microbeam radiation therapy, and its possible foundation, the "endothelial replacement" hypothesis, provides new hope in effective cancer research. Furthermore, this innovative radiotherapy modality, supported by the "endothelial replacement" hypothesis might provide the medical community with a viable treatment regimen to treat these highly malignant brain tumors.

NUCLEAR SCIENCE

Operations Modeling of the Fast Flux Testing Facility (FFTF) Fuel Cycle Demonstration. *VERED ANZENBERG (University of California, Berkeley, Berkeley, CA 94720) HUMBERTO GARCIA (Argonne National Laboratory, Argonne, IL 60439)*
Discrete Event modeling is used to simulate complex processes. One such process is the Fuel Cycle Demonstration for the Fast Flux Testing Facility (FFTF). FFTF is currently in consideration of reactivation and relies on fueling the reactor core using facilities at Argonne National Laboratory-West. Using the software Extend, a model is produced portraying relevant facilities and their corresponding stations. The model is to show bottlenecks within the process and to see whether ANLW will be able to support the fueling needs of FFTF. This research produced a preliminary model; a basic structure to the process and is currently awaiting further data.

Transmission-Corrected Barrel Segmented Gamma Scanner Analysis. *ANDREW BARAN (University of Illinois, Urbana-Champaign, Urbana, IL 61820) WILLIAM RUSS (Argonne National Laboratory, Argonne, IL 60439)*
The Barrel Segmented Gamma Scanner is an instrument for the nondestructive mass assay of 55-gallon barrels of low level radioactive waste contaminated with a small amount of fissile Uranium and Plutonium. The analysis of data collected by the Barrel Scanner results in a record of the masses of these isotopes shipped to disposal and is important for safeguarding the non-proliferation of nuclear materials. Currently spectrum data is analyzed using a Microsoft Excel MACRO on a Macintosh platform. The updated analysis software will be written in the more versatile LabVIEW programming language to create a more easily used and adaptable system for obtaining mass data from waste barrels. The code is modular and well documented to facilitate changes and upgrades in the future, and the new software performs

all of the data handling internally from input file data extraction to calibration and the saving of results and error analysis.

Vertex Tracking for the Pixel Detector Group at STAR. *KENNETH GARMON (University of North Carolina, Chapel Hill, NC 27514) HOWARD MATIS (Ernest Orlando Lawrence Berkley National Laboratory, Berkley, CA 94720)*
The goal of the Solenoidal Tracker at RHIC (STAR) experiment is to search for a phase transition in nuclear matter from confinement in hadronic particles to a quark gluon plasma (QGP). The STAR experiment makes use of the new Relativistic Heavy Ion Collider (RHIC) that has been built at Brookhaven National Laboratory (BNL). One important signature that a quark gluon plasma has been created is the enhanced production of D0 mesons. However, the present equipment lacks the sensitivity necessary for detecting D0 mesons. A few members of the STAR group at LBNL are now working on building a new detector component, designed specifically to detect D0 mesons. The main component of this detector will be a chip, which makes use of the new Active Pixel Sensor technology. My work in the Pixel Detector Group has mainly focused on helping to determine the best resolution for the chip. My mentor, Howard Matis, has created Monte Carlo simulations of D0 meson decays and what data will be taken as a result in the detector. My goal has been to write software (using C) that will re-create particle trajectories and find the vertex (where the D0 meson originally decayed). Once we have determined the most accurate algorithm for re-creating D0 meson decays, we can then determine the most accurate resolution for the chip. In addition, my algorithms can also be used in the final software that will be used to actually analyze data from the detector. By actually running my code using a Monte Carlo simulation, I have found that my program produces the correct answers in all except for a few cases (in which the vertex lies very close to the origin).

Gamma-ray Spectroscopy Using A Novel Sorting Routine: "Blue". *SEPEHR HOJJATI (Contra Costa College, San Pablo, CA 94806) STEVE ASZTALOS (Ernest Orlando Lawrence Berkley National Laboratory, Berkley, CA 94720)*
Studying the coincident g-rays is one of the most powerful means to learn about nuclear structure. The GANDS collaboration uses GAMMASPHERE in conjunction with 252Cf (with ~3% spontaneous fission branching ratio) to study the structure of neutron-rich nuclei. For the purposes of studying the coincident relationship between g-rays, one needs to construct a database of coincident g-ray events. Blue, a computer software developed by Mario Cromaz (LBNL), provides a library of subroutines that can be utilized both to construct such a database and to access the database in the desired way by executing queries that would construct one-dimensional histograms from multi-fold database. By writing interfaces in C code, one can call the subroutines provided in Blue to produce spectra that can then be displayed using standard nuclear physics data analysis software. To date, we have read about 60 tapes into Blue and have created several multi-fold (3 through 6-fold) databases which can be used to resolve overlapping photo-peaks which are not otherwise resolvable using traditional nuclear physics databases due to the typical data compression invoked in creating such databases. Moreover, Blue reduces the size of a traditional histogram by ~1000 fold.

Lead Bismuth Eutectic Target. *ROBERT KAPHEIM (University of Illinois, Urbana, IL 61801) JOE HERCEG (Argonne National Laboratory, Argonne, IL 60439)*
The history of nuclear power has been relatively brief, but two of the main players (nuclear reactor and particle accelerator) are coming together. The key component to the hybrid is a spallation target. In this case the Lead-Bismuth eutectic target is developed using Pro/Engineer and analyzed using Computational Fluid Dynamics code Star CD software. A near 2-D slice of the 3-D tube was analyzed for temperature of the solid walls and of the liquid lead-bismuth, and for the velocity of the lead-bismuth. Multiple problems occur with the heat distribution on the solid tube. Major design changes are in order and other current designs may be superior.

Preparation of specimens for nondestructive testing. *ADAM MORASCH (University of Idaho, Moscow, ID 83843) GEORGE SCHUSTER (Pacific Northwest National Laboratory, Richland, WA 99352)*
The researchers, to whom I was assigned, were conducting studies using nondestructive testing to estimate the occurrence of fabrication flaws in welding material for light-water reactor pressure vessels. Researchers at the Pacific Northwest National Laboratory do nondestructive testing on material from cancelled nuclear power plants. The researchers are developing fabrication flaw density and distribution functions for the materials used in fabrication of nuclear reactor pressure vessels. This includes all product forms for vessels shell cores, welding processes, and the stainless steel cladding applied to the inside of the vessel. The information gathered will be used in future machine analysis by the U. S. Nuclear Regulatory Commission to support/improve the technical basis of assessing potential vessel failure due to postulated failure devices, such as pressurized thermal shock. Preparing the metal specimen is one of the most important steps of the nondestructive testing process. The surface of the metal will be sanded, polished, and etched to reveal the specific area of interest. Sanding is perhaps the most important part of specimen preparation because great care must be used to assure that there is no surface damage. During my internship, I was responsible for preparing the metal specimens so that the researchers could then perform ultrasonic testing on them. The material used by the researchers is carbon steel. The pieces that I prepared for testing were small sections that were ultrasonically tested. This paper details my internship and the appendix includes exact steps to perform the preparation of metal specimens.

The Recyclotron Project. *MAISHA MURRY (Tuskegee University, Tuskegee, AL 36088) MARGARET MCMAHAN (Ernest Orlando Lawrence Berkley National Laboratory, Berkley, CA 94720)*
The objectives of the Recyclotron project are to produce medium-lifetime radioactive beams, to test the limits and feasibility of working with them, and to run future reactions with these beams. To produce radioactive beams, radioactive isotopes are prepared in the 88-Inch Cyclotron. The radioactive isotopes are collected and introduced into the Advanced Electron Cyclotron Resonance source (AECR), where a charged particle beam is created and recycled back through the cyclotron to produce a beam of the radioactive isotope. However precautions must be taken to only medium-lifetime radioactive isotopes to prevent contamination of the ion source. The preliminary radioactive beam attempted was Krypton-76, which has a 14.8-hour half-life. In efforts to produce Krypton-76 there was the possibility of creating Selenium-75 with a 119.78-day half-life and Arsenic-73 with a 80.3-day half-life, which are both long-lived radioactive isotopes. It was determined during a test run on June 7, 2001 that very little of the two contaminates were produced and therefore not a problem. Future radioactive beams are anticipated such as bromine-77, -78 and Niobium-92 to study the p-process nuclei, nuclear structure and magnetic moments.

Object-oriented Analysis Code for Hall A Vertical Drift Chambers. *JONATHAN ROBBINS (University of Richmond, Richmond, VA 23173) JENS-OLE HANSEN (Thomas Jefferson National Accelerator Facility, Newport News, VA 23606)*
The high-resolution spectrometers in Jefferson Lab's Hall A use vertical drift chambers to determine charged particle tracks. The current analysis code for the vertical drift chambers is difficult to maintain and modify, which has prompted the development of an object-oriented version, which will be easier to maintain and more able to adapt to changes in the detector configuration. However, the object-oriented approach involves using a slightly different algorithm than ESPACE, which could lead to different results. In this project, a preliminary version of an object-oriented analysis program for the vertical drift chambers is created and its results are compared to the existing software to determine the impacts of the differences in the reconstruction algorithms. In addition, the algorithms themselves are compared and minor differences in track reconstruction techniques are reported.

The Development of Cd1-xZnxTe for X-ray and Gamma Ray Radiation Detection. *CHARLES SHAWLEY (Whitworth College, Spokane, WA 99251) GLEN DUNHAM (Pacific Northwest National Laboratory, Richland, WA 99352)*
Cadmium Zinc Telluride crystals have properties conducive for room temperature radiation detection. Due to the high atomic mass, wide band gap, and good charge carrier mobility, it is a very attractive material. However, lack of understanding of the behavior of trapping levels in the band gap has restricted its advancement as a commercial detector. Such levels are caused by intrinsic defects and impurities,

which control carrier mobility and electrical compensation of the material. The focus of this project was to discover electron mobility by grid-probing the crystal with varying length sources. The electron mobility was then plotted against volume to determine surface impurities from polishing, the effective volume of the crystal, and how changes in the average lifetime of the electron (Üe) are caused. The driving force of the experiment is the need for large crystal detectors with high resolution. Large crystal detectors have better radiation stopping power, but have considerably worse resolution than smaller crystals. Being a large, single crystal capable of excellent resolution makes CZT a good prospect for commercial radiation detectors.

Neutral Kaon-Kaon Correlations at STAR. *CHARLES STEINHARDT (Princeton University, Princeton, NJ 08544) NU XU (Ernest Orlando Lawrence Berkley National Laboratory, Berkley, CA 94720)*

Bose-Einstein statistics predict identical bosons will tend towards the same quantum state. We consider the relativistic momentum difference between a pair of kaons, and pairs of kaons from the same event, which might interact, should have a smaller difference than pairs of kaons from different events, which cannot possibly interact. Theory predicts that the ratio of the two distributions, when properly normalized, should be 1 for large values of momentum difference but should be augmented by a Gaussian of some radius and amplitude 1 for small values. The radius is the uncertainty in momentum, so the uncertainty principle lets us determine a radius of the interaction. We used data taken from Au-Au collisions at RHIC (Relativistic Heavy Ion Collider) and observed by STAR (Solenoidal Tracker at RHIC) and examined the Bose-Einstein correlation of kaons, unstable spinless bosons. The energy at RHIC is initially high enough that the kaons are in equilibrium, and we measure them after they decouple, or "freeze out". One of the reasons this is interesting is that our energies are nearly high enough to create the Quark-Gluon Plasma, a postulated state that existed just after the big bang, and a large freeze out radius would be evidence of quark deconfinement that accompanies this state. However, our preliminary results are that we do not find any correlation. This would appear to conflict with published results from other experiments and other particles, though we developed some theoretical models that remove that conflict.

PHYSICS

Effect of Nearby Conducting Structure on the Macroscopic Stability of NSTX Plasmas. *ANNIE AHNERT (University of Arizona, Tucson, AZ 85721) JON MENARD (Princeton Plasma Physics Laboratory, Princeton, NJ 08543)*

The ability to predict the macroscopic stability of plasma is an important part of current magnetic fusion research. There are many different programs to predict the stability of plasma, but these programs also require approximations, such as idealized shapes for the closest conducting surface adjacent to the plasma. A program that was able to generate the approximate shape of the conducting surface was written with parameters to control the smoothness of the approximation. The program was used to generate conducting wall shapes accurately simulating the effects of the National Spherical Torus Experiment (NSTX) vacuum vessel and passive plates on the n=1 kink mode stability of a high beta=40% NSTX target plasma. Future studies will investigate the effect of the inner and outer conducting wall on lower beta plasmas.

Non-invasive Measurement of Ultrashort Bunch Lengths of Relativistic Charge Particles Using the Electro-optic Technique. *MUSTAFA AMIN (University of Texas, Arlington, TX 76010) T. TSANG (Brookhaven National Laboratory, Upton, NY 11973)*

An Electro-optic probe based on the Linear Pockels effect provides a non-invasive way of measuring the bunch length of charge particles down to the femtosecond time scale. The transient electric field induced by a relativistic charge bunch changes the dielectric properties of an EO crystal placed near the charge beam. The polarization state of an optical beam probing the crystal is modulated during its passage through the crystal by the electric field of the charged particles. The optical beam can then be analyzed to reconstruct the temporal profile of the electric field at the crystal and hence infer the pulse length. In this work an effort is made to understand the relation between the applied electric field, the rotation of the index ellipsoid, and Electro-optic modulation of light passing through an anisotropic crystal. General expressions for the rotation of the index ellipsoid,

Electro-optic retardation and intensity modulation are derived. The rotation of the index ellipsoid and retardation of an optical beam in LiNbO3 induced by a relativistic charge bunch is discussed.

Analysis of Creep Cavitation in Silicon Nitride Using Anomalous Ultra-Small-Angle X-ray Scattering. *JONATHAN ANDREASEN (Illinois State University, Normal, IL 61790) GABRIELLE LONG (Argonne National Laboratory, Argonne, IL 60439)*

The goal of this project is to investigate the deformation of silicon nitride at high temperatures. Silicon nitride is a ceramic used in the construction of gas turbines. It has excellent mechanical properties at high temperatures but deforms under tensile creep when put under a load. This tensile creep limits the application of this material. In commercial materials, the volume fraction of voids that are produced increases linearly with the amount of strain placed on the samples. Secondary phases (rare-earth oxy-nitrides) have been added to the silicon nitride in an effort to limit the creep behavior. Using Anomalous Ultra-Small-Angle X-ray Scattering (A-USAXS), the volume fractions of both the voids and secondary phase in deformed samples of silicon nitride can be measured. To find the volume distributions of the voids and secondary phase, the data from the X-ray scattering must first be reduced, and then analyzed. To find the volume distributions of the voids and the secondary phase, a C computer program was written. For all samples, the volume distributions of both the voids and the secondary phase were found. The results agree with the theory that the volume fraction of voids increases linearly with strain for the Yb-containing material. The ceramic containing Lu oxy-nitrides had very little strain measured and A-USAXS confirmed the small amount of voids present in this material.

Measurement of B to phi K with phi to Three pi. *DAVID ATTANASIO (Tufts University, Medford, MA 02155) THOMAS SCHIETINGER (Stanford Linear Accelerator Center, Stanford, CA 94025)*

Events of the type B to phi K with phi to three pi are isolated using optimized selection criteria from the BaBar 1999-2000 Run I data set (~20 1/fb). The efficiency of these criteria is analyzed using Monte Carlo studies, enabling a comparison to the predicted occurrence of such events. The only results provided are those of the Monte Carlo efficiency study. Suggestions on completion of the study are given.

Partial Discharge in Spherical Voids in Epoxy Insulation at Room and Cryogenic Temperatures. *DON BURDETTE (Indiana University of Pennsylvania, Indiana, PA 15701) ISIDOR SAUERS (Oak Ridge National Laboratory, Oak Ridge, TN 37831)*

Partial discharge, small bursts of current released in a dielectric material under an applied electric field, is a source of degradation and eventual failure in conventional equipment and cryogenic dielectric insulation for super-conducting power cables and transformers. Understanding the partial discharge (PD) patterns of typical defects will aid in the diagnosis of the remaining life span of the insulation. One such defect is a spherical void or bubble created during the curing process of epoxy. In this work, various electric fields are applied across a spherical air-filled void inserted into epoxy to study the PD pattern produced in terms of charge magnitude q and the ac power supply phase angle N. PD patterns of epoxy samples with and without a void are compared in both oil at room temperature and liquid nitrogen at cryogenic temperature. A difference in the observed PD patterns at room and cryogenic temperatures is distinct. It has also been observed that the PD pattern associated with the void is dependent on how long the sample is aged. In order to clarify the PD signals originating from the samples, PD noise from other sources and their associated patterns are discussed along with noise reduction techniques. The electric field in the void and the solid sample is modeled using Ansoft software to gain an understanding of the physical mechanisms at work inside the two samples.

Ion Beam Implantation Induced Au Nano-Cluster Formation in MgO (100). *ANDREW CAVANAGH (Fort Lewis College, Durango, CO 81301) THEVA THEVUTHASAN (Pacific Northwest National Laboratory, Richland, WA 99352)*

The formation of nano-clusters within an oxide via ion beam implantation is of significant interest because of the ability to parametrically alter the physical characteristics of the cluster formation. This allows for the creation of a variety of optical properties by optimizing the size and density distribution of the nano-clusters within the crystal. These

parameters include altering the energy of the implantation ion, the fluence, the temperature of the crystal and post implantation annealing. For this experiment the implantations were carried out on MgO (100) with a 2 MeV Au^{2+} ion beam at a range of temperatures from 300K to 975K with fluences ranging from 1 to 20 x 10^{16} ions/cm^2. Characterization of the crystals was completed using Rutherford backscattering analysis (RBS) with multi-axial channeling, high-resolution transmission electron microscopy (TEM) and optical absorption. Measurements of the samples were conducted directly after implantation and following ex-situ annealing at 1475K. RBS and channeling measurements were used to characterize the individual samples for both virgin and implanted regions in three of the major crystalline axis, (100), (110) and the (111). These measurements will be discussed further.

On Radiation Levels at the PHOBOS Detector. *JOEL CORBO (Massachusetts Institute of Technology, Cambridge, MA 02139) ALAN CARROLL (Brookhaven National Laboratory, Upton, NY 11973)*
Because of its large number of silicon-based sensors, the PHOBOS detector is very sensitive to radiation levels, and a great deal of time is spent monitoring these levels with thermoluminescent dosimeters (TLDs), beam loss monitors (BLMs), and chipmunks. It was noted that there is an asymmetry between the radiation levels on the two sides of the beampipe. A calculation was done to show that it is possible that alpha particles generated by the gold ion beam might be causing this asymmetry. It was also noted that there is a very steep falloff of radiation levels near the beampipe. A study using TLDs verified that this falloff is exponential and that it falls to background levels at approximately 15 cm from the beampipe. Finally, a study was done using radiation data from the chipmunks and beam data from RHIC to calculate "beam quality", a measure of whether the radiation levels present are acceptable based on the beam currents and energy.

Development of Laser Beam Image Analysis System and Characterization of Flash:Ti Laser Beam. *SEAN CORUM (Augustana College, Sioux Falls, SD 57197) AXEL BRACHMANN (Stanford Linear Accelerator Center, Stanford, CA 94025)*
Lasers are highly important in medicine, industry, and physics. In particle accelerators, lasers are used in Photo Injectors for attaining polarized electron beams. As such, a clean beam profile is crucial to the role photo injecting lasers have in particle physics experiments. However, qualitative analysis methods of a laser beam profile (such as burn paper) are difficult and waste precious particle beam experiment time. An efficient, quantitative method of beam profile analysis is required to maintain performance of the polarized light source. A laser beam image acquisition and analysis system is developed using a CCD camera, a frame grabber card, an IBM compatible computer, and Labview (National Instruments, G programming language). The system analyzes the beam profile in continuous real-time and single shot formats. The program is versatile and calculates axis lengths, ellipticity, elliptical fit, tilt, Gaussian fit, Gaussian parameters, and 3D intensity plots. This system will be used at the Stanford Linear Accelerator Center to monitor the health of the Photo Injectors. To demonstrate the systems ability to quickly and efficiently analyze a laser beam profile, it is used to characterize thermal lensing of a single-mode and a multi-mode Flash:Ti laser beam in the Laser Development Lab. The focal range due to thermal lensing of the laser rod was observed. The system shows promise as an important tool in the diagnostics and problem solving of the particle accelerator's Polarized Light Source.

Z-axis and photomultiplier calibration for the KAMLAND detector. *AIDAN CRAIG (University of California, Berkeley, Berkeley, CA 94720) STUART FREEDMAN (Ernest Orlando Lawrence Berkley National Laboratory, Berkley, CA 94720)*
Ever since the 1998 report of a deficiency in atmospheric neutrino flux by the SuperKamiokande detector, neutrino physics has sought an explanation for the shortage of detected neutrinos from the sun, reactors, and other neutrino sources. The most popular answer to this puzzle has involved neutrino flavor oscillation, which would itself require non-zero neutrino mass eigenstates. The KAMLAND experiment, itself the successor to SuperKamiokande, seeks to provide a definitive measurement of the neutrino oscillation parameters sin2B and DM2 by measuring electron antineutrino flux from several reactors around Japan, as well as the difference in azimuthal and solar neutrino fluxes. Unprecedented precision is to be achieved from the combination of a relatively long baseline (approx. 150 km), as well as an extremely large detector volume of 1150 cu. meters of liquid pseudocumine scintillator. As such, the experimentally determined

neutrino energy spectrum will allow physicists to distinguish between the Large Mixing angle, Small Mixing Angle, and the "just so" Vacuum models of MSW-enhanced oscillation put forth to explain the undercount. Given the notoriously weak coupling of neutrinos to normal matter, proper calibration of the detector will be vital, both to better characterize neutrino energies and to eliminate radioactive background, particularly from solar neutrino data. This is to be accomplished through the deployment of radio- and photo-active sources of known energy along a Z-axis and eventually a 4-pi deployment mechanism, along with an event reconstruction scheme requiring detailed information about phototube time response within the detector.

Evaluation of the Performance of PGT RG-11A/C and Amptek A250 Preamplifiers in Configuration with a Germanium Detector. *SHELECE EASTERDAY (University of Notre Dame, Notre Dame, IN 46556) HARRY MILEY (Pacific Northwest National Laboratory, Richland, WA 99352)*
Radiation detection is an increasingly important branch of science. Gamma-ray detection has applications in several fields, including high-energy physics. Germanium detectors are employed in many experiments of this sort. Gamma ray events picked up by a germanium detector are sensed by a charge-integrating preamplifier. A charge-integrating preamplifier is comprised of a field effect transistor (FET), an operational amplifier, and an RC circuit that integrates the charge of the radiation event and dissipates the charge over a time constant. In determining the performance of a particular preamplifier, one must test the energy resolution of the detector-preamplifier configuration and analyze the fall time of the preamplifier signal. The resolution of a preamplifier can be tested by exposing it to a radioactive source and analyzing the resulting energy peaks with data acquisition equipment. Using a pulser to simulate a radioactive source of a particular energy, one can look at the fall time of the preamplifier signal with an oscilloscope and determine its quality. In this project, the performance of a Princeton Gamma Tech RG-11A/C preamplifier and an Amptek A250 preamplifier were evaluated through the testing of energy resolution, the observation of leakage current on the Ge detector, and the analysis of preamplifier signal characteristics and baseline noise measurements.

Luminosity Calculation and Data Quality Analysis of Peripheral Collisions. *DREW FORMAN (Yale University, New Haven, CT 06520) FALK MEISSNER (Ernest Orlando Lawrence Berkley National Laboratory, Berkley, CA 94720)*
The STAR experiment searches for signatures of the quark-gluon plasma (QGP) formation and investigates the behavior of strongly interacting matter at high energy density. In the experiment two beams of gold ions, traveling at relativistic speeds, intersect to produce collisions. Two properties of these beams, cross-section and luminosity, are fundamental to the experiment and need to be accurately calculated. The cross section is known from theoretical computation, however the luminosity must be determined using the equation N = rLe, where N is the number of events, r is the cross section of the gold beams, L the luminosity, and e the efficiency of the detector. With r now known and e found through Monte Carlo computer simulations, the Luminosity can be calculated by determining the number of events in the experiment. However, events during which the beam lines were unstable or the detectors had inconsistent readouts must be eliminated from the count and subsequent luminosity calculation. To remove such events, a detailed analysis of several variables must be made both over time and over each of the 2000 event data files. Large fluctuations in the variables of the beams coordinate position (x, y, and z vertexes) would reveal unstable beamline tuning and possible bad data. More importantly, a disparity among the detector readouts, specifically the ZCD (Zero degree Calorimiter) and the TPC (Time Projection Chamber) would signify unusable events.

Development of an Ultra High Vacuum End Station with Surface Science Capabilities. *CARA GAINCOLA (Columbia Basin College, Pasco, WA 99301) SHUTTA SHUTTANANDAN (Pacific Northwest National Laboratory, Richland, WA 99352)*
There is a growing interest in physics labs about the epitaxial growth of model oxides on various oxide and metal substrates to obtain high-quality surfaces and films. A number of single crystal oxide films on various substrates have recently been synthesized in our laboratory using oxygen-plasma-assisted molecular beam epitaxial growth. In the

present work, we have developed an Ultra High Vacuum (UHV) end station with surface science capabilities including Auger Electron Spectroscopy (AES) and Low Energy Electron Diffraction (LEED) for oxide studies. This end station will be connected to the channeling beam line at the accelerator facility to incorporate ion beam capabilities in addition to the surface science capabilities. A TiO_2 (110) single crystal was used to test the processing and analytical capabilities in the chamber. Ceria single crystal thin films on yitria-stabilized zirconia were used for channeling investigations in a similar chamber. A brief description of the UHV chamber, preliminary results from the spectrometers and Rutherford Backscattering Spectroscopy (RBS)/channeling results from the ceria films will be presented.

A new Muon Trigger for the Measurement of the Quark Distribution Functions in the Proton with the PHENIX Detector. *HAROLD HAGGARD (Reed College, Portland, OR 97202) MATTHIAS GROSSE-PERDEKAMP (Brookhaven National Laboratory, Upton, NY 11973)*
Results from the first polarized Deep Inelastic Scattering (DIS) measurements led to the so called "proton spin crisis", the observation that quarks only carry a small fraction of the proton spin. Parton Distribution Functions (PDF) describe the contributions of the various constituents of the Proton to its overall spin and are well understood over a large range in x Bjorken. Direct measurements of the PDF at low x will constrain both DG (the gluon contribution) and DS (the quark contribution) in the near future. Measurements of asymmetries in W± production at RHIC will allow discrimination between a flavor symmetric and flavor-broken picture of the polarized (and unpolarized) light sea quarks. The Relativistic Heavy Ion Collider (RHIC) will produce polarized proton-proton collisions with center of mass energies up to 500 GeV. These energies along with two large muon spectrometers provide the Pioneering High Energy Nuclear Interaction eXperiment (PHENIX) with high sensitivity to the production and decay of W±, an excellent channel for measuring the quark and anti-quark distributions. Monte Carlo simulations of both W± decay and hadronic jet background yielded a muon rate that is larger than PHENIX can accept online. A method for reducing this rate, by placing a detector near the interaction point to distinguish jet showers from W events, was studied and shows promise.

BPST Coil Design and Optimization. *ERIC HARKLEROAD (Princeton University, Princeton, NJ 08544) NEIL POMPHREY (Princeton Plasma Physics Laboratory, Princeton, NJ 08543)*
We seek an optimal configuration of Ohmic Heating (OH) and Equilibrium Field (EF) coils for the proposed Burning Plasma Spherical Tokamak (BPST) at PPPL. To determine the EF coil positions for the new device, we scale the design of the National Spherical Torus eXperiment (NSTX), and determine a discrete set of candidate coil positions. We then employ the Tokamak Simulation Code (TSC) to isolate which small subset of these coils experience the greatest changes in current as plasma shape and current profile vary. We select these as our design. Upon fixing the EF coil positions, we optimize the height of the center stack by varying the height and noting variations in the ohmic field error, selecting a height at which these errors are acceptably small. We next seek an ohmic current distribution-a set of EF and OH coil currents which produces little or no field within the plasma. The field produced by an arbitrary current distribution is invariant under addition of a scalar multiple of an ohmic distribution. We outline two methods of approximating an ohmic distribution and implement them in Fortran 90, calling on subroutine E04UNF from the Numerical Algorithms Group (NAG) Library, a specialized routine designed to minimize a function of many variables. We also include provisions for efficient optimization of a center stack of ohmic heating coils. Coupled with other studies and simulation codes, our coil design and optimization codes have the potential to make significant contributions to the design of BPST.

ATLAS / RIA Website. *TERESA HASLINGER (Richard J. Daley College, Chicago, IL 60629) FRANK E. MOORE (Argonne National Laboratory, Argonne, IL 60439)*
During my summer internship at Argonne my assignment was to work on a new website for the Physics Division. This website has two parts. For the first part, this website includes the ATLAS Accelerator Facility (ATLAS) that needed to be updated. ATLAS is a system that accelerates ions for the production of heavy ion beams. Such beams are valuable in the understanding of basic nuclear physics. Dr. Frank Moore, my mentor, drew the site plan from which originated the first part of the website. The information that was used for this site was

taken from many sources in the Physics Division. The second part of the website includes a proposed facility - the Rare Isotope Accelerator (RIA) - which Argonne is bidding for. RIA produces and accelerates beams of short-lived nuclei, which will help to understand nuclei far from stability. The information is basically the same (the information is mostly taken from the original site), but the design is much improved. For both parts of the website, images and text were used. The use of images in combination with text made it possible to make the information clear and easy to understand for the reader. The implementation of this site is at www.phy.anl.gov/atlas/index.html.

Development and Analysis of an Electrically Tunable Optical Filter. *KRISTI HULTMAN (Harvey Mudd College, Claremont, CA 91711) FRED LEVINTON (Princeton Plasma Physics Laboratory, Princeton, NJ 08543)*
The focus of my research experience was the development of an electrically tunable optical filter using a He-Ne laser and a combination of polarizers (P), LN crystals (C), and retarders (R). A variable high voltage power supply was attached to the LN crystals, allowing us to optimize transmission of specific wavelengths. The retarder used was made from 3 polarizing lenses, with the middle lens rotated 59.0° off axis. For analysis of the filter transmission, a LabView program was written to display the image of the beam captured using a CCD camera, as well as peak and average intensities, and save the data. We were successful in tuning the laser to a minimum and maximum in both the PCP and PCRCP configurations, and can resolve wavelength variations of less than 0.1nm. A stable, easily tunable optical filter would allow for a cleaner signal when looking at a specific wavelength or allow you to block out a certain wavelength, thus the noise from unwanted wavelengths would be reduced.

Predicting Neutralino Continuum Annihilations Using DarkSUSY. *SAMEH KAMEL (Santa Clara University, Santa Clara, CA 95053) EDUARDO DO COUTO E SILVA (Stanford Linear Accelerator Center, Stanford, CA 94025)*
Physicists do not fully understand the nature of dark matter although we infer its existence from experimental observation. This project is part of the dark matter detection searches with GLAST. We are investigating one of the WIMP candidates called the neutralino, a particle predicted by the Minimal Supersymmetric Standard Model. In particular, we ran a computer simulation called DarkSUSY that predicts the signature that we expect to see in the data from GLAST that pertains to the detection of the neutralino in the galactic halo.

A New Electron for Gluon Polarization Measurements Through Heavy Flavor Production in PHENIX. *SUSAN KANE (Rensselaer Polytechnic Institute, Troy, NY 12180) MATTHIAS GROSSE PERDEKAMP (Brookhaven National Laboratory, Upton, NY 11973)*
In the endeavor to better understand the universe, physicists strive to understand the smallest "elements" of matter. The make-up and behavior of these particles affect everything around us, even the distribution and motion of the galaxies. In an attempt to better understand one of the four fundamental forces, the so-called strong nuclear force, physicists examine the spin-dependent structure of the proton. The Relativistic Heavy Ion Collider will collide two beams of polarized proton beams, starting in November. At full luminosity, protons will collide an average of 1.2 times every 106 ns. At high collision rates, the amount of data generated in the detectors exceeds the capacity of the data acquisition system. Using fast event selection electronics and processors, triggers, the data volume can be reduced without loosing the quality of the information. For the PHENIX detector we have studied how to use information from the Electromagnetic Calorimeter, and the Ring-Imaging Cherenkov Counter to filter out the interesting physics events thus reducing the raw rate by a factor of 5000.

Exploring Aspects of Neutrino Physics Using a Web-based Interactive Learning Module. *RICHARD KOGEN (University of Illinois, Chicago, Chicago, IL 60607) PETER KASPER (Fermi National Accelerator Laboratory, Batavia, IL 60510)*
The purpose of this research is to aid in the design and implementation of a "work-in-progress" Web-based interactive learning module based on the MiniBooNE neutrino experiment at Fermilab National Accelerator Laboratory. The MiniBooNE Neutrino experiment is a high-energy neutrino oscillation experiment that was initiated to confirm and extend, or deny the findings of neutrino oscillations detected by the LSND experiment at Los Alamos National Laboratory. The BooNE Educational Web Module is an attempt to provide an opportunity for high school and college level students taking physics to learn about and virtually experience high-energy neutrino physics research through an

experiment simulator. This simulator will be widely available through the BooNE Website. This is a qualitative research study focusing on students' navigational processes as they interact with the BooNE Website.

Tile Calorimeter and MySQL Database. *TOM KOTSAKOS (Wilbur Wright College, Chicago, IL 60634) BOB STANEK (Argonne National Laboratory, Argonne, IL 60439)*
A Large Hadron Calorimeter is being built at CERN in Geneva, Switzerland. This collider will be able reach energies of seven TeV. Many experiments require high energy. One of the main goals is to discover the Higgs Boson, which can be created by a high-energy collision. One section of the Tile Calorimeter is being built at Argonne National lab. The construction and testing data are being put into a database using MySQL as the RDBMS. The Tile Calorimeter measures the energy of particles that are generated by the collision of the protons. When a particle goes through a tile, it sends a photon down the fiber to be amplified and read. The database works by joining tables on unique keys. Any other secondary program can utilize the output of a query. The database will be accessible through the web with a graphical interface and forms for search criteria. When the LHC and ATLAS are completed, the database will have further use in integrating with new data or other databases.

Electron Bernstein Wave Polarization Measurements on CDX-U. *THOMAS KRAMER (Brown University, Providence, RI 02912) PHILIP EFTHIMION (Princeton Plasma Physics Laboratory, Princeton, NJ 08543)*
Mode-converted (MC) EBWs offer an attractive path for electron temperature measurement, heating, and current drive in overdense plasmas (Plasma frequency >> Cyclotron frequency). A quad-ridged antenna was installed in CDX-U with a movable limiter, which shortens electron density scale length at the MC layer and hence optimises MC efficiency. Electrostatic EBWs are expected to MC to X-mode electromagnetic waves. Measurements were made with both the X- and O-mode aligned antennas, and the X/O ratio was calculated. An X/O ratio > 2 was observed with the antenna near the MC layer, in contrast to a ratio of 1.2 measured previously with an antenna outside the vessel. A ratio of ~1 was seen with the antenna far from the MC layer, possibly due to reflections between the plasma and vessel wall causing polarization scrambling. Reduction of the X/O ratio was observed when the limiter was extended, likely due to polarization mixing caused by reflection or refraction at the limiter surface in front of the antenna.

Development of Novel Infrared Photonic Devices in Bulk Chalcogenide Glasses. *ANDREW LAFORGE (University of Puget Sound, Tacoma, WA 98416) RICHARD M. WILLIAMS (Pacific Northwest National Laboratory, Richland, WA 99352)*
We explore the permanent photomodification of bulk chalcogenide glasses, with the prospect of incorporating the processes into the development of infrared photonic devices. Effects include photoexpansion, photodarkening, and change of refractive index. Illumination of AsS and GeAsSe with HeNe laser light produced surface expansions of up to 5 microns and darkened regions 175 microns into the material, values considerably larger than those typically reported for thin films. Optical microscopy shows evidence of the creation of subsurface lenses. Although intensity variations affect the speed at which the process occurs, the type and degree of modification are largely dependent upon wavelength and exposure of writing light. The results suggest bulk samples can be used in the fabrication of discrete waveguide-based photonic devices for infrared laser applications.

Exploring the Limitations of the Dipole Approximation with Electron Time of Flight Technology. *SIERRA LAIDMAN (Bryn Mawr College, Bryn Mawr, PA 19010) FRED SCHLACHTER (Ernest Orlando Lawrence Berkley National Laboratory, Berkly, CA 94720)*
Single photoionization is a process in which a photon collides with an atom or molecule and an electron with a certain kinetic energy is emitted, leaving behind a residual ion. The dipole approximation describes the angular emission of these electrons. It assumes that the electromagnetic field of the radiation, expressed as a Taylor-series expansion, can be simplified by using only the first term of the series. It has been known for some time that the dipole approximation becomes inaccurate at high photon energies, and it has recently been determined that there are discrepancies at lower energies as well. In order to enhance our understanding of these limitations, we measured the electron emissions of nitrogen and neon using the latest technology. Beamline 8.0.1 at the Advanced Light Source was used with an electron Time-of-Flight (TOF) end station. Data were collected over a broad range of photon energies (254 - 664 eV) using five analyzers placed at different angles. We also collected the spectra at 15 rotation angles, between 0 degrees and -90 degrees, about the axis of the photon beam. The data from this experiment will likely take a year to fully analyze, but preliminary analysis seems to indicate that these results confirm that the dipole approximation breaks down at photon energies well below 1 keV and that this breakdown is greatly enhanced in molecules just above the core-level ionization threshold.

Automation of the Vacuum System in Area II of the ATLAS Super-Conducting Linac. *DANIEL LASCAR (University of Chicago, Chicago, Il 60637) GUY SAVARD (Argonne National Laboratory, Argonne, IL 60439)*
The system of vacuum pumps and valves that exists throughout area II of the ATLAS was becoming more and more complex to control manually. Furthermore, simply pumping down the system was becoming a very cumbersome, time consuming, and increasingly specialized task. With increasing beam-time being wasted, automation of the vacuum system became a necessity. To do this it was decided a Programmable Logic Controller (PLC) should be used to control and monitor the system. With the PLC, it was possible to run the system both automatically and manually via the use of buttons and switches. In addition, error localization could be performed by the PLC rather than the having to test each possible failure when one part of the target area went down. To automate this system, new pneumatic valves and thermocouples had to be ordered, a procedure for the operation of the vacuum system had to be constructed, a program in the ladder logic of the PLC had to be written, and a board containing both the manual controls for the system and the LED's that would indicate the status of the system had to be designed and constructed.

Prepping USA X-ray Pulsar Data for Analysis. *CHRISTOPHER LAWYER (Florida A & M University, Tallahassee, FL 32307) EDUARDO DO COUTO E SILVA (Stanford Linear Accelerator Center, Stanford, CA 94025)*
The USA satellite was used to record data on several pulsars. In this project data produced by the satellite was altered so that it could be entered into a program called TEMPO. Through TEMPO several characteristics (referred to as the orbital parameters) of the pulsars will be defined. Using two well-documented pulsars, Crab and Cen X-3, the tools for analysis will be tested. If they prove to be adequate, then they will be used to study a special class of pulsars called AXPs. Through study of AXPs, it is believed that light can be shed on many of the mysteries now associated with pulsars.

Ultrafast Time-Resolved X-Ray Science at the ALS. *DAVID LE SAGE (University of California, Berkeley, Berkeley, Ca 94720) ROGER FALCONE (Ernest Orlando Lawrence Berkley National Laboratory, Berkley, CA 94720)*
The group that I did research with this summer conducts ultrafast time-resolved x-ray diffraction and absorption experiments on materials undergoing structural phase transitions. These experiments are conducted at the Advanced Light Source (ALS) synchrotron at the Lawrence Berkeley National Laboratory (LBNL). The group uses 100 fs laser pulses to induce ultrafast phase transitions in the material being studied. These laser pulses are synchronized with X-ray pulses from the ALS, which are used to probe the sample at various times before and after the laser pulse arrives. An x-ray streak camera with single-shot time resolution better than 1 ps is then used to collect the x-ray data. The streak camera is triggered by the laser pulse with a GaAs photoconductive switch, resulting in a camera timing jitter of less than 2 ps. With this time resolution, it is possible to directly probe the structural dynamics of materials undergoing phase transitions, and to make measurements on states of the material that can only exist for a brief period of time after laser excitation. I personally assisted in several experiments of this nature during my summer research appointment, and helped to assess the possibility of increasing the resolution of the streak camera.

Accelerator Orbit Simulation. *BRENDAN LYON (Jamestown Community College, Jamestown, NY 14702) ALFREDO LUCCIO (Brookhaven National Laboratory, Upton, NY 11973)*

Computer simulations are necessary tools to apply theory to a subject matter being studied. It is applicable to particle accelerators especially because it deals with theory on a microscopic scale. With modern physics, it is possible to determine trajectories of particles (in this case, electrons) due to magnetic fields of quadrupole and sector magnets. Using a program called MAD, developed by CERN, we generate the necessary lattices for a particular accelerator, for example, an accelerator with bends or no bends. These FODO lattices represent force vectors of individual elements (quadrupoles) with respect to the experimental particle distribution. By applying each individual lattice to the distribution, we generate output files using C/C++ programming, which represents the same distribution with different positions and velocities. Output files are visualized using a Linux based graphing tool called Gnuplot, and Data Visualization Explorer (DX). Our major disadvantage is the output files are represented by two-dimensional slices; therefore, we are unable to fully use DX's three-dimensional rendering capabilities. In addition, we also investigated certain attributes of the distribution such as beta components, which represent the relative maxima of the distribution's envelope, energy distribution, and charge densities.

Restoration of BaBar Prototype Drift Chamber. *MARY MANNING (University of Virginia, Charlottesville, VA 22904) MICHAEL KELSEY (Stanford Linear Accelerator Center, Stanford, CA 94025)*
A drift chamber tracks the paths and energies of particles by measuring the charge pulse of electrons liberated by those particles as they traverse the chamber. The BaBar drift chamber (IR-2) is currently operational, but the prototype chamber (Proto II) was not. The prototype drift chamber was restored so that it could be used as a test stand for new drift chamber hardware and software. The scintillator telescope trigger system, front-end electronics, high voltage supplies, water chiller, and gas system were installed, tested, and activated. Diagrams and text documentation describing the setup and running procedures for Proto II were created. Calibration and data acquisition software were modified to be compatible with two drift chamber platforms. Initial calibrations failed due to compatibility problems between drift chamber configuration maps and hardware. Subsequent calibrations were successful.

A Proton Detector Array For Deeply Virtual Compton Scattering. *MICHAEL MASKELL (Old Dominion University, Norfolk, VA 23529) CHARLES HYDE-WRIGHT (Thomas Jefferson National Accelerator Facility, Newport News, VA 23606)*
A Deeply Virtual Compton Scattering (DVCS) experiment involves scattering an electron off of a proton and observing the paths of the proton, electron, and the photon emitted. In order to perform such an experiment, three detectors are required, one for each particle. For the DVCS experiment at TJNAF, a 100-element, semiannular proton detector array will be used. The core of each element is the scintillator material that actually does the detecting. For cost effectiveness, plastic scintillators will be used in this experiment. The design of the detectors must take into consideration protection of the scintillator material, maximizing light collection from each individual scintillator, minimizing light collection from neighboring scintillators, and preventing magnetic fields from altering the paths of collected photons. The scintillators must be wrapped to protect them from contaminants such as skin oils, which can attack them, as well as to prevent leakage of light from one block to the next. A reflective Mylar wrapping will provide this layer of protection, and help direct more light into the photomultiplier tubes by reflecting stray photons back to the tubes. To shield the photomultiplier tubes from external magnetic fields, the tubes will be encased in a mu-metal shield. The base plate will be made of Aluminum, with a mu-metal plate attached to provide additional shielding, particularly from the fringe fields produced by the mu-metal tube. Following this basic design for each of the 100 elements of the proton detector array should allow the array to perform with the desired accuracy.

Hybrid Calorimeter Algorithm Development for PrimEx Experiment. *EUGENE MOTOYAMA (Massachusetts Institute of Technology, Cambridge, MA 02139) ASHOT GASPARIAN (Thomas Jefferson National Accelerator Facility, Newport News, VA 23606)*
The PrimEx Collaboration seeks to measure the lifetime of the pi^0 meson (neutral pion) at high precision. The decay rate of the pion is considered to be the most fundamental prediction of low-energy quantum chromodynamics (QCD). Pions will be produced by the Primakoff Effect: a few GeV photon interacts with the coulomb field of a nucleus to produce a pion. The pion then decays almost immediately ($\sim 10^{-16}$ seconds) into two photons. The decay photons will be detected by an electromagnetic hybrid calorimeter (HYCAL), an array of lead tungstate and lead glass crystals. An algorithm is needed to calculate the angular separation of the two decay photons (and thus the invariant mass of the pion) from the energies deposited in HYCAL. A GEANT Monte Carlo simulation of the experiment is used to test and develop the algorithm to achieve the best angular resolution. The development of the algorithm is essential to the PrimEx project.

Derivation of an Optical Filter to Optimally Combine Solar and Electric Light Using Computational Modeling. *TIMOTHY MOWRER (North Carolina State University, Raleigh, NC 27607) JEFF MUHS (Oak Ridge National Laboratory, Oak Ridge, TN 37831)*
Combining collected solar light with conventional electric lighting could drastically reduce energy consumption in buildings. Because the luminosity of solar light fluctuates from hour to hour and generally does not match the color values of conventional electric lights, such a hybrid lighting fixture would require a filter to optimize the appearance of the incoming solar light. The solar spectrum data is acquired via a computer algorithm written by the National Renewable Energy Laboratories (NREL). This data is further manipulated by an algorithm to simulate the effect of the fiber optic cable that will carry the light to the fixture. This data is generated for an entire year in thirty-minute increments. A genetic algorithm is then employed to determine an appropriate filter. Concentrating on the visible spectrum only, the filter is designed to optimize luminosity, chromaticity coordinates (color values), efficiency, and operation time (after sunrise and before sunset). All of these algorithms are combined into a single, customizable program with a Windows Graphical User Interface written in Borland C++. The program is designed to keep the color difference within a 1-step MacAdam ellipse, the minimum amount of color difference perceivable by the human eye. The use of a genetic algorithm will also allow future researchers to easily redefine the criteria for determining the optimal filter.

Electron cyclotron emission diagnostics of the VASIMR plasma rocket concept. *RYAN MUNDEN (Stetson University, DeLand, FL 32720) D.A. RASMUSSEN (Oak Ridge National Laboratory, Oak Ridge, TN 37831)*
Advances in space exploration and sciences have led to great benefits for humankind. To continually enjoy those benefits and advances, it becomes necessary to improve the basic tool of space exploration, the rocket. Current chemical burn rockets are very useful for near-earth tasks and for breaking free of the Earth's gravitational field. The next step in space propulsion is a continuous burn, variable impulse rocket, which may be achieved through the VASIMR plasma rocket. The plasma rocket enables variable throttling of the propellant to maximize fuel efficiency. The plasma, an ionized gas, is created and accelerated by radio frequency (RF) fields launched with a helicon antenna. It attains much higher exhaust velocities enabling very rapid transit through space. By measuring the intensity and frequency of electron cyclotron emission in the plasma, a correlation to the electron temperature can be found. Preliminary tests with a helicon plasma source at Johnson Space Center showed promise that emission was in accordance with the predicted values based on the applied magnetic fields in the system. Continued tests on the Mini-RFTF helicon plasma system at ORNL have so far been inconclusive. Further testing with improved amplification and receivers is planned so that this diagnostic technique can be fruitfully applied to the VASIMR system. Determination of the electron temperature is important in developing models of the experiment.

Pulsewidth Calculations Using a Photodetector and Two-photon Absorption Measurements Compared to Interferometric Autocorrelation. *ANDREA MUNRO (University of Washington, Seattle, WA 98195) MICHELLE SHINN (Thomas Jefferson National Accelerator Facility, Newport News, VA 23606)*
We attempted to determine through experimentation, that two-photon absorption would be the ultrafast pulsewidth measuring technique best suited to be used as a reliable diagnostic for the Free Electron Laser at Jefferson Lab. Two-photon absorption was to be compared with interferometric autocorrelation as methods of pulsewidth measurement that allowed for a large bandwidth and relative ease in alignment. Experimenting parasitically we were unable to collect data

that would allow us to draw useful conclusions about our hypothesis. I did learn the inherent difficulties of experimentation and this experience increase my interest in both laser technology and in becoming an experimentalist.

Detection of Pions and Kaons in Meson Electroproduction.

NADIA NOVIKOFF (Houston Baptist University, Houston, TX 77478) ROLF ENT (Thomas Jefferson National Accelerator Facility, Newport News, VA 23606)
We performed numerous tests to determine if it is possible to separate and then detect pions and kaons emitted by meson electroproduction using an HMS Aerogel Cherenkov detector in Hall C. The case of interest was that of the accelerator beam passing through a hydrogen target, producing a meson that subsequently passes through an aerogel Cherenkov detector, after which the electrons are detected by the SOS and the pions and kaons by the HMS spectrometers. The aerogel detector would contain sixteen photomultiplier tubes and aerogel of a refraction index of either 1.015 or 1.030. We found that it would be possible to separate pions and kaons in this manner, particularly using aerogel with a refraction index of 1.015. We also tested the photomultiplier tubes to be placed in the aerogel Cherenkov detector for gain.

Development and Redesign of an Effective Educational Particle Physics Website.

LAURA OCHOA-FRONGIA (University of California, Berkeley, Berkeley, CA 94720) R. MICHAEL BARNETT (Ernest Orlando Lawrence Berkley National Laboratory, Berkley, CA 94720)
Particle physics is a subject virtually untaught in high schools in the United States, largely because an extensive mathematical and physical background is required to grasp the complex theories and principles. A joint venture between Lawrence Berkeley National Laboratory (LBL) and Fermilab conceived the original "Run II Discovery" website featuring an investigation of the existence of the Higgs boson. After analyzing the website, it was deemed that a new structure and motivation were needed to effectively bring particle physics to pre-collegiate audience. By engineering a site that is a self-contained goal-oriented research simulation, students and teachers are given all the tools to learn a considerable amount of particle physics without encountering the heavy math that often prevents the instruction of this subject in high schools. The new website contains background on the field and a tutorial to aid the students in analyzing real data from Fermilab's Tevatron and Monte Carlo simulations. The goal of exposing younger students to advanced research topics is to increase scientific curiosity, and diversify the high school curriculum. The redesigned website, which is pending approval, will replace the first draft at http://quarknet.fnal.gov/run2/.

TSC Plasma Simulations for NSTX Center Stack Upgrade.

ANDREW OSGOOD (Muhlenberg College, Allentown, PA 18104) STANLEY KAYE (Princeton Plasma Physics Laboratory, Princeton, NJ 08543)
The National Spherical Torus Experiment, or NSTX, is the primary fusion device at PPPL. In an effort to continue efficient use of the machine, a planned center stack upgrade needs numerous computer simulations to determine its practicality. Using specially designed programs called Tokamak Simulation Code, or TSC, numerous qualities and quantities can be accurately simulated. Initially, a shape range had to be determined using the static version of TSC, since the shape of the plasma is integral in many other practical aspects such as stability. Once a stable static shape range was determined, the pf coil currents could be used in the dynamic TSC version to develop a more plausible plasma that evolved through time. For both 1.5MA and 3.0MA plasmas (the only two plasma currents simulated) the TSC produced acceptably wide shape ranges. The 1.5MA plasmas found a wider range, since much higher values of li and a lower current allowed control from pf coils through lower currents. (The pf coils have maximum current limits that restrained most 3.0MA runs.) These runs produced values that were used as input for the dynamic TSC runs, but also illustrated that an adequate shape range could be produced using the new center stack upgrade parameters. The coil currents produced in static simulations will be used in continuing dynamic simulations that strive for specific plasma properties according to future needs. Starting the dynamic runs has shown that this is possible and can produce viable results, and many more simulations will follow.

Study of Magnetic Damping in Liquid Metal Surface Waves.

DAVID PACE (University of the Pacific, Stockton, CA 95211) HANTAO JI (Princeton Plasma Physics Laboratory, Princeton, NJ 08543)
Knowledge of liquid metal surface waves and instabilities provides insight regarding turbulence in plasmas and the magnetohydrodynamic (MHD) model used to describe plasmas generally. Such work is also critical in the development of liquid lithium walls to be used in fusion reactors. The Liquid Metal Experiment (LMX) is designed to study magnetically induced damping of liquid gallium surface waves by driving such waves in the presence of a magnetic field. Previous work measured the dispersion relation and confirmed that a magnetic field aligned perpendicularly to the direction of wave propagation has no effect. More recent findings have demonstrated that a magnetic field aligned parallel to the direction of wave propagation causes significant damping of the waves that follows a Gaussian dependence, and confirmed that the wave number varies in the presence of a magnetic field.

Using the Electron Time of Flight Technique to Analyze the Limitations of the Dipole Approximation.

MONICA PANGILINAN (Cornell University, Ithaca, NY 14853) FRED SCHLACHTER (Ernest Orlando Lawrence Berkley National Laboratory, Berkley, CA 94720)
Understanding the electronic structure of atoms and molecules is fundamental in determining their basic properties as well as the interactions that occur with different particles such as light. Theoretical models of electronic structures use the dipole approximation to simplify x-ray interactions with atoms and molecules. This approximation takes the exponential describing x-ray radiation and truncates everything but the first term. However, at both extremes of the photon energy, the dipole approximation is inaccurate. The electron time-of-flight technique is used to measure the time required for electrons emitted by photoionization to travel a fixed distance. Photoionization is a process describing the collision of a photon with an atom or molecule that produces a free electron and a residual ion. Using the electron time-of-flight technique, five analyzers were used to detect the electrons produced from neon and nitrogen gas at fifteen different chamber angles. From the spectrum produced, the dipole and nondipole parameters were experimentally determined at moderate photon energy values to examine whether nondipole effects must be taken into consideration at energy values far from the extremes. Results indicate that nondipole effects must be taken into consideration at energy values close to the core-level ionization threshold. Furthermore, other molecules and atoms were tested before and show the same conclusions, leading us to believe that these effects are universal. As a result, new theoretical models must be made that use higher order terms that were previously truncated.

X-ray Variability in Seyfert 1 Galaxies: The Correlation Between Spectral Index and Flux.

KAREN PETERSON (Yale University, New Haven, CT 06520) GREG MADEJSKI (Stanford Linear Accelerator Center, Stanford, CA 94025)
The process of energy radiation from active galactic nuclei (AGN) is not well understood. Variability of the radiation occurs on the shortest time scales in the X-ray energy band, hence X-rays must originate nearest the power source of AGN that is suspected to be a black hole surrounded by an accretion disk. The examination in this paper of the X-ray emission of three Seyfert 1 galaxies identifies a direct relationship between spectral index and flux. This finding refutes the simplest proposed model for X-ray radiation of AGN, and an improved model with a feedback mechanism is discussed here.

Fluka Benchmark of Neutron Energy Spectra at 90-degrees.

ANDREW PURYEAR (Texas A&M University, College Station, TX 78752) SAYED ROKNI (Stanford Linear Accelerator Center, Stanford, CA 94025)
This paper presents a comparison between results of FLUKA particle interaction and transport code benchmarked with experimental measurements of neutron energy spectra at 90-degrees produced by the irradiation of various targets by a 2.04-GeV electron beam. Neutron fluence, integrated yield, and time of flight calculated by FLUKA are compared with experimental results. Also, the effects of various components of the experimental set up on neutron energy spectra are studied.

Validating Performance of the PHOBOS Silicon Detector Through Noise Values. *MARC RAFELSKI (University of Arizona, Tucson, AZ 85721) MARK BAKER (Brookhaven National Laboratory, Upton, NY 11973)*

In order to further the understanding of the evolution of the Universe and Quark Gluon Plasma, the detector must send non-defective data to be analyzed. Thus, the performance of the PHOBOS silicon detector is of utmost importance to the experiment. It is imperative that we know the condition of the silicon sub detectors. The programs written in this research do exactly that; validate the performance through average noise values of the sub detectors. Through these programs, it is evident if something were to go wrong. If the detector suddenly had radiation damage due to higher luminosity runs at RHIC, or some other problems, the shift crew would be made aware of the problem right away. This allows for quick validation of the performance of the detector before more lengthy analyses down the road. The result is a graphical program that displays the average noise values of the seven sub detectors, and would show increased noise values if there were any problems. If the noise increased, the PHOBOS collaboration would be immediately aware of the situation and could deal with it appropriately. The work on the noise of the detector aided in the processing of data for the analysis, which yielded a paper during the internship. The paper is called "Energy Dependence of Particle Multiplicities in Central Au + Au Collisions". This paper was submitted to *Physical Review Letters*.

ATLAS at LBNL. *JAMES REED (University of Illinois, Champaign-Urbana, IL 61820) M. GILCHRIESE (Ernest Orlando Lawrence Berkley National Laboratory, Berkley, CA 94720)*

I worked on the strips components of the inner detector of the ATLAS project. We were in the testing phase doing temperature studies of noise and gain. The chips on the module were injected with a constant input charge while the threshold on each chip was raised. In a perfect world once the threshold reached the input voltage, the occupancy would drop to zero (It would read "no hit" instead of "hit"). However, do to noise, the response curve fit to a complimentary error function - nicknamed an "S-curve." I first learned a bit of C++ and then ROOT, then I wrote macros which extracted the S-curves from each channel of a chip and averaged them for each of 12 chips producing 12 different S-curve averages for each chip. These were used to compare the behavior of each chip with respect to the others. The two separate sets (streams 0 and 1) of chips (chips 0-5 and 6-11) were corresponding well within each stream, but across streams the chips did not match up as well (i.e. chip 2 was offset from any of the chips in stream 1). Upon examination with an IR camera, a temperature difference was found between the two sets of chips. A gap between the aluminum mounting and the module at stream 1 was responsible for the decreased thermal conduction. This was fixed by moving the place where the module was fastened to the aluminum mounting. The module is now functioning very well and we are finishing up testing.

Improving the Tune Monitor of PEP-II Asymmetric B Factory. *JOLENE ROBIN (University of New Orleans, New Orleans, LA 70148) ALAN FISHER (Stanford Linear Accelerator Center, Stanford, CA 94025)*

PEP-II is a high luminosity 2.2-kilometer circumference collider in which 9-GeV electrons in the high-energy ring collide with the 3.1 GeV positrons in the low-energy ring to produce B and B-bar meson pairs for the study of CP violation, an asymmetry between matter and antimatter that may account for the predominance of matter in the universe. One of the most important diagnostic systems in PEP-II is the tune monitor. The PEP-II tune monitor was evaluated and redesigned to accomplish several tasks. First, the new tune monitor will have more sensitivity (lower noise floor); this will be accomplished by redesigning the downconverter. Second, an additional measurement plane (in the z or longitudinal direction) so that the synchrotron tune using the sum of the four buttons can be analyzed. Third, another spectrum analyzer, with a much higher bandwidth (at least 10 GHz) so that physicists can look for special spectral features at high frequencies that have, up until now, been unavailable. Last, a way for a computer to track and record changes to the tune automatically. A component called a lock-in amplifier was evaluated and shows promise.

Particle Detection Using Very Thin Scintillator Counters. *GUY RON (Tel Aviv University, Tel Aviv, Israel) BOGDAN WOJTSEKHOWSKI (Thomas Jefferson National Accelerator Facility, Newport News, VA 23606)*

Very thin (1.5 mm & 3 mm) scintillator counters were tested using both

Monte Carlo and experimental techniques. The thin detector plane is needed for use in the Big Bite spectrometer in JLAB's Hall A. Results of the tests indicate that these detector configurations are acceptable for the Big Bite detector and allow an approximation of the expected efficiency for the scintillator plane. This paper presents an overview of the tests performed, recommends the use of 1.5 mm detectors and proposes a construction method.

Search for a Novel Antihypernucleus. *DAVID SCHMIERER (University of Pennsylvania, Philadelphia, PA 19104) DAVID HARDTKE (Ernest Orlando Lawrence Berkley National Laboratory, Berkley, CA 94720)*

I searched for the lightest antihypernucleus, which is known as the antihypertriton. The search for a novel antihypernucleus was made possible by the STAR (Solenoidal Tracker At RHIC) experiment. Antihypertriton is composed of an antiproton, antineutron, and an antilambda particle. Antihypertriton is unstable and was therefore searched for by the identification of its decay products, which are antihelium 3 and a pion. The identification of antihypertriton required extensive studies of the background signal. The first step in searching for antihypertriton was to simulate its production and test the analysis software on this data. In addition, simulations of background were made in order to study ways to reduce background in the real data. Following the simulation studies I looked at year one STAR data where 29 antihelium 3 tracks had already been identified. However, the data yielded too much background to conclusively identify any antihypertriton production. Subsequently a mixed event background was produced by embedding real antihelium 3 tracks in STAR events that have none. The analysis of the mixed event background permitted us to set an upper limit on the production of antihypertriton. We calculated the ratio of antihypertriton to antihelium 3 to be < 1.4 with a 90% confidence level and in fact expect this ratio to be < 0.9. Although my search for antihypertriton did not identify any production, it shows nonetheless that such a search is feasible and will be worthwhile pursing in the future when STAR collects more data.

An Algorithm to Control Decoherence in a Quantum Gate. *JEFFREY SCHMULEN (Texas A&M University, College Station, TX 77840) VLADIMIR PROTOPOPESCU (Oak Ridge National Laboratory, Oak Ridge, TN 37831)*

Quantum computation relies on the laws of quantum mechanics to operate on quantum bits (qubits) and thereby process information faster than classical computing. Each qubit is realized in a two-level quantum system (e.g. a two level atom, a spin, a photon, etc.). Due to inherent interactions with the environmental noise, the two-level quantum system loses its initial/desired configuration; this process is called decoherence. Thus, to maintain the qubit in the state needed for quantum computation (i.e. prevent it from decohering), suitable control algorithms must be implemented. This report outlines a Matlab/Maple program that calculates these controls. A two by two density matrix yields eight real quantities that describe the two level quantum system. From the general theory, these quantities are calculated for an ideal (unitary) situation and realistic (decohered/controlled) situation. At each time step, the unitary and the decohered/controlled quantities are equated to find the control value that restores the decohered state to the unitary state. Application of the calculated controls shows an almost perfect restoration of unitarity.

Microwave Calibration Device. *ALEXANDER SEKON (University of California, Santa Cruz, Santa Cruz, CA 95062) JOSEF FRISCH (Stanford Linear Accelerator Center, Stanford, CA 94025)*

The Next Linear Collider Test Accelerator requires accurate calibration of X-band (11.424GHz) microwave signals. In this project we built a prototype of a device to calibrate power loss across low power components of the Next Linear Collider Test Accelerator. This device measures the output power of a Gunn diode using a detector as the receiver. These measurements are taken by reading the output of the detector with a voltmeter or oscilloscope. This device can be operated for hundreds of hours on 9-volt batteries and is small enough to hold in your hand.

Stability Tests of Hydrodynamic Flows in Water for Laboratory Study of Magnetorotational Instability. *ETHAN SHOSHAN (Rutgers University, New Brunswick, NJ 07751) HANTAO JI (Princeton Plasma Physics Laboratory, Princeton, NJ 08543)*

Magnetorotational Instability (MRI) is a powerful candidate mechanism for the fast transport of angular momentum in magnetized accretion disks. In an accretion disk, when the mass spirals in towards the

stellar object, due to gravity, the velocity increases to conserve angular momentum. When the force of gravity is balanced with the centripetal force, the viscosity pulls it in towards the central compact object, which is too small to explain the fast transport of mass, so there must be another reason. Hydrodynamic (HD) instabilities, like the Rayleigh instability, are ineffective in producing turbulence in accretion disks because it requires a negative gradient of specific angular momentum. Magnetohydrodynamics provides a better description of plasma in hot accretion flows where angular momentum has an extra degree of freedom due to the presence of the magnetic field. The radial transport of angular momentum due to MRI will hopefully explain how mass gets accreted onto a stellar object. Despite the popularity of MRI, it has never been tested in the laboratory. In an attempt to demonstrate MRI in the laboratory, a magnetized couette flow experiment using gallium is proposed. Before gallium is used, a prototype experiment using water has been constructed to study linear and nonlinear HD instability in the (omega1, omega2) space. HD stability can be monitored using particle imaging velocimeter techniques, which will serve as a reference for effects due to the MRI mechanism.

Construction and Calibration of a Tri-Directional Magnetic Probe for Investigation of Field Structure in the VASIMR Helicon Plasma Source. *HANNA SMITH (Smith College, Northampton, MA 01063) RICHARD H. GOULDING (Oak Ridge National Laboratory, Oak Ridge, TN 37831)*
The performance of a helicon plasma source as a propulsion device depends upon the structure of the magnetic fields generated by the RF antenna that ignites and maintains the plasma. The EMIR2 code predicts the configuration of these fields in three dimensions for the helicon plasma source on mini-RFTF. Due to a lack of appropriate diagnostics, however, the theoretical results from EMIR2 still await experimental confirmation. Inductive loop probes provide a convenient means of investigating magnetic fields inside experimental plasmas of moderate energy density. Conventional single loop probes sample one component of dB/dt, the time-rate-of-change of the magnetic field. Acquisition of data in three dimensions for comparison with EMIR2 results demands the use of three mutually perpendicular (and physically proximate) loops. Moreover, mapping the fields associated with the helicon source on mini-RFTF requires a small probe of high frequency response. This paper details the design, construction and calibration of a tri-directional magnetic probe for the VASIMR experiment on mini-RFTF.

Regression Analysis Program for the Characterization of Photovoltaic Devices. *JASON STOKE (Colorado State University, Fort Collins, CO 80523) KEITH EMERY (National Renewable Energy Laboratory, Golden, CO 80401)*
Characterization of photovoltaic devices is key for understanding of how the devices perform. With a characterized photovoltaic panel, module, or array, one can have an idea of how well that device will produce power under any climatic condition. This program is able to take recorded data and fit it to the Photovoltaic Utility Scale Application (PVUSA) model. The fit will produce coefficients that are then substituted back into the model to give a power rating at the project test conditions. This allows predictions to be made about the performance of the device under varying degrees of weather. It can analyze recorded data and give the power rating of that device under the project pest conditions of air temperature of 20°C, wind speed of 1 m/s, and an irradiance of 1000 W/m^2.

Shiftwork Automation Using the Tcl Language. *TIMOTHY THARP (DePauw University, Greencastle, IN 46135) STEVE WOOD (Thomas Jefferson National Accelerator Facility, Newport News, VA 23606)*
My work this summer has been invested in improving the shiftwork environment to make setting up and watching over experimental runs easier on the shift personnel. The purpose of this paper is to be a complete and informative reference and report of two new systems I helped install and program this summer. The first project involved creating GUI's (Graphical User Interfaces) that interface with hardware. I did this using the Tcl ("tickle") language to control a set of relays. These relays short the reset signal line of a specific computer

to ground which results in a hard reset of the computer. The second project takes information from the data acquisition system and displays it in a GUI. This display has been useful in keeping track of the rates of photo-multiplier tube (PMT) counts, and will hopefully aid in monitoring experiments to make sure the PMT's are working correctly.

Designing a LabVIEW Program to Determine the Electrical Properties of New Superconducting Materials. *JENNIFER TOBIN (Albion College, Albion, MI 49224) DAVID K. CHRISTEN (Oak Ridge National Laboratory, Oak Ridge, TN 37831)*
Superconductivity has the ability to revolutionize the distribution of energy in the form of electrical power. The negligible resistance in superconductive materials makes them much more efficient than existent materials as carriers of electricity. Presently materials found to be superconductive do so at low temperatures (near or below the boiling temperature of liquid nitrogen, 77K). A cryocooler is a mechanical device with the ability to reach and maintain these low temperatures using compressed helium gas. In a cryocooler, superconductivity was measured through a four terminal reading on the sample (current, voltage, voltage, current). LabVIEW (a graphical programming language) was used to develop a program to control the temperature, evaluate the amount of current applied to and forced through the superconductive film sample and measure the voltage across the sample. These values were stored in LabVIEW, were transformed into resistance readings and stored in data files. The program was customized to provide a sufficient density of recorded and plotted values during the abrupt resistance decrease that occurs at the superconducting transition temperature, T_c, below which the resistance is zero. Data were taken for a thin film sample of irradiated Hg1212/LaAlO$_3$ that yielded a T_c of 113.142K when cooling and a T_c of 114.015K when warming due to thermal hysteresis. When compared to data of the sample before radiation, it was found that resistance had increased in the irradiated sample at comparable temperatures. The T_c was lowered after radiation from 117.55K to 113.142K.

Neutron Activation Analysis. *CHUE VUE (California State University, Fresno, Fresno, CA 93704) ERIC B NORMAN (Ernest Orlando Lawrence Berkley National Laboratory, Berkley, CA 94720)*
Neutron activation analysis (NAA) is a useful technique for identifying the elemental composition of materials in a non-destructive way. This can be done by irradiating a sample with neutrons and then studying the decays of the radioactive nuclei that are produced. Sensitivities of the method are sufficient enough to measure certain elements down to extremely low concentrations (parts per billion). NAA can be performed to determine the concentration of several different elements within a single sample of a material. Since neutrons have no charge they only interact with the nucleus of an atom, not the electrons. In addition, this technique sees all the elements in a sample, regardless of their chemical form or oxidation state. The basic requirements to carry out analysis of samples by NAA are: the detailed knowledge of the reactions that occur when neutrons interact with the target nuclei, a source of neutrons, and an instrument that can detect gamma rays accurately. Because of its accuracy and precision, NAA is widely performed in many different fields of sciences. In this project we neutron activated zinc (Zn), iridium (Ir), potassium bromide (KBr), molybdenum (Mo), calcium fluoride (CaF$_2$), and a banana. The spectra were obtained, identified and will be posted on the Internet for use in high school basic nuclear science curriculum. With this web site and access to the Internet, teachers and students can use actual experimental results to back up theory and technique that had long been studied and used by many scientists. The goal is that by doing this, nuclear science will be less abstract and more understandable.

Laser Fluorimetric Characterization of Sorption of Gd^{3+} by ä-Alumina and Mesoporous Silica. *JENNIFER WASSMUTH (Lewis Clark State College, Lewiston, ID 83501) ZHEMING WANG (Pacific Northwest National Laboratory, Richland, WA 99352)*
With the growing concern for environmental cleanup, it is important to understand how radioactive materials interact with soils. Radioactive waste from underground tanks has leaked to the soil at the Hanford Site. The radioactive elements in this waste such as americium and curium migrate through the soil. Determining how these materials migrate is essential to selecting the appropriate soil cleanup strategy. Americium and curium are very difficult to study in a lab. Because of

this, gadolinium is used due to its analogous properties. Soil is made up of many different components including ä-alumina and mesoporous silica, which were used to study gadolinium sorption. Nine samples with different concentrations of gadolinium were analyzed in four trials. During the first two trials, the adsorption of gadolinium to silica was studied by adding 0.4 grams of silica to each sample. During the next two trials, the adsorption of gadolinium to ä-alumina was studied by using an ä-alumina suspension of 4 g/L concentration in each sample. The samples were placed in a shaker and then centrifuged to separate the supernatant from the paste. Samples were analyzed using a laser fluorimeter. The resulting graphs show that as concentrations of gadolinium increased, so did fluorescence intensity of the gadolinium peaks. The ä-alumina paste graphs showed that an impurity might be interfering with the fluorescence measurements. Further experiments will determine where the impurity comes from and how gadolinium is adsorbed onto soil. Preliminary indications are that laser fluorimetric analysis will be useful in characterization of sorption of gadolinium.

Airflows Through Large Horizontal Apertures. *WILLIAM WATTS (City College of San Francisco, San Francisco, CA 94112) DAVID LORENZETTI (Ernest Orlando Lawrence Berkley National Laboratory, Berkley, CA 94720)*
Data collected from experiments does not sufficiently characterize airflows through large horizontal apertures that connect multiple zones. Experimental work must be done to fill gaps in data to allow for the accurate modification of building simulation programs, such as COMIS and CONTAM. Two chambers connected by a vertical shaft were used in this experiment to replicate two floors in a building. Outside air was driven into the top chamber, exiting the bottom chamber, to model the effect of air infiltration in buildings. The bottom chamber was heated in order to induce a buoyancy driven flow that opposed the mechanically driven external flow. Tracer gas was injected in the bottom chamber and measured with uniformly distributed sample tubes in each chamber to determine the size of the buoyancy driven and mechanically driven flows. Sufficient data was not gathered to fill experimental gaps due to the inability to achieve a well-mixed temperature in the heated chamber.

Designing a Superfluid Helium Test Dewar for Testing SQUIDs. *CHARLEZETTA WILSON (Howard University, Washington, DC 20001) JOHN WEISEND (Stanford Linear Accelerator Center, Stanford, CA 94025)*
A large superfluid helium test dewar was designed and constructed. The dewar will be used in the near future for testing Superconducting QUantum Interference Devices (SQUIDs). The goal is to test the SQUIDs at 4.2K and 2K.

Thermal Qualification of ATLAS Pixel Detector Disk Sectors. *WILLIAM WISE (Harvard University, Cambridge, MA 02138) MURDOCK GILCHRIESE (Ernest Orlando Lawrence Berkley National Laboratory, Berkley, CA 94720)*
Two prototypes of ATLAS pixel disk sectors were tested to determine if they met thermal requirements. Sector temperature was determined after thermal cycling, thermal shock, pressure, irradiation, and loss of coolant tests, and compared to the sector baseline temperature. The hottest point on either sector after testing was 9.5°C above coolant temperature. This is well within ATLAS specifications, which require that all points on the sectors be less than 15 degrees above coolant temperature. Therefore, these two sector prototypes thermally qualify for use within the ATLAS detector.

Simulation Studies of High Intensity Proton Accumulator Rings. *KATHERINE WOODY (Tennessee Technological University, Cookeville, TN 38505) JEFF HOLMES (Oak Ridge National Laboratory, Oak Ridge, TN 37831)*
The Spallation Neutron Source (SNS) will have the highest intensity proton beam to date. Because of this high intensity, SNS will also have unprecedented low beam loss requirements and an array of physics concerns impacting the beam dynamics. Computer simulation proves to be the most productive method for investigating the SNS beam dynamics, and the computer code, ORBIT, is at the forefront of these studies. The present work involves a novel study using the ORBIT code: new three-dimensional space charge and transverse impedance models that will allow the investigation of a whole new range of

phenomena have been developed. These models increase the amount of computational work by one three orders of magnitude, even with the use of fast solution algorithms. It is therefore important to benchmark these methods both for accuracy and computer time. This is carried out here.

Investigation of Rotating Arc Spark Plugs. *JACOB YODER (Case Western Reserve University, Cleveland, OH 44106) JOHN WHEALTON (Oak Ridge National Laboratory, Oak Ridge, TN 37831)*
The fuel to air ratio in an internal combustion engine piston is an important factor in the fuel efficiency of automobiles. A lower fuel to air ratio can yield greater fuel efficiency, but the rate of misfires increases. A rotating arc spark plug can allow leaner ratios without the misfire problem. An axial magnetic field is applied on the spark gap, and the spark rotates. Because the spark effectively occupies more volume, it is hoped that the ignition probability will remain high in the lean burning scenario. In addition to occupying more volume, rotating sparks tend to have a higher electron temperature. The temperature of the sparks from Capacitive Discharge, Inductive, and Multiple Spark Discharge ignition systems were investigated with a spectrometer. It was found for each system, applying an axial magnetic field resulted in higher electron temperatures (i.e., a preponderance in the lower wavelength bands). When the arc lasted for more than 100 ms, a noticeable rotation of the spark occurred, in accordance with the Lorenz force, measured via digital photography. Implementation of the rotating arc spark plug in an engine is currently in progress, as well as a study of electrode erosion using spectroscopic techniques.

SCIENCE POLICY

Patents and Genomes To Life: A Compounding Issue. *JACQUELINE COHEN (Brown University, Providence, RI 02912) DANIEL DRELL (DOE Headquarters, Washington, DC 20585)*
Intellectual Property emerged as a major issue in the Human Genome Project, originally surprising program managers and researchers. This buttressed the argument that the ethical, legal, and social implications that accompany new initiatives should be explored. The Genomes To Life Initiative builds on the results of the Human and Microbial Genome Projects by characterizing the proteins coded for, the interactions of those proteins to form molecular machines and then gene regulatory networks, and the interactions of microbes acting in combination. The goal is to use this information to advance DOE missions and create computer models of living systems. With the benefit of the experience of the HGP, the research agenda for ethical, legal and social implication of the DOE's next big genetic initiative will include a significant portion of research into patent issues. Looking at the Intellectual Property potential of this initiative suggests the possibility of patent stacking; each of the initiative's steps involve elements that are currently patentable. By the time a model is assembled, more than a dozen layers of patents, with each patent possibly held by different owners, may cover each element going into the model. Unless measures are taken by the government, researchers, or industry, patents could pile on top of each other and become obstacles to further research and even completion of the initiative.

DNA Dilemma: A Perspective on Current USPTO Philosophy Concerning Life Patents. *KALE FRANZ (Colorado School of Mines, Golden, CO 80401) PETER FALETRA (DOE Headquarters, Washington, DC 20585)*
The lack of a solid set of criteria for determining patentability of subject matter—particularly subject matter dealing with life—has recently been of increasing public concern in the U.S. and worldwide. Alarm for patent practices related to life systems ranges from patents being granted on biochemical processes and the knowledge of these processes to the patenting of entire organisms. One of the most volatile concerns is the patenting of human genes or parts of genes since this genetic material is the basic informational molecule for all human beings. Current patent law, legislated in 1952, has been interpreted by the U.S. Supreme Court to allow broad patents of DNA, biochemical processes, and what are generally considered "inventions" of life systems. Several issues are addressed in this paper regarding the unsound reasoning underlying both the interpretation and execution of patent law. Lapses in logic provide a gateway for businesses and individuals to take patenting to an illogical and unworkable extreme. Patent Office disorder of this magnitude is

unnecessary and has great potential for harming the mission that the patent office was designed to serve. Recently disclosed patent-granting guidelines suggest the United States Patent and Trademark Office is not upholding its Constitutional responsibility of promoting the progress of science.

From Berkeley Lab to Marketplace: Technology Transfer Success Stories. *SONYA GABRIELIAN (University of California, Berkeley, Berkeley, CA 94704) CHERYL FRAGIADAKIS (Ernest Orlando Lawrence Berkley National Laboratory, Berkley, CA 94720)*
Lawrence Berkeley National Laboratory is hailed as "a world of great science". Though the sciences comprise the fundamental core of the lab, they cannot stand-alone. To commercialize a laboratory invention, the Technology Transfer Department must construct an effective marketing, patenting, and licensing strategy. Collaborative research can also be facilitated, allowing for increased resources and additional modes of reasoning. Berkeley Lab has met with much success in its relationship with the private sector. To communicate this aspect of the Lab to LBNL scientists and the general public, I have written the "success stories" of five spin-off companies that have evolved from the Lab's licensed technologies: Aeroseal, Inc., Berkeley HeartLab, Inc., Quantum Dot Corporation, Symyx Technologies, Inc., and WaterHealth International, Inc. Since 1990, sixteen startup companies have been launched from LBNL research, creating over 500 new jobs. Though these startups span a broad spectrum of scientific areas, each has an interesting story to tell. In addition, I have constructed a report about The Berkeley Lamp, one of the Lab's most recent technology transfer successes. In an unprecedented coordination effort, Berkeley Lab's Technology Transfer Department partnered with three major California utilities to bring this energy-saving, top quality lighting device to the public.

Carbon Sequestration: Geologic and Oceanic Carbon Sinks. *STEPHEN LEMARBRE (Trinity College, Hartford, CT 06106) ROBIN ABRUZERE (DOE Headquarters, Washington, DC 20585)*
Anthropogenic carbon dioxide escaping into Earth's atmosphere is a central concern of today's environmentalists, scientists, and political leaders. Because fossil fuels will continue to be used in power plants for decades to come, the mitigation of this problem needs to work hand-in-hand with the use of fossil fuels. Carbon sequestration allows for the capture and secure storage of CO_2, while allowing the continued mass use of fossil energy. The injection and sequestration of CO_2 into deep, unmineable coal seams, or into the ocean are two methods being developed to control this problem. Currently, the full technology needed for sequestration is not available, and many are concerned over the possible environmental impacts. However, as more research is performed and more experiments are completed, carbon sequestration will achieve the potential to rise to the forefront of the challenges posed by increasing CO_2 in the atmosphere.

WASTE MANAGEMENT

Characterization of Mark IV and Mark V Electrorefiners. *JARED BARBER (Montana State University, Bozeman, Bozeman, MT 59717) HUMBERTO GARCIA (Argonne National Laboratory, Argonne, IL 60439)*
Concern over uranium depletion drove the US to investigate the possibility of fast reactors and plutonium fuel production in industry. Electrorefiners were developed at first in the late eighties to assist in this end but then, with fear of nuclear proliferation, they were made to assist in clean and efficient disposal of radioactive wastes from fast reactors. In the United States efforts to develop such electrorefiners have resulted in two electrorefiners that were built at Argonne National Laboratory-West. In an attempt to understand how to improve the performance of the electrorefiners, characterization of the process was undertaken. Many experimental runs were made with the level of factors and responses being recorded. Using statistical analysis techniques, these factors and responses were leafed through in order to find important factors that would help improve the electrorefiners' performance. The findings suggest that agitation and decreasing anode loading may help to improve the Mark V Electrorefiner's

performance. Also higher average cell voltage, lower average current, and lower maximum cell voltage may help to improve the Mark IV Electrorefiner's performance. Many improvements can be made to enable better statistical analysis. In addition, further statistical analysis could help to find more useful relationships in the future.

Decontamination Factors for the Mark-IV and Mark-V Electrorefiners. *OLIVER EAGLE (Colorado School of Mines, Golden, CO 80401) BRIAN WESTPHAL (Argonne National Laboratory, Argonne, IL 60439)*
This paper explores the decontamination factors from treating nuclear fuel from the Experimental Breeder Reactor-II (EBR-II) via electrometallurgical treatment (EMT). Decontamination factors are a measure of the removal of an impurity from material that is desired for reuse. To calculate decontamination factors, composition data was used from before and after spent material was processed in the Mark-IV and Mark-V electrorefiners in the Fuel Conditioning Facility (FCF). Decontamination factors are particularly useful in the area of fuel recycling because they effectively show the reduction of contaminants to very low levels. For the EMT process they are useful as a comparison to other separation technologies both past and present, as well as to examine changes in process variables which affect performance. Although decontamination factors for EMT are not quite as favorable as some other technologies the EMT process requires less infrastructure and thus has considerable economic advantages.

Mop Water, Trim Sol, and Recycling. MELISSA ROBERTSON (Washington State University, Pullman, WA 99163) KATHY POSTON (Pacific Northwest National Laboratory, Richland, WA 99352) .
Throughout the summer I have been working on a major trash-recycling project and managing a Mop water/Trim Sol waste stream. I have been following up on these three projects for about eight weeks. I conducted all of the research by interviewing, sampling, Internet researching, and document requests. The two waste streams had many options for treatment and I had to narrow it down to one consistent and effective method. S ome of the options looked at were evaporation, extending life/paired with evaporation, disposal/incineration, and recycling/filtering. The dumpsters were surveyed by volunteers on a weekly basis according to a pickup schedule. A database was created in order to track the building, time, date, level, and material in the dumpsters. From this information I was able to go back and see what actions need to take place. A meeting was held concerning the Trim Sol and Mop water waste streams where we discussed the options at hand. The best option chosen was extending life/paired with evaporation. A "new technology" cutting fluid product will be used, demineralized water, an antimicrobial agent will be added to the sumps, and the waste will be evaporated. A meeting was held where the data was reviewed and a proposal was produced. We are going to separate the buildings into two categories; opportunity for reduction and no reduction needed. The buildings that have an opportunity for reduction will be continually surveyed to collect more data to produce a plan of action. Both projects served the purpose of reducing the amount of waste being returned to the environment. The goal was to reduce the quantity of waste being generated and to possibly eliminate the source of waste.

Index of Schools

A

Albion College 136
Alfred State College 121
Allan Hancock College 83, 84
Allegheny College 95
American River College 111
Augustana College 108, 130

B

Bethune-Cookman College 95
Big Bend Community College 104
Binghamton University 127
Bismarck State College 110
Blue Mountain Community College 111
Boston College 119
Bowdoin College 88
Brigham Young University 91, 112
Bronx Community College 102
Brown University 114, 125, 132, 137
Bryn Mawr College 95, 132
Bucknell University 113

C

California State University, Bakersfield 98
California State University, Fresno 84, 136
California State University, Hayward 101
California State University, Long Beach 87
Carnegie Mellon University 103
Case Western Reserve University 99, 137
Central Piedmont Community College 110
Central Washington University 105
Christian Brothers University 114
City College of San Francisco 86, 137
City Colleges of Chicago—Harold Washington 124
Clark Atlanta University 112
Coahoma Community College 101
College, Westminster 105
Colorado School of Mines 25, 137, 138
Colorado State University 113, 136
Columbia Basin College 86, 90, 92, 96, 104, 124, 131
Community College of Rhode Island 84
Contra Costa College 88, 89, 105, 106, 128
Cornell University 34, 64, 82, 86, 91, 134
Cosumnes River College 117
Cumberland University 104

D

Davidson College 83
DePauw University 136

D

Dordt College 120
Duke University 113

E

East Los Angeles College 109
Eastern Oregon University 92, 112
Eastern Washington University 83, 98, 119
Elmhurst College 104

F

Fayetteville State University 100
Florida A&M University 101, 132
Florida State University 116, 123
Fordham University 103
Fort Lewis College 130
Fresno City College 87, 94, 97, 119, 121, 125

G

George Washington University 88, 127
Georgia Tech 123
Goerge Mason University 94
Gonzaga University 105, 106
Guilford College 97

H

Harry S. Truman College 119
Harvard University 107, 137
Harvey Mudd College 131
Holyoke Community College 121
Houston Baptist University 134
Howard University 137
Hudson County Community College 102, 106, 108

I

Illinois State University 129
Indiana University of Pennsylvania 125
Iowa State University 100, 106, 107

J

James Madison University 114, 122
Jamestown Community College 98, 116, 133
Juniata College 124

K

Kansas State University 122
Kenai Peninsula College 101
Knox College 87

Index of Schools

Index of Schools

U

Union College 101
University at Buffalo 114
University of Arizona 129, 135
University of California, Berkeley 91,
    103, 127, 130, 133, 134, 138
University of California, Davis 40, 118
University of California, Riverside 86
University of California, Santa Cruz 83, 136
University of Central Arkansas 92
University of Chicago 102, 132
University of Colorado 90
University of Connecticut 29, 127
University of Georgia 103
University of Idaho 84, 128
University of Illinois 92, 107
University of Illinois, Chicago 86, 120, 132
University of Illinois, Urbana-Champaign 104, 105, 128,
    135
University of Iowa 97
University of Maryland 105, 108
University of Massachusetts, Amherst 82
University of Michigan, Ann Arbor 106, 117, 122, 127
University of Nevada 64
University of New Orleans 135
University of North Carolina 128
University of Northern Iowa 102
University of Notre Dame 85, 130
University of Oregon 100
University of Pennsylvania 135
University of Portland 108
University of Puerto Rico, Cayey 115
University of Puerto Rico, Rio Piedres 115
University of Puerto Rico, San Juan 117
University of Puget Sound 132
University of Richmond 128
University of Rochester 87, 90, 103
University of South Florida 125
University of Tennessee 96, 99, 106, 111, 113, 115, 118,
    125, 126
University of Texas, Arlington 129
University of Texas, Austin 108, 116
University of Texas, Brownsville 126
University of Texas, Dallas 109
University of the Pacific 134
University of Utah 83
University of Virginia 133
University of Washington
    82, 92, 93, 96, 100, 116, 119, 122, 123, 134
University of Wisconsin, Madison 126
Utah State University 114

V

Vanderbilt University 86
Virginia Tech 93

W

Walla Walla Community College 111
Washington State University
    83, 85, 90, 94, 97, 107, 109, 121, 126, 138
Washington State University, Tri-Cities 93, 115, 122, 125
Washington University 100, 107
Western Washington University 90, 123
Westminster College 102
Whitman College 75, 91, 92, 96, 97, 121, 122, 123
Whitworth College 18, 93, 129
Wilbur Wright College 120, 132
Wilkes University 90

Y

Yakima Valley Community College 115
Yale University 112, 130, 135
York College 94

Index of Names

A

AARDAHL, CHRIS 91
ABRUZERE, ROBIN 138
ADAMS, EVAN 122
ADAMSON, TRAVIS 91
ADESANYA, ADEYEMI 101
ADHIKARI, SEAN 82
AHNERT, ANNIE 129
AKRE, RON 108
ALBERTUS, PAUL 106
ALEXANDER, MICHAEL L 111
ALONGI, SHELLEY 115
ANDERSON, KISSIE 98
ANDREASEN, JONATHAN 129
ANDREWS, CULLEN 98
ANZENBERG, VERED 127
APTE, MICHAEL G. 111
ARAMAYO, GUSTAVO 107
ARROYO, YAHAIRA 115
ASZTALOS, STEVE 128
ATTANASIO, DAVID 129
AVERIN, DIMITRY 98
AYLWARD, ERIN 107
AYON, ANGELA 115

B

BAER, NATHANIEL 91
BAEZ-CAZULL, SUSAN 115
BAGNASCO, JOHN 110
BAKER, ANN 122
BAKER, MARK 134
BAKER, ROGER 98
BAKER, SARAH 116
BARAN, ANDREW 127
BARBER, JARED 138
BARNETT, R. MICHAEL 134
BARTON, JOHN W. 121
BATEMAN, KENNETH J. 112
BAVYKIN, SERGEI 85
BECKER, JIM 93
BELL, GEOFFREY C. 108, 114
BERGHUIS, PETER 124
BERNSTEIN, ARON 48
BERRELLI, JENIFER 82
BHATNAGAR, SAURABHA 82
BIBLE, DON II 98
BIRNBAUM, JEROME 123
BLAKELY, ELEANOR 84
BLAU, PETER J. 122
BODEN, TOM 103
BOETTCHER, KATE 91

BOSTICK, DEBRA 97
BOTT, KARLYN 91
BOWER, NATHAN 98
BRACHMANN, AXEL 130
BRAUN, ARTUR 117, 124
BRESNAHAN, CATHY 92
BRITT, PHILLIP F. 95
BROCKWELL, REBECCA 116
BROUGHTON, DAVID 100
BROWN, AARON 91
BROWN, HUNTER 98
BROWN, WILLIAM S. 115
BRUCKNER-LEA, CYNTHIA 106, 109
BRUEMMER, MEGAN 92
BRUEMMER, STEPHEN M. 123
BUNN, AMORET 104, 119
BURDETTE, DON 129
BUSEY, JESSICA 116
BUTCHER, THOMAS 108
BUTRYN, RYAN 116

C

CADA, GLENN 116
CALDWELL, DUSTIN 107
CAMAIONI, DONALD 91
CAMPBELL, ALLISON A. 83, 96
CAMPBELL, JAMES A. 91, 94
CARMODY, CARLY 92
CARPENAY, MARK 99
CARROLL, ALAN 130
CARROLL, BRIAN 116
CARTER, MARK D. 106
CARVER, COLIN 92
CASPI, SHLOMO 113
CASTELEIN, MATTHEW 107
CASTILLO, VINCENT 108
CASTRO, JOHN II 107
CAVANAGH, ANDREW 129
CERVENY, STEVEN 99
CHAN, ANTONIO 106
CHAN, CHIN 99
CHEERS, TIMOTHY 99
CHEN, ZHONGNING 117
CHESTNUT, RON 98
CHIN, TIMOTHY 122
CHRISTEN, DAVID K. 136
CHU, HENRY 71, 112
CHU, STEPHANIE 82
CHUNG, HELEN 82
CHUU, JENNY YJ 99
CIALELLA, ALICE 115
CLARK, SCOTT 99

Index of Names

COHEN, JACQUELINE 137
COOK, BRIANA 82
COOK, LESLIE 83
COOPER, PRISCILLA 90
CORBETT, JEFF 105
CORBO, JOEL 130
CORDERO, AREL 100
CORSA, TODD 102
CORUM, SEAN 130
COSTENARO, DAVID 107
COTTS, BENJAMIN 108
COWIN, JAMES P. 119
COX, APRIL 100
CRAIG, AIDAN 130
CRANSHAW, JUSTIN 100
CRUSSELLE, VALERIE 83
CUNNIFF, SARAH 92
CURTIS, LAURA MS 100

D

DAI, SHENG 94, 97
DATKSOS, PANOS G. 83, 94, 108, 109, 111
DAVID, STAN 125
DAVIS, AARON 108
DEATHERAGE, BROOKE 83
DECHAND, DAWN 122
DELGADO, MATTHEW 108
DELMAR, MONIQUE 108
DEMKO, JONATHAN 115
DENBEAUX, GREG 85
DICKERHOFF, DARRYL 116
DIEFENDERFER, HEIDA 89
DILMANIAN, AVRAHAM 127
DINSMORE, MICHELE 117
DIXON, WARREN 100
DO COUTO E SILVA, EDUARDO 59, 131, 132
DOBBS, GARY 92
DOKTYCZ, MITCH 87, 89
DOLGASHEV, VALERY 107
D'OTTAVIO, TED 103
DOWNS, JANELLE L. 89, 115
DRAGOO, KRISTI 100
DRELL, DANIEL 137
DUCKWORTH, DOUGLAS C. 92
DUMITRESCU, DELIA 122
DUNHAM, GLEN 128
DUNSTAN, ROSHITHA 100
DZIUBAN, DOUGLAS 83

E

EAGLE, OLIVER 138
EAKIN, ALISON 83

EARNEST, THOMAS 87
EASTERDAY, SHELECE 130
ECKERT, MICHAEL 108
EFTHIMION, PHILIP 132
ELLINGSON, WILLIAM 123
ELLIS, PAUL 88
EMERY, KEITH 136
EMIGH, CHRISTINE 83
ENT, ROLF 134
ERIAN, FADEL F. 111
EVANS, BOB 112

F

FAHLSTROM, CARL 92
FALCONE, ROGER 132
FALETRA, PETER 1, 25, 137
FALL, SARA 84
FANNING, THOMAS 102
FAULTERSACK, LIZ 106
FELTS, SHARON 84
FERNANDEZ, SUSAN 108
FERRADA, JUAN 99, 101
FINN, MEGHAN 92
FINNERTY, MAUREEN 84
FISCHER, MARC 120
FISHER, ALAN 135
FISHER, MATTHEW 108
FOLLETTE, DAVID 117
FONNESBECK, JACQUELINE 95
FORMAN, DREW 130
FOSTER-MILLS, NANCY 122
FOWLKS, ALISON 117
FRAGIADAKIS, CHERYL 138
FRANKLIN, A. LYNN 105
FRANZ, ELIZABETH 123
FRANZ, JAMES A. 96
FRANZ, KALE 25, 137
FREEDMAN, STUART 130
FREYMAN, CHRISTINA 123
FRIAS, CARMEN 109
FRISCH, JOSEF 111, 135
FUJA, RAY 109
FUJINAMI, KACEE 84
FUJITA, ETSUKO 94
FULLER, DOUGLAS 100

G

GABRIELIAN, SONYA 138
GAEDE, NEIL 101
GAINCOLA, CARA 130
GARCIA, ABRIL 84
GARCIA, HUMBERTO 127, 138

Index of Names

GARCIA, MICHAEL 84
GARCIA, STACI 117
GARMON, KENNETH 128
GASPARIAN, ASHOT 48, 133
GATLEY, JOHN 29, 126
GAUGER, AMBER 93
GAVIN, IGOR 34
GEORGE, BRENT 109
GHATIKAR, GIRISH 101
GHEBREBRHAN, MICHAEL 101
GIESFELDT, KATHLEEN 109
GIFFORD, ANDREW 29, 127
GIFFORD, MICHAEL 112
GILCHRIESE, M. 135
GILCHRIESE, URDOCK 137
GLINIAK, DOUG 123
GOFF, CATHERINE 109
GOMEZ, JOSE 117
GONZALEZ, ANA 95
GOODRICH, ERICA 84
GORBY, YURI 89
GOTH-GOLDSTEIN, REGINE 84, 91
GOULD, OMAR 112
GOULDING, RICHARD H. 136
GRAY, LEONARD J. 101
GREEN, TIMOTHY 82, 117
GREENE, DAVID L. 116
GRIFFITH, ADAM 101
GROSSE PERDEKAMP, MATTHIAS 131
GRUBE, CRAIG 101
GUILLEMIN, RENAUD 65
GULL, DEAN 84
GUNDERSON, CARLA 118
GUNTER, DAN 99
GUNTER, LEE E. 118
GUTOWSKA, ANNA 91, 92

H

HABTEAB, ADEN 85
HAFALA, RAY 114
HAGAN, BETHANY 109
HAGGARD, HAROLD 131
HAINES, JOHN 110
HALE, RYAN 109
HALLEN, RICHARD T. 93
HAM, KENNETH 120
HAMMAN, KELLY 85
HAMMOND, SUSAN 110
HANSEN, JENS-OLE 53, 128
HANSON, JON 94
HARDTKE, DAVID 135
HARKLEROAD, ERIC 131
HARVEY, EVERETT 99, 106

HASLINGER, TERESA 131
HAZEN, TRACY 40, 118
HE, GEORGE 121
HEATHERLY, TERRY 98
HEEB, LIBBY 93
HEITSCHMIDT, COREY 93
HEMMENS, OLIVER 65
HERCEG, JOE 128
HERNANDEZ, MIRIAM 85
HILSON, BRYAN 110
HIND, GEOFFREY 82, 90
HINMAN, ROCHELLE 18, 93
HLOHOWSKYJ, IHOR 120
HOERTKORN, MATTHEW 93
HOJJATI, SEPEHR 128
HOLBEN, BROOKE 85
HOLBROOK, JEREMY 123
HOLBROOK, STEPHEN 82, 87
HOLMES, JEFF 137
HOPKINS, ADAM 123
HOPKINS, LINDSAY 110
HOTCHKISS, ERIN 118
HOWARD, JOSHUA 101
HUBERMAN, ELIEZER 34, 86
HUBLER, TIM 92, 96
HULTMAN, KRISTI 131
HURST, ANNA 101
HUSTON, MICHAEL 119
HUTTON, REBEKAH 118
HYDE-WRIGHT, CHARLES 133
HYLDEN, KATHRYN 85

I

ICENHOWER, JONATHAN 118
IGBOKWE, ANTHONY 102
ITON, LENNOX E. 95

J

JAGANI, TEJASKUMAR 102
JAGER, YETTA 103
JAN-FANG CHENG 86
JANSSEN, MICHAEL 102
JARDINE, PHILIP M. 118
JENKINS, WILLIAM 126
JI, HANTAO 134, 135
JOHNSON, BRANT 104
JOHNSON, KIMBERLY 121
JOHNSON, LINDSEY 110
JOHNSON, ROGER N. 122
JOHNSON, TIM 93
JONES, KEITH W. 116, 121
JUAREZ, ANA 85
JUSTICE, THOMAS 110

Index of Names

Index of Names

Index of Names

Index of Names

SUNG WOO YU 65
SWANSON, KEN 98
SWINGER, HEATHER 96

T

TAKAI, HELIO 102
TERRY, KENNETH 102
THARP, TIMOTHY 136
THERSLEFF, THOMAS 126
THEVUTHASAN, THEVA 122, 129
THOMAS, LMP (MAY-LIN) 97
THOMPSON, VICKI 87
THORNTON, MATTHEW 96
THRALL, BRIAN D. 18, 88, 93
THRALL, KARLA 93, 94
THUNDAT, THOMAS 88
TILLER, BRETT 86
TOBIN, JENNIFER 136
TOMLINSON, JJ 107
TONTCHEVA, PETIA 120
TOROK, TAMAS 83, 88
TORRES, MARIA 120
TOWNSEND, ROBERT 114
TRUE, BRIAN 126
TRUJILLO, KATHLEEN 120
TSANG, T. 129
TSOURIS, COSTAS 117
TUHUS-DUBROW, DANIEL 114
TURNER, JOHN 75, 97
TURNER, SABRINA 105

U

ULLOA, KARINA 126

V

VALENTINE, DANIEL 114
VAN GEET, OTTO 90
VANSCHOIACK, LINDSEY 96
VAUGHEY, JOHN T. 96
VIRDONE, MICHAEL 114
VODRASKA, CHRISTOPHER 121
VUE, CHUE 136

W

WADE, JENNIFER 97
WALDEN, GENEVIEVE 121
WALKER, ANDY 113
WALKER, BRITTANY 90
WALTON, ROD 120

WANG, ZHEMING 136
WARE, LINDA 122
WARREN, SCOTT 97
WARRINER, SARAH 97
WASSMUTH, JENNIFER 136
WATTS, WILLIAM 137
WEAVER, MICHAEL 97
WEIMER, THERON 106
WEISEND, JOHN 137
WEMPEN, JACOB 114
WESTFALL, DANIEL 121
WESTPHAL, BRIAN 138
WHAM, ROBERT 100
WHEALTON, JOHN 137
WHITE, KATHERINE 106
WILCHER, KENT 126
WILCOX, WYATT 121
WILKINSON, TOMMY 97
WILLIAMS, ELISHA 121
WILLIAMS, ERNEST L. JR. 99
WILLIAMS, GUS P. 119
WILLIAMS, GUSTAVIOUS P. 119
WILLIAMS, RICHARD M. 132
WILLIS, CARL 97
WILSON, CHARLEZETTA 137
WINKLER, JONATHAN 114
WISE, WILLIAM 137
WITHERS, ALEXANDER 106
WOJTSEKHOWSKI, BOGDAN 135
WOOD, MARY 85
WOOD, STEVE 136
WOODS, MIKE 103
WOODY, KATHERINE 137
WRAY, CRAIG 114
WU, PA-YI JACKIE 115

X

XIAOHONG, LI 96
XU, NU 129
XU, TENGFANG (TIM) 117

Y

YERSHOV, GENNADIY 85, 110
YEUNG, TSUHAO 90
YODER, JACOB 137
YOU, YUN 88
YOUNG, JAMES S. 124
YOUNG, MARCUS II 115
YOXALL, BRIAN 106

Index of Names

Z

ZAHEDKARGARAN, CHAKAMEH 106
ZALAVADIA, NIKUNJ 106
ZAMORANO, JESUS 126
ZELLHOEFER, JESSICA 90
ZEMANIAN, THOMAS S. 112
ZHEN, YILI 91
ZHOU, JIZHONG 100

Education Programs Offered by the U.S. Department of Energy Office of Science

http://www.scied.science.doe.gov

Undergraduate Research Programs

These programs are designed to give undergraduate students direct experience in scientific research or science policy and guidance in planning a career in science.

SULI: *Student Undergraduate Laboratory Internship.* Formerly ERULF (Energy Research Undergraduate Laboratory Fellowship), this program is open to all undergraduate students attending 2 or 4 year colleges or universities. The students participate in 10 or 16 week internships throughout the year.

CCI: *The Community College Institute*. This program is open to students attending Community Colleges. The internship is available in the summer and is designed to enrich and enhance the student's academic education with research projects and career development activities.

PST: *Pre-Service Teacher Program*. This program is designed for students aspiring to be the science, math and technology educators of the future. It is an opportunity to spend 10 weeks in a summer internship while strengthing science, math, and/or technology content knowledge and skills with guidance on transfering the knowledge/skills to a classroom environment.

Other Programs

Science Bowl: A math and science competition for teams of public and private high school students.

Albert Einstein Distinguished Educator Program: This program brings Science, Math and Technology teachers in the K-12 arena to Washington D.C.… "where Education Practice meets Education Policy."

ERLE: *Used Energy Related Laboratory Equipment*. This is a clearing house of equipment no longer being used at the DOE. It makes the equipment available (and free) to post-secondary academic institutions.